ESO Workshop on

The Need for Coordinated Ground-based Observations of Halley's Comet

Paris, 29 – 30 April 1982

Proceedings

Edited by P. Véron, M. Festou and K. Kjär

ESO Workshop on

The Need for Coordinated Ground-based Observations of Halley's Comet

Paris, 29 – 30 April 1982

Proceedings

Edited by P. Véron, M. Festou and K. Kjär

September 1982

EUROPEAN SOUTHERN OBSERVATORY
Karl-Schwarzschild-Str. 2, D-8046 Garching bei München
Federal Republic of Germany

ISBN 3-923524-14-5

INTRODUCTION

Observing comets has always been a very difficult task because cometary phenomena are of a transient nature. Almost all spectacular comets, i.e. bright objects coming close to the Earth and thus displaying large tails, appear suddenly in the sky as tiny nebulosities and fully develop within a few weeks. Not only the time available for preparing instruments is very short and standard (non specific) equipment has to be used, but invariably, even if one gets ready in time, all the observing time in observatories has already been allocated for the next six or twelve months! As a consequence, despite the comprehension which is manifested by colleagues who kindly accept to give up their observing time, our knowledge of these objects progresses very slowly.

The last ten years have been marked by two events which leave us to think that we are coming out of Stone Age in cometary physics. Firstly, the far ultraviolet wavelength range is now accessible by means of sophisticated experiments flown on board rockets or spacecraft. Emissions of four of the main atoms in the Universe (H, C, O, and S) are now observable in comets and this allows us to measure the nucleus gaseous output through the determination of its atomic balance. Secondly, it has been decided to send space probes to proceed to direct observations of the nucleus of a comet and of its environment.

Does it mean that ground based observations have become obsolete? Certainly not. A few molecules are (or will soon be) observable in the radio range; it is reasonable to hope to detect the main parent molecules in the millimeter range in the near future; very sensitive detectors working in the near IR or in the visible ranges are being developped and will enable the detection of new faint and important emissions as well as to permit the gathering of data with high spatial, spectral, and temporal resolutions.

The bright Halley's comet has been chosen as the target for the first space missions. A tremendous effort will be devoted to the study of that comet, not only because of those space programs but because it is the only bright periodic comet which is due to return to perihelion in the next twenty years. Consequently, a very important practical obstacle for programming an appropriate observing campaign - the unknown arrival time - disappears in that case. Ample time is left for reflection, preparation and coordination. This workshop is intended to help the setting of a wide cooperation between European astronomers.

It is a pleasure to thank the chairmen of the various sessions, the invited speakers, and the authors of contributed papers, who all made this workshop possible.

P. VERON
M. FESTOU

EDITORS' NOTE

Our approach to the publication of this report has been similar to that followed for previous ESO workshop and conference proceedings: the speakers were asked to submit their texts typed on standard appropriate sheets, which were then used directly for offset printing. We are grateful to most of the speakers for providing us with their papers shortly after the end of the workshop.

The discussions after the papers were printed only when they were confirmed in writing by their authors.

We would like to express our gratitude to all those who helped us in the organization of this workshop, and especially to Mrs. C. Blamont, M. Levasseur, M-C. Pantalacci and R. Verschuren.

The editors

Participants

Dr. A. Ammar	CNES, Paris France
Dr. C. Andersson	Onsala Space Observatory, Onsala Sweden
Dr. P. Angebault	Observatoire de Besançon France
Dr. C. Arpigny	Université de Liège, Cointe-Ougrée Belgium
Dr. J. Audouze	Institut d'Astrophysique, Paris France
Dr. C. de Bergh	Observatoire de Meudon France
Dr. J.-L. Bertaux*	Service d'Aéronomie du CNRS, Verrières-le-Buisson France
Dr. J.J. Berthellier	CRPE, Saint-Maur France
Dr. J.P. Bibring	Laboratoire R. Bernas Faculté des Sciences, Orsay France
Dr. J. Blamont	Service d'Aéronomie du CNRS, Verrières-le-Buisson France
Dr. A. Boischot	Observatoire de Meudon France
Dr. R. Boyer	DASOP Observatoire de Meudon, Meudon France
Dr. M. Combes	Observatoire de Meudon, Meudon France
Prof. C.B. Cosmovici	DFVLR, Wessling Germany
Dr. G. Courtès	LAS, Marseille France
Dr. J. Crovisier	Observatoire de Meudon France
Dr. P. Cruvellier	LAS, Marseille France
Dr. A. Danks	ESO, Garching bei München Germany
Dr. D. Despois	Observatoire de Bordeaux France

Dr. C. d'Uston	Centre d'Etude Spatiale des Rayonnements, Toulouse France
Dr. A. Ekelund	Onsala Space Observatory, Onsala Sweden
Dr. L. Ekelund	Onsala Space Observatory, Onsala Sweden
Dr. C. Emerich	LPSP, Verrières-le-Buisson France
Dr. T. Encrenaz	Observatoire de Meudon France
Dr. H. Fechtig	Max-Planck-Institut für Kernphysik, Heidelberg Germany
Dr. P. Felenbok	Observatoire de Meudon France
Dr. M. Festou	Service d'Aéronomie du CNRS, Verrières-le-Buisson France
Dr. E. Gérard	Observatoire de Meudon France
Dr. R.H. Giese	Ruhr Universität Bochum, Bochum Germany
Dr. J. Guérin	Institut d'Astrophysique, Paris France
Dr. F. Hechler	ESOC, Darmstadt Germany
Dr. M. Hechler	ESOC, Darmstadt Germany
Dr. J.-L. Heudier	Telescope de Schmidt, CERGA, Saint Vallier de Thiey France
Prof. D.W. Hughes	Department of Physics, The University, Sheffield England
Dr. J.F. James	The Schuster Laboratory, The University, Manchester United Kingdom
Dr. K. Jockers	MPI für Aeronomie, Kathenburg-Lindau Germany
Dr. J. Klinger	Laboratoire de Glaciologie et de Géophysique de l'Environnement, Grenoble France
Dr. C.-I. Lagerkvist	Astronomiska Observatoriet, Uppsala Sweden

Dr. P. Lamy	Laboratoire d'Astronomie Spatiale, Marseille France
Dr. Y. Langevin	Laboratoire R. Bernas Faculté des Sciences, Orsay France
Dr. J.F. Le Borgne	Observatoire du Pic du Midi, Bagnères France
Dr. A. Levasseur-Regourd	Service d'Aéronomie du CNRS, Verrières-le-Buisson France
Dr. Rh. Lüst	MPI für Astrophysik, Garching bei München Germany
Dr. D.J. Malaise	Université de Liège, Cointe-Ougrée Belgique
Dr. M. Malinovski	LPSP, Verrières France
Dr. B. Morando	Bureau des Longitudes, Paris France
Dr. G. Moreels	Observatoire de Besançon France
Dr. P. Morel*	CNES, Paris France
Dr. R.P. Norris	Nuffield Radio Astronomy Labs, Macclesfield England
Dr. J.P. Parisot	Observatoire de Besançon France
Dr. J.P. Picat	Observatoire de Meudon France
Dr. J. Rahe*	Remeis Sternwarte, Bamberg Germany
Dr. R. Reinhard	Space Science Department of ESA, Noordwijk The Netherlands
Dr. E. Rieger	Max Planck Institute für Extraterrestrial Research Garching bei München, Germany
Dr. H.E. Schuster	ESO, Garching bei München Germany
Dr. G. Schwehm	Bereich Extraterrestrische Physik Ruhr-Universität Bochum, Bochum Germany
Dr. P. Stumpff*	Max-Planck-Institut für Radioastronomie, Bonn Germany

Dr. P. Véron	ESO, Garching bei München Germany
Dr. M.K. Wallis	University College, Cardiff Great Britain
Dr. R. West	ESO, Garching bei München Germany
Prof. L. Woltjer	ESO, Garching bei München Germany
Dr. D.K. Yeomans	Jet Propulsion Laboratory, Pasadena USA
Dr. R. Zerull	Ruhr-Universität Bochum, Germany
Dr. J.M. Zucconi	Observatoire de Besançon France

* The asterisk denotes the chairmen.

TABLE OF CONTENTS

WELCOMING ADDRESS

Jean Audouze
Directeur
de
l'Institut d'Astrophysique du CNRS

On behalf of the Institut d'Astrophysique du CNRS I am both happy and honoured to welcome the participants to this ESO workshop which is an attempt to coordinate the research efforts which will be devoted to the study of Halley's Comet.

This workshop is important because, as will be stated later at length in this conference, comets are indeed the best tools we have at our disposal to scrutinise the nature of the solar system and have some insight into its evolution. In this respect, future programmes which will be conducted to study in detail Halley's Comet are indeed a unique opportunity for reaching this goal.

I wish you a very enjoyable and profitable workshop and every success in your work and I thank the organisers who chose our Institute to hold such an important meeting.

OPENING ADDRESS

L. Woltjer, ESO

Four years from now, the main part of the Comet Halley observations will have been completed. In the normal ESO schedule, frequently a year passes between receipt of an observing proposal and the performance of the observation. If some modest instrumentation requirements are to be dealt with, this interval may become much longer. It is thus none too soon to see now what will be needed at ESO for the Halley event. We therefore have responded with much enthusiasm to the proposal by Professor Blamont to have an ESO workshop on comet Halley.

A second reason why the present workshop may be timely is provided by the NASA "International Halley Watch". It will be necessary to see what our response to the IHW should be and to investigate in which way it may be made truly international.

Professor Audouze has kindly offered to make the facilities of the Institut d'Astrophysique available for this workshop. I would like to thank him and his staff for their efforts.

IS COMET HALLEY REALLY DANGEROUS?

P. VERON, ESO Munich

After the discovery of the cyanogen bands in the coma of comet Morehouse (1908 c) by de la Baume Pluvinel and Baldet at the Juvisy observatory near Paris on October 4th, 1908 (CRAS 147, 666) the well known French popularizer, Camille Flammarion, could write in the weekly magazine "l'Illustration" of 24 October 1908 that this comet was mainly made of cyanogen, a deadly gas; and that if, by chance, this comet would approach the Earth too much, the Earth atmosphere could get mixed with a few million cubic kilometers of cometary gas. He was in fact suggesting that crossing a comet tail could be very dangerous for the Earth inhabitants, although this danger did not exist in the case of comet Morehouse.

Comet Halley was rediscovered by Max Wolf at Heidelberg on September 11, 1909. It was then realized that the comet would pass in front of the solar disk on May 18, 1910. Comet tails were known to point away from the Sun, and the possibility that the Earth could cross the comet tail arose. C. Flammarion felt it necessary to write an article dated December 31, 1909 and published in the "Bulletin de la Société astronomique de France" in January 1910, to explain that there was no danger at all because of the very small density of comet tails. But it was already too late: in the meantime, the French astronomers H. Deslandres and A. Bernard, from Meudon observatory, had observed the cyanogen bands in the coma of comet Halley (CRAS 149, 1103, December 13, 1909); this was soon confirmed by the American astronomers Frost and Parkhurst who announced in a telegram dated December 31, 1909 and published in the Astronomische Nachrichten of January 5, 1910: "Prismatic camera shows light of Halley's comet to be now largely due to third cyanogen band."

Hell, this is even worse than my wife.

Proceedings of the ESO Workshop on "The Need for Coordinated Ground-based Observations of Halley's Comet", Paris, 29 – 30 April 1982.

Comets have always been feared, without any scientific reasons; and now a comet was coming, containing the lethal cyanogen gas; its tail was known to be due to sweep the Earth; and, a year earlier, a well known astronomer had announced that these circumstances could be the cause of a great catastrophe (Annuaire pour l'an 1911, publié par le Bureau des Longitudes, p. 203). Very quickly a great number of newspapers, in France first, and soon in other countries, Italy, Germany, Spain, the U.S.A.,... were announcing the end of the world for May 18th, 1910. Many people got scared; "comet pills" were sold, which were supposed to ward off the evil effects of the comet (Barnard 1914, Astrophys. J. 39, 373);

C. Guillaume, associate director of the very serious "Bureau des Poids et Mesures" in Paris, was suggesting various methods to clean the air from any cyanogen traces before it could enter houses (BSAF 24, 189, 1910); more dramatic were the reported cases of people committing suicide rather than waiting to be killed by the comet, or the story of a mother throwing her six month old baby in a well (C. Flammarion 1910, CRAS 24, 249 and l'Illustration, May 14, 1910).

Fortunately a number of people took this terrible prediction with more philosophy as it is shown by numerous humoristic post cards published in 1910.

In 1986, comet Halley and its tail will stay well away from Earth; we shall be safe.

WHY SHOULD WE OBSERVE HALLEY'S COMET?

Rhea Lüst
Max-Planck-Institut für Physik und Astrophysik
Institut für Astrophysik
Karl-Schwarzschild-Str. 1, 8046 Garching b. München, FRG.

General remarks. The title of this introductory talk is a question which has certainly various aspects. In this meeting, the participants have come together to discuss the reasons why we expect to gain more information from comet Halley during its next apparition in 1986 than from all other comets observed until now, and how we can optimize the observations and the world-wide cooperation among astronomers. This question is closely related to the choice of C/Halley as the first target for a cometary space probe, and therefore the coordination of ground based, satellite and space craft observations will be a special point of these considerations.

Indeed C/Halley has an outstanding position among the 600 - 700 comets presently known. Its orbit puts it somewhere between the periodic comets with typical revolution times below 20 years (there are only 16 comets with periods longer than 20 years among the roughly 110 periodic comets observed until now), and those which are usually classified as "non-periodic", perhaps because their periods are long as compared to a human life. Comet Halley which returns every 76 years is by far the brightest and the most famous comet among the periodic ones, mentioned already in Chinese reports several centuries B.C. and observed in an almost unbroken series of about 30 perihelion passages, at first only in China, Japan and Korea and since the 13^{th} century also in Europe. None of the other 15 comets with longer periods has been seen during more than 4 apparitions, and only C/Encke with the shortest known period of 3.3 years which has been discovered in 1786 has a larger record of 52 observed perihelion passages. However, this long epoch of observations is not the only reason for C/Halley's fame, nor does it sufficiently explain the activities which are planned for its next apparition four years from now.

Proceedings of the ESO Workshop on "The Need for Coordinated Ground-based Qbservations of Halley's Comet", Paris, 29 – 30 April 1982.

Fig. 1. C/Halley during its 1682 apparition, the one which was witnessed by Edmund Halley, from an old broadsheet.
The picture shows the comet observed from the city wall of Nuremberg (J. Classen, "Die Sterne" 52, 1976)

According to the Öpik-Oort theory, a vast reservoir of about 10^{11} cometary nuclei is surrounding the sun within 50 000 a.u. Though their history is not yet fully understood, they seem to be the most pristine objects of the solar system which are still reflecting the composition of the presolar nebula. This makes them important for the study of their own origin as well as for the origin of the solar system. "New" comets coming into the inner planetary system for the first time are usually brighter than those which are not on their first voyage to the sun. This is demonstrated by a catalogue of 200 original high accuracy orbits issued by Marsden et al. (1978) in which the perturbations by the planets are taken into account. The values of the original semi-major axes show that almost all comets with perihelion distances larger than 3 a.u. were "new", indicating that the newcomers are intrinsically brighter, probably because of a larger content of frozen volatiles in their outer layers which had never before been exposed to the irradiation of the sun. But

since the appearance of non-periodic comets is unpredictable and since they are in most cases already fairly close to the sun at their discovery (if not past their perihelion), they are, in the near future, impossible targets for a space probe. On the other hand, the periodic comets have apparently lost some characteristics of the non-periodic ones, and their surfaces may be depleted of volatiles.

Comet Halley is the only periodic comet which has preserved many of the properties of bright new comets in spite of multiple perihelion passages fairly close to the sun (q = 0.58 a.u.). Both in photography and in visual observations it presented itself as a very active object with varying structures and jets in its coma and with a long plasma tail. Since it came rather close to the earth during its last apparition (minimum distance ~0.16 a.u.), it was a bright object in May 1910, easily visible with the naked eye, and has been investigated by many observers. These old observations are of course a major source in the preparation of the future observing program. Already now we possess a set of accurate orbital elements and parameters of the non-gravitational forces as a basis for the precalculation of the future ephemeris which will hopefully enable an early recovery. The special geometry of the tail when the earth grazed through a part of it on May 19, 1910, allowed to draw conclusions about the nature, the accelerations and the size of the dust grains (Sekanina 1981). This geometry was caused by a coincidence of two events: the earth passing through the orbital plane of the comet and the comet passing through the ecliptic plane with a time difference of only 82 minutes, so that the tail was seen edgewise. Furthermore the old observations have been used for a deduction of the physical conditions which we may expect near the comet, though no detailed model of the coma can yet be calculated since at that time the present techniques of high precision photometry and spectroscopy were just in their beginnings and the photographic plates had not been properly calibrated. One has additionally tried to compare these results with others derived for recently observed comets which show some similarity with C/Halley, as e.g. C/Bennett 1970 II and C/West 1976 VI, and to draw conclusions from this analogy. We must, however, be aware that at present we do not possess much more than a very preliminary qualitative model of C/Halley with some first order quantitative guesses,

but we do have now the great chance to improve this picture considerably by observations in all accessible wavelengths, from the ground, from sounding rockets and earth-orbiting satellites and from the probes which will hopefully succeed in carrying out their in situ measurements. One of the great advantages of this comet is that it gives us enough time to coordinate our efforts, and the International Halley watch program, initiated by scientists in the United States, has already started with the organization of a world-wide cooperation.

To emphasize the importance of an international coordination we should for a moment think of the results which came from observations of C/Kohoutek in 1973/74. This comet was discovered 8 months before its perihelion passage, and the first predictions of its brightness evolution suggested that it would become one of the brightest comets of the century. Though this was not true - a demonstration that the evolution of the gas and dust coma can vary considerably due to different chemical and structural properties of cometary nuclei -, we learned more from this object than from any other comet. We will certainly be able to do much better with C/Halley which is not unknown to us and which gives us years for the preparation and coordination of earth based and in situ observations.

Obviously C/Halley combines many advantages as a first target for a space mission. It does not make much sense to weigh against each other the efficiencies of ground based and in situ observations which both have their special possibilities and restrictions. A principal difference is of course the fact that in a fly-by mission a space probe will only be able to give a snapshot, though a very good and detailed one, while ground based observations or observations from earth-orbiting spacecraft can follow the comet during its evolution in space and time. Some measurements will thus be restricted to one of the two methods, but many will complement each other by investigating the same problem by different means. In the following, I shall try to outline a few points which may be important. Most of them will be treated in more detail during the subsequent reports of this meeting.

Nucleus. Up to now, practically no systematic observations of comets in large solar distances exist. There are, however, different reasons why an early recovery of a bright comet followed by a

continuous tracking would be of great value. In the case of C/Halley, I should first mention the corrections of the pre-calculated orbit which are necessary for the planning of the space missions. In fact, the search for this comet has already started in November 1977, so far with negative results. Unfortunately the comet is and will be in a rather star-crowded region of the milky way near Monoceros, Gemini and Orion till 1984, and only very slowly will it then move into Taurus. In the moment (April 1982) its heliocentric distance is about 12 a.u. It is difficult to estimate its present magnitude since the extrapolation of the light curve from the solar distance at which C/Halley had been recovered in 1909 (~3.5 a.u.) out to its present distance is very problematic. Observations of three recent non-periodic comets indicate that the brightness parameter n can be as high as 7 for large distances from the sun (West, 1982), and though the value may be somewhat smaller for C/Halley (see e.g. Yeomans, 1981 and Ferrin, 1982), we might have to wait until late 1983 before we see the comet which may then be of about 24th magnitude. At that time its heliocentric distance will be around 8.5 a.u.

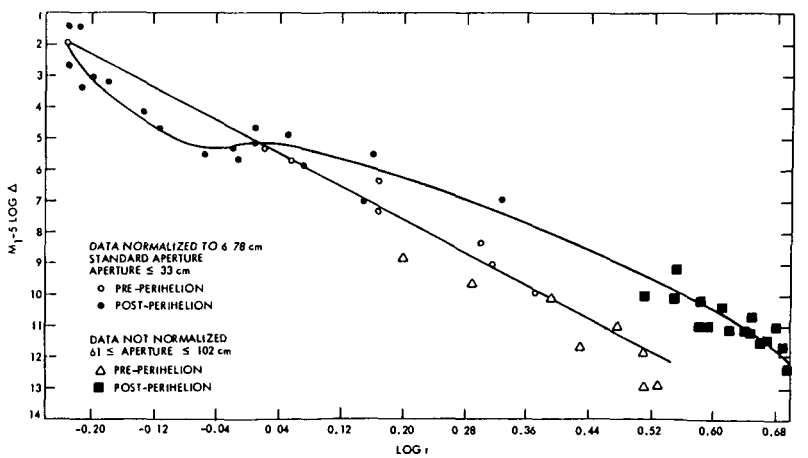

Fig. 2. Light curve for C/Halley from the best 1910 visual estimates, compiled by Newburn and Yeomans (1982)

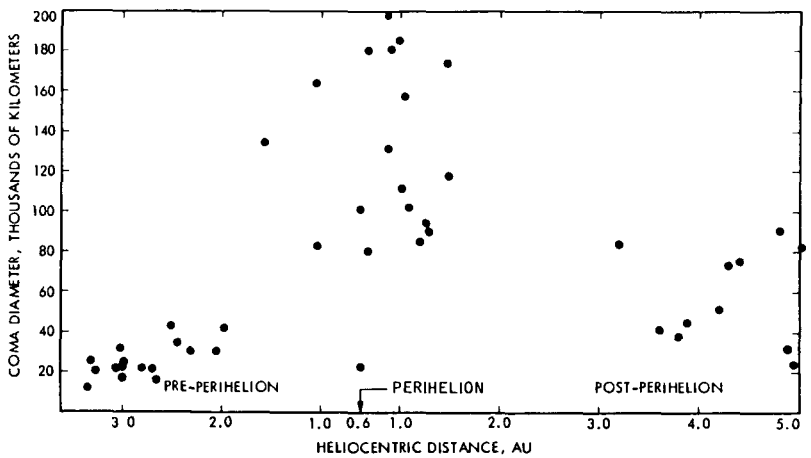

Fig. 3. Variation of coma diameter for C/Halley from its 1910 apparition, compiled by Newburn and Yeomans (1982).

Fig. 2 gives an impression of the quality of the available light curves. The rather large scatter indicates the need for better data, especially for data in larger solar distances. Fig. 3 shows the variations of the coma diameter with a very large scattering especially around the time of perihelion passage and later which are partly due to differences of the used instruments. Certainly much better measurements could be achieved today.

Besides photometry of the integrated light, interference filter photometry in selected wavelength intervals will be important. It will yield further information about the structure, the surface conditions and the chemistry of the nucleus, especially if we obtain series of data from pre- and post-perihelion observations for comparison. In a paper by Newburn et al. (1981) reporting the results of interference filter photometry of the periodic comet Ashbrook-Jackson, the authors state that up to 1977 "there was no published photoelectric photometry for any comet beyond 2 a.u.". Contributions in this field are therefore highly desirable.

An analysis of such measurements would for instance allow to detect turn-on distances of the ices which make up the outer layers of the

nucleus. The ratio of water ice with an evaporation distance of 2 - 3 a.u. to frozen compounds of higher volatility such as CH_4, CO, CO_2 and some others which start to evaporate much earlier would be of special interest. There is evidence that the abundances of CO and/or CO_2 are rather large in some nuclei (see e.g. Feldman, 1978). Since large amounts of high volatiles cannot be stored in a lattice of water ice, the assumption of a clathrate structure could be tested.

Changes of the brightness and activity of nuclei manifesting themselves by sudden flares and outbursts may be taken as signs of inhomogeneities in the outer layers. Such outbursts have been reported in both periodic and parabolic comets, indicating that local active spots are a common property of the surfaces of nuclei in spite of differences in the composition and structure at least of their outer layers. The frequency of such brightness irregularities can be used for deriving the rotation periods of nuclei, while the parameters of the non-gravitational forces deduced from the orbits give the sense of rotation which for C/Halley has been found to be in the same direction as its revolution (Yeomans, 1977). Whipple (1981) has calculated the rotation times for 47 comets, among them Halley with a period of a little over 10 hours, from periodic features of expanding halos. Such halos may be caused by repeated ejections from icy spots on the surface of the nucleus. The median rotation period for the 47 comets was found to be 15 hours. By a somewhat different method basing on an interpretation of spiral dust structures, Larson and Minton (1972) have derived a rotation period of 34 hours for C/Bennett 1970 II as compared to 28 hours for the same comet deduced by Whipple.

Coma

a) Gas. Though our knowledge of the composition of cometary comae has greatly improved during the last decades by the extension of spectroscopy into the ultraviolet and into the longer wavelength regions, we are yet far from having a detailed model of the coma, not to speak of the nucleus. Very few parent molecules have so far been identified by their spectral emissions, partly because of observational difficulties, partly because most of them have very short life times due to their rapid dissociation or ionization by chemical interactions and by the solar radiation and the solar wind.

So the detection of neutral water - presumably the most abundant constituent - in the radio spectrum of C/Bradfield 1974 III is still waiting for confirmation. There is evidence that either CO_2 or CO or both are very abundant in some nuclei. CO_2 has so far only been observed in its ionized state, the very stable CO molecule has been found in some ultraviolet spectra, and recently also some lines in the visual spectrum of C/Bradfield 1980 XV were found to coincide with CO emissions (Cosmovici et al., 1982). Furthermore there is a rather marginal identification of HCN and CH_3CN in the radio spectrum of C/Kohoutek 1973 XII which also could not yet be repeated in other objects. The discovery of CS in some recently observed comets points to the existence of CS_2 as its parent molecule, (Jackson et al., 1982).

It will therefore be one aim of the Halley probes to investigate the coma by neutral and ion mass spectroscopy. However, mass spectroscopy, as important as it will be, can only reflect the conditions in a certain solar distance, fixed by the moment of intercept. If simultaneous spectroscopy in all accessible wavelengths from ground based and earth orbiting instruments complement these measurements, it will be possible to calibrate these spectra by combining their results with those from the space probes. In this way, variations in the abundances and their ratios may be found from series of spectra taken at different solar distances, and a comparison with theoretical model calculation may then lead to a better understanding of the processes taking place in the coma, and of the primary composition of the nucleus.

In the past years the question has been brought up whether a cloud of water ice grains is surrounding the nuclei. Though there is as yet no direct evidence for such an icy grain halo, its existence would explain scale lengths and life times of some molecules which, according to this model, would not only evaporate directly from the surface of the nucleus but additionally in the more distant parts of the coma to which they have been transported in the icy grains. There may be a chance to detect these grains by their scattering in the infrared 3 m ice band (Hanner, 1981).

b) Dust. Coma and dust tail observations of various comets have yielded that the ratio of dust to gas emitted from the nucleus is

generally in the order of 1 by mass or a little less. There is no calibrated photometry which would allow to deduce reliable figures for comet Halley, and it is a serious restraint for the preparation of the space probes that we do not have more than rough lower and upper limits for the dust density and its variation with distance from the nucleus. Recent observations of C/Bowell 1980b have indicated the release of dust at extreme heliocentric distances, namely at 7 a.u. Spectra obtained by Cochran and McCall (1980) at Kitt Peak observatory have shown a halo of 12" or 60 000 km diameter. The continuum contained no traces of any kind of emission lines. The mechanism by which the dust has been ejected is not yet fully understood, the release from dusty ice grains (water or methane) has been suggested as well as an electrostatic blow-off of CO_2 (Houpis and Mendis, 1981). In this respect, early spectroscopy of C/Halley with high spatial resolution in the visual and infrared will be important. Polarization measurements of the scattered sunlight in the coma and in the dust tail will be useful for a deduction of the dust particle sizes. Here, observations of the Orionid and Eta Aquarid meteor shows which are presumably debris from Halley's comet are to be recommended both from ground based instruments or by impact sensors of spacecraft. The composition and density of the dust could be deduced from such observations.

Tails. C/Halley will also give us the possibility to study a bright plasma tail. We know from various coma and tail observations that the interaction between the solar wind and interplanetary magnetic fields with the cometary molecules contributes to the ionization of the neutral cometary material in the outer parts of the coma and is responsible for the acceleration of the ions as well as for the formation of structures in the plasma tails. However, these investigations have never covered a large continuous time span, and the material was always very inhomogeneous due to different instruments tracing a comet on its 24 hours path over the sky. It has also been attempted to correlate tail activity with variations in the solar wind parameters and with active phenomena on the sun. These attempts have suffered from the lack of simultaneous interplanetary measurements and observations of the comet. Efforts to obtain longer series of homogeneous photographs, for instance from a net of satellite cameras which can follow the comet around the globe and a coordination with solar and interplanetary observations should

therefore be encouraged.

Dust tail observations will yield information of the dust particle sizes and masses with all their consequences on the structure of the outer layers of the nucleus and the dust emission mechanism. Such investigations have been made in the past by Sekanina for several bright comets, and they should be repeated for C/Halley.

Concluding I would like to emphasize again the great importance of an early recovery and of observations beginning at the moment when the comet will be located until it will fade again. The apparition of C/Halley in 1986 will provide a unique chance to increase our knowledge about comets and their origin, and as it looks now we may trust that the scientific community is utilizing this chance by preparing a well organized international cooperation.

Current Literature

Cochran A.L. and McCall M.L.	1980	Publ.Astron.Soc.Pacific 92, 854
Cosmovici C.B., Barbieri C., Bonoli C., Bortoletto F., Hamzaoglu E.	1982	to be publ. in Astron.Astrophys.
Feldman P.D.	1978	Astron.Astrophys. 70, 547
Ferrin I.	1982	Astron.Astrophysics. 107, L7
Hanner M.	1981	Icarus 47, 243
Houpis H.L. and Mendis D.A.	1981	preprint, in press
Jackson W.M., Halpern J., Feldman, P.D., Rahe J	1982	Astron.Astrophys. 107, 385
Larson S.M. and Minton R.B.	1972	in "Comets Scientific Data and Missions" ed. Kuiper and Roemer Libr.Congr.Cat. No. 62-619613
Marsden B.G., Sekanina Z., Everhart E.	1978	Astron. J. 83, 64
Newburn R.L., Bell J.F., McCord T.B.	1981	Astron. J. 86, 469
Newburn R.L. and Yeomans D.K.	1982	Annual Review of Earth and Plan. Sciences 10 (in press)
Sekanina Z.	1981	Comet Halley Dust and Gas Environm. Workshop ESA SP - 174, p 55.
West R.M.	1982	preprint, report of this meeting
Whipple F.	1981	Smiths.Astroph.Obs. preprint No. 1500
Yeomans D.K.	1977	Astron. J. 82, 435
Yeomans D.K.	1982	"The Comet Halley Handbook" NASA - JPL 400-91

Review Papers

Newburn R.L. and Yeomans D.K. (editors)	1980	The International Halley Watch Report of the Science Working Group NASA TM 82181
Wyckoff S.	1981	Overview of Comet Observations preprint, to appear in "Comets", ed. L.L. Wilkening, Univ. of Arizona Press

DISCUSSION

K. Jockers: You mentioned that there are no calibrated plates of Comet Halley's dust tails. There is a series of objective prism plates of Comet Halley obtained at Lowell observatory containing trailed stellar spectra which would allow a calibration and a determination of the light emission of comet Halley's dust tail.

M. Wallis: An icy grain halo to explain curious scale lengths and lifetimes has been postulated for several years. Is there still no direct evidence of such a halo and does the infrared evidence not suggest it does not exist.

E. Gérard: From IR data there seems to be no "optically " thick halo larger than $\sim$ 30 to 50 km. From radio data this limit is somewhat larger, although there may have been around C/West and C/Kohoutek a transient halo of diameter $\sim$ 500 km but not a permanent one. Finally the radar echo from Encke is compatible with a target of 1 km radius so, in conclusion, the halo may exist but it is then "optically" quite thin.

R. Reinhard: The light curve which you showed has been updated in the meantime (see Marcus, J.N. 1981, The "Delta Effect" in Halley's 1910 light curve, Comet News Service, 81-3, 1981). The updated curve is shown e.g. in Newburn, R.L. 1981, A semiempirical photometric theory of gas and dust production (ESA SP-174, page 8, Fig. 6). In this new curve the post perihelion dip which you showed has disappeared. The pre and post perihelion curves run approximately parallel to each other, the post perihelion curve being slightly higher.

J. Klinger: The light curve for comet Halley that you showed is rather different compared to the light curve published by F. Whipple (1978, The Moon and the Planets 18, 343). In particular the post perihelion dip is much more pronounced in your curve compared to Whipple's. Where does this come from?

Rh. Lüst: The light curve has been compiled by Newburn and Yeomans (1982) from the best visual 1910 estimates. I cannot comment on the differences with Whipple's curve. The post perihelion dip is explained by a breaking-up of the nucleus by Ferrin (Astron. Astrophys. 107, L7, 1982). This explanation is however doubtful.

D. Yeomans: Concerning the light curve published by Newburn and Yeomans, at least part of the post perihelion brightness dip is certainly due to observations made when the comet was very close to the Earth in May 1910. At that time visual observations by E.E. Barnard and others systematically underestimated the comet's apparent magnitude. Much of the observational scatter post perihelion is probably due to intrinsic brightness variations of the comet itself.

D. Hughes: Cometary magnitude as a function of heliocentric distance has been reinvestigated by Morris and Green (1982, Astron. J. 87, 918) who show that the pre and post perihelion light curves are much more alike than was shown by Yeomans.

THE COMET PROBES

THE GIOTTO MISSION TO HALLEY'S COMET

R. Reinhard

Space Science Department of ESA
European Space Research and Technology Centre
Noordwijk, The Netherlands

1. INTRODUCTION

It is estimated that of the order of 10^{11} comets exist in a vast cloud around the Sun at a distance of $\sim$ 50 000 AU. Each year, $\sim$ 100 comets are newly deflected into the Jovian capture region (4-6 AU from the Sun) as a result of chance gravitational perturbations occurring in the distant reaches of the solar system. Occasionally the orbit of such a comet is then perturbed into a short-periodic orbit by the gravity of one of the major planets.

Unlike the planets, which all move in roughly co-planar orbits, the long-periodic comets have a spherical distribution of orbits around the Sun. Their distribution in space is reminiscent of the distribution of globular clusters about the centre of their parent galaxy. There are cosmogenic hypotheses that suggest that these spherical symmetries represent a memory of the symmetry of the parent cloud of material that later collapsed and flattened to form the main system. This has suggested to some researchers that comets may be very old, possibly predating the ages of the planets themselves. Consequently, the material they contain may be representative of the earliest condensations in the interstellar cloud that ultimately formed the Sun and the planets. The likelihood that the nuclei of new comets are possibly pristine samples of condensates from the protosolar system (possibly mixed with surviving pre-solar-system interstellar dust) implies that measurements of their composition and physical constitution would yield fundamental information on the chemical and physical conditions that existed near the time of planetary formation.

The cometary nucleus is thought to consist of a mixture of ices - mainly water, but also many other volatile molecules composed of H, C, N and O - and rocky material. The dimensions and mass of most cometary nuclei are inferred to be in the range of 1 - 10 km and 10^{15} - 10^{18} g, respectively. As a result, the gravitational attraction or, equivalently, the escape velocity is 1 - .5 m s^{-1}, which is minute in comparison with that of planets.

Our knowledge of comets comes from the fact that the nucleus, which itself is too small to be observed from the Earth, becomes active as it approaches the Sun. Heated by insolation, the nucleus releases large amounts of gas and dust during its passage through perihelion. This unpredictable and often violent process

Proceedings of the ESO Workshop on "The Need for Coordinated Ground-based Observations of Halley's Comet", Paris, 29 – 30 April 1982.

produces an atmosphere of enormous extent. Neutral molecules, some highly reactive, are formed by sublimation and possibly by other processes occurring very close to the nucleus (< 10^3 km) and expand to distances of 10^5 - 10^7 km. Ionised molecules, also produced by very rapid but poorly understood processes, have on occasion been observed even in the inner parts of this atmosphere. In addition, ions are accelerated out of the central region to form a plasma tail. Such a tail shows visual evidence of complex hydromagnetic phenomena (filaments, rays, kinks and helices).

The gas streaming out of the nucleus carries with it quantities of fine dust, which is responsible for much of the visual brightness of a comet. At distances > 10^4 km from the nucleus of a very active comet, solar radiation pressure exceeds the aerodynamic drag force on the dust, which is then swept out of the comet's atmosphere to form a large curved dust tail.

Although there is a large set of observations of comets over many centuries our knowledge on comets is still very limited. Most of this knowledge consists of the determination of cometary orbits, phenomenological descriptions of the coma and the tails, and analysis of cometary spectra. Observations of comets from Earth (ground-based or from near-Earth space) can only provide line-of-sight integrations limited to molecules with strong emission lines in suitable wavelength ranges. In particular, the parent molecules released from the nucleus can only be detected by in-situ measurements which are needed to unravel the complex physical and chemical processes in the cometary atmosphere. Cometary research cannot advance significantly beyond the present state unless certain fundamental questions, such as the existence of a nucleus, are answered which can only be addressed by a cometary mission.

Scientists on both sides of the Atlantic have tried for over a decade to obtain approval for a first cometary mission. Finally, a rather ambitious mission, combining a Halley flyby in 1985 and a Tempel 2 rendezvous in 1988, was planned jointly by NASA and ESA in 1978/79. NASA was to provide the main spacecraft, which was to carry a small ESA procured probe to Halley's comet and later to continue to Tempel 2. When it became apparent in early 1980 that the Solar Electric Propulsion System, an essential element of this mission, could not be funded by NASA, ESA proceeded independently and developed the probe further into an autonomous spacecraft.

Halley's comet (Fig. 1) has been selected for ESA's first cometary mission because of its high dust and gas production rates which are comparable to those of 'new comets', its well-known orbital characteristics, the moderate launch energy requirements, and its outstanding role in history. The Italian painter Giotto di Bondone saw Halley in 1301 and was so impressed by its appearance that

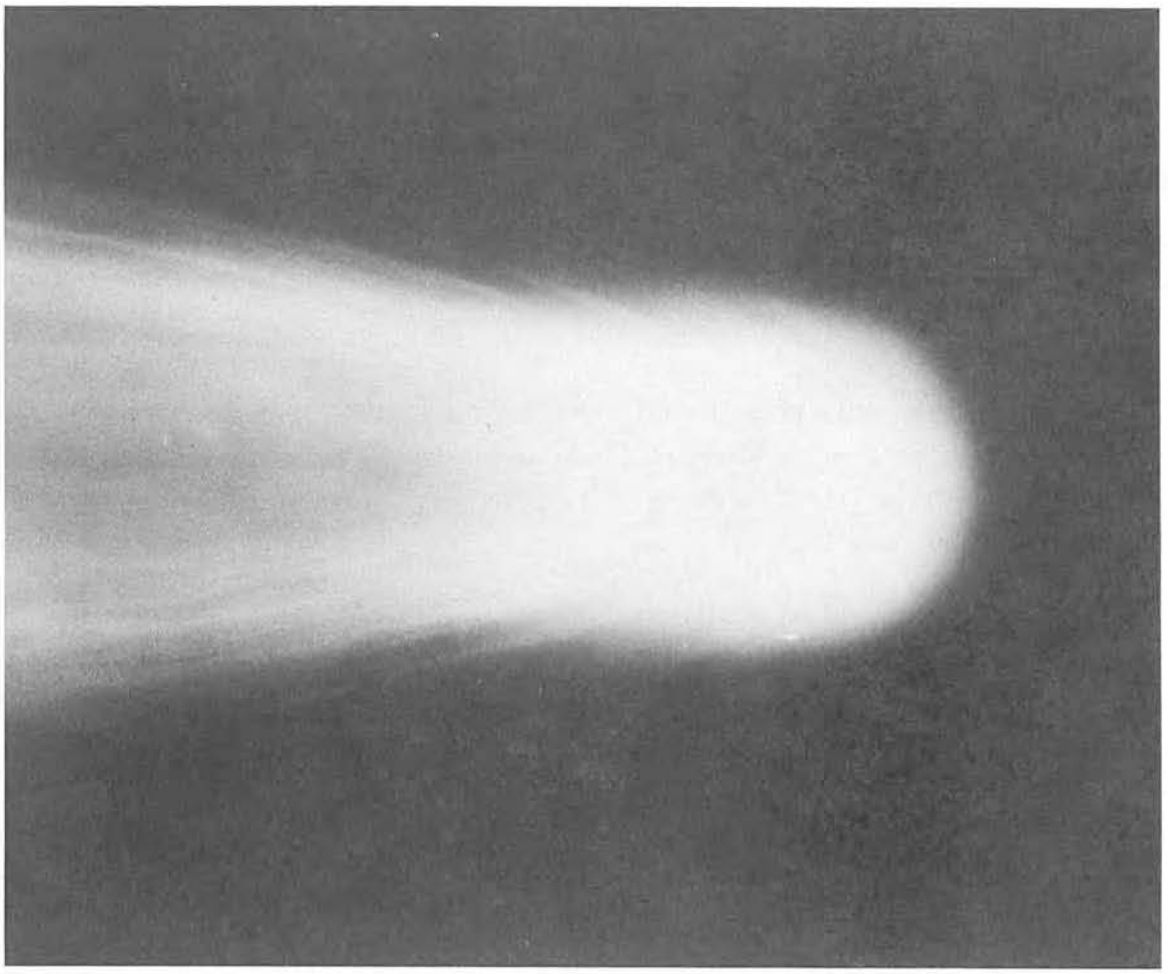

Figure 1 - Head of comet Halley 1910 II on 8 May 1910 (courtesy Mt. Wilson and Palomar observatories)

he incorporated it a few years later as the 'Star of Bethlehem' in one of the frescoes in the Scrovegni chapel in Padova. The painting shows details of the comet coma and the tail not unlike the drawings made in the 19th century by scientists. This is why ESA has given the name 'Giotto' to its comet mission to Halley.

The Giotto project was approved in July 1980, allowing precisely 5 years between approval and launch. During the study phase of the Giotto mission a Scientific Working Group formulated the scientific objectives and defined a mission concept and a model payload. The Giotto scientific objectives are:

- *to provide the elemental and isotopic composition of the volatile components in the cometary coma, in particular to identify the parent molecules*
- *to characterise the physical processes and chemical reactions that occur in the cometary atmosphere and ionosphere*
- *to determine the elemental and isotopic composition of the cometary dust particles*

- *to measure the total gas production rate and the dust flux and size/mass distribution and to derive the dust-to-gas ratio*
- *to investigate the macroscopic system of plasma flows resulting from the interaction between the cometary and the solar-wind plasma*
- *to provide numerous images of the comet nucleus with a resolution down to 50 m (from these the nucleus size and rotation may be deduced and its mass may be estimated).*

An intense Earth-based observation programme is a natural and necessary complement to the Giotto mission.

To accomplish these objectives the Giotto spacecraft will carry ten scientific experiments some of them having more than one sensor. They were selected in January 1981 and are listed in Table 10 together with their mass/power/data rate allocations as of June 1982.

Table 1. Halley's Comet

Orbital characteristics (for Epoch 1986 Feb. 19.0 (E.T.))	
perihelion passage T	1986, Feb 9.6613 (E.T.)
perihelion distance q	0.587096 AU
eccentricity e	0.967267
argument of perihelion ω	111.8534
ascending node Ω	58.1531
orbital inclination i	162.2378
Historical	
earliest recorded apparition	240 BC
number of recorded apparitions	28
last perihelion passage	20 April 1910
shortest/longest period	74.42/79.25 years

2. THE SCIENTIFIC PAYLOAD

2.1 Halley Multicolour Camera (HMC)

The camera is designed to detect and image the nucleus of comet Halley, to measure the nucleus size, shape and albedo and to observe the active sublimation process of the nucleus. By following the moving comet nucleus, the camera's microcomputers can determine the trajectory parameters of the spacecraft relative to the nucleus in real time.

The optical system of the camera is a modified Ritchey-Chrétien design with correcting field lens. The telescope is mounted behind the spacecraft bumper shield and therefore protected from direct dust-particle impacts. A 45^{o} deflecting mirror is used to look at the comet. A baffle assures adequate reduction of

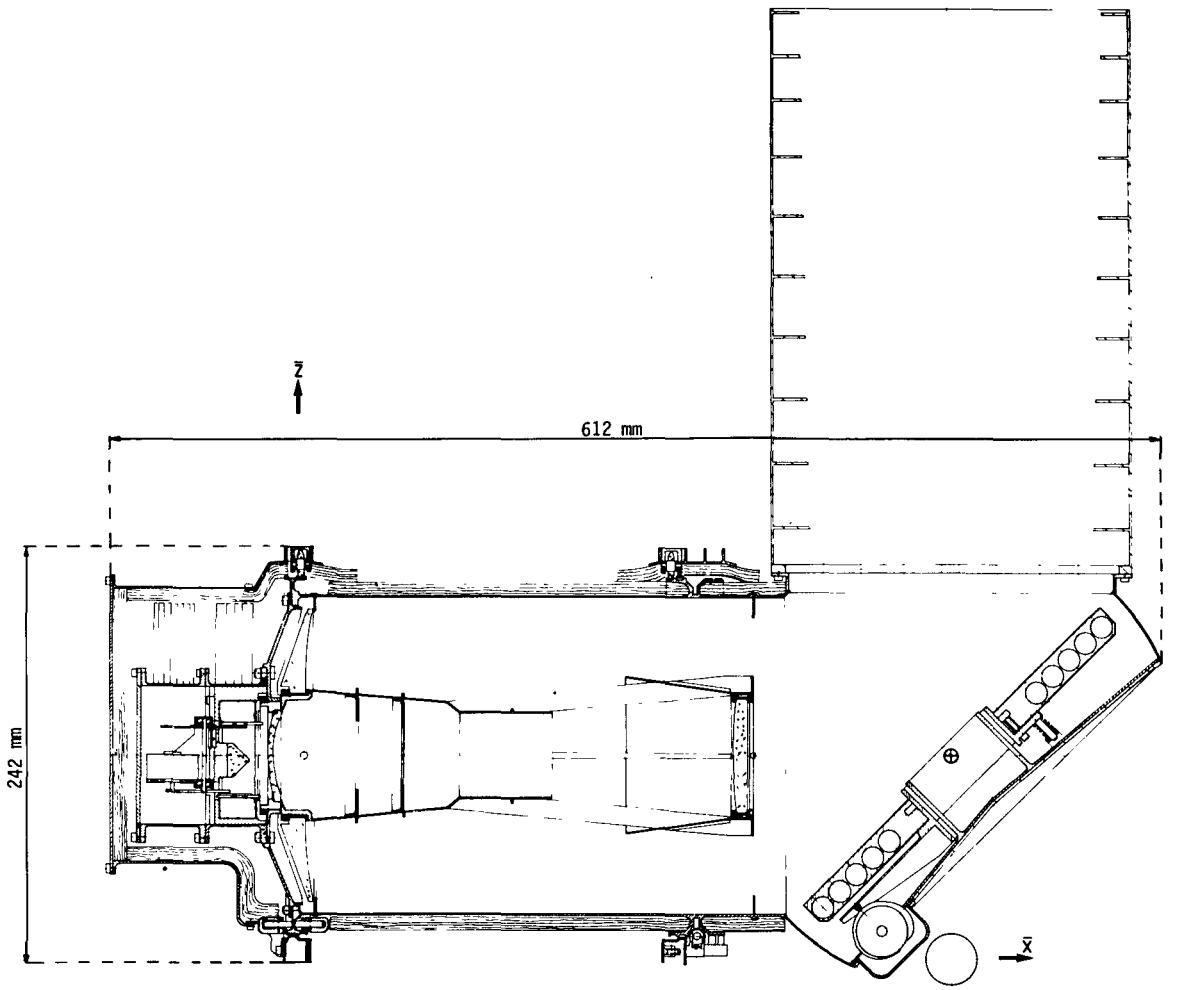

Figure 2 - The Halley Multicolour Camera (HMC). The baffle with its 10 elements is shown in the upper right, the deflecting mirror in the lower right, the primary and secondary mirror in the lower left and center, respectively, and the focal plane layout (Reticon, CCD's, filter wheel) to the left of the primary.

diffuse sunlight and spacecraft-reflected light.

The telescope images onto a focal-plane arrangement of one Reticon and two area CCD's (charge-coupled device). The Reticon is used to detect the nucleus and later to clock the two area CCD's. The area CCD's are used in a mode in which only a few active lines scan the image of the comet during its apparent motion across the rotating (because of the spacecraft spin) field of view; the remaining lines are masked and used as a low-power, highly efficient data buffer. The contents of the exposed lines are shifted into the masked CCD lines with precisely the rate of motion of the nucleus image. Using CCD's as intermediate storage for a line scanner permits exposure times as short as 10 μs to be achieved. Smear due to the spinning motion of the camera is then negligible, even for such a high resolution as 22 μrad per pixel of the detector. In the nucleus imaging

mode the camera works best if the nucleus is slightly ($\gtrsim 1^{o}$) off spin axis. The two area CCD's each have two segments, three of the four segments being tinted to provide colour pictures.

Table 2 Halley Multicolour Camera Characteristics

Telescope	Ritchey Chrétien with corrector lens focal length : 1000 mm, effective F/7.68 aperture : 160 mm field of view : 1.5^{o}
Detectors	1 multidiode array : Reticon, 2 lines with 936 diodes each diode size 30 x 375 µ 2 area CCD's : TI, virtual phase each 2 x 292 lines with 390 pixels per line pixel size 22.3 x 22.3µ
Resolution	22 m/pixel at 1000 km slant range
Field of view	linear CCD : 1.61^{o} (1.5^{o} unvignetted) area CCD : 0.65^{o}
Filters	1st area CCD : lines 5 - 10 : red* lines 11 - 292 : masked lines 297 - 302 : filter wheel* lines 303 - 584 : masked 2nd area CCD : lines 5 - 8 : clear* lines 9 - 292 : masked lines 297 - 304 : blue* lines 305 - 584 : masked *more than one line because of TDI

Filter Wheel (Ø 56 mm)

Shutter	
clear	300 - 1100 nm
red	710 - 1100
orange	590 - 690
blue	300 - 480
$P_{\parallel}$	300 - 1100
$P_{\perp}$	300 - 1100
continuum	442 - 454
continuum	718 - 740
OH	306 - 316
C_3	402 - 412
C_2	504 - 516
(H_2O^+	694 - 706)

The camera can be rotated through 180^{o}, allowing the nucleus to be followed during approach and imaged even after the flyby. Already at 1400 km from the nucleus, the camera will be able to resolve its surface structure down to 30m.

2.2 Neutral Mass Spectrometer (NMS)

As the spacecraft flies through the cometary coma, cometary neutrals will be encountered at the flyby velocity of 68 km/s. Since the gas outflow velocity is much smaller (< 1 km/s), one might think that the mass of the cometary neutrals could be determined simply by measuring their energy (since $E = \frac{1}{2}mv^2$). However, the daughter molecules can derive significant kinetic energies from energetic interactions such as photo-dissociation and ion-molecular reactions, which appear either as a change in the incident direction or as an increase or decrease in energy, e.g. an O atom with a velocity of 5 km/s can appear anywhere between mass 14 and 18. Consequently, an energy spectrum will be smeared, predominantly in the lower mass ranges, and individual peaks corresponding to

particular masses cannot be resolved. In the higher mass ranges the cometary neutral velocity distribution will be 'cold' and the energy spectrum will correspond to the mass spectrum.

This calls for the following approach. In the lower mass range (1 - 34 amu) a double-focussing (angle and energy) mass spectrometer is used consisting of a parallel-plate electrostatic energy analyser followed by a magnetic sector field momentum analyser. The particle beam is imaged onto a microchannel plate with linear readout, where each position corresponds to a particular mass. The energy information that is lost in the 'M-analyser' is provided by the 'E-analyser', which is simply a parallel-plate electrostatic analyser with single focussing (angle) properties. Again, the particle beam is imaged onto a microchannel plate with linear readout, where each position corresponds to a particular energy. For analysis the beam of cometary neutrals first has to be transformed into a beam of ions; this is achieved by bombardment with an electron beam with the electrons being emitted from either of two redundant filaments.

Table 3 Neutral Mass Spectrometer Characteristics

	M-Analyser	E-Analyser	
Energy range	-	20 - 860 eV	730 - 2110 eV
Mass range	1 - 36 amu	1 - 35 amu	30 - 86 amu
Resolution	0.25 amu 1 amu for particles 4.5^{o} off axis and 10 eV thermal energy	4.4 eV	7.2 eV
Field of view	9^{o} cone	9^{o} cone	
Integration time			
neutrals	1.4 s	0.7 s	
ions	0.1 s	0.05 s	
Density range			
neutrals	10 - 10^{7} cm^{-3}	30 - 10^{7} cm^{-3}	
ions	1 - 10^{5} cm^{-3}	1 - 10^{5} cm^{-3}	

Both sensors have separate and nearly identical gas inlet systems with an electron beam ion source of fly-through geometry. The ion source operates in two modes. In the neutral mode cometary ions are reflected by deflecting plates in front of the entrance slit, in the ion mode the deflecting plates are switched off and the electron emission is suppressed allowing cometary ions to enter the analyser. Further away from the comet nucleus the instrument will measure predominantly ions, close to the nucleus predominantly neutrals.

2.3 Ion Mass Spectrometer (IMS)

The Ion Mass Spectrometer comprises two sensors, a High Energy Range Spectrometer (HERS) optimised for measurements in the outer coma where a turbulent transition between solar wind and cometary ions is expected, and a High Intensity Spectrometer (HIS) optimised for measurements in the inner coma where high fluxes of relatively cold cometary ions are expected.

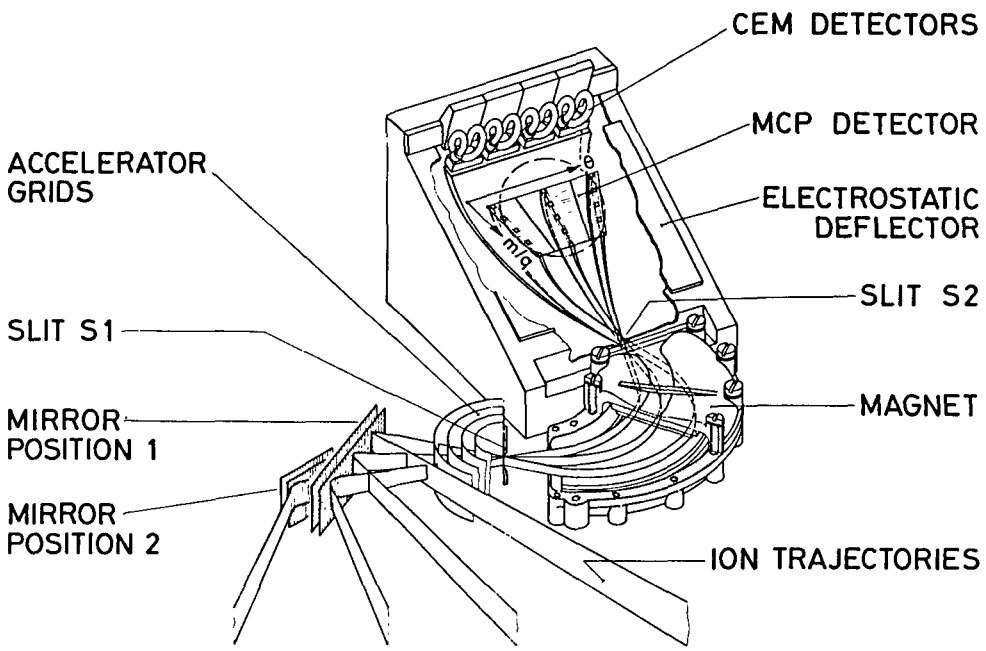

Figure 3 - The High Energy Range Spectrometer (HERS) of the Ion Mass Spectrometer

The HERS sensor consists basically of an electrostatic mirror to deflect the cometary ions into the instrument, a pair of grids with variable applied voltage, a sector magnet which serves as momentum per charge filter, and an electrostatic deflector which spreads the momentum-analysed ions according to their energy per charge. The beam is then imaged onto a two-dimensional microchannel plate, with one dimension a measure of mass per charge and the other a measure of the elevation angle of the ion's velocity vector. Azimuth angle is scanned by the spacecraft spin and the energy distribution is determined by variation of the voltages applied to the pair of grids.

The HIS sensor employs two quadrispherical electrostatic analysers with magnetic deflection and an array of 4 x 4 channeltrons as detectors. The energy per charge of the particles to be analysed is selected by the differential voltage applied to the first electrostatic analyser while the momentum per charge (and thus mass per charge) is determined by the acceleration potential applied between

Table 4 Ion Mass Spectrometer Characteristics

	HERS	HIS
energy range	20 - 8000 eV	300 - 1500 eV
mass range	1 - 64 amu/q	12 - 60 amu/q
$m/\Delta m$	$\geq$ 20 at $\sim$ 20 amu/q	$\geq$ 20 at $\sim$ 20 amu/q
elevation range/resolution	1) $+15^{o}$ to $+45^{o}$ / 7.5^{o} 2) $+45^{o}$ to $+75^{o}$ / 7.5^{o}	-2.5^{o} to $+27.5^{o}$ / 5^{o}
azimuth range/resolution	spin scanned / 5.6^{o}	spin scanned / 22.5^{o}
time resolution	24 s	4 s
dynamic range	10^{-3} - 10^{2} cm^{-3}	10^{-2} - 10^{4} cm^{-3}

a pair of plane parallel grids located behind the exit of the first electrostatic analyser. The ion species expected to be seen at the selected energy is imaged at the centre of the one-dimensional detector array of 4 channeltrons. Hence, the mass spectrum and the temperatures of all individual species can be measured by just scanning through the energy-per-charge range. The other direction of the channeltron array provides resolution in elevation, while azimuth angle is scanned by the spacecraft spin.

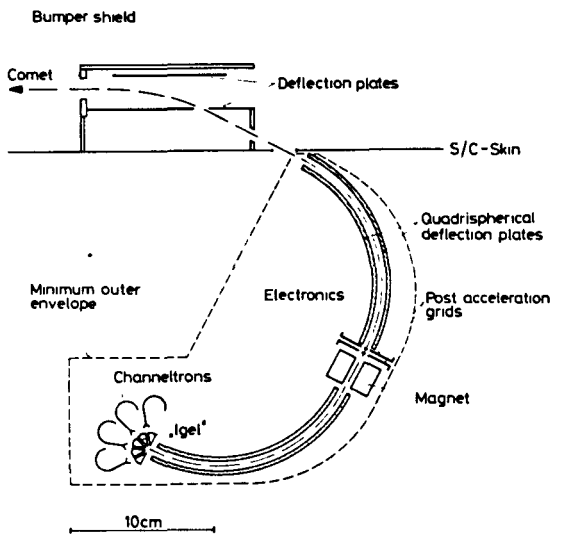

Figure 4 - The High Intensity Spectrometer (HIS) of the Ion Mass Spectrometer

2.4 Dust Mass Spectrometer (PIA)

This instrument measures the chemical and isotopic composition of individual dust particles. When a dust particle impacts on the instrument's target, a plasma is generated from which ions are extracted and accelerated via a 1.5 kV acceleration grid. The acceleration ions fly through a time-of-flight tube approximately 1 m long where they are separated in time according to their mass. The spectrum of elements of which the dust particle is composed is recorded by an electron multiplier at the end of the drift path. Since the elemental abundances of typical minerals found in meteorites vary significantly it is possible to identify

the predominant mineral in the impacting dust grain from the quantitative abundance in the spectrum.

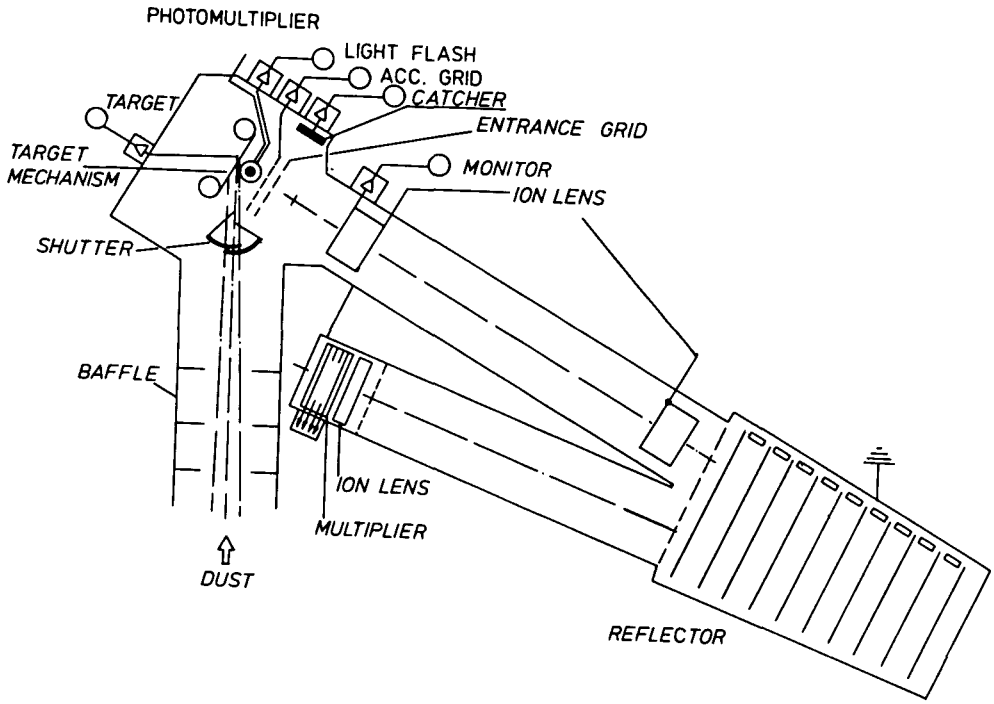

Figure 5 - The Dust Mass Spectrometer (Particulate Impact Analyser (PIA))

Impact-ionisation mass spectrometry is ideally suited for a fast cometary flyby such as Giotto will make because the number of positive ions released upon impact increases significantly with the impact velocity. The time-of-flight tube consists actually of two tubes at an angle of 8^{o}, with an ion reflector in between, used for energy focussing. This, together with the high ion yield, gives

Table 5 Dust Mass Spectrometer Characteristics

dust mass range	$\sim 3 \cdot 10^{-16} - 5 \cdot 10^{-10}$ g
atomic mass range	1 - 110 amu
mass resolution	separation of peaks possible if $I_{m+1} : I_m \geq 1:50$
time resolution	$\sim 10^{-4}$ s time of flight in the tube $\sim 10^{-2}$ s for impact counting 0.25 s for spectral analysis of individual dust particles
target area/material	0.01 - 5 cm^2 (shutter controlled) / Ag

excellent mass resolution, so that isotopic ratios such as $^{7}Li/^{6}Li$, $^{11}B/^{10}B$, and $^{13}C/^{12}C$ can be resolved. Because of its small target area, which can be varied through a shutter mechanism, the instrument will predominantly analyse the most common dust particles, which are expected to be in the mass range 10^{-15} - 10^{-11} g.

2.5 Dust Impact Detector System (DID)

Although larger dust particles are more infrequent, the bulk of the mass released from the comet nucleus in the form of solids is contained in them. Impacts of these large dust particles on the front sheet of the spacecraft bumper shield are detected by three piezo-electric elements (microphones) mounted 120°

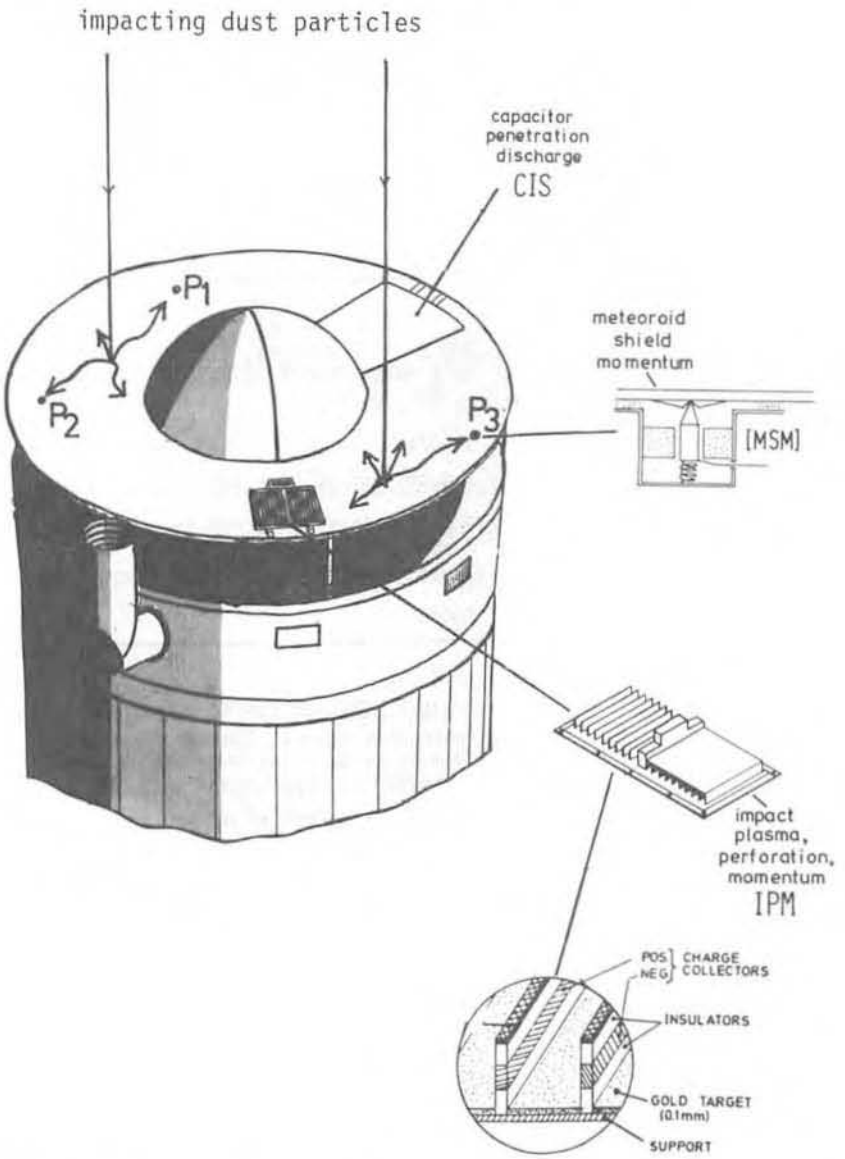

Figure 6 - The Dust Impact Detector System (DID), mounted on the front sheet of the bumper shield. Details of the Meteoroid Shield Momentum Sensor (MSM) and the Impact Plasma and Momentum Sensor (IPM) are shown on the right.

apart at the outer edge of the front sheet (meteoroid shield momentum measurement, MSM). They register the shock wave which is generated by each dust-particle impact and propagates through the front sheet. In this way the whole area of the front sheet ($2m^2$) can be used as 'detector'. A similar element is also placed on the rear sheet (rear shield momentum measurement, RSM) and measures the mass of even larger dust particles that are able to penetrate the front sheet (> 10^{-6} g) and impact on this rear sheet.

A Capacitor Impact Sensor (CIS) of 1000 cm^2 area measures the flux of dust particles > 10^{-10} g penetrating a thin (70μ) Mylar dielectric material. Aluminium deposits on both faces act as capacitor. Upon impact by a sufficiently large particle the dielectric of the capacitor is perforated and the device is discharged through the impact-generated plasma. The counting rate is limited by the recharging process of the capacitor to ∿ 1000 impacts/s.

Table 6 Dust Impact Detector System Characteristics

IPM	
a) sensor area	100 cm^2 (Au target), ½ of sensor covered by a metallised film (1 μ thick)
impact charge range	10^{-14} - 10^{-8} C
maximum count rate	1000/s
density resolution	1 g cm^{-3} at 10^{-13} - 10^{-15} g
b) impact detector	1 piezo-electric PZT-5H longitudinally resonant element
momentum range	10^{-11} - 10^{-8} Ns
maximum count rate	100/s
MSM/RSM	
impact detectors	4 piezo-electric PZT-5H longitudinally resonant elements, 200 kHz (3 mounted on front sheet, 120° apart, 1 mounted on rear side of rear sheet)
sensor area	2 m^2 (front sheet of bumper shield)
momentum range	10^{-11} - 10^{-8} Ns
maximum count range	10/s at 10^{-10} g 1/s at 10^{-6} g
CIS	
sensor area	1000 cm^2
capacitor configuration	10 μ electrode (Al foil) 70 μ dielectric (Teflon) 0.1 μ electrode (Al foil) 10 μ insulation (Teflon)
threshold sensitivity	10^{-9} g
maximum count rate	1000/s

Very small dust particles are detected by an impact plasma detector (IPM) having very high count-rate capability. This sensor is also located on the front sheet of the spacecraft bumper shield. The impact-generated plasma electrons and ions are separated by an electric field, the total charge being proportional to the particle mass. The impact plasma detector has two arrays, one without a foil, the other covered by a metalised penetration film of 1μ thickness, which observes a somewhat reduced number of impacts depending on the penetrating power or bulk density of the dust particles. A piezo-electric microphone sensor (as in MSM) is part of IPM and detects simultaneously the impact momentum independent of the ambient plasma. The impact momentum is different depending on whether the dust particle impacted on the covered (momentum of the debris cloud) or uncovered (momentum of dust particle only) part of the IPM. Further, a thin metallic probe with a -20V potential insulated from the spacecraft structure forms part of the impact plasma detector and monitors the saturation current of the secondary electrons emitted by impacts of cometary gas and dust particles. The response of this sensor will be used to assess the density of the plasma cloud which forms around the spacecraft during its critical passage through the inner coma.

The main objective of this system of dust impact detectors is to provide the dust-particle mass spectrum between 10^{-17} and 10^{-3} g.

2.6 Fast Ion Sensor (FIS)

This sensor measures the three-dimensional velocity distributions of solar wind ions, giving the flow speed and direction, temperature and density, and follows the development of the solar wind as it is thermalised, slowed-down and deflected. Ions streaming parallel to the relative velocity vector will not be measured as these are expected to have very high fluxes near the comet.

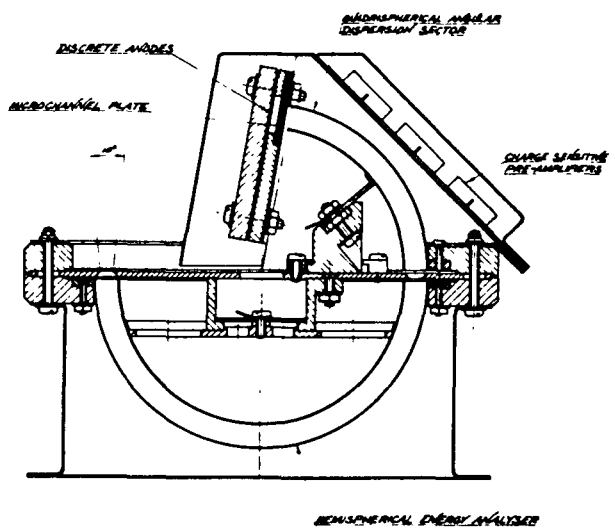

Figure 7 - The Fast Ion Sensor (FIS)

The sensor consists of a hemispherical plate electrostatic energy analyser with a subsequent quadrispherical sector (80^{0}) to disperse the trajectories according to the polar angle of incidence before they are registered by a microchannel plate with a series of 8 metal anodes behind it. The

energy band selected can be varied by changing the voltages on the plates of the energy analyser.

The experiment is operated in different modes depending on the angular width and the energy spread of the ion distribution.

2.7 Implanted Ion Sensor (IIS)

Some cometary neutrals may reach large distances from the nucleus before they are ionised and become 'implanted' in the solar wind. The task for the Implanted Ion Sensor is to search for these cometary ions. It combines an electro-

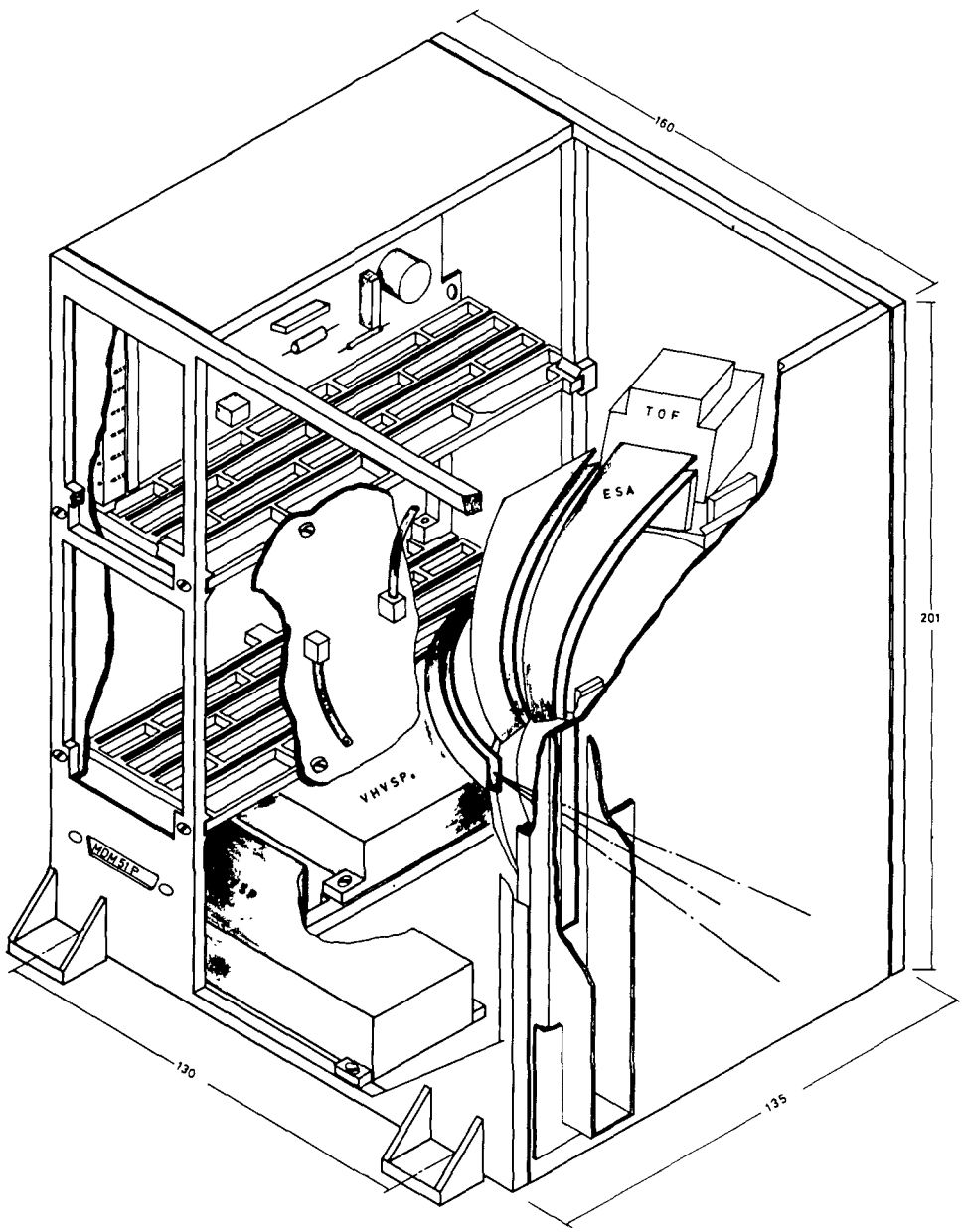

Figure 8 - The Implanted Ion Sensor (IIS) and electronics box. 3 of the 5 electrostatic analysers and 1 of the 5 time-of-flight tubes are shown

static analyser with a time-of-flight measurement. The quadrispherical electrostatic analyser selects positive ions of a given energy per charge E/Q, which are then accelerated by a potential difference, V, before the time T to travel a path length D is determined. By measuring these quantities the mass to charge ratio can be determined

$$\frac{M}{Q} = 2\,(V + \frac{E}{Q})\,\frac{T^2}{D^2}$$

Since cometary neutrals are ionised by charge exchange or photons the charge state is predominantly Q = 1, allowing the ion mass to be determined.

The instrument has a total of 5 electrostatic analysers each followed by a time-of-flight tube. The ions enter one of the electrostatic analysers depending on their incident elevation angle. As the ions leave the analyser they are accelerated before they enter the time-of-flight tube which is only 4 cm long. The 'start' signal is provided by secondary electrons generated by the ion passage through a thin carbon foil, the 'stop' signal by secondary electrons generated in the surface layer of a spherically-shaped aluminium absorber. In both cases the secondary electrons are accelerated by 1.5 kV and deflected towards a microchannel plate. In the '4D' mode the ions are sorted into 5 different mass groups in the range 1 - 40 amu, in the 'TOF' mode they are sorted into 256 groups depending on their time-of-flight.

2.8 Electron Electrostatic Analyser (EESA)

This sensor measures the pitch angle distributions of suprathermal electrons in the energy range 10eV - 30 keV. These measurements together with the FIS will define the solar wind plasma and its interaction with the comet. EESA is an electrostatic analyser which is hemispherical in shape but has the characteristics of a quadrispherical analyser. The particles enter through a circular opening in the centre of the hemisphere and are deflected through 90^{o} before they are detected by one of the 17 sections of a ring-shaped microchannel plate depending on their incident polar angle. Azimuthal resolution is provided by the spacecraft spin. The potential between the analyser plates is varied in 39 steps, providing a 10% energy resolution.

2.9 Positive Ion Cluster Composition Analyser (PICCA)

This sensor is intended for operation in the innermost part of the coma where the cometary ions are expected to be singly charged and to have negligible thermal velocities. In the spacecraft frame of reference these particles will flow strictly radially towards the spacecraft with a velocity of 68.7 km/s and their kinetic energy will range from 245 eV (10 amu) to 4.9 keV (200 amu). As the energy E and the charge Q of the ions are assumed to be known, an E/Q measurement directly translates into a mass measurement. Of particular interest are the

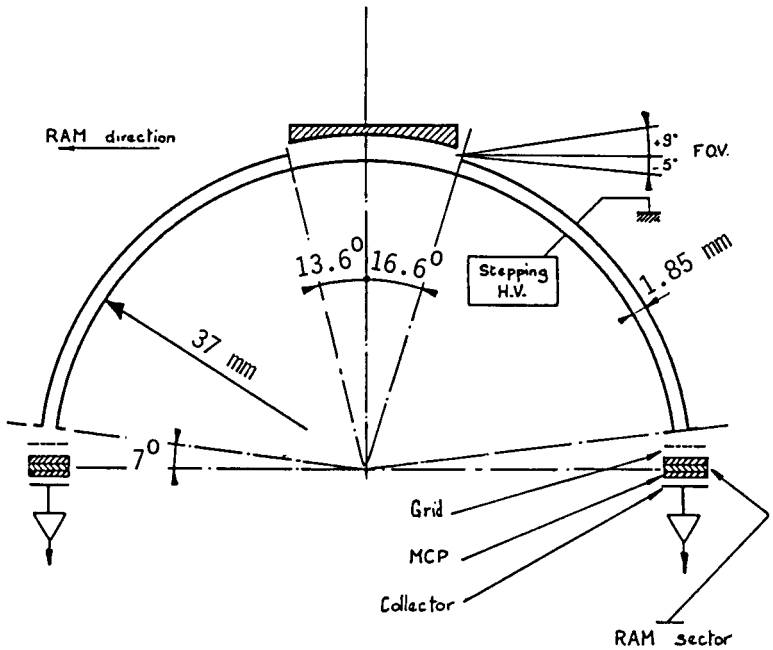

Figure 9 - The Electron Electrostatic Analyser (EESA). Although the analyser is hemispherical in shape the electrons only traverse a quadrisphere after entering through the top cap

clathrate hydrates (e.g. $CO \cdot 6\ H_2O$) which are formed when some of the more volatile species such as CO, CO_2, NH_3 are trapped in a cage of H_2O molecules. Once these clusters are ionised ($I^+ \cdot (H_2O)_m$) PICCA has the capability of detecting them because of its high mass range.

PICCA is a hemispherical electrostatic analyser with 2 channeltrons as detecting devices. By varying the potential between the top and bottom part of the aperture the particles will be deflected from the general flow direction and will enter the analyser according to their mass. To obtain a good and constant mass resolution the ions are decelerated before entering the electrostatic analyser. The hemispherical analyser itself is operated at 2 different fixed voltages corresponding to 2 mass ranges.

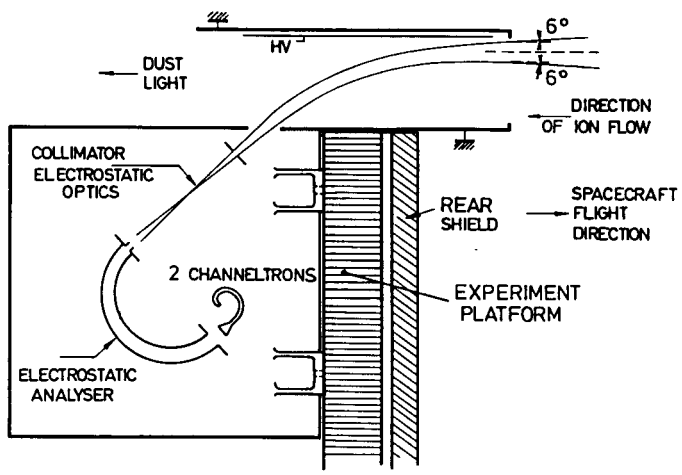

Figure 10 - The Positive Ion Cluster Composition Analyser (PICCA)

Table 7 Plasma Experiments Characteristics

FIS (ions)

energy range	10 eV - 20 keV						
FOV	5^0, azimuthally						
geometric factor	$\sim 10^{-2}$ cm^2 ster						
max. count rate	10^6/s						
detector	microchannel plate with 8 metal anodes						
	modes						
	Solar wind			HAR		FTR	
energy range	?						
energy resolution	$\Delta E/E$ = 6%			26%		52%	
time resolution	8 s			12 s		4 s	
azimuthal range	-22.5 to +22.5 (wrt Sun)			0 - 360^0		0 - 360^0	
azimuthal sectors	8	1		8	16	8	
elevation range	46 - 98^0	46 - 150^0		20 - 180^0	72 - 124^0	20 - 180^0	
elevation sectors	1	5		4	2	3	

IIS (ions)

energy range	100 eV - 70 keV		
energy resolution	$\Delta E/E$ = 10%		
mass range	1 - 40 amu in 5 groups		
geometric factor	$1.23 \cdot 10^{-4}$ E(keV) cm^2 ster keV		
max. count rate	$3 \cdot 10^4$/s		
background count rate	< 1/d		
azimuthal range	0 - 360^0		
elevation range	15 - 165^0		
time resolution	128 s		
FOV	12^0, azimuthally		
	modes		
	4D	TOF	
azimuthal sectors	16	1	
polar sectors	5	1	
mass groups	5	256 ("time" groups)	

EESA (electrons)

energy range	10 eV - 30 keV
energy resolution	$\Delta E/E$ = 10% (39 energy steps, 1 sweep takes 0.25 s)
FOV	360^0 x 14^0 (from -5^0 to $+9^0$ from ram direction)
elevation range/ resolution	360^0 / 14 sectors with 22.5^0, 2 sectors with 19.5^0 1 sector with 6^0 (centred around ram direction)
azimuth range/ resolution	360^0 / 22.5^0
time resolution	2 s
geometric factor	$7 \cdot 10^{-3}$ cm^2 ster
detector	circular ring microchannel plate with 17 sectors

PICCA (ions)

mass range/resolution	10 - 21 amu / ΔE = 10 eV, $\Delta m \approx 0.4$ amu 21 - 200 amu / ΔE = 25 eV, $\Delta m \approx 1$ amu
FOV	6^0 x 6^0
time resolution	2.25 s
dynamic range	$2 \cdot 10^{-4}$ - $2 \cdot 10^2$ cm^{-3}
acceptance area	0.1 cm^2
detector	2 channeltrons (1 fast, up to 10^7 counts/s 1 normal, up to 10^5 counts/s)

2.10 Energetic Particles Experiment (EPA)

The prime purpose of the Energetic Particles Experiment is to extend the range of the Giotto plasma analysers to higher energies. It will detect particles which are accelerated in the cometary environment from solar wind energies ($\sim$ 1 keV), and it will allow determination of the dust column density as the low energy solar particles are absorbed by the dust. Monitoring the energetic solar particle flux will also provide useful background information, in particular during times of a solar flare, to instruments using devices which are sensitive to these particles, such as channeltrons, channel plates and CCD.

This experiment consists of three identical very small telescopes, each with two solid state detectors. Two telescopes are mounted side by side at 45^{o}, a third one at 135^{o} from the relative velocity vector. This allows observations of field-aligned particle streaming for all inclinations of the magnetic field vector, in other words, together with the spacecraft spin, this allows 3-dimensional viewing of particle pitch angle distributions. Of the two telescopes mounted side by side one is covered by a thin foil, while the other is open. Low energy protons cannot penetrate the foil, therefore the covered telescope measures electrons only, while the open telescope measures protons and electrons. Neglecting statistical fluctuations the count rate difference then refers to protons only.

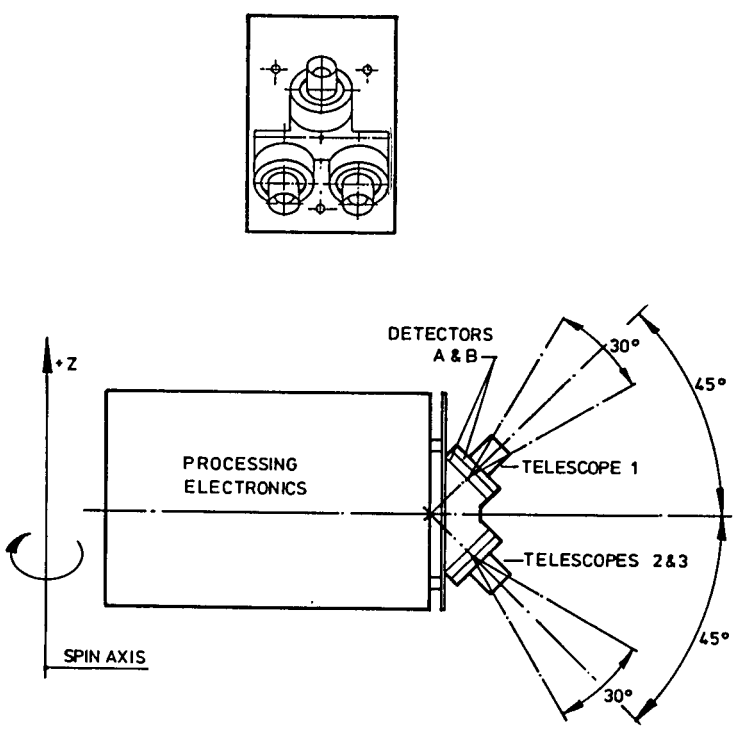

Figure 11 - The Energetic Particles Experiment (EPA)

The energy of the incoming charged particle is determined by measuring its energy loss in the solid state detectors in various channels and logic combinations (see Table 8). Particles of different species and energy ranges are identified using the dE/dx vs. E technique. The low energy threshold of 15 keV is essentially determined by the detector noise. It overlaps with the upper energy threshold of the Fast Ion Sensor (20 keV).

Table 8 Energetic Particles Experiment Characteristics

detectors	totally depleted surface barrier detectors, circular in shape		
		A	B
	area	0.384 cm^2	2.0 cm^2
	thickness	100 μ	200 μ
geometric factor	$8.2 \cdot 10^{-2}$ cm^2 ster per telescope		
FOV	30^o (full cone)		
azimuthal range/resolution	$360^o/45^o$ (8 sectors)		
temporal resolution	0.5 s		
elevation range	30^o - 60^o (telescopes 2 and 3) 120^o - 150^o (telescope 1)		
channel specification	energy range	species	detector threshold logic
telescope 1 (open)	15 - 30 keV	p e	$A_1 \cdot \overline{A_2} \cdot \overline{B_1}$
	30 - 60 keV	p e	$A_2 \cdot \overline{A_3} \cdot \overline{B_1}$
	60 - 140 keV	p e	$A_3 \cdot \overline{B_1} \cdot \overline{A_4}$
	0.14 - 3.4 MeV	p	$A_4 \cdot \overline{A_5} \cdot \overline{B_1}$
	4.7 - 20 MeV	p	$A_4 \cdot \overline{A_5} \cdot B_2$
	>20 MeV	p	$A_4 \cdot B_1 \cdot \overline{B_2} \cdot \overline{A_5}$
	3.5 -12.5 MeV	alpha	$A_5 \cdot \overline{B_1}$
	>180 keV	e	$A_1 \cdot \overline{A_4} \cdot B_1 \cdot \overline{B_2}$
telescope 2 (with foil)	15 - 30 keV	e	$A_1 \cdot \overline{A_2} \cdot \overline{B_1}$
	30 - 60 keV	e	$A_2 \cdot \overline{A_3} \cdot \overline{B_1}$
	60 - 140 keV	e	$A_3 \cdot \overline{B_1} \cdot \overline{A_4}$
	0.14 - 3.4 MeV	p	$A_4 \cdot \overline{B_1} \cdot \overline{A_5}$
telescope 3 (open)	15 - 30 keV	p e	$A_1 \cdot \overline{A_2} \cdot \overline{B_1}$
	30 - 60 keV	p e	$A_2 \cdot \overline{A_3} \cdot \overline{B_1}$
	60 - 140 keV	p e	$A_3 \cdot \overline{B_1} \cdot \overline{A_4}$
	0.14 - 3.4 MeV	p alpha	$A_4 \cdot \overline{B_1}$

During the encounter phase spectral and angular information concerning particle fluxes will be provided with high time resolution (0.5 s). During the cruise phase, approximately 30 min average particle flux measurements and angular information in one energy channel will be generally obtained. An experiment internal memory of 64 kbit ram will be used which allows up to 13 days of data storage.

2.11 Magnetometer (MAG)

The magnetic field is measured by a wide range (0.004 - 65536 nT) triaxial ringcore fluxgate magnetometer mounted on the antenna tripod where it is furthest from the spacecraft and also protected from dust impacts (see Fig. 14). The Giotto magnetometer is identical to the GSFC fluxgate magnetometers on Voyager and intended for flight on ISPM, apart from improved noise characteristics by use of different sensor core alloys.

The principle of the fluxgate magnetometer is as follows: Suppose in the simplest sensor arrangement a ferromagnetic core of soft magnetic material is periodically driven into saturation by a drive coil generating a periodic magnetic field strength of suitable wave shape at the drive frequency f_0. An additional sense coil around the core will then exhibit a distorted signal composed of frequency components at f_0 and odd harmonics. Addition of an ambient magnetic field component along the core axis will lead to the appearance of even harmonics. Generally, in fluxgate magnetometers the second harmonic is detected because its amplitude turns out to be proportional to the ambient field component parallel to the core or the sense coil axis. In order to obtain good linearity a feedback coil is generally added to compensate the ambient magnetic field in response to the output from the sense coil. In this case, the sense coil is essentially used for zero detection only.

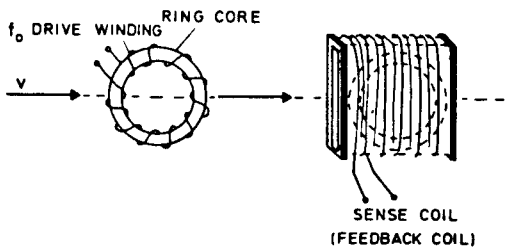

Figure 12 - The principle of the fluxgate magnetometer sensor (MAG)

The measurement of the ambient magnetic field is disturbed by the spacecraft field which generally has two sources: perm fields and induced fields due to magnetic materials, and stray fields due to varying electric currents. Because of their potential lack of stability magnetically soft materials are particularly disturbing for magnetic measurements. The same is true for stray fields. Major sources of contamination are: The antenna despin motor, the NMS and IMS magnets, the 3 HMC and the PIA motor, the HMC Invar, the antenna feed, the TWT's and the Latching Relays. Present estimates indicate a combined experiment/spacecraft field strength of $\sim$ 30 nT with $\sim$ 10% variability at the location of the outer sensor.

The magnetometer has two sensors, an outboard sensor located about 1.1 m above the upper face of the spacecraft body and an inboard sensor located about 0.5 m above it. From the difference in the readings of the two sensors the spacecraft field can be estimated and its contaminating effect on the ambient

field can be eliminated to some extent. The outboard sensor is triaxial (three orthogonal sensors for the measurement of the three components of the ambient magnetic field vector) while the inboard sensor is biaxial (1 ringcore with 2 pick-up coils for the measurement of two magnetic field components only). The available data rate allows transmission of 25.4 vectors/s in Formats 1 and 2, 8.8 vectors/s in Format 3 and 1.2 vectors/min in memory mode (assuming the experiment 16 kbyte memory is read out after 24 hours).

2.12 Optical Probe Experiment (OPE)

Observations of cosmic dust have traditionally been classified as either 'remote' (essentially optical) or 'in-situ' (mass spectrometers or impact detectors). Optical remote sensing results in a column brightness (integration

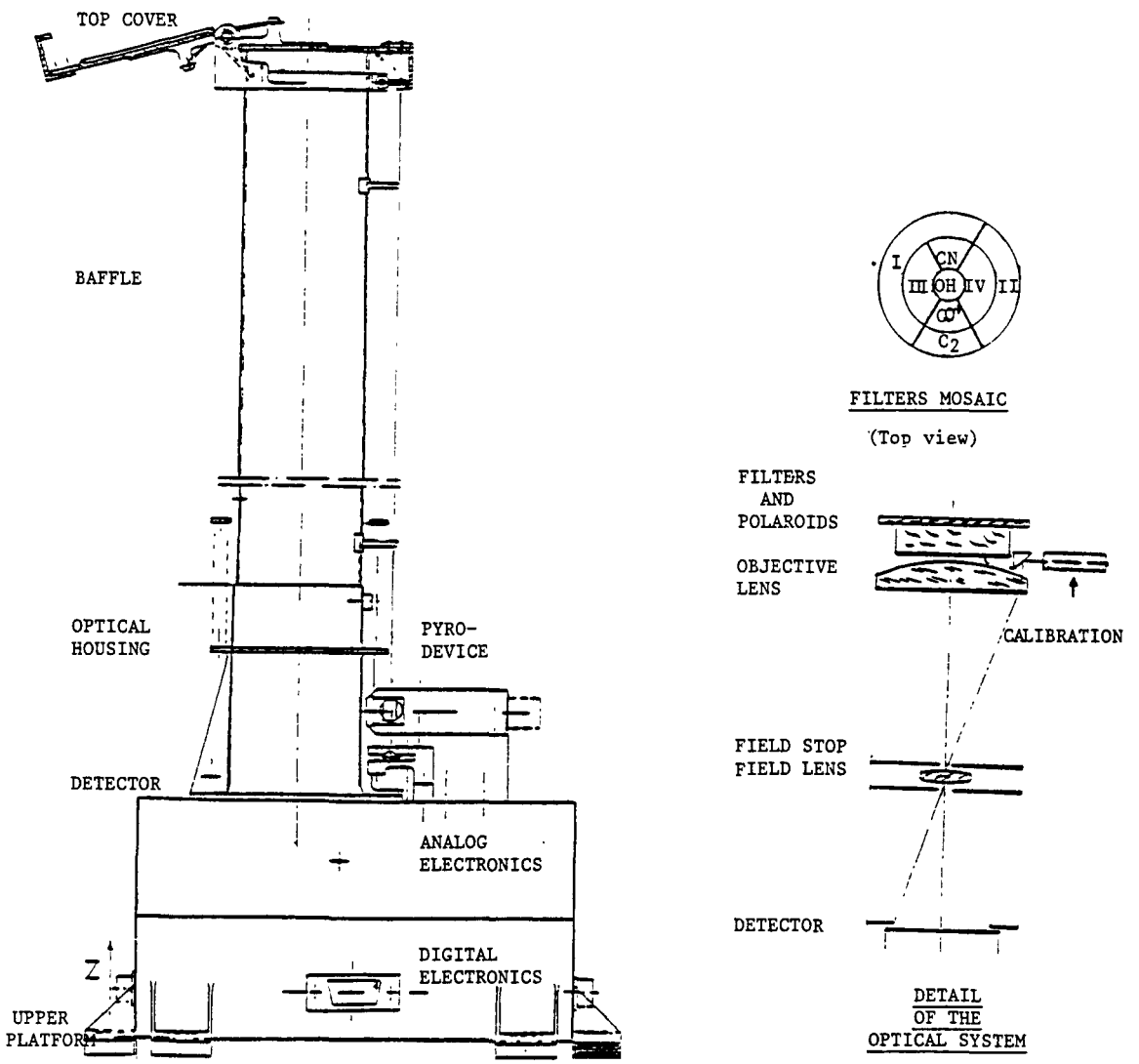

Figure 13 - The Optical Probe Experiment (OPE). Shown on the left is the experiment housing, shown on the right are details of the optical system

over the line of sight), interpretation of which is impossible without assumptions about both the spatial distribution of the dust grains and their scattering properties. In a cometary flyby a third type of observation, in-situ photopolarimetric observation - referred to as optical probing - is possible. For a photopolarimeter aimed tangentially to the spacecraft orbit, inversion of the brightness integral is rigorous and provides, without any assumptions, in-situ observation of the local spatial density of dust and gas and of the scattering properties of dust grains.

The requirement to observe tangentially offers two possibilities: forward or rearward, corresponding to a phase angle of 72.8^{o} or 107.2^{o}. Because of the less critical engineering demands (smaller baffle, no dust particle impacts) a rearward-looking instrument was chosen.

The photopolarimeter utilises a small refracting photometer with an objective lens of 24 mm diameter (18 mm effective), eight interference filters, two spectrally matching polaroid foils and a microchannel plate for spectral analysis. The rotation of the anlysers needed to determine the polarisation is provided by the spin of the spacecraft. One complete polarisation measurement is performed during half a spacecraft spin. The difference between successive line-of-sight measurements refers to the brightness and polarisation of a small volume of space only (a 'cylinder' of about 140 km in length and 7 km (corresponding to the instrument's 3^{o} field of view) in diameter).

The dust will be observed in four spectral bands which are free or almost free of gaseous emissions. Simultaneously, the discrete gaseous emissions of OH, CN, CO^{+} and C_2 will be observed.

Table 9 Optical Probe Experiment Characteristic

optics	objective lens Ø 24 mm (18 mm effective) field lens Ø 8 mm
FOV	3^{o} (full cone)
viewing direction	- 180^{o} (rearward, i.e. phase angle 107.2^{o} at encounter)
filters	continuum (dust) / discrete (gaseous emissions) 361 - 375 nm / OH 307.5 ± 40 nm 439 - 448 / CN 387 ± 20 565 - 585 / CO^{+} 426 ± 20 714 - 721 / C_2 514 ± 30 2 polaroid foils (UV, visible)
time resolution	0.5 s (2 s for polarization measurements)
sensitivity	S/N > 20 at < $2 \cdot 10^{5}$ km from the nucleus
detector	microchannel tube

2.13 Radio Science (GRS)

It is possible to determine the total electron content in Halley's ionosphere if two phase-locked (coherent) RF signals with different frequencies are transmitted and their phase difference

$$\Delta\phi = \phi_1 - \frac{f_S}{f_X}\phi_X = A \cdot f_S \left(\frac{1}{f_S^2} - \frac{1}{f_X^2}\right) \cdot I$$

is measured at the receiver. f_S = 2.3 GHz (S-band), f_X = 8.4 GHz (X-band), A is a constant of proportionality and $I = \int N_e \, ds$ is the total electron content between the spacecraft and the receiving ground station.

It is estimated that the cometary electron content is $\sim 3 \cdot 10^{16}$ m^{-2} while the interplanetary electron content is $\sim 10^{18}$ m^{-2} and the electron content in the Earth's ionosphere is $\sim 10^{17}$ m^{-2}. Evidently, the electron content of the comet is only a fraction of the total electron content. Therefore, the cometary electron content as measured during the encounter will appear as a small time variation of 10 - 15 min duration superimposed on the background total content which is relatively constant over this time period apart from variations in the Earth's ionosphere (diurnal variations, wave-like fluctuations, solar flare effects). It is therefore necessary to monitor the ionospheric electron content during the comet encounter.

Table 10 Giotto Scientific Payload (June 1982)

Experiment		Mass (kg)	Power (W)	Data Rate (bps) Format 1/2/3*			Principal Investigator	Main collaborating institutes (hardware)
Camera		11.48	12.2	20058		723	H U Keller MPI für Aeronomie, Lindau	Laboratoire de Physique Stellaire et Planétaire, Verrières-le-Buisson Institut d'Astrophysique, Liège Istituto di Astronomia, Padova DFVLR, Oberpfaffenhofen Ball Aerospace Systems Division, Boulder
Neutral Mass Spectrometer	M-analyser E-analyser	10.94	10.1	4156		–	D Krankowsky MPI für Kernphysik, Heidelberg	Physikalisches Institut, Universität Bonn Physikalisches Institut, University of Bern Laboratoire de Géophysique Externe, CNRS, Saint-Maur The University of Texas at Dallas
Ion Mass Spectrometer	High Energy Range Spectrometer High Intensity Spectrometer	8.76	9.5	3253		1084	H Balsiger Physikalisches Institut, University of Bern	MPI für Aeronomie, Lindau JPL, Pasadena Lockheed Palo Alto Research Laboratory
Dust Mass Spectrometer		10.00	11.6	2891	5782	–	J Kissel MPI für Kernphysik, Heidelberg	
Dust Impact Detector System	Meteoroid Shield Momentum Sensor Impact Plasma and Momentum Sensor Capacitor Impact Sensor	2.00	1.9	361	903	–	J A M McDonnell Space Sciences Laboratory, University of Kent, Canterbury	MPI für Kernphysik, Heidelberg ONERA/CERTS/DERTS, Toulouse ESA Space Science Department
Plasma Analysis 1	Fast Ion Sensor Implanted Ion Sensor	4.08	4.2	3975	1265	1355	A Johnstone Mullard Space Science Lab., Holmbury St. Mary	Istituto Plasma Spaziale, Frascati MPI für Aeronomie, Lindau
Plasma Analysis 2	Electron Electrostatic Analyser Positive Ion Cluster Composition Anal.	2.85	3.7	2530	1807	904	H Rème Centre d'Etude Spatiale des Rayonnements, Toulouse	MPI für Aeronomie, Lindau Space Sciences Laboratory, Berkeley
Energetic Particles		0.50	0.7	181			S M P McKenna-Lawlor, St. Patrick's College, Maynooth	Dublin Institute for Advanced Studies MPI für Aeronomie, Lindau
Magnetometer		1.25	1.2	1265		407	F M Neubauer Institut für Geophysik und Meteorologie, Braunschweig	Laboratory for Extraterrestrial Physics NASA/GSFC Istituto di Fisica, University of Rome
Optical Probe Experiment		1.1	1.2	723		–	A C Levasseur-Regourd, Service d'Aéronomie du CNRS, Verrières-le-Buisson	Laboratoire d'Astronomie Spatiale, Marseille Space Astronomy Laboratory, University of Florida, Gainesville
Total		52.96	56.3	39393		4654		

* Format 1: From t_o - 4 hrs until t_o - 1 hr
Format 2: From t_o - 1 hr until mission end
Format 3: During cruise and pre-encounter

3. THE SPACECRAFT

Figure 14 shows the Giotto spacecraft in cross-section. The spacecraft will be spin-stabilised, nominally at 15 rpm. During the comet encounter the spin axis will be aligned with the relative-velocity vector ('relative' means in the comet frame of reference), i.e. cometary particle streaming is from below in Figure 14.

At launch the spacecraft will weigh 950 kg, reducing to 512 kg when the solid-propellant kick motor has burnt out and the hydrazine has been used up for the various mid-course attitude and orbit-correction manoeuvres.

The spacecraft will be protected from hypervelocity dust-particle impacts by a dual-sheet bumper shield, composed of a thin front sheet and a thick rear sheet separated by 23 cm. Details of the bumper shield composition are given in Table 11. Two quadrispherical shell sectors close over the kick motor nozzle after firing to complete the front sheet of the bumper shield.

Table 11 Dust Shield

front sheet	0.1 mm white Aluminium Oxide 1 mm Aluminium
230 mm spacing	
rear sheet	7.5 mm Epoxy Kevlar 5 mm Polyurethane Foam 2 mm Epoxy Kevlar 15 mm MLI (Mylar) 40 mm Aluminium honeycomb structure (exp. platform)

The spacecraft has three equipment platforms: from top to bottom (Fig. 14), the 'upper' and the 'lower' platforms carrying spacecraft equipment boxes, and the 'experiment' platform mounted on top of the rear bumper shield (with a small separation). The sensors of the dust-impact detector system (DID) are mounted on the front bumper shield, the magnetometer sensor (MAG) is mounted on the carbon-fibre tripod as far away from the spacecraft magnetic field sources as possible, and the optical probe experiment (OPE) is mounted on the upper platform inside the spacecraft, looking rearward. All other experiment sensors and electronics boxes are mounted on the experiment platform (camera shown as example). The experiment sensors can protrude from the spacecraft side wall up to 17 cm to allow measurements in the undisturbed flow of cometary particles.

A solar-cell array will provide 190 W of power during the encounter, which is not quite sufficient when one of the two redundant X-band travelling-wave-tube amplifiers (TWTA's) (78 W), all other spacecraft subsystems (70 W), and all

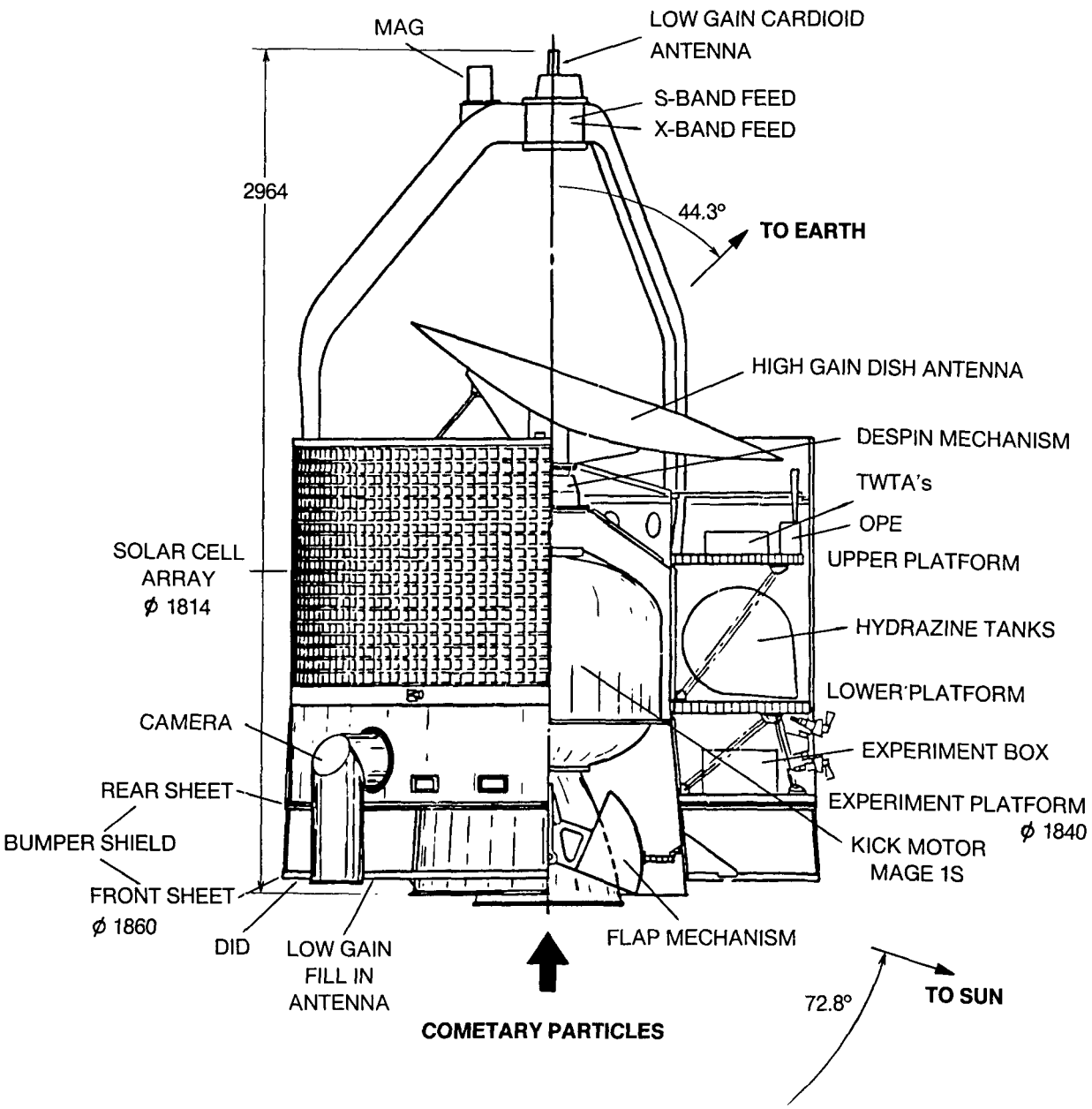

Figure 14 - The Giotto Spacecraft

experiments (56 W + 6 W margin) are switched on. Batteries are required in addition to the solar cells not only to bridge this gap, but also to provide full power during the last part of the encounter in case the solar cells' power output deteriorates due to dust-particle impacts.

The main spacecraft antenna is a high-gain dish antenna (HGA) with an effective reflector diameter of 1.47 m. The HGA can be operated in either S-band (2.1 GHz uplink, 2.3 GHz downlink) or X-band (8.4 GHz downlink). The HGA beam is inclined at 44.3° with respect to the spacecraft's spin axis and despun so that it points permanently at the Earth during the encounter. The pointing requirements in X-band are rather stringent: if the spacecraft spin axis is not well aligned with the spacecraft relative velocity vector or if the spacecraft attitude changes due to the impact of a large dust particle, the telemetry link to the ground receiving station may be lost (antenna gain decreases by 3 dB for 0.8° misalignment in X-band and 3° in S-band). For operations in the geostationary transfer orbit and near Earth, two low-gain antennas operating in S-band are used. They are located at either end of the spacecraft; a cardioid antenna at the upper end of the hollow carbon-fibre tripod, a fill-in antenna (microstrip patch) flush-mounted on the front bumper shield.

The X-band link budget shows that 40 kbps of scientific data can be achieved during the encounter including a 5 dB weather margin (rain at the receiving station). During cruise the spacecraft will be controlled from ESA's European Space Operations Centre (ESOC) in Darmstadt, Germany. For the Halley encounter, the Australian CSIRO Institute has offered the use of its 64 m antenna at Parkes, which is normally used for radio-astronomy. This antenna will be linked via a communications satellite to ESOC, where quick-look data, including the first images of the nucleus, will be available during the encounter.

4. THE MISSION

The Giotto mission is a fast flyby of comet Halley around midnight UT of 13 March 1986, near the comet's post-perihelion crossing of the ecliptic plane, about 1 month after the comet's perihelion passage. At this time the comet is most active. The baseline approach is a launch by Ariane in tandem with a geostationary spacecraft. The possibility of a pre-perihelion encounter was also considered, but analysis showed that it cannot be realised under the constraints of the geostationary transfer orbit imposed by the second passenger on Ariane.

During a 14-day nominal launch window in the first half of July 1985, Ariane will launch the two spacecraft into a geostationary transfer orbit, where their separation will take place. After some revolutions in this orbit, Giotto's on-board solid-propellant motor will be fired close to perigee to inject the space-

craft into its comet transfer trajectory. This heliocentric trajectory (Fig. 15) lies completely in the ecliptic plane and has a closest approach to the Sun of 0.7 AU. After a cruise phase of eight months Giotto will encounter Halley's comet on 13 March 1986. At that time Halley will be 0.89 AU away from the Sun and 0.97 AU away from the Earth. The phase angle to the Sun will be 107.2^{o} (Fig. 16), i.e. the spacecraft will approach the comet nucleus from 'behind', which is very favourable for spacecraft survival bearing in mind that large particles are injected predominantly into the sunward hemisphere. The flyby velocity will be 68.7 km/s.

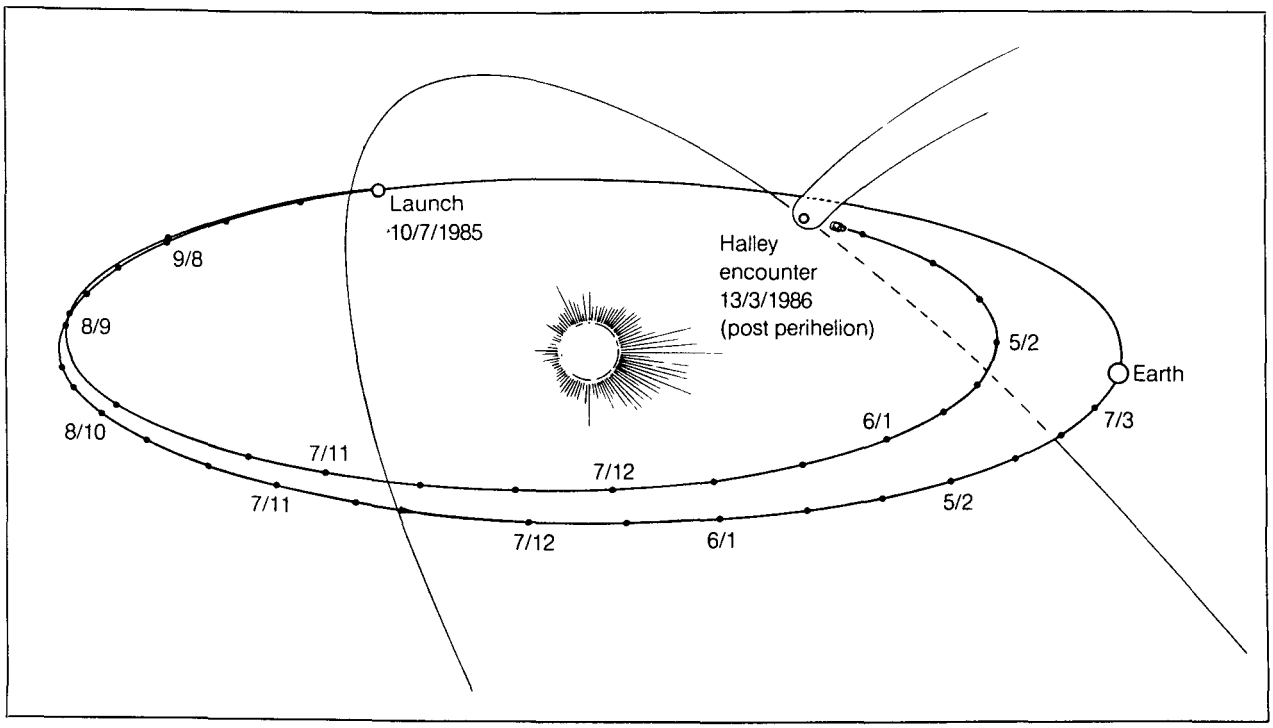

Figure 15 - Reference trajectory for Giotto from launch on 10 July 1985 to post-perihelion encounter with Halley on 13 March 1986. Halley's orbit is retrograde and inclined at 18^{o} with respect to the ecliptic.

During the transfer (or cruise) phase a number of mid-course manoeuvres will be required to target the spacecraft at the comet nucleus. Analysis indicates that with a ΔV capability of $\sim$ 180 m/s, the spacecraft can be delivered with an accuracy of 100 km at the time of encounter. The distance at which Giotto will pass the comet will probably be much larger because the position of the nucleus is not very well known. Although Halley's comet has been observed during 28 apparitions and although the comet will probably be "re-discovered" already in the winter 1982/83 the position of the nucleus within the coma at the time of the launch will only be known with an accuracy of 30 000 km. During the following eight months the knowledge on the position of the nucleus will be continuously

improved through extensive observations from Earth. It is expected that about 2 days before the encounter when the last orbit correction manoeuvre will have to be made the position will be known to within 500 - 1000 km. This residual uncertainty is largely due to the size of the nucleus which is too small to be seen from Earth and the effect of the non-gravitational forces due to asymmetric outgassing which is difficult to calculate. In order to obtain good quality images of the nucleus surface it would be desirable that Giotto passes the nucleus on the sunward side. Probably Giotto will be targetted at a point 500 km sunward from the nucleus which is a compromise between the conflicting requirements of spacecraft survival and imaging (further away) and plasma experiments and neutral mass spectrometer (as close as possible).

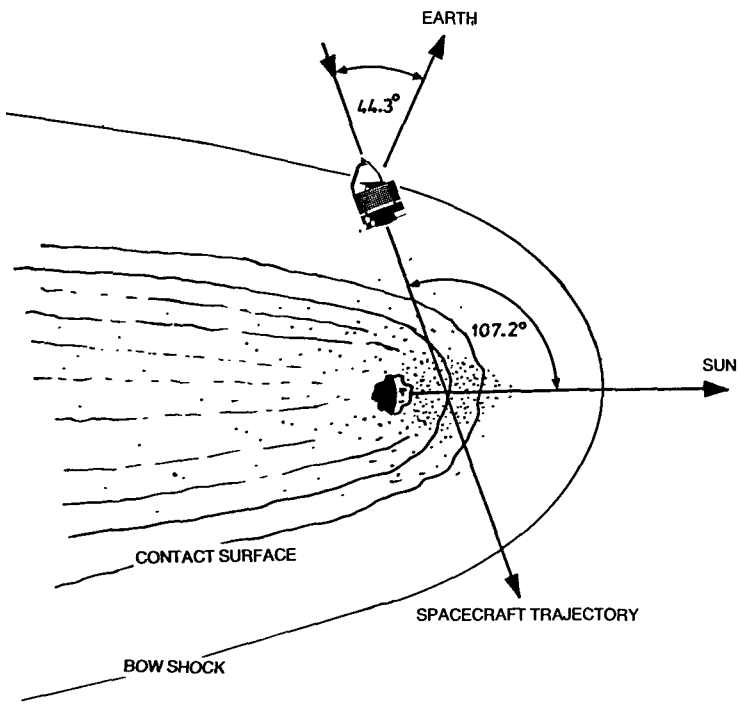

Figure 16 - Geometry at Halley encounter. The spacecraft will be targetted to pass the nucleus on the sunward side. A bow shock is expected at ∿ 10^5 km, a contact surface at ∿ 10^3 km from the nucleus

At about 4 hours before the time of closest approach (t_0) the scientific instruments will be switched on. Initially, only a few 'events' will be registered, but the rate of events will rise quickly (quadratically). The first impacts of dust particles are expected at t_0 - 1 hour. Therefore, for the first three hours the two dust experiments will operate at a reduced data rate (Table 10, Format 1) allowing the plasma experiments a higher data rate in the turbulent transition zone between the solar wind and the cometary 'ionosphere'. The most important measurements will be made in the last minutes and seconds. The camera will start to resolve nucleus surface features from about 30 000 km

(t_o - 10 min) onwards, the contact surface which separates the cometary ions from the turbulent transition region is expected at about 1000 km (t_o - 15 sec) and some rare parent molecules having low densities and short lifetimes may only be detectable inside 1000 km. In view of the potential hazard posed to the spacecraft by impacting cometary dust, the data will be transmitted to Earth in real time. No spacecraft memory is provided. The mission nominally ends at t_o because spacecraft survival is unlikely beyond this point. The duration of the science data take is also limited by spacecraft battery capacity and the availability of ground receiving stations.

The Australian Parkes antenna will be available for three periods of five 8-hour passes each during the cruise phase, at approximately 100, 190 and 220 days after launch and during five 8-hour passes on five consecutive days immediately before and during the encounter. During these times data will be transmitted at 40 kbps. In addition, there is the possibility to transmit science data at a low rate (4.6 kbps; see Table 10, Format 3) during cruise at intervals dictated by operational contraints (approximately once per week).

The NASA DSN 64 m station at Tidbinbilla, Australia will be used as a hot back-up during the encounter. For the 24 hours preceding the encounter the NASA 34 m network will be used allowing data transmission in Format 3 to bridge the gap between the last two Parkes passes providing continuous coverage for 32 hours before and during the encounter.

5. ENVIRONMENTAL EFFECTS

The particular comet environment, in combination with the high flyby velocity, leads to problems never before encountered on space flights. As the spacecraft approaches the nucleus, cometary neutrals, ions and dust particles will impact on the spacecraft with a velocity of 68 km/s. Dust particles with masses $\gtrsim 10^{-6}$ g impacting at these velocities can easily penetrate the spacecraft structure. Each time, a cloud of debris would be formed inside the spacecraft and would impact with high velocity on spacecraft components leading to their destruction. Presently discussed dust models for Halley at 0.9 AU post-perihelion predict that the first of these large dust particles will be encountered long before the spacecraft comes close to the nucleus. Figure 17 shows a dust particle believed to be of cometary origin. Particles of this type are collected in the Earth's stratosphere by high flying aircraft.

At 68 km/s the impact energy is so enormous that the dust particles are completely vaporised and even partly ionised, the degree of ionisation depending on the particle's mass. Also, the cometary neutrals and ions impacting on the spacecraft cause emission of secondary ions. It is estimated that one ion-

electron pair is produced by each neutral or ion impacting on aluminium. This impact-generated plasma causes a space-charge cloud in front of the spacecraft and a spacecraft potential, and presents a serious background problem for cometary plasma experiments.

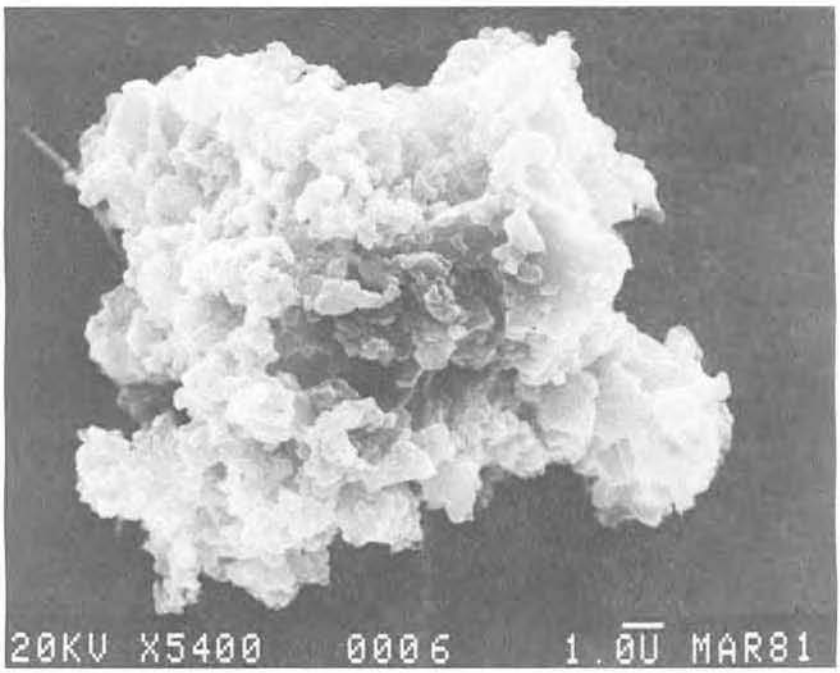

Figure 17 - Typical example of a dust particle collected by a U-2 aircraft in the Earth's stratosphere. It is believed that these particles are of interplanetary origin being released earlier from a comet. The size of this particle is 0.016 mm. (courtesy D. Brownlee)

Protection of the spacecraft against dust particles of at least 0.1 g is mandatory to ensure its survival until it comes within a few hundred kilometres of the nucleus, where the best images and the most valuable scientific data will be obtained. A single sheet of aluminium would have to be more than 8 cm thick to provide protection against 0.1 g particles and would weigh more than 600 kg, which is prohibitive. An ideal and in fact the only solution to the problem is a 'dual-sheet bumper shield', consisting of a thin front sheet and a thick rear sheet with a large space between. Upon impact on the front sheet, the dust particle is completely vaporised, even if the front sheet is very thin. The vapour cloud expands into the empty space between the two sheets and impacts on the rear sheet, where its impact energy is distributed over a large area.

Particles above 1 mg in mass cannot be accelerated much above 10 km/s in Earth laboratories, therefore hypervelocity impact phenomena at 68 km/s can only be studied by computer simulation. (For Giotto the explicit Lagrangian finite differences code has been used.) Details of the shield are given in Table 11. Equipped with this shield, Giotto has a good chance of surviving until within a

few hundred kilometres of the nucleus. However, as soon as Giotto enters the sunward hemisphere, where most of the large dust particles are expected, its survival becomes doubtful.

To improve the probability of spacecraft survival by using a thicker rear sheet would not help because dust particles above a certain mass impacting on the edge of the shield will cause the spacecraft's attitude to change. Anything more than a 1^{o} change would result in a loss of the telecommunications link, which could not be recovered quickly.

The calculations show that a major attitude change ($\gtrsim 1^{o}$) can occur following the impact of a large dust particle ($\gtrsim 0.1$ g). This result in combination with the nominal dust model which predicts a high probability of such impacts within 1000 km from the nucleus, leads to the conclusion that the Giotto mission will probably end at that distance due to loss of the telecommunications link.

The adverse effects of the impact-generated plasma around the spacecraft have been quantified using present best estimates for the Halley gas production rate. The calculations show that a positive spacecraft potential of no more than a few tens of volts and a slightly higher potential in the space-charge cloud in front of the spacecraft can be expected. In the innermost part of the coma the density of the impact-generated plasma is several orders of magnitude higher than that of the cometary plasma. The adverse effects on detector background, however, will be limited because the highest densities of impact-generated plasma will be above the front sheet and not at the location of the plasma sensors, and secondly the impact-generated ions can be distinguished from the cometary ions by their distinctly different velocity distributions (in the spacecraft frame of reference the distribution of cometary ions will be centred at 68 km/s, while the distribution of the impact-generated ions will be at rest).

Mission planning, spacecraft and experiment design depend to a large extent on educated guesses on the cometary environment and its effects on the spacecraft and the experiments. This has led to the formation of three working groups:

i) Halley Environment

This working group is deriving model parameters for Halley (Table 12), from the observations during previous apparitions, from analogy with other comets, and from theory. From these model parameters a dust and gas model for Halley is derived which is updated once or twice per year as new information becomes available.

ii) Plasma

This working group is mainly investigating the effects of the impact-generated plasma around the spacecraft. It also provides a forum for discussion

TABLE 12 Model Parameters for P/Halley (April 1982)

Comet brightness	$m_1 = H_0 + 2.5n \log r + 5 \log \Delta$
	pre-perihelion: $H_0 = 5.47$, $n = 4.44$ — *post-perihelion*: $H_0 = 4.94$, $n = 3.52$ for $r < 1$ AU, $n = 3.07$ for $r \geq 1$ AU
Nucleus: radius	$R_N = 2.2$ km
mean bulk density	$\rho_N = 1$ g cm^{-3}
surface temperature	$T_N = 185$ K
albedo	$\bar{p}_N = 0.1$
shape	spherical
rotation period	10 h, direct sense
rotation axis	perpendicular to orbit plane
Composition of the volatile component	83.4% H_2O 16.6% all other molecules with mean molecular mass 44 amu
Resonance fluorescence efficiency	$R = 2 \times 10^{-55}$ m^2 s
Mean heat of sublimation	$L = 8 \times 10^{-20}$ J/molecule (corresponding to H_2O)
Ratio of specific heats	$\gamma = 1.33$
Ratio of dust to gas production rates by mass	$\mu = 0.5$
Gas momentum transfer efficiency	$\varepsilon = 1$
Radiation pressure efficiency	$Q_{pr} = 1$
Dust size distribution	Sekanina (a) as described in Reinhard (1979)
Dust bulk density	$\rho = 0.8 + 5 \cdot 10^{-6} \cdot a^{-1.2}$ g cm^{-3}
At 0.9 AU post-perihelion	
Total gas production rate	$Q_g = 2.6 \times 10^{29}$ molecules s^{-1}
Gas molecule lifetime	$\tau_g = 1.6 \times 10^4$ s (corresponding to H_2O)
Other useful parameters derived from the above set	
Nucleus mass	$M = \frac{4\pi}{3} R_N^3 \rho_N = 4.5 \times 10^{16}$ g
Escape velocity	$(\frac{2GM}{R})^{\frac{1}{2}} = 1.65$ m s^{-1}
Gas terminal velocity	$V_g = 1.8 (\frac{8KT}{\pi m})^{\frac{1}{2}} = 754$ m s^{-1}
Mean molecular mass	$0.834 \times 18 + 0.166 \times 44 = 22.3$ amu
At 0.9 AU post-perihelion	
Total gas production rate	$M_g = 9.6 \times 10^6$ g s^{-1}
Total dust production rate	$M_d = \mu M_g = 4.8 \times 10^6$ g s^{-1}
Variation of the density of gas molecules with distance r from the nucleus	$n_g(r) = \frac{Q_g}{4\pi r^2 V_g} \exp(-\frac{r}{\tau_g V_g})$

between the plasma experimenters participating in the three missions to Halley (Giotto, Venera-Halley, Planet-A) and for studies of the various plasma physical processes resulting from the solar wind/comet interaction.

iii) Mission Optimisation and Spacecraft Navigation

Since the Halley nucleus is too small to be seen from Earth its position within the coma can only be estimated within several hundred kilometres. Predict-

ing its position which is required for Giotto targetting is only possible through an extensive observation programme of Halley during its next apparition and modelling of the non-gravitational forces. An elegant solution for improving the targetting accuracy would be to use the first spacecraft that encounters Halley (Venera-Halley 1) as a path-finder for the following spacecraft (Giotto). The task of the Mission Optimisation and Spacecraft Navigation Working Group is to investigate this and other possibilities to target Giotto as closely as possible to a predetermined optimum flyby point. In addition, the Working Group tries to enhance the science return of all three cometary missions by stimulating cooperation in sequencing the experiment-active times or exchange of real-time information on cometary behaviour (location of bow shock, dust envelope, etc.).

ACKNOWLEDGEMENT

The helpfulness of the Principal Investigators on Giotto and of the Project Team to provide drawings and data is gratefully acknowledged.

DISCUSSION

A. Danks: Is the resolution of the Mass Spectrometer sufficient to resolve the expected isotopes, e.g. H/D, $^{12}C/^{13}C$, $^{14}N/^{15}N$, $^{16}O/^{17}O/^{18}O$?

R. Reinhard: All three mass spectrometers intend to measure isotopic ratios. The Ion Mass Spectrometer (HERS as well as HIS) has a mass resolution $M/\Delta M > 20$ at $\sim$ 20 amu/q, the dust mass spectrometer has a mass resolution $m/\Delta m = 200$, the neutral mass spectrometer (M-Analyzer) has an average mass resolution of 0.25 amu over the mass range of 1 to 36 amu. Whether you can or cannot measure a specific isotopic ratio will depend, of course, largely on the relative abundances. For the dust mass spectrometer the isotopic ratios $^{6}Li/^{7}Li$, $^{10}B/^{11}B$, $^{12}C/^{13}C$ are of particular importance, as it may be possible to infer the probable age and origin of the comet. However, the carbon isotopic measurement may be masked by the presence of ^{12}CH.

H. Fechtig: Concerning masking of ^{13}C by ^{12}CH: due to the high impact velocity of 70km/sec the dust impacts produce temperatures of 10^4 to 10^5K. At these high temperatures this particular masking on mass 13 most probably will disappear.

A. Danks: Will the filters flown in the photopolarimeter be available for ground based observers?

A.C. Levasseur-Regourd: For Hope/Giotto instrument, 4 channels almost free of gaseous emissions and having bandwidths as large as possible have been chosen for studying the continuum emission: 362-375nm, 439-448nm, 565-585nm and

714-721 nm. In addition, 4 gaseous species will be studied: OH 307.5 nm, CN 387 nm, CO^+ 426 nm, C_2 514 nm. It would be of great interest to have ground based observations made at the same wavelengths. Our filters are built in the LAS (Marseille) and detailed information is available. However, it should be remarked that the continuum to gas emission ratios in ground based and in-situ measurements are quite different and require specific filters.

C. Cosmovici: Which is the situation of the Radio Science Experiment?

R. Reinhard: Giotto radio science experiment was strongly recommended by the selection committee. However, as Giotto is a low cost project, it was agreed that a final selection should only be made when the spacecraft TT & C subsystem and the ground segment were fully defined which was expected to be done at the end of Phase B. During that time a low level dialogue should be maintained between the Project and the two teams of proposers. This dialogue in fact took place in several meetings in 1981, a final decision is now expected at the next meeting which is scheduled to take place on 7 May 1982. I would like to add that Giotto radio science would be very valuable for the Giotto mission in that it would complement the presently accepted payload towards lower electron energies and I hope that the final decision will be positive.

THE USE OF GROUND BASED OBSERVATIONS OF HALLEY'S COMET IN THE GIOTTO NAVIGATION

Martin Hechler and Friedhelm Hechler
European Space Operations Centre, ESA
Darmstadt, West Germany

Abstract

The GIOTTO spacecraft probably cannot make use of its on-board camera for targetting purposes. Therefore the spacecraft navigation has to rely on information on the Comet position derived from earth based astrometric measurements.

It is planned to gather the data in the frame of the Comet Halley Watch and to execute the cometary orbit determination at JPL and at ESOC.

1. Introduction

The GIOTTO spacecraft will be launched in the first half of July 1985 from Kourou. ARIANE will launch two spacecraft into a geostationary transfer orbit, from which GIOTTO will depart after about 2 days by firing its solid boost motor close to perigee. It will enter into an excess hyperbola and will leave the sphere of influence of the earth about 3 days later. After approximately 8 months interplanetary cruise phase it will encounter Comet Halley at midnight on March 13/14th 1986. In the last 4 hours before closest approach with the Comet scientific data will be transmitted at a rate of 40 kilobits per second. Survival of the probe after closest approach is not envisaged.

The mission objective is to obtain in situ measurements from the cometary environment. Therefore the objective of spacecraft navigation is to

Proceedings of the ESO Workshop on "The Need for Coordinated Ground-based Observations of Halley's Comet", Paris, 29 – 30 April 1982.

accuracy of such measurements without reference directions in the image.

Presently it is unsure whether the GIOTTO mission can make use of information on the target position which will be obtained from the Soviet Venera spacecraft arriving at the comet a few days before GIOTTO. Such information could essentially improve the GIOTTO targetting.

2. Midcourse Navigation

The overall system of orbit determination and orbit manoeuvres we call Navigation. For the GIOTTO mission the comet ephemeris determination is an intrinsic part of the navigation.

Position and velocity of the spacecraft and the comet will never deviate far from those obtained along the nominal trajectory which is selected at launch. The motions can be linearized relative to this reference trajectory and for simple representation position and velocity deviations of spacecraft and comet are combined to an n=12 dimensional state vector which may be extended by further parameters in the estimation process.

We distinguish between the following random variables:

$$(1) \qquad \underline{x} \;:\; \text{actual state deviation}$$
$$\underline{\hat{x}} \;:\; \text{estimated state deviation}$$

The actual state deviation $\underline{x}$ cannot be known on ground, therefore manoeuvre calculations will be based on $\underline{\hat{x}}$.

In the linearized theory the random variables will remain Gaussian and they are fully described by the evolution of their means and covariance. $\underline{x}$ and $\underline{x} - \underline{\hat{x}}$ have zero mean by definition of the reference orbit and by using an unbiased estimator.

deliver the spacecraft as precisely as possible to a fly by region which has been selected such that the overall scientific return will be optimized. This targetting will also take into account the dust hazard.

To target the spacecraft at its fly by trajectory a series of orbit correction manoeuvres will be required. First the perigee injection manoeuvre of 1400 m/s has a considerable error in size and direction which is planned to be corrected within two days as soon as the actual trajectory has been determined with sufficient accuracy. Later in the cruise unpredictable dynamical effects acting on the spacecraft, e.g. inaccuracies of the radiation pressure modelling or fuel leakage, have to be compensated for by correction manoeuvres. Other retargetting manoeuvres are required to take into account the improved knowledge of the target position at encounter time.

In fact, the major contribution to the targetting error is introduced by the cometary position uncertainty. The knowledge of the cometary ephemeris will improve in November/December 1985 from earth based observations during this time of close approach to the earth.

Therefore a correction manoeuvre will retarget the spacecraft trajectory towards an updated predicted encounter point which will deviate from the point which was used as best estimate at the time of launch window calculations in July 85.

Important for spacecraft targetting will be those observations of the comet which are obtained after perihelion passage. As the comet will be recovered from earth only a few days before encounter, a fast and reliable processing of astrometric observation data will be essential. They probably provide the only source of information on stochastic effects on the cometary motion during perihelion passage.

An optimum means for such terminal navigation would be the use of direction measurements of the comet as seen from the spacecraft (on board guidance) because it would link the spacecraft trajectory directly to the target trajectory without any transformation errors. Unfortunately the scientific camera on the dual spin spacecraft will not be capable of resolving reference stars in the field of view in the background of the comet. The attitude motion of the spinning spacecraft will not admit a sufficient

The dynamics of the system, the measurements and the orbit corrections can be described by a set of linear equations between state vectors at discrete times $\{t_i\}$.

State propagation:

$$(2) \qquad \underline{x}_i = \Phi_i^{i-1} \underline{x}_{i-1} + \underline{w}_i$$

measurements:

$$(3) \qquad \underline{z}_i = H_i \underline{x}_i + \underline{v}_i$$

manoeuvres:

$$(4) \qquad \underline{x}_i^+ = \underline{x}_i^- + \Lambda_i \bar{\underline{x}}_i + \underline{n}_i$$

where:

Φ_i^{i-1} is the state transition matrix between time t_{i-1} and time t_i,

H_i are the measurement partials at t_i,

Λ_i is the guidance matrix which is explained later,

and $\underline{v}_i$, $\underline{w}_i$, $\underline{n}_i$ are properly chosen noise terms (measurement noise, dynamical system noise, manoeuvre errors).

The measurements may be range or range rate measurements of the spacecraft or directional measurements of the comet from the earth or from the spacecraft.

The Guidance Matrix

In the linear system the calculated correction manoeuvre $\Delta\underline{v}_i$ at time t_i is a linear function of the estimated state $\bar{\underline{x}} = \begin{pmatrix} \bar{\underline{x}}^P \\ \bar{\underline{x}}^C \end{pmatrix}$

The estimated miss vector from the preselected encounter point at time t_F is

$$(5) \qquad \Delta\underline{\tilde{r}} = \underline{\tilde{r}}_p - \underline{\tilde{r}}_c$$

where $\underline{\tilde{r}}_p$ and $\underline{\tilde{r}}_c$ are the position deviations of probe and comet respectively predicted from the current state estimate. If the state transition matrix from time t_i to time t_F is decomposed into independent 6 x 6 matrices of probe and comet and the corresponding 3 x 3 blocks referring to positions and velocities

$$(6) \qquad \Phi^P = \begin{bmatrix} \Phi_1^P & \Phi_2^P \\ \Phi_3^P & \Phi_4^P \end{bmatrix}, \quad \Phi^C = \begin{bmatrix} \Phi_1^C & \Phi_2^C \\ \Phi_3^C & \Phi_4^C \end{bmatrix}$$

then

$$(7) \qquad \Delta\underline{\tilde{r}} = \begin{bmatrix} \Phi_1^P & \Phi_2^P \end{bmatrix} \underline{\tilde{x}}^P - \begin{bmatrix} \Phi_1^C & \Phi_2^C \end{bmatrix} \underline{\tilde{x}}^C .$$

This predicted miss vector has to be compensated by a velocity increment

$$(8) \qquad -\Delta\underline{\tilde{r}} = \Phi_2^P \cdot \Delta\underline{v}$$

If the last two equations are solved for $\Delta\underline{v}$ the guidance matrix is defined as

$$(9) \qquad \Lambda = J \left(\Phi_2^P\right)^{-1} \cdot \left[-\Phi_1^P, -\Phi_2^P, \Phi_1^C, \Phi_2^C\right] ,$$

where J is a n x 3 matrix which carries the $\Delta\underline{v}$ into the probe velocity part of the state vector.

These notations lead to a uniform Kalman-type algorithm for covariance analysis and propellant estimation.

The orbit correction manoeuvres correlate the state of the spacecraft with the state of the comet. The comet ephemeris estimation process can be treated separately if on board observations are not involved, but it has to be taken into account in any covariance analysis for the spacecraft if manoeuvres are included.

3. The use of Astrometric Data

Without on board guidance the GIOTTO spacecraft delivery error is dominated by the uncertainty of the position of Halley's Comet or - more precisely - the uncertainty in the position of its nucleus as it is predicted from earth based observations. This prediction is uncertain mainly for three reasons

- the errors in the optical observations;
- the imprecisely known location of the nucleus in the visible dust cloud;
- the cometary specific force modelling problem.

As regards the first two problems ESA relies on the provision of sufficiently dense optical observations from various observatories which are coordinated in the frame of the Comet Halley watch by the astrometry discipline specialist. The requirements on this observations system from the space mission are more stringent than those usually imposed by the observing scientist. A consistent and fast evaluation of the photographic plates must be guaranteed in particular towards the end of the mission. An early recovery of the comet after its perihelion passage is essential to increase the time interval for data acquisition and data processing before the encounter date.

At some other time intervals e.g. in November 1985, an intensive observation campaign is required.

The data are planned to be reduced to a joint reference system by the observers and transmitted in real time (= as fast as possible) to both the centres at which the orbit determination is going to be performed, namely to the Jet Propulsion Laboratory (JPL) at Pasadena, and to the European Space Operations Centre (ESOC) at Darmstadt. Operational reliability will be improved by a link between ESOC and JPL.

The orbit determination system is being developed in collaboration by JPL and ESOC (ref.[4]). The main concern of the orbit determination is with above error source no. 3, namely the modelling of non-gravitational accelerations and the determination of parameters in the model such that a minimum variance prediction at the encounter date is obtained.

The non-gravitational forces affecting the motion of the comet are generally agreed to be caused by a rocket-like thrust impacted upon the comet's nucleus when the nuclear ice vaporizes in the sun's neighbourhood (Marsden, Sekanina, Yeomans). These forces are mainly observable through their secular effect on the orbital period of revolution of the comet; they lengthen it by about 4 days in 75 years. Therefore processing of observations over long orbital arcs including those of the 1909 -1911 apparition of Halley's comet is mandatory (see also [2]).

Different models will be fitted to the data of previous apparitions of the comet in order to assess the quality of various non-gravitational force models (see also [3]), in particular their capability for orbit prediction. However, each model tested will have to reflect the expected physical process of the comet's activity. Consequently the orbit determination software has been separated into a Comet Model Analysis Program and a Comet Operational Program which finally performs the refined parameter estimation and predicts the most likely target miss vector together with its uncertainty regions. The bar chart (Fig. 1) summarizes the data and task flow in the above software.

The first error source, the optical observation errors, naturally will be a subject for the observers. The coordinating function of the Halley Watch could establish a refined catalogue of background stars along the path of the comet and organize simultaneous observation of the comet from different observatories. Common standards for data reduction and reference system transformations will be established. A transfer of information on the character of the remaining errors into the orbit determination processes would be appreciated.

The problem of the location of the cometary nucleus within the observed gas cloud has to be a joint effort between observers, and the Comet Halley Watch and the orbit determination centres. The problem can only be partially treated within the orbit determination system. A standardized approach in resolving a certain point in the gas cloud, e.g. a definition of the 'centre of light' is required. Based on this definition the location displacement of the nucleus can be introduced into the observation models and a bias can be removed from the observation noise. Again a consistent physical model foundation will have to be maintained.

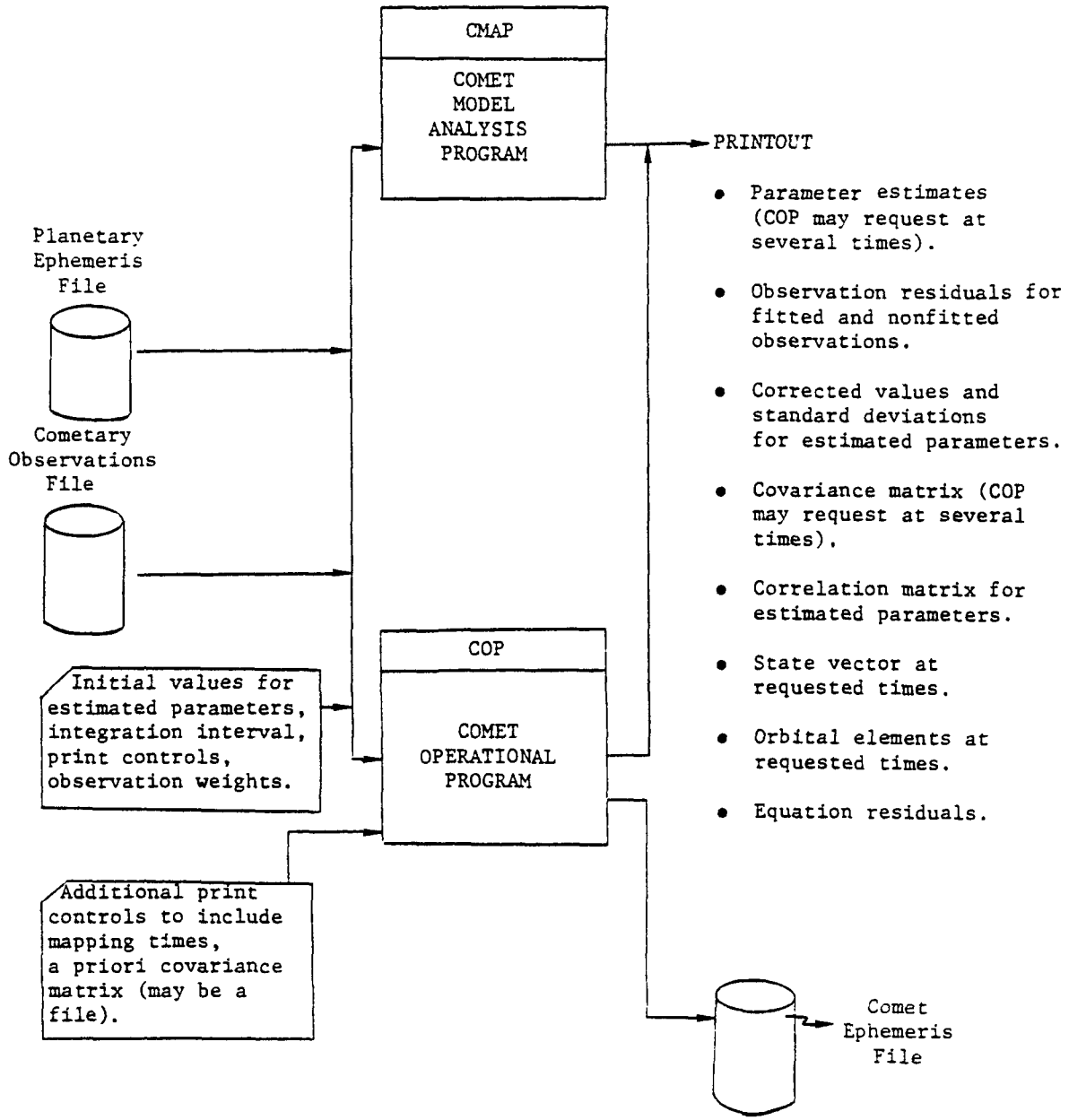

FIGURE 1. COMET MODEL ANALYSIS PROGRAM AND COMET OPERATIONAL PROGRAM

In this area a feedback from the orbit determination centres to the observers might be useful, provision of addition information on the light distribution may improve the model estimates.

4. Other Navigational Information derived from Ground Based Observations

Other observation data may directly support the modelling of the outgasing effect, e.g. if the spin axis and the spin rate of the comet can be well determined from earth the observable secular effect on the cometary orbit can be correlated with the badly observable accelerations transverse to the motion, which will improve the prediction capability of the algorithms.

The occasion of special events on the comet, like big gas bursts etc. should be communicated to the orbit determination centres as well.

Another type of information which has an indirect effect on spacecraft navigation is that which influences the dust model around the comet. The targetting strategy will be a function of the dust model, therefore it should be envisaged to organise a real time flow of information on this subject, similar to that on astrometric data within the Comet Halley Watch.

5. Conclusions

- All cometary missions to some extent depend on ground based observations, GIOTTO in particular.

- Operational data processing and communication has to be established by the Halley Watch between the spacecraft control centres and prime observers who have assumed an obligation to provide standardised astrometric observations on a coordinated schedule.

- An early recovery of the comet after perihelion passage is particularly important for the spacecraft navigation.

- Additional exchange of information on the observation errors and on the location of the nucleus in the Coma of the Comet would support the modelling of the cometary motion.

References

1 M. Hechler and F. Hechler, Midcourse Navigation for the European Comet Halley Mission, Proc. Int. Symp. Spacecraft Flight Dynamics, Darmstadt, May 1981 (ESA SP-160).

2 Yeomans, D.K., Comet Halley - The Orbital Motion, The Astronomical Journal, Vol. 82, No. 6, June 1977.

3 Marsden, B.G., Z. Sekanina, D.K. Yeomans, Comets and Non-Gravitational Forces, The Astronomical Journal, Vol 78, March 1973.

4 Yeomans, D.K., J.E. Ekelund and F. Hechler, Comet Ephemeris Generation Programs Software Structure Document, JPL/ESOC, December 1981.

DISCUSSION

D. Malaise: How can you situate the nucleus with respect to the dust head? One observes that the maxima of luminosity of dust and various molecules do not coincide. Position differences are in the 500 to 2000 km range. The nucleus can be in front, at the center of, or behind the central dust patch. If you give yourself a model (isotropic dust emission, fountain model, ...) you will be able to find the position of the nucleus but this will be arbitrarily model dependent. I do not see how to reduce the uncertainity on the actual gravitational center under, say, ± 500 km.

D. Yeomans: To minimize the possible offset between the comet's center of light and the actual necleus, observers could filter out gas emissions and take the shortest exposure that can still be measured. Offsets between the region of highest continuum emission and the actual nucleus will be minimized in this fashion.

RADIO AND INFRARED OBSERVATIONS

THE RADIO AND RADAR OBSERVATIONS OF COMETS : A REVIEW

Eric Gérard - Observatoire de Meudon - Département de Radioastronomie
92190-Meudon - France

I-INTRODUCTION

Thousands of hours of radio telescope time have been spent on comets (some would say wasted) with yet only one molecule definitely detected, OH, which has been known in comets for decades and one nucleus detected by radar, that of P/Encke. There are sound reasons why most results were negative so far, this review is aimed at spelling out some of them.

II - RADAR OBSERVATIONS

The observing technique consists in transmitting a powerful CW signal (one sense of polarization) with a high gain antenna towards the comet during the round trip echo time of flight and integrating the return signal (both senses of polarization) during a similar interval over repeated emission-reception cycles. From the echo spectrum one can deduce the radial velocity, the limb-to-limb velocity and the radar cross-section of the rotating target while the degree of depolarization measures its surface roughness.

In November 1980, Kamoun et al. (1982) detected the nucleus of P/Encke with the Arecibo radar operating at S-band (12.6 cm), providing the first direct evidence for the presence of a solid body with a radius of 1.5 km.
In July 1976, Pettenghill et al. (unpublished) using the same radar system failed to detect P/d'Arrest and an upper limit of 1 km was suggested for the radius of its nucleus.
Even with the most powerful radar systems namely Arecibo at S-band (12.6 cm) and Goldstone at X-band (3.5 cm) a comet of radius 1 km can only be detected if its geocentric distance (Δ) is less than 0.4 AU. Future opportunities are P/Grigg-Skjellerup (May 1982), P/Churyumov-Gerasimenko (Nov. 1982), P/Haneda-Campos (Sept. 1984) and P/Halley (April 1986).

The acquisition and interpretation of radar data rely heavily on visual observations which can provide an accurate ephemeris and an estimate of the spin vector. In this respect, short period comets are safer targets than long period or new comets. On the other hand

Proceedings of the ESO Workshop on "The Need for Coordinated Ground-based Observations of Halley's Comet", Paris, 29 – 30 April 1982.

the nucleus of a bright comet like C/Bennett (1970 II), C/Kohoutek (1973 XII) or C/West (1976 VI) may reach a radius of 5-10 km (Ney, 1974) and be detectable at 1 AU from the Earth. However a large intrinsic brightness by no means guarantees a large radar cross-section since comet nuclei are known to be unequally active.

Finally the dust and ice grains of mm and cm size around the nucleus may also contribute a significant echo at X-band (Chaisson et al., 1975) : according to Rayleigh scattering the radar cross-section follows a $\lambda^{-4}a^{-6}$ law with a the particle size. In fact Gibson and Hobbs (1981) argue (next section) that the passive continuum emission once detected from C/Kohoutek (1973 XII) and C/West (1976 VI) may be due to an Icy Grain Halo (IGH) opaque at cm wavelength. Such a halo composed of cm-size grains could be easily detected in bright comets at 1 AU from the Earth by short wavelength radar.

III - PASSIVE CONTINUUM OBSERVATIONS

A black body of 1 km radius and 200 K temperature located 0.4 AU from the Earth produces a flux density of 2.2 μJy (1 micro Jansky = 10^{-32} Watt m^{-2} Hz^{-1}) at λ 1.5 cm : thus there is little hope of ever detecting the thermal radiation of a cometary nucleus like that of P/Encke or P/d'Arrest except in a close encounter with Earth and no such case is predicted for short period comets in the 1980's. On the future 30 m - IRAM millimeter radio telescope a 10 km size nucleus also at 0.4 AU would only contribute a 2.8 mK antenna temperature at λ 1.5 mm, well beyond the realm of present day receiver sensitivity.

There is however a fair chance of detecting thermal emission from an IGH : Delsemme and Miller (1971) developed the theory of such a halo in order to explain the optical observations. Gibson and Hobbs (1981) in their review of the continuum radio emission of comets suggest that an IGH with a diameter of the order of 100km made of cm-size grains could account for the microwave signals detected in C/Kohoutek (1973 XII) and C/West (1976 VI) at 2.8 and 3.7 cm. However those signals appeared and disappeared in a day or so and the halo is most likely a transient phenomenon associated with an outburst. Furthermore the microwave IGH was not seen in C/Kobayashi-Berger-Milon (1975 IX), P/d'Arrest (1976 XI) and C/Bradfield (1978 VII), although the geocentric distance of

P/d'Arrest was only 0.15 AU. But Gibson and Hobbs (1981) argue that old comets may lack the volatiles to lift off and maintain a significant IGH. Besides possible new bright comets, P/Halley is the best opportunity for the next years.

IV - SPECTRAL LINE OBSERVATIONS

The preceding sections have demonstrated the first drawback of cometary radio observations : the signal is always weak and requires hours of integration to be extracted from the receiver noise. The scanty results obtained after one decade of spectral line observations prove that the situation is not any better there : in his review of the radio observations of comets, Snyder (1982) gives a detailed account of the numerous attempts at detecting molecular lines starting with C/Bennett (1970 II). Lengthy integration times are necessary and this raises another difficulty : cometary ephemerides need to be very accurate in order to guarantee that the target remains in the beam of the radio telescope. For instance the Effelsberg 100 m - and the Onsala 20 m - antennae have a Half Power Width (HPBW) of about 40 arcsec respectively at 1.3 cm (H_2O) and 3.4 mm (HCN, J = 1-0) ; the situation will be even more critical when the IRAM (Spain) 30 m antenna operates at 2.6 mm (CO, J = 1-0) with a HPBW of 20 arcsec . Our own experience is that such radio observations require almost real time astrometric positions and should never rely on ephemerides extrapolated weeks in advance. Unfortunately, as evidenced by the recent crisis in astrometry, the painful and time consuming work of visual comet observers has largely gone unrewarded both professionally and academically (Roemer, 1981). Yet it is a sine qua non condition of the success of future cometary line work.

The reason why most molecular searches were unsuccessful is essentially threefold.

- (i) most observations lack sensitivity by at least a factor of 10
- (ii) there was a dearth of bright comets in the last eight years but also an inadequate selection of the best targets and or of the best epoch.
- (iii) due to the special excitation conditions prevailing in comets the optimum transitions for detecting a given species have not always been chosen.
- (i) while the OH radical was extensively studied at 18 cm wavelength(Biraud et al., 1974 ; Snyder et al, 1976 ; Gerard et al.,

1977 ; Webber and Snyder, 1977 ; Despois et al, 1979 ; Giguere et al, 1980 ; Despois et al., 1981 ; Bockelée-Morvan et al., 1981)

the antenna temperature at 1667 MHz seldom exceeded 0.1 K : yet OH is a major constituent of cometary comae, more than 90 percent of the OH molecules are in the ground state where the 18 cm transition occurs and the populations of the upper and lower levels of the Λ doublet are strongly inverted (or anti-inverted) by solar UV pumping. It is therefore not surprising that most molecular searches other than OH have failed so far : the antenna temperature upper limits are generally well above 0.1 K. Likewise many upper limits to the mean column density averaged over the telescope beam (N) and to the gas production rate (Q) fall above what can be

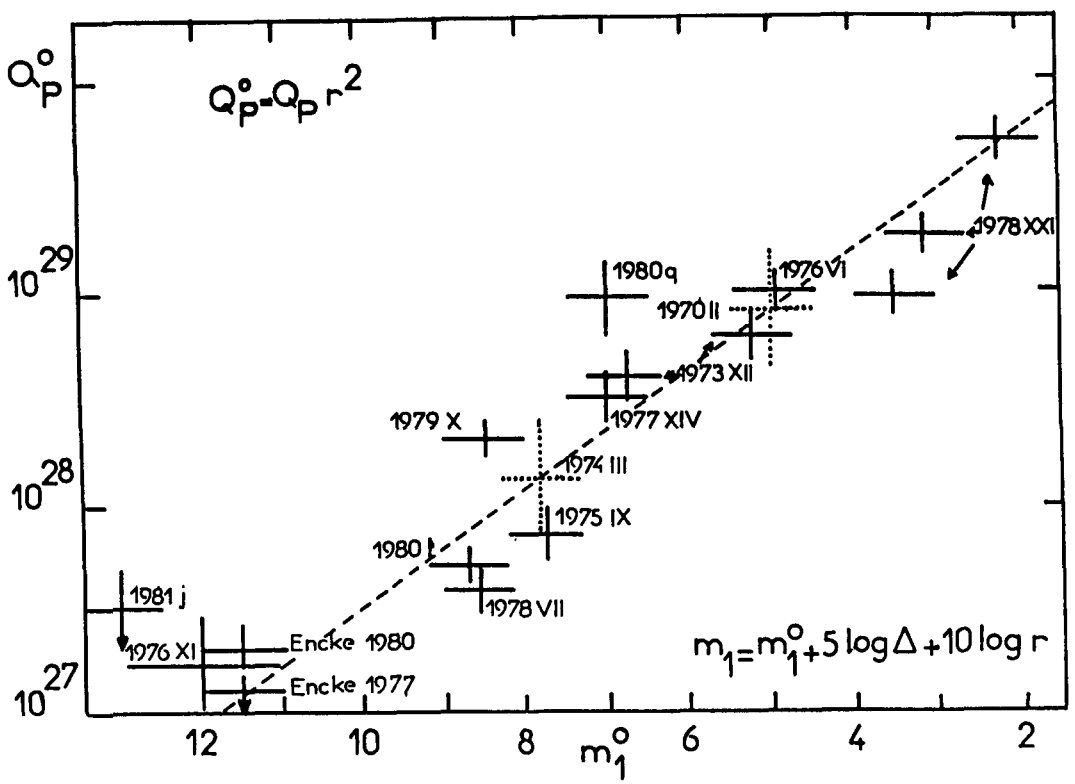

Fig.1 : Intrinsic production rate versus absolute magnitude - The 3 arrows for 1978 XXI refer to June (middle) July-August (upper) and November (lower) 1978 data. The 2 arrows for 1973XII refer to pre (upper) and post (lower) perihelion periods. The 2 downwards arrows at the bottom indicate upper limits. The dashed line corresponds to log Q_p^o = 30.3 - 0.28 m_1^o (Despois et al., 1981).

reasonably expected from visible, UV and radio OH data. For medium bright to bright comets like C/Kohoutek (1973 XII), C/West (1976 VI) P/Halley at a heliocentric distance (r) = 1AU the production rates of the major constituents (H, H_2O, OH, CO, C, O, NH_3, CH_4) are probably in the range 10^{28}-10^{29} mol. (atom)s^{-1} while the minor constituents (CO_2, HCN, CN, C_3, C_2 CS_2, CS, NH...) lie in the range 10^{26}-10^{27} mol. s^{-1}. At Δ = 1AU, the corresponding N values for a 2 arcmin beam are respectively 10^{13}-10^{14} mol. (atom) cm^{-2} and 10^{11}-10^{12}mol cm^{-2}, considerably smaller than in the interstellar medium.

- (ii) In fact there is a large spread of intrinsic gaseous production rates among comets as shown on Fig. 1 : thus the OH parent production rate reduced to r = 1AU according to a r^{-2} law (Q_P^o) is 100 times larger in C/West (1976 VI) than in P/Encke (1977, 1980) or P/Swift-Gehrels (1981).

As expected Q_P^o is correlated with the absolute visual magnitude (m_1^o) reduced according to $m_1^o = m_1 - 5 \log \Delta - 10 \log r$. A'Hearn and Millis (1980) have even found 3 orders of magnitude variation for the intrinsic production rates of C_2, CN and C_3 (measured in the visual spectrum) in a larger sample of comets and confirmed the correlation with m_1^o.

Thus as soon as a total visual magnitude estimate is available it becomes possible to predict approximate values for N(OH, CN, C_2, C_3), Q_P(OH, CN, C_2, C_3), N_P (OH, CN, C_2, C_3) (where the subscript P refers to the parent species) using models of comet comae (e.g. Giguere and Huebner, 1978)

The actual N values expected at any given r and Δ may be calculated knowing the linear size ($\Delta\theta_B$) , the scalelength (L) of the molecule and assuming a r^{-2} dependence for Q or the dependence already observed in the case of a periodic comet. Despois et al. (1981) have analysed OH data over a large range of heliocentric and geocentric distances namely $0.4 < r < 2.6$ AU and $0.2 < \Delta < 3.2$ AU. When $\Delta\theta_B > 2L$, N generally varies slowly with r since to increase of production rate is compensated by the shrinking of the scalelength as the comet approaches the Sun : for C/West (1976 XI), N remainded nearly constant between r = 0.37 and r = 1.4 AU while Δ varied from 0.8 to 1.2 AU. (Snyder et al., 1976 ; Despois et al., 1981). On the other hand, at constant r N follows a Δ^{-2} law as long as $\Delta\theta_B > 2L$ and a Δ^{-1} law when $\Delta\theta_B < 2L$ i.e. when the molecular source is resolved by the antenna beam.

All comets searched for molecular lines are shown on Fig. 1 including C/Bennett (1970 II) and C/Bradfield (1974 III) which were not observed at OH-18 cm wavelength and are represented as dotted crosses corresponding to their absolute visual magnitudes of 5.0 and 7.8 respectively. Concerning the molecules that were detected the following may be said :

- CH_3CN : for the ν_8 vibrationally excited transition Schloerb et al., (1979) deduce $N < 210^{14}$ mol. cm^{-2} in C/Bradfield (1978 VII), 100 times less than the value found by Ulich and Conklin (1974) in C/Kohoutek (1973 XII) while the gaseous production rate was only 10 times weaker For ground state CH_3CN their limit is $N < 10^{13}$ mol. cm^{-2} and $Q < 310^{27}$ mol. s^{-1}, of the same order as the major constituents so that at least a factor of 10 improvement is necessary to obtain a meaningful limit.

- HCN : from their upper limit to the J = 1 - 0 transition in C/Bradfield (1979 X) Ekelund et al. (1981) determined $Q^o(HCN)/Q^o(OH) < 0.03$, half the ratio observed by Huebner et al., (1974) in C/Kohoutek (1973 XII). Since $Q^o(CN)/Q^o(OH)$ is close to 0.01 (A'Hearn and Millis, 1980 ; A'Hearn et al., 1981), a factor of 10 improvement $Q^o(HCN)/Q^o(OH)$ should lead to detection if CN is produced by dissociation of HCN (Combi and Delsemme, 1980) : this may be achieved by observing a bright comet at moderate Δ.
Snyder et al. (1982) also attempted to detect HCN from C/Meier (1978 XXI) in November 1978 but the intrinsic production rate had considerably decreased since August (as indicated by the lower cross on Fig. 1) and with Δ = 2 AU the conditions were less favourable than for C/Kohoutek (1973 XII).

- CH : Rahe et al. (1977) have set an upper limit $N = 10^{14}$ mol.cm^{-2} in C/West (1976 VI). Since CH is a minor constituent this limit is too high by a factor of 10 if the ground state population inversion is as large as for OH and a factor of 100 in the case of LTE.

- H_2O : a thorough discussion of all the λ 1.35 cm observations is given by Crovisier et al. (1981) : doubt is cast on the detection claimed by Jackson et al. (1976) in C/Bradfield (1974 III) and even if it were genuine the λ 1.35 cm transition is not appropriate for solving the problem of the water vapor abundance in comets.

Regarding the upper limits reported on CO, CS, H_2CO, CH_3OH and NH_3 a few additional remarks can be made :

- CO and CS : respectively major and minor constituents they are studied by their UV spectrum and both production rates are lower

than the radio upper limits.

- H_2CO and CH_3OH : while nothing is known about their possible abundance, the reported upper limits are again those expected from major constituents and thereby not very significant.

- NH_3 : is a more favourable case : the upper limits reported by Mango et al. (1974) and Hollis et al. (1981) are probably close to what is needed to explain the NH_2, NH observations in the visible (Giguere and Huebner, 1978) so that again of a factor of 10 would be quite valuable.

- (iii) Except for the inner coma where collisions tend to populate the energy levels according to the Boltzmann partition function (LTE), the excitation by the radiation field is dominant (UV, visible or IR from the Sun and possibly far - IR from dust) and drastic departures from LTE can occur (e.g. OH).

For H_2O,Crovisier (1982) has shown that IR fluorescence does not predict any excitation of the rotational lines previously detected in the interstellar medium (6_{16} - 5_{23} at 226 Hz ; 3_{13} - 2_{20} at 183 GHz ; 4_{14} - 3_{21} at 380 GHz). However strong lines are expected in the submillimeter region : since they belong to the IR fluorescence cascade down to the ground state, their intensity should vary as r^{-2}, unlike the OH - 18 cm line.

For NH_3, the (1,1) ; (2,2) ; (3,3) inversion transitions near λ 1.3 cm could well be detected in comets since rotational transitions occuring in a time of the order of 10 seconds bring the molecule to the lowest rotational states for J = K which are metastable states Since the lifetime of ammonia is very short the radiation field may not alter the initial partition function established in the inner coma.

For heavier molecules like HCN, CO, CS, CN, CH_3CN, CH_3OH the rotational lines fall in the mm wavelength region) thus the upper rotational levels will be populated by collisional or radiative excitation (although the strength of the dipole moment will play a major role : for CO and HCN the radiative lifetime of the J = 1 level is respectively 210^7 and 410^4 s. Thus the lower rotational levels will be easily populated and it is more appropriate to search for the CO J = 2 - 1 and J = 3 - 2 at 230 and 345 GHz when a sensitive system is available (both a large collecting area and a low noise receiver). For HCN however the radiative excitation rate may be of the same order as the lifetime so that the partition function will change with r :therefore the J = 1 - 0 transition is probably a

good choice. As shown by Malaise (1970) the excitation of CN is dominated by UV fluorescence as well as collisions.
A careful examination of all possible excitation schemes must be carried out for each molecule not only for interpreting the radio data but most of all to determine what are the optimum transitions to attempt a detection. In fact it may turn out that certain molecules should rather be searched outside the radio spectrum.

REFERENCES

A'Hearn, M.F. and Millis, R.L. : 1980, A.J. 85, 1528

A'Hearn, M.F. Millis, R.L. and Birch,P.V. : 1981, A.J. 86, 1559

Biraud,F. Bourgois,G., Crovisier,J., Fillit,R., Gerard,E., and Kazes,I. : 1974, Astron. Astrophys. 34, 163

Bockelee-Morvan,D., Crovisier,J., Gerard,E., and Kazes,I.: 1981 Icarus 47,464

Chaisson,E.J., Ingalls,R.P., Rogers,A.E.E. and Shapiro,I.I. : 1975 Icarus 24, 188

Combi,M.R. and Delsemme,A.H. : 1980, Ap.J. 237, 641

Crovisier,J., Despois,D., Gerard,E., Irvine,W.M. Kazes,I., Robinson, S.E. and Schloerb,F.P. : 1981, Astron. Astrophys. 97,195

Crovisier,J. : 1982, ESO Workshop, 29-30 April Institut Astrophysique Paris

Delsemme,A.H. and Miller, D.C. : 1971, Planet. and Space Sci.19,1229

Despois, D., Gerard,E., Crovisier,J.and Kazes,I. : 1979, Paper presented at the IAU General Assembly XVII, Commission 15 Montréal

Despois,D. Gerard,E., Crovisier,J. and Kazes,I. : 1981, Astron. Astrophys. 99, 320

Ekelund,L., Irvine,W.M. and Andersson,Ch. : 1981, Icarus 47, 431

Gerard,E., Biraud,F., Crovisier,J., Kazes,I. and Milet,B. : 1977 in "Comets, Asteroïds and meteorites, ed. A.H. Delsemme, University of Toledo, p. 65

Gibson,D.M. and Hobbs,R.W. : 1981, Ap. J. 248, 863

Giguere,P.T. and Huebner,W.F. : 1978, Ap. J. 223, 638

Giguere,P.T., Huebner,W.F., and Bania,T.M. : 1980, A.J. 85, 1276

Hollis,J.M., Brandt,J.C., Hobbs,R.W., Maran,S.P. and Feldman,P.D. : 1981, Ap. J. 244,357

Huebner,W.B., Snyder,L.E.and Buhl,D. : 1974, Icarus 23,580

Jackson,W.M., Clark,T. and Donn,B. : 1976, in "The study of comets" ed. B. Donn, M.Mumma, W. Jackson, M. A'Hearn and R.Harrington, NASA SP. 393, p 272

Kamoun,P.G., Campbell,D.B., Ostro,S.J., Pettenghill,G.H. and Shapiro I.I. : 1982, Science 216, 293

Malaise,D.J. : 1970, Astron. Astrophys. 5, 209

Mango,S.A., Johnston,K.J., Chui,M.F., Cheung,A.C. and Matsakis,D. 1974, Icarus 23,590

Ney,P.N. : 1974 Icarus 23,551

Rahe,J., Churchwell,E. and Keller,H.U. : 1977, Astron. Astrophys. 61,765

Roemer,E. : 1982, private communication

Schloerb,F.P., Irvine,W.M. and Robinson,S.E. : 1979, Icarus 38,392

Snyder,L.E., Webber,J.C., Crutcher,R.M. and Swenson,G.W. Jr : 1976 Ap. J. 209, L 49

Snyder, L.E. : 1982, preprint

Snyder,L.E., Hollis,J.M. and Webber,J.C. : 1982, in preparation

Ulich, B.L. and Conklin,E.K. : 1974, Nature 248,121

Webber, J.C. and Snyder,L.E. : 1977, Ap.J. 214, L45

DISCUSSION

R. Norris: If the 18 cm flux from inverted OH should exceed that ($\sim$ 0.3 Jy) from previously detected comets such as comet West by a factor of $\sim$3, it will be possible to make an aperture synthesis radio map of the OH emission with an array such as Merlin. How likely do you think it is that the 18cm flux will reach this value?

E. Gérard: There is little chance that the OH 1667 MHz flux will exceed 0.3 Jy. What we are looking at is improving our system noise at 18 cm: presently the Nançay antenna has a system noise of 45 K but there are plans to decrease it to 30 K. May be you have similar plans. We should discuss those matters in the frame of the IHW Radio Science team of NASA where I will hopefully be serving on the European side.

D. Malaise: Comment on slide showing OH production against total magnitude. In my opinion the content of information of this diagram is nil because total magnitude is used. The total number of photons emitted by a molecule does not depend on r_h, so that the total brightness in OH light is accurately proportional to the production rate of OH. This is however not true for the dust because their lifetime is infinite (for observation purpose) so that, even with the most simple physical model, the total brightness including a mixture

of dust and molecules cannot be proportional to the production rate of OH. I just want to stress that this kind of diagram would contain much information if the total magnitude was given for cleanly separated components of the head and not for a varying mixture.

E. Gérard: I fully agree that one cannot attempt any physical interpretation of this slide showing OH production rates versus total magnitudes and I never did it. However, I want to point out that this diagram can be used to derive an estimate of the radio intensity from the total magnitude which is the only quantity one generally has to decide whether an observation can be made or not. Furthermore this diagram shows that there are intrinsically bright and dim comets, the production rates varying by more than a factor of 100.

M. Festou: In order to interpret radar observations, you have to know what are the rotation period of the nucleus, the inclinaton of the rotation axis on the orbital plane, etc. Are there any plans to complement radar observations with visual observations in order to determine those parameters?

E. Gérard: To interpret the radio echo you have to know the following nucleus characteristics: inclination of axis, rotation period, radar reflectivity and radius. The faster the rotation, the wider the spread in frequency. For Halley we know the rotation period and we hope that the orientation will be determined before 1985. In any case we do not need all the parameters: one can measure the total intensity of the echo (integrated over frequency) and get the radius by assuming a radar reflectivity like Encke for instance.

Finally the echo may be analysed differently if a pulsed radar is used. No frequency analysis is made, only a range (distance) analysis. Thus if the diameter is 4 km, there will be a delay of about 2/300000 = 7 microseconds.

C. Cosmovici: Which is the maximum distance and the minimum diameter of an object detectable with the Arecibo antenna?

E. Gérard: There is no simple answer to your question: The intensity of the echo varies as $\Delta^{-4}D^2$ with Δ the geocentric distance and D the nucleus diameter. Comet Encke was easily detected at Δ = 0.33AU with D = 2. With the same radar set up and receiver sensitivity at Arecibo one could detect (with the same integration time) in similar conditions another comet with $\Delta \propto D^{1/2}$ or $D \propto \Delta^2$ so that any close passage to Earth is a good candidate. But within a few years both the transmitter power and the receiver sensitivity might be improved (factor 1.5. in power, factor of 2 in sensitivity → factor of 3 gain).

M. Bird: What are the chances of detecting radar echoes from Comet Halley to improve the navigation of the Giotto mission?

E. Gérard: The chances are as follows: the echo intensity is proportional to $\Delta^{-4}\ D^2\ T_r\ \tau^{1/2}/T_N$ with D the nucleus diameter, T_r the transmitted power, τ the integration time and T_N the receiver noise. P/Encke was detected at Δ = 0.33 with D = 2 in 1980. In November 1985 P/Halley comes at Δ = 0.6 so that a factor of 16 must be gained to have the same signal to

noise ratio. We can foresee a gain of 4 in T_R/T_N. Now it appears that D=5 (Comet Halley Handbook) so that detections should be possible. The detection in April 1986 will be much easier since Δ = 0.4 AU but too late for improving navigation of Giotto.
The interest of getting the echo is twofold for navigation:
(i) range measurement: obtain accurate Δ
(ii) Doppler measurement: derivation of Δ with respect to time.

? : Could a radar observation in November 1985 improve the ephemeris of comet Halley?

D.K. Yeomans: An Arecibo Doppler observation of comet Halley in late November could substantially improve the comet's ephemeris at the time if an accuracy of say 6 cm/sec could be achieved. However it is not yet clear whether or not the ephemeris improvement realized in November 1985 can be maintained until the spacecraft flybys in March 1986.

PROPOSED RADIO OBSERVATIONS OF INVERTED OH IN HALLEY'S COMET

R.P. Norris
University of Manchester
Nuffield Radio Astronomy Laboratories
Jodrell Bank
Macclesfield
Cheshire
SK11 9DL
ENGLAND

Stimulated emission and absorption at 1665 and 1667 MHz from cometary OH was first detected in Comet Kohoutek[1,2]. Subsequent observations of other comets and calculations have led to a good understanding of the pumping and emission mechanisms of the cometary OH[3], and will no doubt continue to contribute to the understanding of cometary chemistry. It is the purpose of this short contribution to point out some of the potential uses of the OH maser emission which have not so far been explored, and to suggest observations which should be made of Halley's comet.

The intensity of OH maser emission from comets fluctuates rapidly as a function of heliocentric velocity as a result of the u-v pumping mechanism. Comparison of the ephemeris[4] for Halley's comet with the calculated population inversion[1,3] shows that the OH maser emission should reach a peak in late 1985, shortly before the closest pre-perihelion approach of the comet to the Earth. A further but weaker maximum in the maser intensity should occur after perihelion in early March 1986, shortly before the encounter with the spacecraft Giotto.

Throughout late 1985 to early 1986, it is important that the OH emission should be monitored using large single dish telescopes. It is expected that the pumping mechanism for the masers will distinguish between magnetic sublevels[5], and consequently the emission may be linearly polarised. The single dish observations should therefore record all four Stokes parameters, hence giving complete polarisation information.

Single dish observations[3] indicate that the size of the OH emission region is $\sim 10^5$ km, giving an angular size of a few arcmin at 1 a.u. However, the maser process is extremely sensitive to inhomogeneities in the gas[6] and so small scale structure within the gas is expected.

It is proposed that spectral line aperture synthesis observations of the OH would give a great deal of information about the dynamics and chemistry of the gas in

Proceedings of the ESO Workshop on "The Need for Coordinated Ground-based Observations of Halley's Comet", Paris, 29 – 30 April 1982.

the coma. The distribution of the OH may be mapped as a function of frequency provided that the maser emission is sufficiently intense, using synthesis arrays such as MERLIN (including the 425m MK IA-MK II baseline), Westerbork or the VLA. The most opportune epoch for these observations will be in late November 1985, when the maser emission will be near a maximum in flux density, and the comet will be close to the Earth with a high ($\sim +20^{o}$) declination. These observations should also provide an absolute position of the OH, thereby locating it relative to the cometary nucleus.

An additional observation of the OH emission may become useful shortly after perihelion in February-March 1986. Stochastic accelerations of the comet during perihelion, together with the stringent requirements of the navigation of the Giotto spacecraft, mean that the ephemeris of the comet must be redetermined between perihelion (February 9 1986) and the Giotto encounter (March 13 1986). The proximity of the comet to the Sun may prevent early optical recovery. However the comet may be recovered at radio frequencies as soon as the heliocentric velocity becomes such that the OH maser turns on. If the November 1985 OH observations have been successful, then aperture synthesis observations of the OH emission shortly after perihelion may provide additional data for the Giotto navigation group. Unfortunately, however, this suggestion must remain speculative until we can see whether the nucleus can be located accurately within the OH aperture synthesis maps.

REFERENCES

1. Biraud, F., Bourgois, G., Crovisier, J., Fillit, R., Gerard, E., & Kazes, I., 1974. Astron.Astrophys. 34, 163.
2. Turner, B.E., 1974, Astrophys.J., 189, L137.
3. Despois, D., Gerard, E., Crovisier, J. & Kazes, I., 1981, Astron. Astrophys., 99, 320.
4. Yeomans, D.K., 1981, 'The Comet Halley Handbook', Jet Propulsion Laboratory, Pasadena.
5. Mies, F.H., 1974. Astrophys.J., 191, L145.
6. Norris, R.P. & Booth, R.S., 1981, Mon.Not.R.astr.Soc., 195, 213.

INFRARED OBSERVATIONS OF COMET HALLEY

Michel Combes
Observatoire de Paris-Meudon

I. Introduction

This study will not present a complete review of all the results concerning comets derived from the infrared spectral range. It will be focussed on three key questions that future ground based observations in the infrared range could help to solve in connection with the space missions to P/Halley, Giotto and Vega.

1. Where are the ices ?
2. What are the nature and the distributions of dust grains ?
3. What can be learnt about parent molecules ?

These questions are related to the chemical and physical properties of the inner coma in the close environment of the nucleus.

Sublimation of ices and in particular of water ice, if it exists would dominate the thermal regime and the temperature structure of the inner coma. Dust grains play a major role in the cometary energy budget through the solar light absorption and radiative transfer. Dust grains may also strongly influence the efficiency of chemical reactions through catalysis properties. Moreover there are some reasons to believe that the classical model of the cometary nucleus - a bare nucleus like a dirty snow ball - could be unrealistic. The nucleus might be closely and permanently surrounded by a dusty and/or icy cocoon of some hundred of kilometers thickness. Such a structure of the inner coma would strongly differ from current models of comets.

The inner coma is also the region where some parent molecules might be identified directly. Up to now, we have only indirect evidences about the nature of parent molecules, not in conflict with the basic assumption that H_2O is the major parent molecule. Nevertheless, various reasons may be given to argue against this common assumption (Wallis, 1982).

Next encounter of comet Halley will induce extensive observational studies. Studying the close vicinity of the nucleus should be a major goal of these observations.

II. Specific interest of the IR spectral range.

As shown in Fig. 1, a typical cometary spectrum exhibits in the visible spectral range the spectrum of the scattered solar light and in the infrared the thermal emission of the coma itself, with a maximum ranging between 5 and 20 microns depending on the coma temperature, i.e the heliocentric distance. The point of interest is that the spectrum shown in Fig. 1 is mainly due to the dust. The nucleus itself gives only a minor contribution to the total flux, except for

Proceedings of the ESO Workshop on "The Need for Coordinated Ground-based Observations of Halley's Comet", Paris, 29 – 30 April 1982.

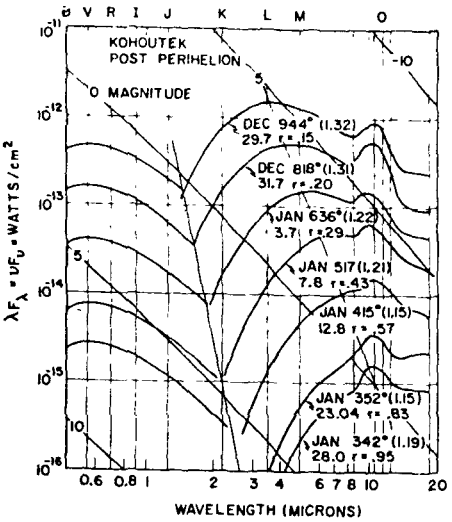

Fig. 1 : Spectra of comet Kohoutek at various heliocentric distances (From Ney, 1974).

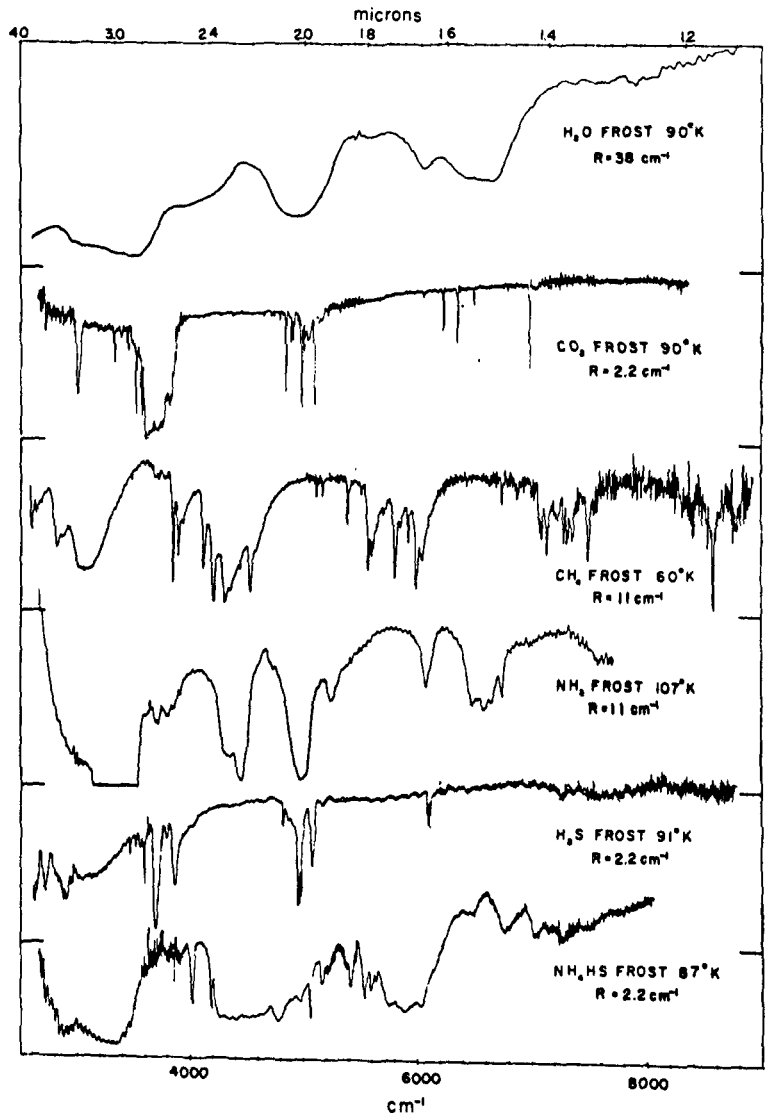

Fig. 2 : Frost absorption spectra (From Larson and Fink, 1977).

close fly-by space experiments. Emissions due to gases are negligible in terms of energy in the infrared spectral range. At low spectroscopic resolution the cometary IR spectrum is entirely due to dust and ices. The IR spectral range is thus an ideal region for studying the cometary dust and ices.

Moreover the infrared spectral range is well suited for identification of minerals and ices. Fig. 2 shows typical absorption spectra of various frost species : H_2O, CO_2, CH_4, NH_3, H_2S and NH_4SH.

The well known spectral signature of silicates may be found in the thermal infrared spectral range around 10 and 20 microns, as shown in Fig. 3 where SiO_4 absorption modes induce absorption spectra of olivine and piroxene.

Search for parent molecules in the infrared spectral range looks promising since most of the expected parent molecules have absorption bands in the near and thermal infrared ranges. Products of the absorption coefficients by the expected abundances as given in the NASA Comet Science Working Group Report (1979) have been plotted in Fig. 4 for various molecular species (Encrenaz et al., 1982). Fig. 4 shows that the best candidates to be detected as parent molecules in the IR range are H_2O, CO, CO_2, CH_4, NH_3, N_2H_4 and H_2CO. If the assumed model is not correct, Fig. 4 shows that several other molecules exhibit spectral signature in the infrared.

In conclusion, the infrared spectral range seems to be well adapted for a study of the inner coma. The IR cometary spectra are dominated by dust and ices properties at low spectroscopic resolution. Dust and ices exhibit characteristic spectral features in this spectral range. Moreover most of the expected parent molecules have absorption bands in the IR range which could be present as high spectroscopic resolution features on cometary spectra.

III. Where are the ices ?

Several spectra of faint comets, Stephan-Oterma, Tuttle, Meier and Bowell, have been obtained in the JHKL photometric bands by A'Hearn et al. (1981) which do not show any evidence for ices spectral features. CVF spectra of Comet Stephan-Oterma between 1.4 and 2 microns (A'Hearn et al., 1981) and of Comet West (1975n) between 2.8 and 3.6 microns (Oishi et al., 1978) confirm the absence of any absorption features of H_2O ice at 1.5, 2.0 and 3.0 microns. This result led A'Hearn et al. to ask the question "where are the ices ?".

M. Hanner has discussed the problem in details (Hanner, 1981). Several reasons may explain the lack of detectable water ice signature.

1. Significant absorptions features cannot be produced at 1.5 and 2:0 microns by micron sized particules due to the well known properties of light scattering.

2. The 1.5 and 2.0 microns bands are not very strong. While the depth of the

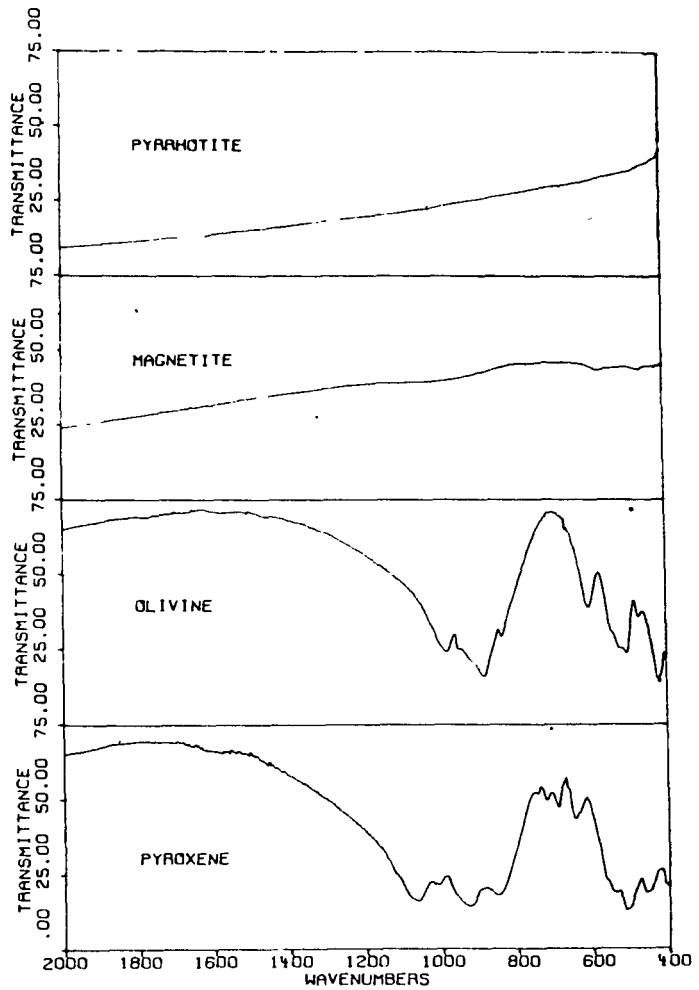

Fig. 3 : Minerals absorption spectra (Fron Fraundorf et al., 1981).

bands depends on particle size the 3μ band is always stronger than the 1.5 and 2.0μ bands, by about two orders of magnitude for 5 and 20μ diameter grains. But the contrast at 3μ may be reduced by the thermal emission of the coma for comets close to the Sun (∿1 AU).

3. The lifetime of the ice particles might put severe constraints on the detectability of an icy halo. Except for very pure water ice grains, the maximum size of an icy halo would be limited to a few hundred kilometers at heliocentric distances < 2.5 AU. In such a case ice absorption features may be masked by the surrounding dust emission.

4. For distant comets (> 5 AU) it is not clear that the gas flow escaping from the nucleus could be sufficient to strip large particles far from the nucleus.

If such an analysis is right, the icy halo of Comet Halley may have a small extension (∿ 100 km) at the time of the fly-by of Halley by the Giotto and Vega space missions. In spite of its short fly-by miss distance Giotto might miss water ice particles. The infrared remote sensing experiment IKS on Vega (Encrenaz et al., 1982) with a field of view at closest approach of about 200 km in diameter, might be more successful if scattering ice grains are sufficiently large at the time of the encounter.

Undoubtly an active search for water ice from ground, before the perihelion and at large heliocentric distances would be of major interest. To conclude it may be of interest to summarize the optimum conditions for such an observations ; 1) observations should start at large heliocentric distance (Δ > 2.5 AU) ; 2) the field of view should not exceed ∿ 3 arc sec ; 3) the spectroscopic resolution should be $\frac{\lambda}{\Delta\lambda} \sim 50$; 4) the 3μ band seems to be the best candidate for detection.

IV. Nature and distribution of dust grains

Fig. 1 shows a sample of spectra of the tail of Comet Kohoutek at various heliocentric distance. The maximum of brightness is shifted towards long wavelengths as the Comet moves to large heliocentric distance. So the brightness temperature of the tail is directly dependent on the distance to the Sun but is always warmer than the black-body temperature at the same distance. That means that the dust particles are small. An upper limit of their diameter is 3μ. If the same particles are responsible for the scattered light in the visible spectral range, their diameter must be larger than 0.2μ.

Such spectra can give constraints not only on the particles sizes but also on the chemical nature of the grains. All the spectra shown in Fig. 1 exhibit the silicates signature around 10μ, superimposed to a "black-body emission". Silicates grains cannot be the unique constituent of the dust, some absorbing material is also needed. In contrast the anti-tail spectra do not show the silicates

signature and the brightness temperature is always close to the equivalent black-body temperature. So anti-tail particles are larger than 20μ or are not due to silicates.

Additional data may be obtained from low resolution photometry in the infrared. From analysis of M/L magnitudes ratio vs heliocentric distance or colour-index (J-H, H-K) variations vs phase angle Campins and Hanner (1982) have obtained new constraints on the nature of the dust. Up to now, the coverage in phase angle and heliocentric distance for a given comet is not sufficient.

Such observations are needed for Comet Halley on a long time basis. Some spectroscopic resolution ($\lambda/\Delta\lambda \sim 100$) as well as spatial resolution (some arc-sec) would be needed and above all simultaneous measurements in a large spectral range covering both the thermal infrared and the reflected light ranges. Continuous observations during several days, especially at the time of the Giotto and Vega encounters with Halley will be of major interest as indications on changes in the cometary dust structure and cometary activity.

A specific photometer dedicated to such a programme is being studied at Paris-Meudon Observatory. It will be able to record the cometary spectrum between 1.5 and 20 microns on 5 points of the coma simultaneously, with a resolution of 3 to 5 arc-sec and a spectroscopic resolution of $\sim$ 100. A second channel will produce high resolution images of the coma in the visible spectral range using a CCD camera which may be used also to observe stellar occultations by the coma (cf. D. Malaise, this meeting).

V. Parent molecules

As shown previously most of the expected parent molecules have absorption bands in the near and thermal infrared ranges. The sub-mm spectral range is also promising. This paper is restricted to the near and thermal IR. For a discussion of possible detection of parent molecules in the sub-mm spectral range, the reader is referred to Crovisier (1982, this meeting) or Encrenaz et al. (1982b).

A synthetic spectrum of a Halley type Comet has been computed, using the data given in Fig. 4 by Encrenaz et al. (1982) between 2 and 15 microns. Emission lines of H_2O, CO, CO_2, CH_4, NH_3, N_2H_4 and H_2CO could be detectable from a fly-by mission. Such a detection is a major goal of the infrared spectroscopy experiment (IKS) of the VEGA mission to Halley. From the ground, search for parent molecules is a very difficult task. In view of the low column densities of the various expected molecules, spectral lines are faint and narrow. Most of the expected molecules are also present in the atmosphere of the Earth. The intense emission of the cometary dust and the noise due to the terrestrial atmosphere prevent any detection at low spectroscopic resolution. Nevertheless some attempts should be made from high altitude observatories or from airplanes, using very high

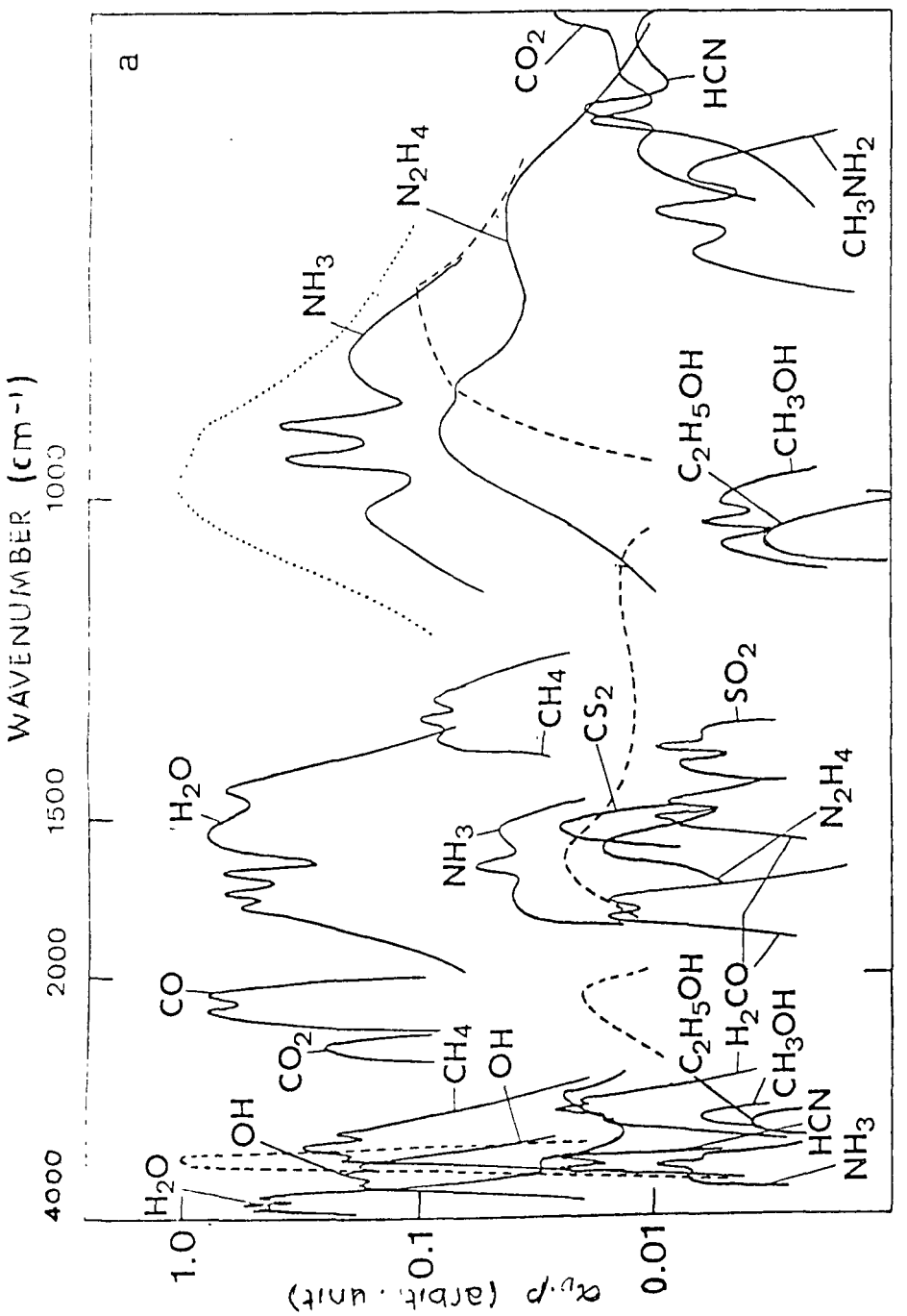

Fig. 4 : Comparative absorptions of molecules between 2.5 and 15 microns. The absorptions due to H_2O ice and silicates are plotted an arbitrary scales (From Encrenaz et al., 1982).

spectroscopic resolution devices like interferometers or heterodyne systems and taking into account the Doppler shift due to the motion of the Comet relatively to the Earth.

Unsuccessful search for CH_4 at 3.3 microns in Comet Kohoutek has been reported by Roche et al. (1975). The experiment was made from an aircraft using a Fabry-Perrot interferometer. A search for CO in the entire 4 microns band was also unsuccessful from the ground (Wollmann et al., 1974).

However these negative conclusions might be revisited. Indeed an accurate distribution of the energy among the individual lines of a given band must be known. Except in the inner-coma, lines are formed by fluorescence and a Boltzmann distribution of the energy levels within each molecular band is not expected. As a consequence the total energy of a band is distributed in only a few lines. The needed calculations require a long and tedious computation, specific to each molecule (Encrenaz et al., 1982). This computation has been performed (Crovisier et al., 1982b) in the case of the H_2O molecule : only 9 lines in the ν_2 band and 6 lines in the ν_3 band are excitated.

In conclusion, detection of parent molecules from ground based observations could be marginally expected in the near and thermal infrared spectral range. New attempts should be made by means of interferometry or heterodyne spectroscopy from an airborne observatory, like the KAO and perhaps Astroplane, in the case of H_2O and CH_4. From the ground, CO, NH_3 and C_2H_2 are the best candidates for detection. Complete calculations of the energy distribution are needed for each molecule in order to maximize the detection probability.

References

- A'Hearn M.F., Dwek E., Tokunaga A.T. 1981, Astrophys. J. (in press).
- Campins H., Hanner M.S. 1982, Comets : Gases, Ices, Grains and Plasma (in press).
- Crovisier J. 1982, Ground-based Observations of Halley's Comet. ESO Workshop, Paris.
- Crovisier J., Combes M., Crifo J.F., Encrenaz T. 1982b, XXIVth COSPAR Meeting, Ottawa.
- Encrenaz T., Crovisier J., Combes M., Crifo J.F. 1982, Icarus (in press).
- Encrenaz T., Combes M., Crovisier J. 1982b, Scientific Importance of Submillimeter Observations , ESA Workshop, Noordwijk.
- Fraundorf P., Patel R.I., Freeman J.J. 1981, Icarus 47, 368.
- Hanner M.S. 1981, Icarus 47, 342.
- Larson H.P., Fink U. 1977, Appl. Spectrosc. 31, 386.
- Malaise D. 1982, Ground-based Observations of Halley's Comet. ESO Workshop, Paris.

- NASA International Comet Mission Halley/Temple 2. Mission Baseline. Vol. III NASA 626.2, 1979.
- Ney E.P. 1974, Icarus 23, 551.
- Oishi M., Kawara K., Kobayashi Y., Maihara T., Noguchi K., Okuda H., Satao S. 1978, Publ. Astron. Soc. Japan 30, 149.
- Roche A.E., Cosmovici C.B., Drapatz S., Michel K.W., Wells W.C. 1975, Icarus 24, 120.
- Wallis M. 1982, Third European IUE Conference, Madrid.
- Wollmann E.R., Geballe T.R., Greenberg L.T., Lacy J.H., Townes C.H., Rank D.M. 1974, Icarus 23, 593.

DISCUSSION

M. Wallis: A comment first: Ney's observations of a 9.7 μm feature in comet Kohoutek can only be interpreted as evidence of the Si-O bond, not silicates. My question next: Why can Hanner find a decrease in grain lifetime by a factor of a million, while Patashnik and Rupprecht (Ap. J. 197, L79, 1975) found only a 10 or 10^2 decrease? Might it be due to the unphysical assumption of absorptivity independent of wavelength adopted by Hanner?

M. Combes: I don't know.

P. Lamy: The "traditional" way of making "dirty" ices, as far as optical properties are concerned, is to introduce a constant, more or less large, absorption coefficient k. This is a completely unphysical description and you can get whatever results you want just by playing with the values given to k, hence get a 2 or 3 orders of magnitude difference in comparison with pure H_2O.

M. Schwehm: Remark on ice grain lifetimes::
Calculations of the extent of an icy grain halo using mixtures of grains from different materials - instead of just adding a constant value to the absorption part of the complex refractive index of ice like M. Hanner did - shows that the halo could extend to several 10^4 km at least for grains of an original size > 10 μm. These calculations have been done for the Halley encounter geometry (cf. paper by Schwehm and Kneißel in Comet Halley Environment Working Groups Report, ESA-SP, 174, p.77, 1981).

OPTICAL OBSERVATIONS: NUCLEUS AND COMA

THE NUCLEAR REGION OF COMETS

D. MALAISE

Université de Liège
Institut d'Astrophysique
5, avenue de Cointe

B - 4200 LIEGE-COINTE
BELGIUM

There is no originality in saying that what we see from comets is the head and the tails, that is, a very tenuous end evanescent part which altogether weights no more than 3.10^{11}g. This mass is dispersed in a huge volume comparing with that of the sun.
The source of all this material is thought to be a solid chunk of dirty snow a few kilometer diameter, weighting some 10^{15} to 10^{18} g and commonly called the nucleus.
No need to say that the only physically and cosmogonally relevant part of the comet is precisely this nucleus. The continuing frustration of cometary physicists is that the nucleus of a comet has never been observed or even detected due to its small size. Its existence is however prooved beyond any doubt by the study of phenomena observed in the coma. We, of course, want to know much more about it and to this purpose, the European Space Agency is building a probe due to meet Comet Haley in summer 1986. The Russians have transformed two Venera missions to the same aim and the Japanese are also going to visit the comet. But even at this stage, those planning the instruments for the probes are in a deep embarassement and the same question arises again and again : what is the close environment of the nucleus ? The two Russian venera probes are not planned to approach closer than a few thousand km from the nucleus by fear of destructive interaction with material surrounding the nucleus. The Europeans plan a much closes approach ($\sim$ 500km) but, although some weight has been allocated to a sophisticated dust shield, the mission is not expected to survive its closest approach to the comet. Moreover, those planning the on-board camera do not know how and whether to protect the first optical element, they are in deep hesitation about how to model an image of the comet nucleus and its environment in order to program their pattern recognition microprocessor. Think how dramatic it would be to program it to aim at the brightest spot and to go all the way to the comet and to take 2000 pictures of an undifferenciated bright halo 2000 km in front of the nucleus. Even the people having to make the mid-

Proceedings of the ESO Workshop on "The Need for Coordinated Ground-based Observations of Halley's Comet", Paris, 29 – 30 April 1982.

course correction do not know where to aim at : they realize that the actual nucleus could be about anywhere within say 1000 km from the center of luminosity as seen from earth.

These difficulties reflect a peculiar situation : on the one hand extensive observations and their theoretical interpretation concern the part of the comets comprised between 5.10^3 and 5.10^5 km radius: this I will call cometary aeronomy. On the other hand, extensive theoretical studies are bearing on the nucleus itself; but they are all implicitely based on the simple original "Whipple" model of a bare snowball directly lit by the sun and vaporizing into space. The region surrounding the nucleus up to say 1000 km radius not only is unknown and nearly out of reach of ground based observation, it is also mostly ignored by theoreticians. This region is what I call the nuclear region : its observation is the subject of this talk. When in 1965 I objected to Delsemme about his thermodynamical model of the nucleus, that the picture would be quite different if the nucleus, instead of being bear, would be imbeded in a deep layer of dusty material he eluded the question by saying that this would simply modify the albedo. Let us look a little closer into this problem :

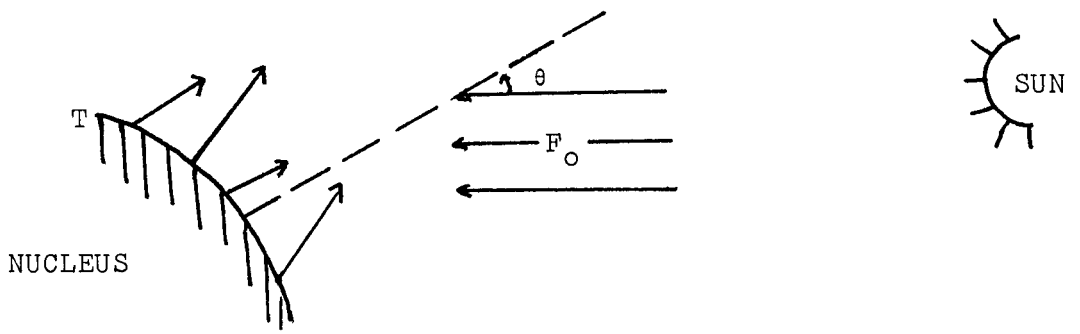

Figure 1.

Delsemmes thermodynamical model :

$$F_o(1-A_o)r^{-2} \cos\theta = \sigma(1-A_1)T^4 + Z(T).L(T)$$

$$Z(T) = p_s(T)\ (2\pi mkT)^{-1/2}$$

Where F_o is the solar flux at unit solar distance, A_o the visible albedo of the nucleus, A_1 the infrared albedo, T the nucleus temperature, Z(T) the vaporization intensity (molecules cm^{-2} sec^{-1}), which can be approximated by the second relation in term of the saturation pressure p_s. L(T) is the heath of sublimation. It is found that the temperature is controlled by evaporation (of the

most volatile component if there is a mixture) when the heliocentric distance is small enough. As r increases, Z(T) drops quite suddenly and the temperature is then controlled by the radiative terms only. In this model, evaporation stops at various heliocentric distances for various volatiles (typically 2.6 AU for H_2O, 8.5 AU for CO_2, 15 AU for CH_2O, 38 AU for CH_4, 60 AU for CO and 80 AU for N_2).

Malaise's dusty nuclear region model :

The transfer of radiation in an optically thick dusty nuclear region is of course much more complicated :

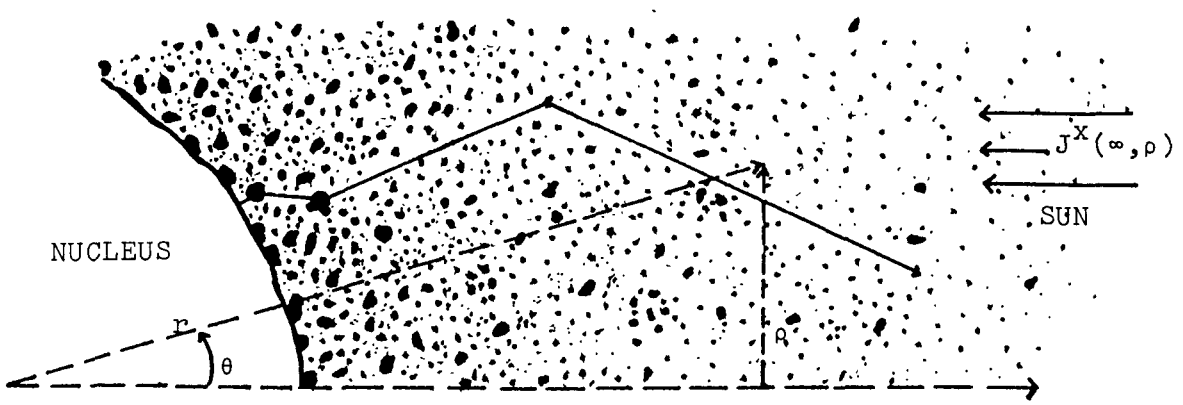

Figure 2.

- The first step is to consider a spherically symetric cloud of dust limited by two surfaces : inside the nucleus, and outside the surface where $I_o(\theta,\rho) = I_o(\infty)e^{-1}$. Between the two surfaces a dust repartition f(r,a) where a is the radius of the dust yielding an absorption coefficient at r $\kappa(r) = \int_o^\infty f(r,a)\pi a^2 da$.

The diffusion inside the cloud is described by the medium albedo $\omega(r) = A \int_o^\infty f(r,a)\pi a^2 da$ where A is the surface albedo of dust.

One obtains easily differential relations for the integrated radiative flux and the radiation pressure in cylindrical coordonates :

$$\frac{d}{dx} J^x(x,\rho) + \frac{d}{d\rho} J^\rho(x,\rho) = -4\kappa(r)[(1-\omega)\,\bar{I}\,(x,\rho) - (1-\omega)B(T)]$$

$$\frac{d}{dx} p^{xx}(x,\rho) = -\frac{\pi\kappa(r)}{c} J^x(x,\rho)$$

$$\frac{d}{d\rho} p^{\rho\rho}(x,\rho) = -\frac{\pi\kappa(r)}{c} J^\rho(x,\rho)$$

$$\frac{d}{dy}\, p^{yy}(x,\rho) = o$$

One needs more hypothesis to solve this system of three equations with six unknown functions.

- making the radiation pressure tensor isotropic $p^{xx}=p^{\rho\rho}=p^{yy}=u(x,\rho)$
- assuming thermal equilibrium of the dust $\bar{I}(x,\rho)= B(T)$

yields $$[\frac{d^2u}{dx^2} - \frac{1}{\kappa(r)} \frac{d\kappa(r)}{dx} \frac{du}{dx}\ ] + [\frac{d^2u}{d\rho^2} - \frac{1}{\kappa(r)} \frac{d\kappa(r)}{d\rho} \frac{du}{d\rho}\ ] = o$$

$$J^x(x,\rho) = - \frac{c}{\pi\kappa(r)} \frac{du(x,\rho)}{dx} \; ; \; y^\rho(x,\rho) = - \frac{c}{\pi\kappa(r)} \frac{du(x,\rho)}{d\rho}$$

The general solution of this system has been established for two cases :

1) $\kappa(r) = Cr^{-q} \rightarrow u(r,\theta) = [A_1 + A_2\, r^{-q}][B_1 + B_2\theta]$

$$J^x(x,\rho) = \frac{c}{\pi C} [qA_2 \cos\theta r^{-1}(B_1 + B_2\theta) + B_2 \sin\theta r^{-1}(A_2+A_1\, r^q)]$$

$$J^\rho(x,\rho) = \frac{c}{\pi C} [qA_2 \sin\theta r^{-1}(B_1 + B_2\theta) - B_2 \cos\theta r^{-1}(A_2+A_1\, r^q)]$$

2) $\kappa(r) = Ce^{-qr} \rightarrow$

$$u(r,\theta) = [A_1 + A_2(\ln r + \sum_1^\infty \frac{(-1)^n q^n r^n}{n.n!})](B_1 + B_2\theta)$$

$$J^x(x,\rho) = - \frac{c}{\pi Cr} [\cos\theta . A_2(B_1+B_2\theta) - B_2 \sin\theta\, e^{qr}.(A_1+A_2 \ln r + A_2 \Sigma \ldots)]$$

$$J^\rho(x,\rho) = - \frac{c}{\pi Cr} [\sin\theta\, A_2(B_1 + B_2\,\theta) + B_2 \cos\theta e^{qr}(A_1+A_2 \ln r + A_2 \Sigma \ldots)]$$

- After solving for a given set of boundary values, one can describe the radiation field in the nuclear region and hopefully compute the vaporization of gazes at the nucleus and its walk through the dust cloud.
- Then one would have the dynamical functions necessary to compute the motion of the dust; from this, one could compute the dust repartition function $f(r,a)$ which probably would become $f(x,\rho,a)$ and hence a new $\kappa(x,\rho)$.

Several iterations would then be necessary to reach a coherent solution. I never pursued the solution of the problem to this point but it does not seem that one would find anything like the Delsemme bald nucleus with an adjusted albedo. I claim that the very nature of the problem is different, and that if we start by assuming that

the nucleus is naked, we will find that the nucleus is naked, but this means simply that, maybe the wrong assumption has been done.

The argument against a dusty model of the nuclear region is that the dust is swept away by the molecules. This very fact shows however that the optical depth of the dust is larger than one :
The dust to gaz mass ratio of normally dusty comets is of the order of 1. The final velocity of the dust (reached at a few 10^2 km from the nucleus) is similar to the gaz velocity. Since all the momentum of the dust has been acquired from the gaz, in average, each molecule has hit at least twice a dust grain before free effusion into space. If a molecule leaving the nucleus cannot reach free space without hitting a grain, one does not see how a photon coming from the sun could reach the nucleus without being absorbed or scattered by the same dust.
In fact, the flux of molecules is large enough to clean the nuclear region only near the subsolar point, in a direction depending on the rotation of the nucleus and somewhat on the orbital motion of the comet. The rotation of the nucleus also produces a depleted region around the equator due to diminished escape velocity (see table I).

Surface gravity, escape velocity

ρ \ $r_n(v_p)$	1km(*29cm s^{-1}*)	3km(*87*)	10km(*291*)
	g = .041cm s^{-2}	.123	.410
1	v_c = *90 cm s^{-1}*	*270*	*900*
	M = 4.10^{15} gr	$1.1\ 10^{17}$	$4.2\ 10^{18}$
.3	g = .012	.037	.123
	v_c = *49*	*148.*	*493*
	M = $1.25\ 10^{15}$	$3.3\ 10^{16}$	$1.25\ 10^{18}$
.1	g =	.012	.041
	v_c =	*85.*	*285*
	M =	$1.1\ 10^{16}$	$4.2\ 10^{17}$

r_n : radius of nucleus ρ : density of nucleus
g : gravity acceleration at the surface of nucleus
v_c : *escape volocity* v_p : *equator velocity (T=6HR)*
M : mass of the nucleus.

It must also be noted that the force acting upon a grain is essentially proportional to its cross section, yielding an outwards acceleration inversely proportional to its radius. The smaller particles escape faster and there is a size differentiation of the dust near the nuclear surface.

Some direct consequences of the presence of dust are the following:

- Most of the surface of the nucleus is isolated from direct sun light and yields little amount of material.
- The temperature of the nucleus is determined by the vaporization of the most volatile (Delsemme model) only on a small percentage of its total area; the remaining is controlled by the radiation field in the dust cloud.
- Temperature of the dust cloud at $\tau \sim 1$ is controlled by radiation field and is hotter on the sun side than on the tail side.
- Thermodynamics of the nuclear regions is quite complicated and includes chemical reactions on grains and recondensation in the cold parts.
- A large part of the gaz is vaporized as a direct fan jet directly from the nucleus (following more or less the Delsemme picture).
- Another part of the gaz diffuses through the dust cloud and escapes finally with the thermal velocity of the cloud.
- The ratio of these two components could be around 1 with the strength of the jet varying if the surface of a rotating nucleus is differentiated (Cucchiaro and Malaise 1982).
- Photochemistry would prevail in the jet, while collision chemistry and surface chemistry can play an important role for the molecules crossing the cloud.

Figure 3a shows a possible solution of the spherical symetry dust cloud (no molecular vaporization, no nuclear rotation). Figure 3b shows the same in the case of vaporization and nuclear rotation. Before examining the possiblity of observing the nuclear region or its diagnose through observations in the inner coma, its is useful to show to the observers how the scales are.

Figure 4a shows a large scale photograph of comet Bennett 1970II; the small white rectangle near the head is the size of the whole format of the pictures shown in Figure 4b to f. The latter are pictures of the same comet obtained by Fehrenbach and Malaise

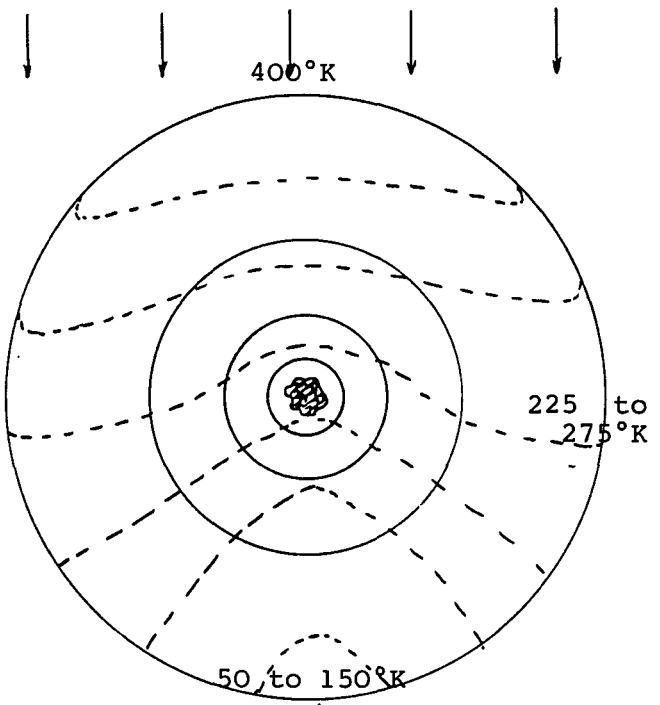

Figure 3a. Spherical symetric dust cloud with negligeable molecular flow. ——— dust isodensity curves
– – – – temperature curves.

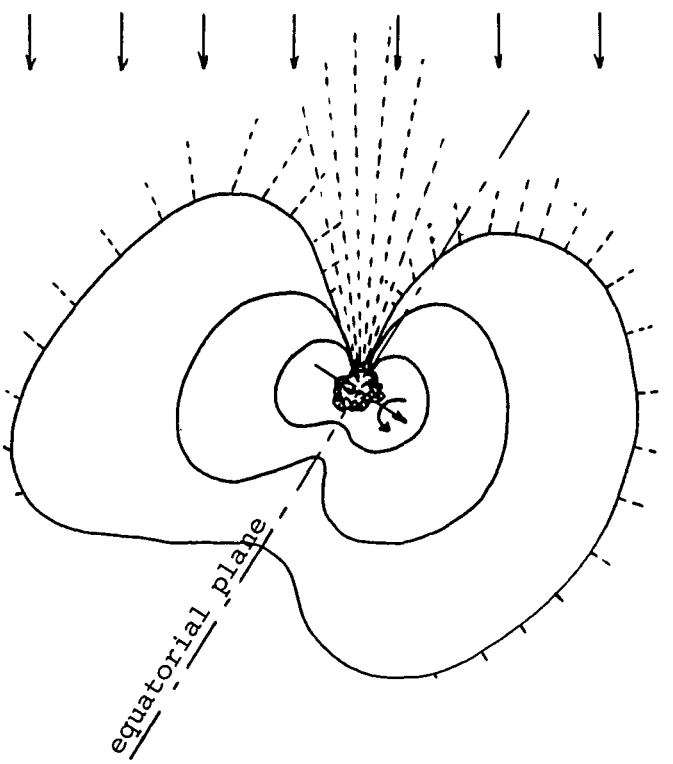

Figure 3b. Rotating nucleus with high molecular flow.
——— dust isodensity curves
------ molecular flow.

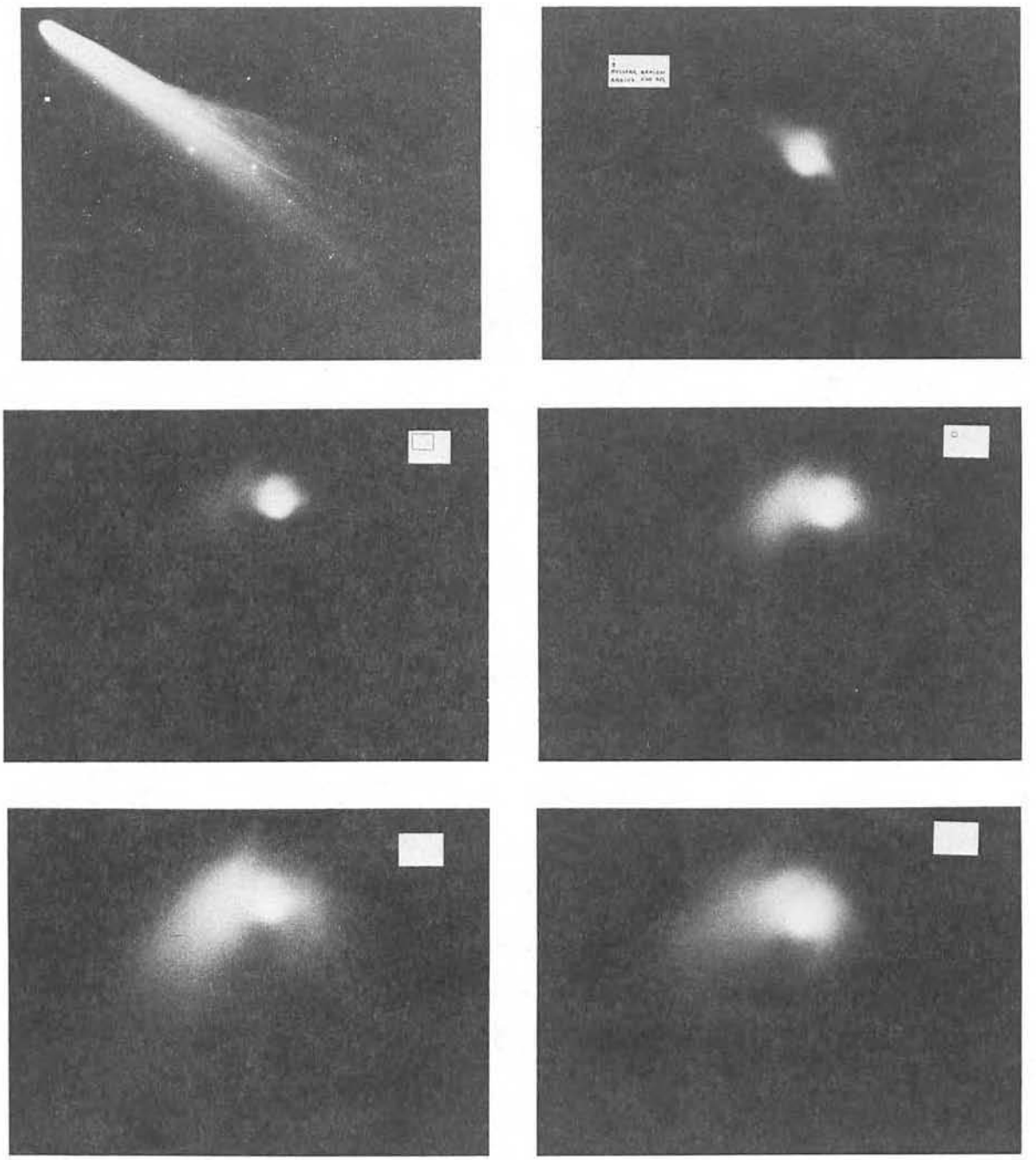

Figure 4 a-f.

directly at the Coudé focus of the 150 cm telescope of the Haute Provence Observatory. Figure 4b shows as a dark dot in the white rectangle the size of the nuclear region we want to observe. Comparison between Figure 4a and b shows dramatically how spatial resolution (including seeing and guiding) is the most important quality for those observations. Figure 4c to f shows as a white rectangle the whole field of the Halley Multicolor Camera on board Giotto four hours before encounter. The small rectangle or the dot show the whole field respectively two hours, one hour and four minutes before encounter. Let us recall that the whole field comprises 10^5 resolution elements and that an image comprising 10^4 resolution elements can be transmitted to the earth each four second.

POSSIBLE CONTRIBUTIONS FROM GROUND BASED OBSERVATIONS.

- Spectroscopy

Classical spectroscopy can be used to study the nuclear region mainly in two ways : - detection and identification of faint cometary emissions in the center of the head - comparing the spectrum at the center to the spectrum farther in the head.

In the nuclear region, the processes might be more complicated than in the head where fluorescence is known to dominate (except for [OI] emissions). Chemiluminescence can take place and its measurement allows to identify which chemical reactions are at work. Collisions within the central region brings about detectable modification in the fluorescence spectrum and gives information on the total density in the comet.

These observations need to be done with the highest possible space resolution with a stigmatic spectrograph, whose vignetting can be corrected. The detector should be linear or proper technique to linearize it without introducing large errors should be at hand. It is an absolute necessity to be able to substract the fraunhofer spectrum, due to the scattering of sun light by the dust of the central coma, from the emission spectrum of the comet.
The effect of this is shown on figures 5 and 6.

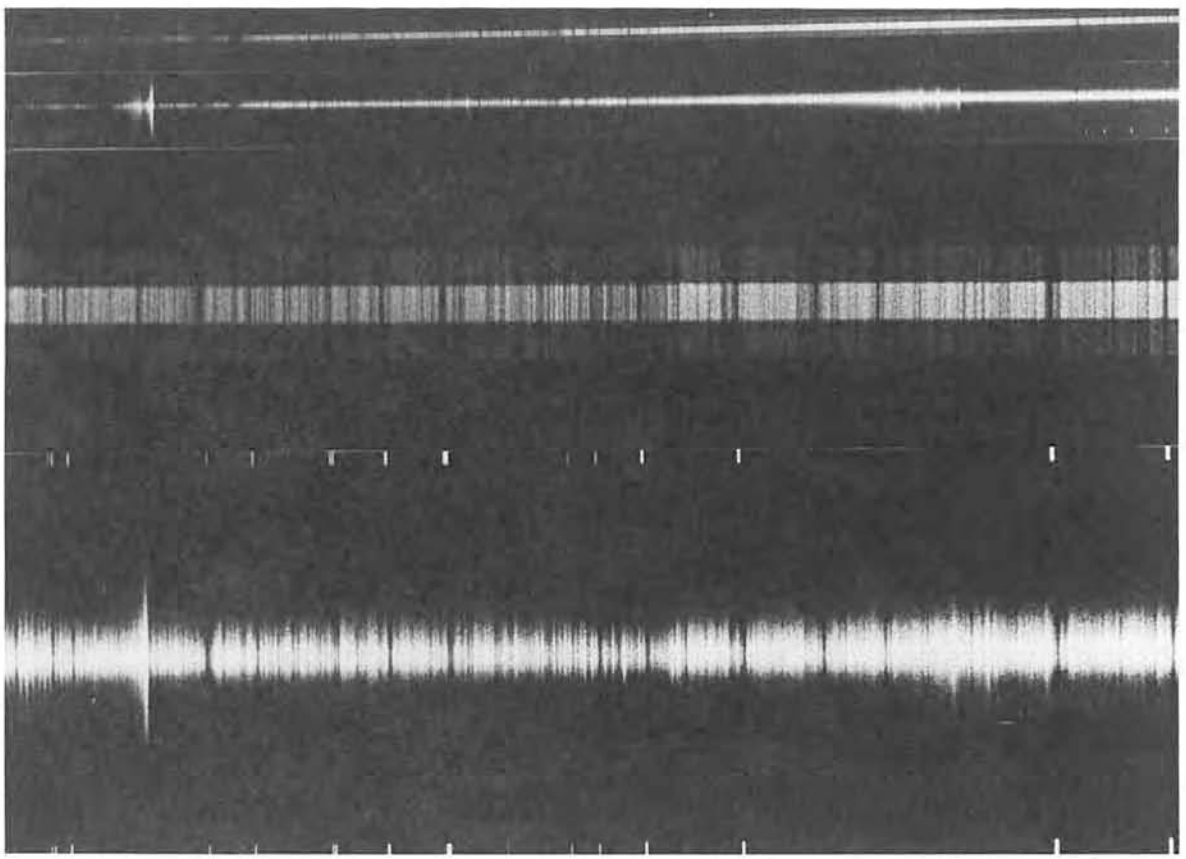

Figure 5.

Figure 5 shows in the upper part two photographic spectra extending from 372 nm to 496 nm; the top one is the spectrum of the sun obtained with two exposure times by pointing the telescope on the twighlight after the comet observation. Under this spectrum is the cometary spectrum; both plates were from the same batch and processed together. The bottom of the picture shows an enlargement of the 420 - 440 nm region of the same spectra.

Figure 6a to f show intensity recordings of these spectra for various spectral regions. For each region, the lower recording is the spectrum as it is on the plate, and the upper recording is the same from which the solar spectrum multiplied by a coefficient $C(\lambda)$ has been substracted. $C(\lambda)$ is adjusted so that the most prominent fraunhofer lines are just erased from the cometary spectrum (if $C(\lambda)$ is choosen too large, the fraunhofer lines would appear in emission).

Figure 6a and b show the CN(o-o) and the C_3-405 nm regions : now, try to imagine how the total intensity of C_3 would be estimated on the lower tracing (which is what one usually does in order to

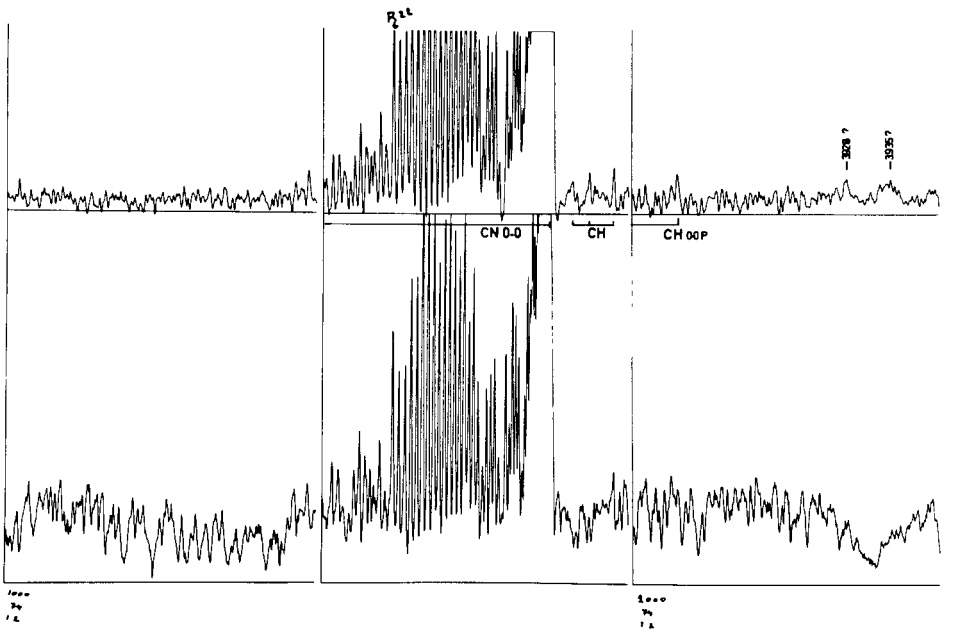

Fig.6a : Spectrum in the CN region; note the two unidentified large feature appearing in the processed spectrum and hiterto hidden in the H line of the scattered Fraunhofer spectrum (lower tracing).

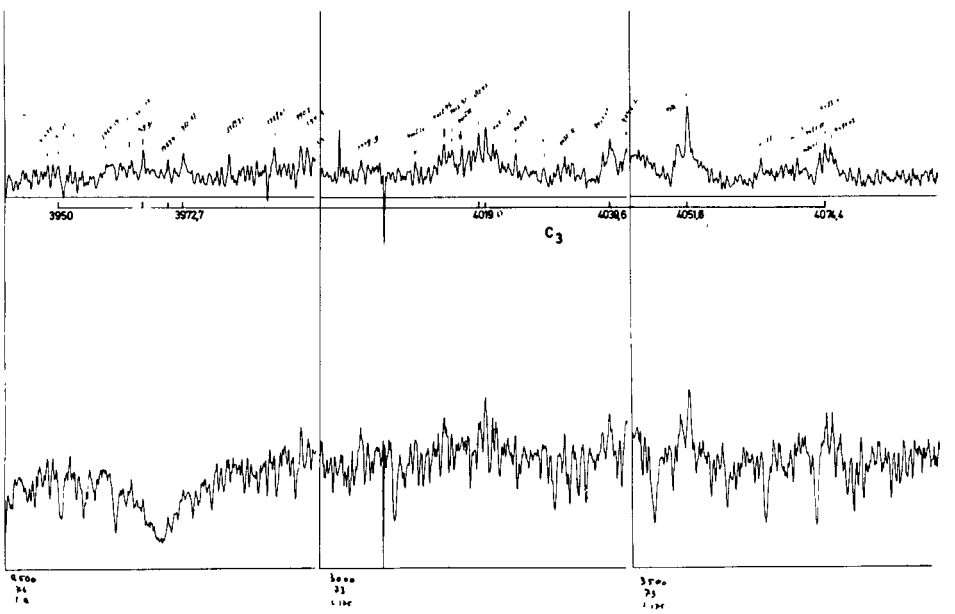

Fig.6b : Spectrum in the C_3 region; the zero intensity is at the coordinate axis showing that the total intensity of C_3 is quite large; on the unprocessed spectrum the intensity of C_3 cannot be measured.

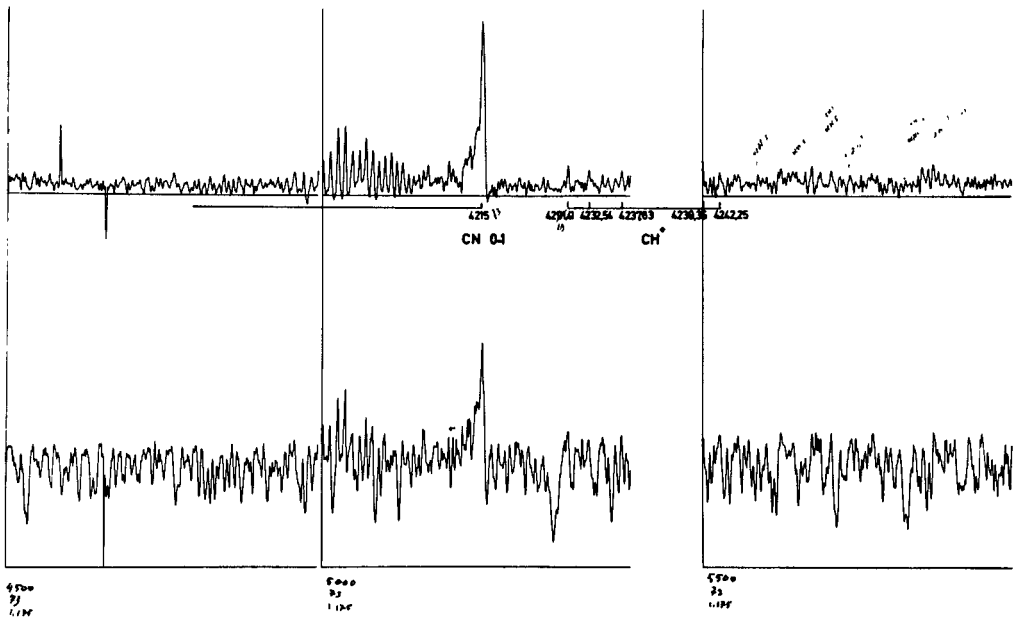

Fig.6C : CN O-1 region : on the processed spectrum, one can measure accurately the intensity ratios in the R-branch of CN; one can measure CH^+ and discover tens of unidentified lines longwards of 425 nm.

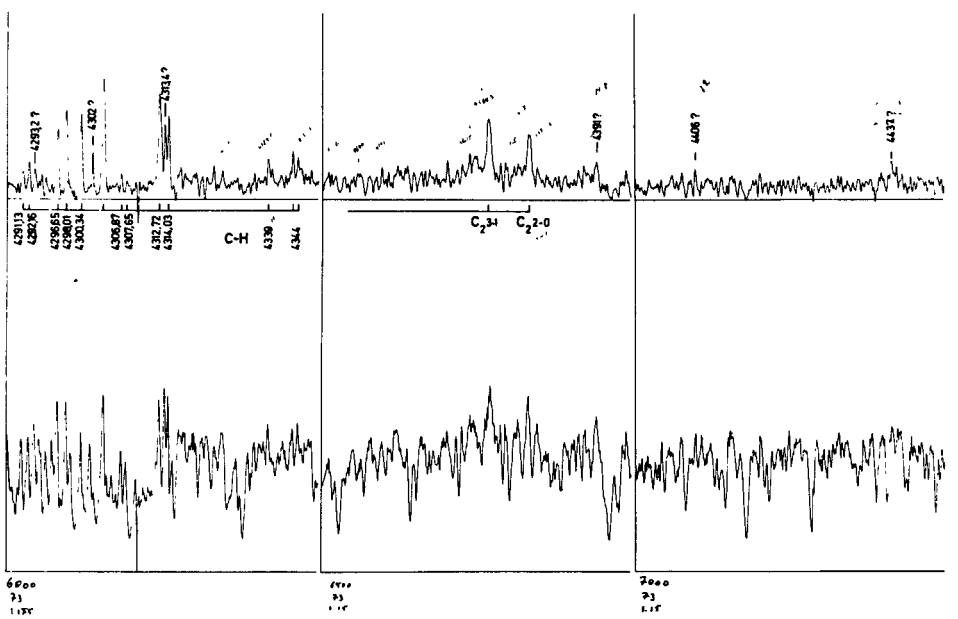

Fig.6d : the CH and C_2(2-O) regions : again, huge accuracy gain in measuring the intensity of CH lines; tens of unidentified lines longwards of 437.2nm.

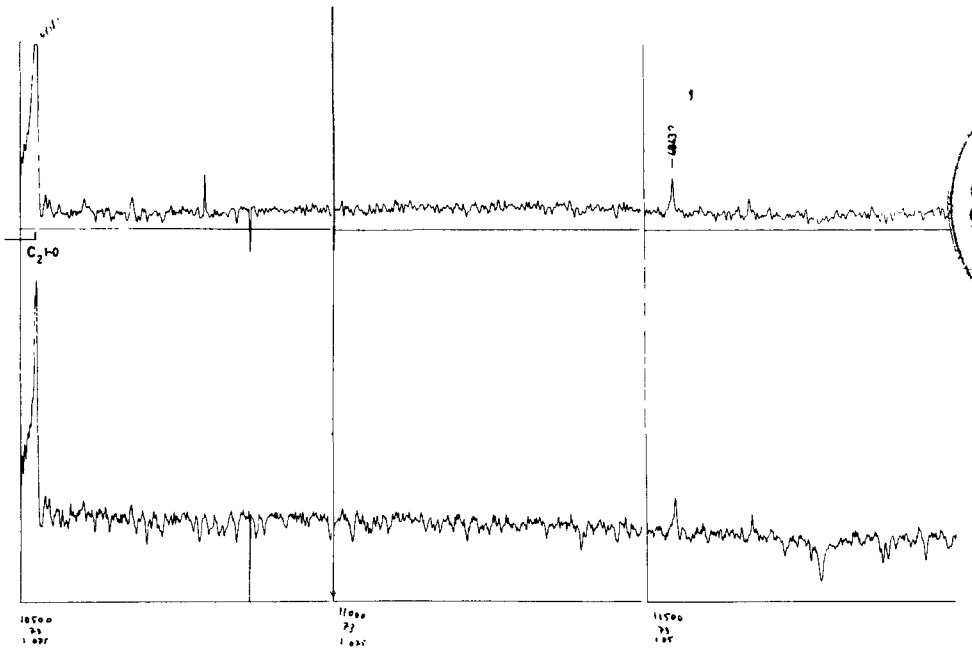

Fig.6e : The region of the spectrum longwards of 473.7nm shows a conspicious continuous proper emission of the nuclear region, peaking around 480nm. The band head at 484nm is also unidentified.

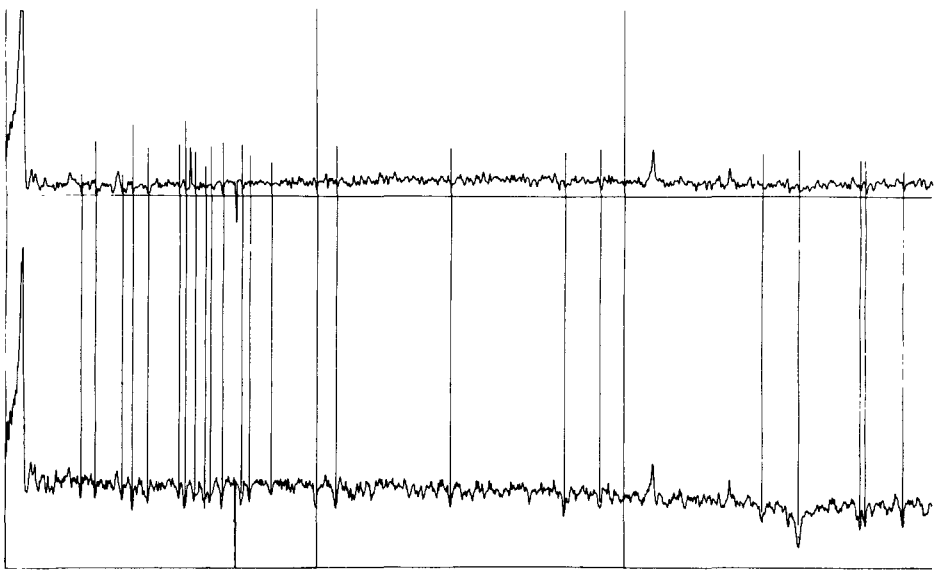

Fig.6f : Although a "feature" is unlikely in the albedo of the scattering dust, a larger fraction of the solar spectrum has been substracted from the comet spectrum in the region 473-487. The continuous glow however has not been removed.

estimate the abundance of C_3). On the upper tracing we see immediately that the close packing of lines shows as a pseudo-continuum and that the total intensity of C_3 is comparable to the one of CN. Also notice two unidentified large features around 392.9 and 393.5 which were hitherto hidden in the wings of the H fraunhofer line. Figure 6c and d show the CN (0-1), CH^+, CH and C_2 (2-0) regions; they highlight the accuracy gained in measuring the intensity ratios of rotation lines in CN and CH, the possibility of estimating the same for CH^+ (while these lines are barely detectable in the unprocessed spectrum), and the discovery of tens of unidentified lines between CH^+ and CH and longwards of the C_2(2-0)head. Figure 6e and f illustrates still another feature of properly processed spectra of the center of the head. Here we have the region longwards of the C_2(1-0) head, between 473 and 489 nm. On the left is the spectrum processed with the coefficient $C(\lambda)$ fitting the whole spectrum. We see that there remains a large continuum emission peaking between 478 and 484 nm. On the right is the same region processed with an increased value of $C(\lambda)$ which brings the interline to zero just longwards of the C_2 head (around the NH_2 emissions which usually hides the $C^{12}C^{13}$ and $C^{13}C^{13}$ heads). Despite this increase of $C(\lambda)$, one still see the large proper emission of the nuclear region. Wheter this is a continuum glow or the result of the close packing of the rotation lines of an unknown polyatomic molecule is not known. The band head at 484.3nm is also unidentified.

Two technical remarks should be added about recording cometary spectra : - the field should not be allowed to rotate during exposure (cassegrain modern spectrographs should be preferred to coudé); the direction of the slit on the sky should be known.

- some fiducial mark should be provided along the slit in order to enable to measure the relative displacement of maximum of luminosity with respect to each other (two hairs accross the slit a few mm apart seem adequate).

Table 2 is a resume of the particular requirements for nuclear region spectrography :

Table 2 : Spectrophotometric observations

Aim	: - compare spectrum of center to the spectrum of the head. - detect and measure very short emissions at the center.
Require	: - large space resolution (∿ 1") and spectral resolution (better than .5Å). - stigmatism of instrument. - no field rotation, perfect guiding on moving target. - photometric accuracy : linearized detector - unvignetting. - substraction of fraunhofer spectrum. - fiducial marks (at least one) on the slit.

- Photometry

Two main contributions of ground based photometry can be identified :

- Global photometry as a function of time (or heliocentric distance). This gives insight in the gross production of the nucleus. It must be remenbered, as a theoretical background, that the interpretation of the light curve, while rather simple when the comet is very far away and approaching, gets more and more model dependant as "activity" sets in and remains model dependant on the receding part of the orbit even when the comet becomes again very faint. It is thus of utmost importance to try to trace the light curve of periodic comets from early discovery on. The work beeing done now with the electronographic camera on P/Halley is a typical exemple of what should be pursued. As soon as the comet is bright enough, however it is necessary to separate the "continuum" light curve from the molecular light curves. In this respect it is most interesting to trace out accurately the early history of each species.
- Photometric profiles or (better) isophotes. These measurements when properly done and followed day after day, give informations on the activity in the nuclear region (see for instance Cucchiaro and Malaise 1982). Their interpretation is very much dependent on the model and if high accuracy is not achieved in all respect (see table 3) it is always possible to interpret the data with a simple Haser model whose parameter are physically meaningless.

Table 3 : Photometric Observations.

Aim	: (1) Light curve of each species, particularily at outset of emission. (2) Photometric profile of each species (isophotes).
Requirements	: - High space resolution ∿1" near center; (2). - Clean separation of bands; (1) and (2); ∿ 2.5 to 5Å resolution. - Photometric accuracy; (1) and (2); (linearized detector). - Substraction of continuum profile from molecular profiles; (2). - Exact morphological relations between various band profiles (2). - Consistant observations covering the longest possible arc of the orbit with frequency adapted to comet's activity. (1) and (2)

- Occultation of stars by the nuclear region

The casual visual observation by Dossin (1962) of stars dimmed by more than one magnitude when passing at less than 600 km from the center of the coma of Burnham 1959K, should be repeated quantitatively. The occultation curves would provide first hand informations on the nuclear region. The possibility of such observations are discussed in details by Cl. Jamar and D. Malaise (1982). They describe a devoted photometer used as an anciliary instrument to a spectrophotometer (see figure 7). These observations could also be attempted with a highly sensitive camera and a spatial resolution of the order of 1". The main points here are :

- The comet should be close to the galactic plane.
- The photometer should be capable of measuring stars of magnitude 15 with a signal/noise ratio of at least 50 and an exposure time of the order of 1 second.
- Band pass limitation is not essential since absorption by molecules is negligeable.

Table 4 show the probability that a 1000 km nuclear region moving at 5 arcmin/hr would occult a star as a function of mpg and galactic latitude b of the star for 1hr of observation.

Table 4 : Star occultation by nuclear region (hr^{-1})

b	0°	60°
mpg		
15	.13	.013
16	.25	.017
17	.68	.030
18	1.58	.052

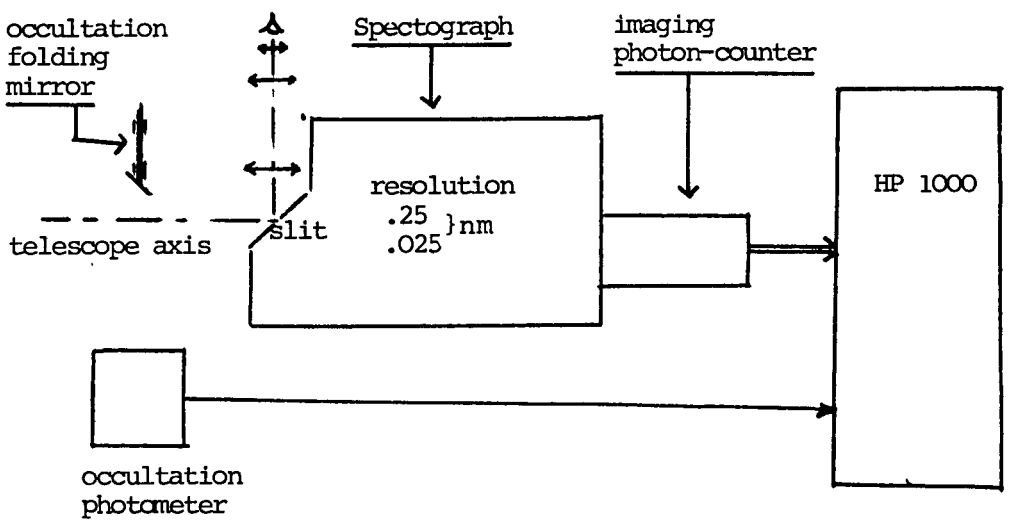

Figure 7. Spectrophotometer block-diagram.

CONCLUSION

There is no doubt that ground based observations can yield invaluable informations about the nuclear region of comets.
It is however clear that only very accurate measurements can be used succesfully.
The instrumental function should be calibrated carefully in order to account for : stigmatism, vignetting and linearization of detector. Spectral separation of bands should be insured and guiding accuracy should match the required space resolution. The fraunhofer spectrum should always be substracted from the band spectrum. In case of a photometric profiles, this requires due attention to the differential refraction in the earth atmosphere.

It is seen that obtaining an overall photometric accuracy of say 1% is not at all a trivial operation; only excellent physicists highly trained in metrology can obtain it.
On the other hand by simple mathematical considerations, it is known that when experimental errors exceed 2 to 3%, the observations impose only very loose constraints on the model. Then, the value of the model rests upon the intuition of the author, i.e. it is highly suspect.

The fashionable work nowadays comprises necesseraly a section on observation, and a section on interpretation and discussion (it is a closed work often defending a thesis). Pure observational work is considered with contempt. The result is that there exists practically no papers (except in astrometry) reporting of professional grade observations. The "universal paper" reports on observation in an illustrative way which excludes further use of the data. In the long run this will impoverish our field and we would like to encourage work and papers whose main aim is to report highly accurate data.
Finally we show on Figure 7 the diagram of an instrument well fitted to the observation of the nuclear region as described in this paper.

It comprises a spectrograph section with selection of plane gratings covering the λ-range 300-650 nm by 120 nm subranges with a resolution of .25 nm for photometry. The high dispersion grating yields a resolution of .025 nm on 12 nm sub-ranges for spectroscopy. In both modes, the entrance slit covers a field of 10' and the

spectrum is imaged on a two dimensional photon-counting detector (microchannel intensifier with TV pick up tube).

The entrance slit is optically polished and the field can be observed during exposure. When a star, due to its apparent motion is expected to cross the comet very close to its center, the spectrograph exposure is interrupted and a diagonal mirror deflects the light of the star into the occultation photometer where its occultation curve is recorded (this last for about 30 sec).
Then, the normal exposure of the spectrophotometer is resumed.

The photon-counting detector needs to be operated with a computer and a mass memory (1024 x 1024).

The instrument is planned to operate with the 2.2 m Max Planck telescope at the Cassegrain focus. The spatial resolution (nominal width of the slit) is 1 arcsec.

REFERENCES

Cucchiaro A., Malaise D., 1982, to appear in Astron. and Astroph.

Jamar Cl., Malaise D., 1982, to appear in Mém. Soc. R. Sc. Liège.

Dossin F., Obs J., 45, 1, 1962.

DISCUSSION

J. Klinger: Delsemme's model and all models derived from it try to establish a law for cometary activity depending only on the heliocentric distance. I think that this is not the right way to proceed and I'll try to show in the paper I will give during this workshop that even in the simplest case of only water ice at least two parameters describing the orbit are necessary to obtain a law for cometary activity.

OBSERVATIONAL NEEDS FOR THERMAL MODELING OF COMET NUCLEI

J.Klinger

Laboratoire de Glaciologie et de Géophysique de l'Environnement
2, rue Très-Cloitres
F38031-Grenoble Cedex France

In order to be able to develop a realistic model for cometary nuclei we need information about chemical composition and physical state of the matter that composes the comet.Until that kind of detailed information will be available the only thing we can do is to make some assumptions concerning the composition and the conditions of formation of the comet and to deduce what the activity may be if these basic assumptions are correct.The purpose of the present paper is to point out what kind of data we need to check some ideas on the heat balance of comet nuclei published recently (Klinger,1980) as well as other models of the nucleus.

Since Whipple (1950) developed his so called "dirty snowball model" many authors consider H_2O as the dominant constituent of comets.For this reason a great number of models consider nuclei of pure water ice (see for example Weissman and Kiefer 1981). As it is generally accepted, that comets condensed at temperatures much lower than 100 K the water ice in the nuclei is considered to be amorphous. According to Ghormley (1968) amorphous ice transforms to cubic ice in an irreversible manner at about 153 K. During the phase transition a heat release of about 67 J/g takes place.As proposed by Patashnik et al.(1974) this excess heat may be responsible for cometary outbursts. As pointed out independently by Smoluchowski (1981) and myself (Klinger 1980) the heat conduction coefficient of the ice increases in an important manner during the phase transition. This effect may even be enhanced at least at high temperatures if the nucleus is a porous medium and contains substances more volatile than H_2O, CO_2 for example. In this case a part of the heat is transported by the vapor phase in the pores (Smoluchowski 1982).

The orbital mean temperature T_m for periodic comets has been defined as follows (Klinger 1981) :

Proceedings of the ESO Workshop on "The Need for Coordinated Ground-based Observations of Halley's Comet", Paris, 29 – 30 April 1982.

$$\varepsilon\sigma T_m^4 = \frac{1}{\Pi}\cdot\int_0^{\Pi}(P(t)-\Phi(t))\cdot dt \qquad (1)$$

with : ε = emissivity
σ = Stefan Boltzmann constant
Π = period of the orbit
P(t) = incoming power
Φ(t) = power lost due to dissipative processes (evaporation for example)

In the same paper a thermal time constant τ has been defined as :

$$\tau = R^2 c \varrho / K\pi^2 \qquad (2)$$

with : R = radius of the nucleus
c = specific heat
ϱ = density
K = heat conduction coefficient

This time constant determines the penetration of heat waves into the nucleus. When $\Pi \ll \tau$ the nucleus acts as a good integrator and after a sufficiently long time the temperature of the center of the nucleus will approach T_m. A sphere of crystalline ice with R = 1 km has a time constant of $400 < \tau < 1400$ years. For a sphere of amorphous ice we have $\tau > 10^4$ years. For short period comets ($\Pi \ll \tau$) T_m determines if the center of the comet is in the amorphous, cubic or even hexagonal state. On the other hand the physical state of the ice in the nucleus determines wether heat conduction to the interior is important in the heat balance equation and in this may influences the activity of the nucleus.

Nuclei containing crystalline (cubic or hexagonal) ice may be less active than nuclei containing amorphous ice. When the ice of a nucleus is partially transformed the activity of the comet will be erratic until all its ice is in the crystalline state. When heat conduction is important in the heat balance the maximum activity will show a phase lag with respect to perihelion.

It has been shown (Klinger 1982) that for albedo values $\leqslant 0{,}3$ short period comets like Encke, Oterma, Schwassmann-Wachmann 2 and Tempel 2 have orbi-

tal mean temperatures > 153 K. For this reason heat conduction may be important in the heat balance equation and that may explain the low activity of these bodies.

T_m for Schwassman-Wachmann 1 varies between 121 and 132 K for an albedo $0 \leqslant A \leqslant 0,3$. This relatively high orbital mean temperature may favor transformations of small portions of the nucleus in an irregular manner. The erratic activity of Schwassmann-Wachmann 1 may be due to this phenomenon.

Halley in the same conditions has T_m values between 81 and 86 K. The ice in the inner part is therefore in the amorphous state. As the thermal time constant of the nucleus is far too high to allow a significant penetration of the heat wave into the nucleus evaporation of the surface layers will be dominant when the comet approaches the sun and only a thin crystalline crust will subsist after each perihelion passage. For this reason the present model predicts a rather constant activity during a long time span.

In order to check the model presented here or any other model, a good knowledge of the evolution of cometary activity and of the chemical composition of the coma is necessary. A good knowledge of the albedo of the nucleus would be very useful as well as some ideas on subsurface thermal gradients in the nucleus.Information about this last point are probably only obtainable by broadband Radiometry in the centimeter range during space mission to comets and will not be further discussed here. It seems clear that the best way to study a comet with earth based and earth orbiting instruments will be a quasi-continuous monitoring during the whole apparition in the spectral range from UV to radio frequencies with a high spacial and spectral resolution. It is evident that such a program is not realistic as telescope time will be limited even for such a prominent comet as Halley is.On the other hand if too much raw data will be available there will not be enough staff able and willing to transform all these data into useful scientific knowledge. This happened in 1910 !On the other hand a well coordinated observational program during well chosen time spans may do nearly as well.In the case of Halley early recovering may perhaps allow to deduce the albedo of the nucleus. When the comet becomes active the easiest way to get some ideas about the evolution of the activity and to refine Whipple's (1980) determination of the rotation period and the rotation axis may be by photometric series obtained with the same instrument.At the same moment it will be necessary to determine the evolution of the elemental abundance especially for H,O,N and C and to compare the intensity evolution of the spectral lines to the evolution of the continuum.At least in some cases ultraviolet and visible spectrophotometry should be synchronized with infrared observations from an earth

orbiting satellite or an airplane flying higher than 14000 m in order to identify the parent molecules. In a similar way the parent molecule of OH detected by means of the 18 cm-wavelength doublet may perhaps be identified.

The most interesting phase of the apparition of Halley may be when the uppermost amorphous ice layer reaches a temperature of about 153 K. When this is the case, we expect a rapid increase in activity. At that moment it would be most useful to organize several well coordinated and if possible well synchronized campaigns with all available observational techniques. As we expect fluctuations of the activity with time constants less than one hour it would be good to synchronize all instruments with a precision of the order of seconds or better if possible and to use integration times as short as the detection techniques allow. The temporal resolution of earth based instruments may be improved if several similar instruments situated in different zones of the earth could be synchronized as well as it is technically feasible in order to eliminate fluctuations of the transparency of the atmosphere.

In Figure 1 we plotted the albedo as a function of heliocentric distance where the surface is supposed to reach the transition temperature between amorphous and cubic ice(153K).We see that the transition temperature is reached in the isothermal approximation at 4 A.U. and for the subsolar point at 8 A.U.,for an albedo of 0.3 as it is used in the model of Weissman and Kiefer (1981).Unfortunately we know nothing about the thickness of the crystalline crust and so it is difficult to predict when the amorphous layers are reached. But there is probably a phase lag with respect to the surface temperature so that the increase in activity may occur closer to the sun. As we see in the upper part of fig.1 the increase in activity may occur when the observational conditions from the earth will be quite favorable. A careful examination of series of photo plates showing the evolution of the activity of Halley's comet in 1910 may indicate us the most favorable time windows for coordinated intensive observation campaigns.If sufficiently precise astrometric data for the nucleus can be obtained the observation of cometary activity may be completed by an evaluation of nongravitational forces as a function of time.A quasi-continuous monitoring of OH production during the whole apparition by means of radiotelescopes would be useful. After perihelion at least some observations in conditions as close as possible to pre-perihelion observations will give us information on asymetric activity with respect to perihelion.

Even if the present propositions look ambitious from an observer's point of view we have to keep in mind that Halley's comet is perhaps the only comet with a highly excentric orbit that we may have the opportunity to study during our lifetime. It is important to elaborate a detailed program for a well coordinated

observational program with all available techniques as soon as possible. The problem of coordination may perhaps be much more difficult to solve than technical problems.

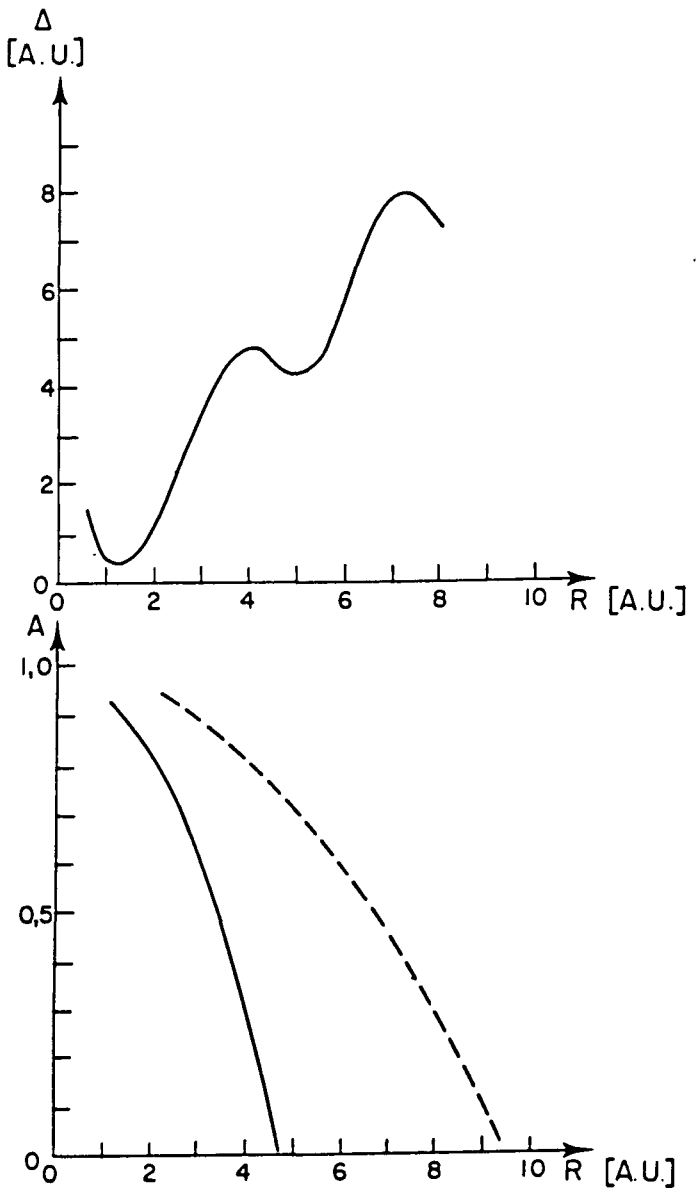

Figure 1 : up : Geocentric distance Δ of comet Halley before perihelion as a function of heliocentric distance R during the 1985/86 apparition.

down : Heliocentric distances where the surface of the nucleus may reach the transition temperature between amorphous and cubic ice (153 K) for different albedos A.

continuous line : isothermal approximation

dashed line subsolar point.

REFERENCES

Ghormley,J.A. (1968).Enthalpy Changes and Heat Capacity Changes in the Transformations from High Surface Area Amorphous Ice to Stable Hexagonal Ice.The Journal of Chemical Physics,48,503-508.

Klinger,J. (1980). Influence of a Phase Transition of Ice on the Heat and Mass Balance of Comets. Science,209,271-272.

Klinger,J. (1981). Some Consequences of a Phase Transition of Water Ice on the Heat Balance of Comet Nuclei.Icarus,47,320-324.

Klinger,J.(1982).Classification of Cometary Orbits based on the Concept of Orbital Mean Temperature (to be published).

Patashnik,H.,Rupprecht,G. and Schuerman,D.W. (1974).Energy Source for Comet Outbursts. Nature,250,313-314.

Smoluchowski,R.(1981).Amorphous Ice and the Behavior of Cometary Nuclei. Astrophys.,J.,244,L 31-L 36.

Smoluchowski,R.(1982). Heat Transport in Porous Cometary Nuclei.13th Lunar and Planetary Science Conference,Houston.

Weissmann,P.R. and Kiefer,H.H. (1981).Thermal Modeling of Cometary Nuclei. Icarus,47,302-311.

Whipple,F.L. (1950). A comet model I. The acceleration of comet Encke. Astrophys., J., 110, 375-394.

Whipple,F.L. (1980).Periodic Comet Halley.IAU, circular N° 3459.

DISCUSSION

D. Hughes: a) What is the density of amorphous ice?
b) can it be produced under "dirty" conditons (I had the incorrect idea that one needed pure H_2O to produce amorphous ice.
c) what conditions are needed to condense amorphous ice (i.e. temperatures and pressures)

J. Klinger: a) Ice formed near 10 K has density of about 1.1 g cm $^{-3}$. Ice formed near 77 K has a density of 0.94 g cm^{-3}, a value which is near that of ordinary crystalline ice (see e.g. Smoluchowski 1981, Astrophys. J. Letters 244, L 31).
b) The condensation in "dirty" conditions do not exclude the formation of amorphous ice. But in this case we may obtain still less ordered systems than in pure conditions. It has been shown that infrared absorption lines of molecular clouds fit better the absorption lines produced by dirty amorphous ice than those of crystalline ice (see e.g. Léger et al. (1979) Astron. Astrophys. 79, 256 and several papers by Greenberg et al.)
c) Amorphous ice is found at low pressures; the upper limit where amorphous ice subsists is not well known but it may be of the order of a few kilobars. The upper limit for temperature condensation is of the order of 120 K. Most authors give 153 K for the transition temperature from amorphous to cubic ice but the onset of the phase transition at lower temperature is reported too.

M. Wallis: Can the heat of the phase transition not provoke a phase change wave propagating inwards?

J. Klinger: Yes. But this requires a sufficiently good heat transmission coefficient of the material in the inner part of the nucleus. All amorphous substances have a very low heat conduction coefficient (between 10^{-2} and 10^{-3} W/cm K). We estimate the heat conduction coefficient of amorphous ice at 150 K to be about 3.10^{-3} W/cm K. In a fluffy medium with small vapor content it must be even lower. Crystalline ice at the same temperature has a heat conduction coefficient of about 4.10^{-2} W/cm K. Further the compactness of the material increases (see for example J. Ocampo and J. Klinger 1982, "Absorption of N_2 and CO_2 on ice", Journal of Colloid and Interface Science 86, 377). When this crystalline ice is heated further, the vapor may contribute to the heat transport between the ice grains. All these arguments lead me to the conclusion that the occurence of an outburst is more likely than the propagation of a heat wave toward the interior with a complete transformation of the nucleus. But I agree with you that further observations and theoretical studies are necessary to clear up this point.

THE COMA OF COMETS

M.C. FESTOU
Service d'Aéronomie du C.N.R.S.
BP N° 3 - VERRIERES le BUISSON
FRANCE

I - INTRODUCTION.

The coma of comets is the transient atmosphere which surrounds the nucleus when this latter approaches the sun. Spectrophotometry of both the neutral and ionized species which form this coma provides information on the nature and on the chemical composition of the nucleus. In this short communication, we shall examine the informational content of coma spectra and discuss how it can be used to derive the abundances of the various species. A more detailed discussion of the aeronomical processes taking place in cometary atmospheres has been presented elsewhere (Festou, 1981). Then, we shall consider what can reasonably expected to be done in the coming years from ground based and/or from earth-orbiting observatories.

II - THE COMA SPECTRUM.

a) Identification.

The main production mechanism of the observed light is fluorescence. However, a few spectral lines result from forbidden transitions and this attests that a few species are directly produced in an excited state. Since cometary atmospheres are collisionless media (with the exception of the very inner coma), only the first few electronic levels of the fundamental state of molecules are populated and the presence of each emitter is signalized by only a few bands. There are three main exceptions :

- The Swan band system connects the $^3\pi_u$ and $^3\pi_g$ states of the C_2 molecule. The $^3\pi_u$ state is not the ground state (which is $^1\Sigma_g^+$) and any theory on the origin of C_2 radicals (photo-

Proceedings of the ESO Workshop on "The Need for Coordinated Ground-based Observations of Halley's Comet", Paris, 29 – 30 April 1982.

dissociation of one or more parent molecules or gas phase reactions) must predict the formation of that state. Since the C_2 molecule is homonuclear, no relaxation of highly excited rotational levels can occur and numerous electronic transitions are observed throughout the visible spectrum. A similar situation occurs in the near IR region where the Philipps bands are located. The C_2 diagram is shown in A'Hearn (1982).

- The NH_2 α-bands are spread in the 4000-8000 Å region. They can usually be distinguished from other emissions because of their small spatial extension.

- In CO-rich comets, the CO^+ comet-tail system is composed of a large number of bands between 3200 and 5500 Å . At moderate spectral resolution, those bands have a doublet structure (Greenstein, 1962) ; at a higher resolution, they reveal a rich and complex structure (Arpigny, 1964).

Only approximative fluorescence calculations have been made for those species. No calculations at all are available on the C_3 radical (3900-4150 Å region), on the OH^+ (3300 - 3700 Å) and CO_2^+ (3000 - 4000 Å) ions emissions. Thus,making the distinction between new faint features and weak lines of these molecules is always a difficult task. The correct assignment of observed lines as due to hypothetical species requires a complete calculation of the fluorescence equilibrium of those possible emitting molecules. One way to solve the problem consists to associate spatial and spectral resolution : all the lines of a given species have the same spatial distribution.

A lot of work remains to be done in the near UV (3000 - 4000 Å) where numerous ion features are observed but are not identified. The 1200 - 3000 Å region is even more promissing since neither a continuum (or only a weak) nor any complicated band systems are observed. Since little energy is available at those wavelengths and since observations must be made from outside the earth atmosphere, it is only recently that results have been obtained in that spectral region (see a review of UV spectra in Feldman, 1982 and a review on the IUE observations in Festou et al., 1982).

b) Production processes

The high chemical reactivity of most species known to exist in cometary comae excludes the possibility of the existence of free radicals in the nucleus. It is why Wurm (1934, 1943) proposed the idea that the nucleus was evaporating stable molecules which are subsequently photolysed by the solar light into the observed molecules and ions. Consequently, the spatial distribution of the coma species should reflect the properties of their production path. Thus, spatial mapping of the emissions is a very useful tool in attempting to disentangle the puzzle that is the search of the production processes taking place inside the coma. The inversion of brightness integrals is very difficult and demands the knowledge of numerous parameters such as the lifetime of the radicals and molecules under the action of the solar light, the effect of other destruction processes (gas phase reactions, interaction with the solar wind), the properties of the nucleus (gas production rate as a function of time, spatial and temporal anisotropies of the production), the velocity field of the coma particles (to compute densities as well as the excitation rates).

Besides the photolysis of complex molecules, there exist some other potential competing production mechanisms. The possible role of dust particles is still unknown. The importance of gas phase reactions (see a recent review in Huebner et al., 1982) will be really undestood only when high spatial and spectral measurements in the inner part of the coma will be available. At the present time, there is no indication that major species are produced via chemical reactions, as attested by the non dependance of the intensity of the most important emissions on the heliocentric distance.

The production of a few species in an excited state may provide information on their parent molecules. As an example, oxygen atoms are produced in the ^3P state in most photodissociations of parent molecules. However, part of those atoms can be produced either in the ^1D or in the ^1S states and then, are observed the well known forbidden lines (Festou and Feldman, 1981). The interpretation of the observations is made difficult by the fact that

ion recombinations are very efficient in producing those excited atoms. Simultaneous measurements of ionic emissions are consequently needed to solve the problem of the origin of the observed atoms. Another example is provided by the ^1D carbon atoms which are thought to be produced by electrons recombinations of CO^+ ions (Feldman, 1978) : it will be concluded on the reality of this possible production process when both CI 1931 Å and CO^+ (Ist negative tail system) emissions will be recorded simultaneously.

c) Physical conditions prevailing inside the coma

High resolution spectra can provide information on the physical conditions which exist inside the coma. The accurate measurement of Doppler displacements and of emission linewidths leads to a better knowledge of the velocity field of coma particles. Since most observed velocities result of non thermal processes - they are determined by the energy budget of reactions which produce the coma species -, one thus have another invaluable information on the nature of the parent molecules. This nature can also be reached by analysing the isophotes of the emissions (the cases of HI and OH led to successful results a posteriori confirmed by direct linewidths measurements). The analysis of the rotational structure of emissions confined to the nuclear region can reveal the existence of collisions. The case of CH has been studied by Arpigny (1976). C_3 and CS emissions can be used in the same manner. The structure of some multiplets (OI, CI, SI) should conduct in the near future to new results. The spatial distribution of the $O(^1D)$ atoms is espacially interesting because they are easily quenched by H_2O and CO_2 molecules (Festou and Feldman, 1981).

d) Coma abundances.

We have briefly examined what has to be known to relate the measured intensities to the actual line of sight column densities. It should be added that the knowledge of the incident solar spectrum is a prerequisite to such an analysis which, in some cases, can be complicated by radiation transfer problems. A recent list of species identified in the coma can be found in Festou (1981) or in Wyckoff (1982). The total coma content of

those atoms and molecules varies from comet to comet. However, there is a clear indication that all comets have the same composition, with the exception of dust and CO (Feldman *et al.*, 1980 ; Festou *et al.*, 1982). Recent works showed it was necessary to simultaneously study the various end-products of production chains to identify the multiple parent molecules and production processes. (Weaver *et al.*, 1981 for the H_2O case ; A'Hearn and Feldman, 1981 for C_2 radicals ; Festou *et al.*, 1981 for the CO and CO_2 cases) In Table 1 are given the estimated water production rates in a sample of 11 comets observed at various heliocentric distances. Those numbers can be combined with those appearing in Table 1 of Festou *et al.* (1982) (Composition of a Halley type comet at 0.9 A.U.) to deduce an order of magnitude of the abundance of the main coma species of any comet at any heliocentric distance in the 0.3 - 2 A.U.range (the CO production cannot be scaled).

TABLE 1

COMET	DISTANCE (AU)	$Q_{H_2O}(S^{-1})$
BENNETT (1970 II)	0.6	$5\ 10^{29}$
K.B.M. (1975 IX)	0.85	$8\ 10^{28}$
WEST (1976 VI)	0.4	$1.5\ 10^{30}$
	1.43	2.10^{29}
P/d'ARREST (1976 e)	1.3	$2\ 10^{29}$ (1)
P/ENCKE (1980)	0.8	$2\ 10^{28}$
BRADFIELD (1979 IX)	0.7	$2\ 10^{29}$
	1.	$6\ 10^{28}$
	1.37	$2\ 10^{28}$
P/TUTTLE (1980 h)	1.02	$5.7\ 10^{28}$
P/STEFAN-OTERMA (1980 g)	1.58	$3\ 10^{28}$
MEIER (1980 g)	1.52	$8.5\ 10^{28}$
PANTHER (1980 u)	1.73	$1.\ 10^{29}$
SEARGENT (1978 XV)	0.87	$3.3\ 10^{29}$

(1) During outburst.

III - FUTURE OBSERVATIONS.

The qualitative works undertaken in the 70's should be continued in a systematic way in order to conduct comparative studies of comets. The correct gathering and interpretation of the observations demands a tremendous cooperation effort : important spectroscopic data concerning some coma species are still missing, rate coefficients of numerous reactions, their dependancy with temperature are unknown, coma models (fluorescence efficiency, density) have to be refined (spatial anisotropies, time dependancy of the source of parent molecules). Coordinated observations should be planned to detect the thresholds of appearance of the most important emissions (OH and CO^+) and to follow their evolution with the heliocentric distance (thermal properties of the nucleus). Coordination is necessary to monitor the activity of the nucleus (continuous survey of the production of species which have short lived parent molecules - CH, CS, C_3, S -) and thus introduce a time dependant source function in coma models. The increase of the sensivity of the detectors should lead to new linewidths measurements at various distances from the nucleus (HI : B α ; OI : red and green lines ; OI, CI, SI ultraviolet multiplets) and provide information on the photochemical properties of their parents. Emphasis should be put on ultraviolet observations since all the main atoms (but N) can be observed between 1.200 and 2.000 Å : it will thus possible to establish what the total gaseous output of the nucleus is. Occultation experiments can provide spectral signatures of the most abundant parent molecules (Smith et al., 1981).

The transient nature and the complexity of the phenomenon called "a comet" make difficult or even impossible for a single observer to gather a completely meaningful set of data. When analysis time comes, there are always missing pieces of information. Then, assumptions are used insteadt. It is hoped that the coming of Halley's comet and the (overrated) importance which is and will be given to the event will result for the first time in the setting of large networks of observers who will add their expertises to attempt solving some of the above mentionned problems.

REFERENCES

A'HEARN M.F. (1982) - In "Comets", pp 433-460. LL. Wilkening Ed. University of Arizona Press.

A'HEARN M.F. and FELDMAN P.D. (1980) - Ap. J,242, L187-L190.

ARPIGNY C. (1964) - Ann. d'Ap., 27, 406-416.

ARPIGNY C. (1976) - NASA - SP 393, 793-839.

FELDMAN P.D. (1978) - Astron. and Astrop., 70, 547-553.

FELDMAN P.D. (1982) - In "Comets", pp 461-479. L.L. Wilkening Ed. University of Arizona Press.

FELDMAN P.D. et al. (1980) - Nature, 286, 132-135.

FESTOU M.C. (1981) - ESA SP-164, 213-219.

FESTOU M.C. and FELDMAN P.D. (1981) - Astron. and Astrop., 103, 154-159.

FESTOU M.C., FELDMAN P.D. and WEAVER H.A. (1982) - Ap. J.,256, 331-338.

FESTOU M.C., FELDMAN P.D., WEAVER H.A. and KELLER H.U. (1982) - To appear in the proceedings of the third IUE conference held in Madrid, Spain, may 1982.

GREENSTEIN J.L. (1962) - Ap. J., 136, 688.

HUEBNER W.F., GUIGUERE P.T. and SLATTERY W.L. (1982) - In "Comets",pp 496-518, L.L. Wilkening Ed. The University of Arizona Press.

SMITH P.L., BLACK J.H. and OPPENHELMER M. (1981) - Icarus, 47, 441-448.

WEAVER H.A., FELDMAN P.D., FESTOU M.C. and A'HEARN M.F. (1981) - Ap. J., 251, 809-819.

WURM K. (1934) - Z. für Astrophysik, 8, 281-291.

WURM K. (1943) - Mitt. Hamburger Sternwarte, 8, 51-92.

WYCKOFF S. (1982) - In "Comets", pp 3-55, L.L. Wilkening Ed. The University of Arizona Press.

DISCUSSION

D. Malaise: When you state that abundances ratios are the same in all comets except maybe for CO_2 related species, I would like you to be a little more critical. Most excitation rates were not computed or cannot be computed in the present state. Abundances or rate of production of C_3 in particular have to be taken with much caution. What are the bounds you would put on your statement?

F. Festou: Absolute figures on coma abundances are highly model dependent. Uncertainties can be classified into two groups: i) those related to the measurements and to coma density models, ii) those related to our knowledge of fundamental parameters such as excitation constants. Errors in the first group amount to 20 or 30 % in most cases. Errors in the second group are evidently very large and, for instance, as you mentioned it, the abundance of C_3 is not known accurately. However, the "atomic" budget of the coma does not indicate that there exists a species which would be more abundant than water. Thus, one is left with the idea that H_2O dominates in cometary comae and that, in some comets, CO and CO_2 could be present in significant amounts. This point of view is well supported by IUE obsèrvations of comets which are numerous enough to allow us to do model and instrument independent comparisons of spectra, i.e. obtained at the same heliocentric or geocentric distance, for the same heliocentric velocity.

K. Jockers: Regarding remark by Malaise, Huebner told me recently that there are laboratory measurements of the oscillator strength of C_3 which would reduce the values quoted by A'Hearn and coworkers by a factor of 30. This produces better agreement with his model calculation but I agree that the chemical models are unlikely to make accurate predictions of minor species.

M. Festou: The so-called "chemical models" never predict the correct abundances of any species through gas phase reactions. If neutral species densities are appropriately predicted by some models, it is because adequate parent molecules which are subsequently photodissociated have been assumed to exist in the mixture released by the nucleus. This does not mean that those models are useless but it seems to me that they are mainly useful for providing a sink for most ions via charge exchange reactions. However, things could be different if reactions implying excited radicals or atoms were introduced in those models.

ON THE IDENTIFICATION OF CO IN THE VISIBLE SPECTRUM OF COMET BRADFIELD 1980 t

C.B. Cosmovici:
Space Research Group (AWF), DFVLR, D-8031 Wessling

L. Biermann:
Max-Planck-Institut für Astrophysik, D-8046 Garching

C. Arpigny:
Institute d'Astrophysique, Université de Liège,
5 Av. de Cointe, B-Liège

Summary

Spectra taken with the 122 and 182 cm Asiago telescopes permitted the first identification of CO emission lines between 4000 and 9000Å. Absolute fluxes of 15 lines could be determined using a Reticon detector. Preliminary theoretical calculations on possible parent molecules and production rates are presented.

Introduction

Neutral Carbon Monoxide has been observed in the new Comet West 1975 n at 1510 Å (4th positive system) by means of a UV-rocket experiment (Feldman and Brune, 1976). The Cameron bands, observed in the Martian Atmosphere, could also be present at 2155 Å and 2064 Å in the spectrum of Comet West 1975 n (Smith et al., 1980). Search for CO in the radio- and in the IR-range at 2.6 mm (Ulrich and Conklin, 1974) and 4.7 μ resp. (Wollman et al., 1974) was not successful.
Biermann (1976) investigated the high-dispersion spectra of Comet Mrkos (1957 V) (not a new comet like Bradfield 1980 t) taken by Greenstein and Arpigny (1962) and remeasured by Woszczyk (1962) where between 5300 and 6550 Å many unidentified lines are present, in order to investigate the possibility of CO-identification.
The results of this investigation favor the identification of the triplet transitions of CO, but the numbers do not seem to be quite large enough to rely entirely on the argument of a small statistical probability (0.2 %) that the presence of the observed bands is merely due to chance.
Biermann suggested therefore a further investigation of the rotational structure of the CO-bands for the triplet system and more detailed observations of cometary UV and visible spectra.

Proceedings of the ESO Workshop on "The Need for Coordinated Ground-based Observations of Halley's Comet", Paris, 29 – 30 April 1982.

A detailed investigation of 20 spectra of the "new" Comet Bradfield 1980 t) taken at the Asiago observatory permitted for the first time a more convincing identification of the Triplet-system in the wavelength region 4000 - 9000 Å (Cosmovici et al., 1982).

The Observations

The observations were carried out between January 8 and 16, 1981 at the Asiago Observatory (Italy).

16 spectra were taken with the 122 cm telescope using a prism spectrograph coupled with an S20 image tube. The dimension of the slit around the central part of the coma radial to the tail varied between 750 x 28000 km^2 and 850 x 49000 km^2.

Three spectra were obtained with the Reticon 512 spectrophotometer of the 182 cm telescope on January 14 and 15, 1981 with the slit oriented E-W, 32 arcsec long and 3 arcsec wide (26100 x 2450 km^2) centered on the bright nuclear condensation.
(For more details see Cosmovici et al., 1982).

Figure 1A shows an example of spectrum taken with the prism-spectrograph and Figure 1B shows the corrected Reticon spectrum obtained January 15 at UT 16^h 38^m with 1 min exposure time.
Black emission lines are CO features.
The identification of the lines of Fig. 1B and the absolute fluxes of the most relevant features are given in Table 1.
The error in the flux determination is about 50 % due to the bad observational conditions. The relative intensities of the lines are known with better precision, typically ± 10 %.
The flux in the continuum is about $8.5 \cdot 10^{-4}$ erg/sec cm^2 Å sr.

In Table 2 the known Triplet and Asundi-bands (Krupenie, 1966) are tabulated with the observed CO-lines.

The identification is strengthened by the fact that the triplet bands of CO are degraded to the red according to Krupenie (1966).

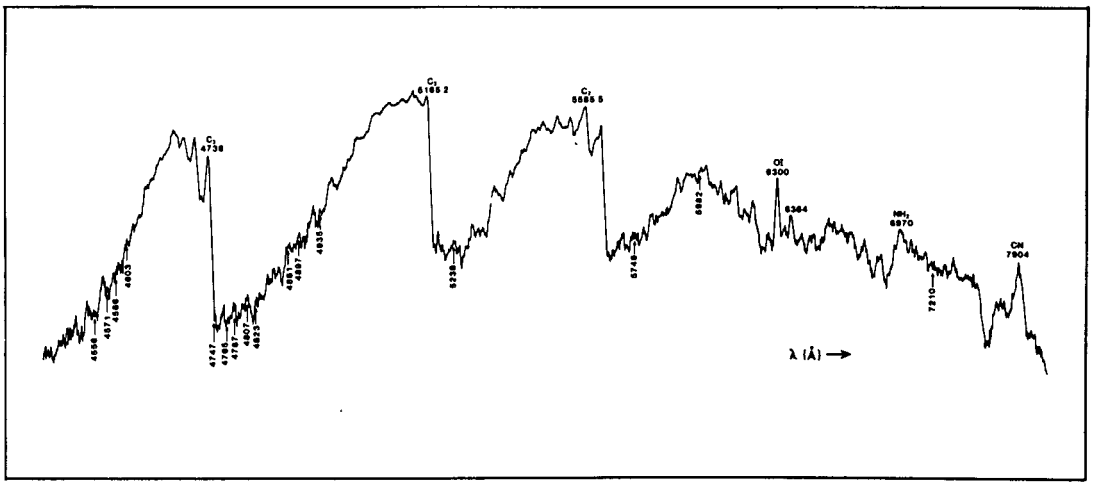
λ (Å) →

FIG. 1 A

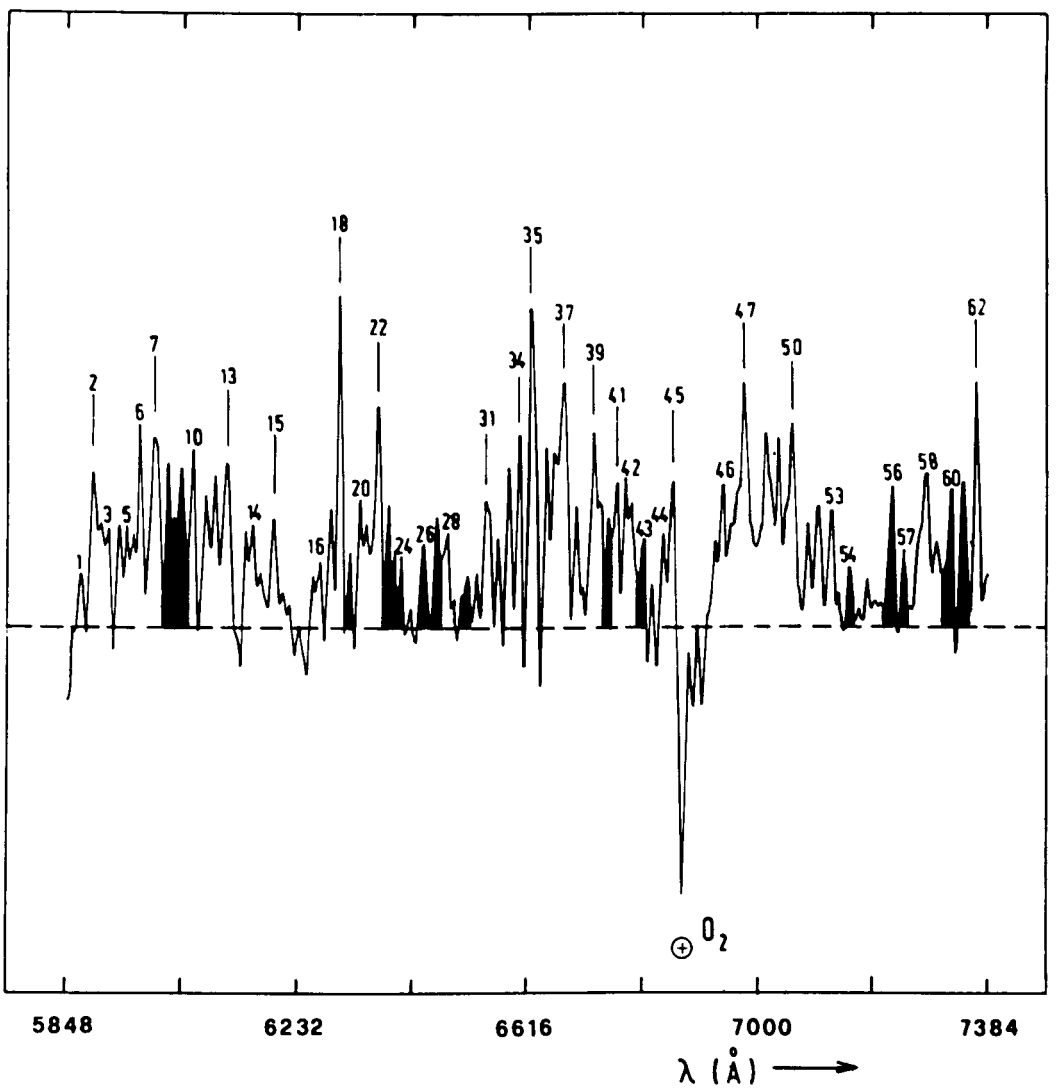
1
2
3
5
6
7
10
13
14
15
16
18
20
22
24
26
28
31
34
35
37
39
41
42
43
44
45
46
47
50
53
54
56
57
58
60
62
⊕ O2
5848
6232
6616
7000
7384
λ (Å) ⟶

FIG. 1 B

TABLE 1

RETICON SPECTRUM 5850 - 7350 Å (3 Å RESOLUTION)

Line No. (Fig.1B)	λ(Å) ± 2 Å	Suggested identification	λ(Laboratory)	F x10^{-3} (erg $s^{-1}cm^{-2}sr^{-1}$)
1	5871	H_2O^+ (0,9,0)	5871.01; 69.71	
2	5891	Na I	5890 + 5896	1.2
3	5916	H_2O^+ (0,9,0)	5917.29; 13.38	
4	5936			
5	5949			
6	5971			
7	5995	NH_2 (0,9,0)	5994.95; 95.01	1.5
8	6015	CO (4-0) T + NH_2 (0,9,0)	6010.5 + 6020	
9	6038	CO (4-0) T + "	6037.0 + 6034	1.2
10	6054			
11	6077	NH_2 (0,9,0)	6077.32	
12	6098	NH_2 (0,9,0)	6098.37	
13	6121	NH_2 (0,9,0)+C_2 (1-3)	6121.12 + 6122.1	
14	6158	H_2O^+ (0,8,0)	6158.64; 58.86	
15	6190	CO^+ (0-2)+ C_2 (0-2)	6189.4 + 6191.3	
16	6265			
17	6286	NH_2 (0,8,0)	6286.14;88.06;88.76	
18	6300	[O I] + NH_2 (0,8,0)	6300.0 + 6300.08; 00.79; 00.91	2.6
19	6318	CO (8-3) T	6319.8	
20	6334	NH_2 (0,8,0)+CN (5-1)	6334.51 + 6332.2	
21	6345	NH_2 (0,8,0)	6345.27; 45.43	
22	6364	[O I] + CO (11-2) T	6363.9 + 6366.9	1.7
23	6384	CO (8-3) T	6383.1	
24	6403	CO (3-0) T	6401.0	
25	6418			

Line No. (Fig.1B)	λ(Å) ± 2 Å	Suggested identification	λ(Laboratory)	F x10^{-3} (erg $s^{-1}cm^{-2}sr^{-1}$)
26	6439	CO (3-0) T	6433.1	
27	6464	CO (3-0) T	6464.6	
28	6478	C_2(5-8)+CN(6-2) ?	6481.8 + 6478.4 ?	
29	6512	CO (9-1) A	6513.5	
30	6526	H_2O^+ (0,7,0)	6525.24; 24.92	
31	6541	H_2O^+ (0,7,0)	6541.48; 41.85	
32	6561	H_2O^+ (0,7,0)	6562.7	
33	6579	H_2O^+ (0,7,0)	6576.77;77.26;77.66	
34	6595	H_2O^+ (0,7,0)+C_2(3-6)	6595.05;93.54+99.1	
35	6619	NH_2 (0,7,0)	6618-6620	2.4
36	6643			
37	6671	H_2O^+ (0,7,0)+C_2(2-5)	6671.14; 71.38; 71.69 + 75.9	
38	6689	H_2O^+ (0,7,0)	6686.56; 85.51	
39	6718	H_2O^+ (0,7,0)	6715.49; 14.65	
40	6740			
41	6760	C_2 (1-4) ?	6762.4	
42	6772			
43	6802	CO (10-2) A	6804.0	
44	6837			
45	6851			
46	6936			
47	6971	H_2O^+ (0,6,0)	6970.14; 73.71	1.9
48	7006	H_2O^+ (---)	7003.94	
49	7017			
50	7040	H_2O^+ (0,6,0)	7040.65; 37.89	
51	7070	H_2O^+ (0,6,0)	7069.5; 70.41	
52	7084	C_2 (6-10)+CN (4-1)	7083.2 + 7089.0	
53	7108	CN (4-1)	7107.0	

Line No. (Fig.1B)	λ(Å) ± 2 Å	Suggested identification	λ(Laboratory)	F x10^{-3} (erg s^{-1}cm^{-2}sr^{-1})
54	7136	CO (11-3) A	7134.0	
56	7208	CO (6-0) A + T	7210.4 + (7200)	1.1
57	7228	CO (6-0) A+T (3-1)	7229.0 + 7231.3	
58	7265	CN (5-2) + T (3-1)	7259.1+7270 ±2 Å	
59	7285	CN (5-2)	7289.0	
60	7310	CO (9-2) A	7314.0	
61	7334	CO (9-2) A	7337.0	
62	7350	NH_2 (0,5,0)	7350.0	1.9

A = Asundi

T = Triplet

TABLE 2A

BAND HEADS OF THE $d^3\Delta \rightarrow a^3\Pi$ CO - TRIPLET SYSTEM (KRUPENIE, 1966)

AND OBSERVED LINES

λ(Å)	I	v'-v"	λ(Å) observed	blended by
(7502.1)?			(7500) ?	
7515	---	1-0		CN (6-3)
(7483)				CN (6-3)
7270			7265	
(7231.3)	---	3-1	(7228)	CO (6-0) Asundi
(7200)			(7208)	
6964.3				H_2O^+ (0,6,0)
6925.2	---	2-0		O_2 Atm
6901				O_2 Atm
6736			6740 ?	
6703	---	4-1		
6669			(6671)	NH_2 (0,7,0)+C_2 (2-5)

λ (Å)	I	v'-v"	λ (Å) observed		blended by	
6464.6			6464			
6433.1	10	3-0	6439	?		
6401.0			6403			
6383.1			6384			
6348.7	1	8-3				
6319.8			6318			
6037.0			6038		NH_2	
6010.5	8	4-0	6015	?	NH_2	
5982			5984		NH_2	
5670.5			5670			
5647.6	6	5-0				
5624					C_2	(Swan)
5554.1					"	
5532.5	5	7-1			"	
5508					"	
5351.2			5340	?		
5330.5	5	6-0	5328		NH_2	(0,12,0)
5308			5301	?		
5258.3			5250	?		
5238.4	5	8-1	5237			
5216			5209	?		
5070.9			5079	?	C_2	(Swan)
5052.7	8	7-0	5046	?	"	
5033					"	
4996.9					C_2	(Swan)
4979.0	6	9-1			"	
4959.0			4960		"	
4935.5			4938		NH_2	(0,13,0)
4917.2	2	11-2			C_2	(Swan)
4897.5			4900		"	
4880.8			4883		C_2	(Swan)
4869.3	---	13-3				

4823.5			4822			
4806.7	8	8-0	4806			
4787			4790			
4764.8			4766			
4747.5	5	10-1	4745			
4729.1					C_2	(Swan)
4716.6					"	
4702	---	12-2			"	
4678					"	
4680.3					"	
4664	---	14-3			"	
4646.7			4647		"	
4602.6			4604		"	
4586.4	7	9-0	4588		"	
4571			4573		"	

λ(Å)	I	v'-v"	λ (Å) observed	blended by
4556.5			4554	
4541.0	5	11-1	(4540)	CO^+ (1-0)
4524.0				
4520.7			(4518)	CO^+ (4-2)
4505.5	---	13-2	(4503)	
4488.4			4490	
4494.4				
4478.8	---	15-3	4477	
4462.9				
4454.5			4456	
4445.5	1	---	4442	
4437			4436	

The wavelengths of the (4-1)band are not tabulated by Krupenie and were calculated on the basis of the given molecular constants.

TABLE 2B

$a'^3\Sigma^+ \rightarrow a^3\Pi$ ASUNDI SYSTEM

8281.0	---			
---	---			
---	--- >	6-1		
---	---			
8222.5	---			
7888.0	---			
---	---			
---	--- >	5-0		
---	---			
7833.9	---			
7598.0	---			
---	---			
7574	--- >	7-1		
---	---			
7552.5	---			CN (6-3)
7359.0	---			
---	---			
7337	--- >	9-2	7334	
---	---			
7314.0	---		7310	
7257.0	---			
---	---			
7229	--- >	6-0	(7228)	CO (3-1) Triplet
---	---			
7210.4	---		7208	
7158	---			
---	---			
7134	--- >	11-3	7136	
---	---			
7116.5	---			

λ(Å)	I	v'-v"	λ(Å) observed	blended by
—	—			
—	—			
7007	—	8-1	(7006)	H_2O^+ (—)
—	—			
6988	—			
6841.5	—			
—	—			
6820	—	10-2		
—	—			
6804.0	—		6802	
6726.3	—			
—	—			
6704	—	7-0		
—	—			
6685.7	—			H_2O^+ (0,7,0)
6551.0	—			
—	—			
6530	—	9-1	(6531)	H_2O^+ (0,7,0)
—	—			
6513.5	—		6512	
6445.3	—			
—	—			
—	6	16-5		
—	—			
6405.0	—			
6397	—			
—	—			
—	6	11-2		
—	—			
6366.9	—		(6364)	OI
6275.0	—			
—	—			
6257.8	6	8-0		NH_2 (0,9,0)
—	—			
6244.7	—			
—	—			
—	—			
6159.5	5	15-4		H_2O^+ (0,8,0)
—	—			
—	—			
6135.0	—			
6127.5	—			
6119.0	6	10-1		C_2 (1-3) + NH_2 (0,9,0)
—	—			
6105.2	—			
5888.7	—			Na I
—	—			
5876.2	5	9-0		H_2O^+ (0,9,0)
5869.4	—			
5855.8	—			NH_2 (0,10,0)

λ (Å)	I	v'-v"	λ (Å) observed	blended by
---	---			
5836.5	---			
---	5	16-4		
---	---			
5812.8	---			H_2O^+ (0,9,0)
5779.6	---			
5773.5	---			
5769.7	5	11-1	(5769)	Hg (NS)
5761	---			
5746.0	---		5746	

FIG. 2

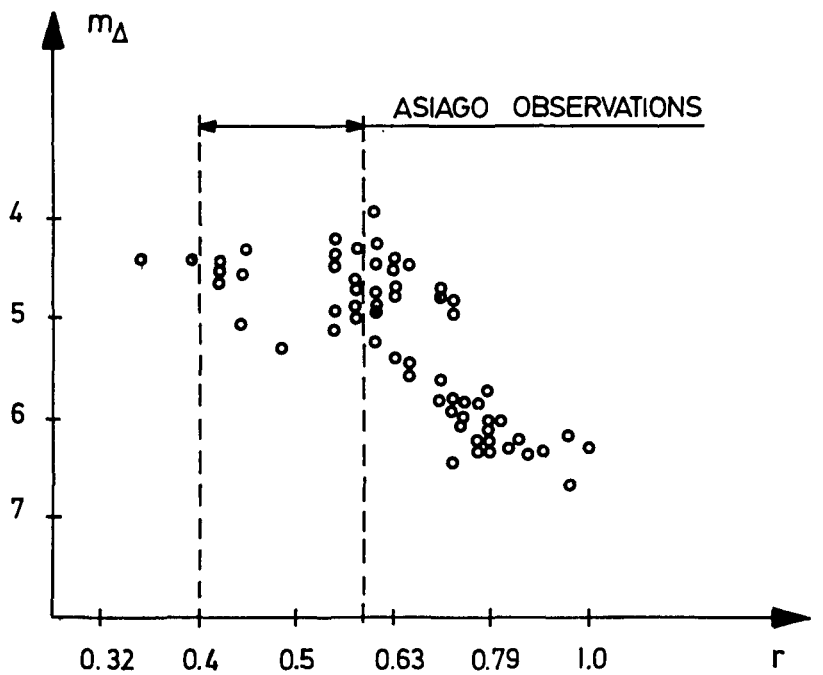

Light curve of Comet Bradfield 1980 t derived from 68 observations carried out by 11 different observers (Fulle and Milani,1982). m_Δ represents the magnitude the comet would have shown if observed always at 1 A.U. from the Earth. r is the heliocentric distance in A.U. The strong outburst starting January 13,which is evident in the figure was also observed in USA and Belgium. A more than twofold increase in the comet's brightness is reported in the period January 14-15,1981. The outburst was short-lived,and within a few days the magnitude had returned to the previous level (Bortle 1981).
A disruption of the comet's nucleus is not confirmed.

DISCUSSION

While the identification of the Asundi band system ($a'^3\Sigma^+ \rightarrow a^3\Pi$) of Carbon monoxide in the spectrum of Comet Bradfield (1980 t) can be deemed rather uncertain, the number of coincidences is much larger in the case of the Triplet system ($d^3\Delta \rightarrow a^3\Pi$), and the presence of these emissions in Comet 1980 t can be established much more convincingly, as we shall see.

Table 3 lists the Franck-Condon factors (McCallum et al., 1972) which are in this case rather different from those listed by Krupenie (1966) for the bands of the Triplet-system together with the quantity:

$$I_{v'v''} = \text{const.} \times q_{v'v''} \nu^4_{v'v''}$$

which gives a measure of the relative intensity of the (v'-v") band, apart from the population factor, $N_{v'}$.
The molecular constants have been taken from Huber and Herzberg (1979).
We have also indicated, for each band, two symbols:

(1) P means that the band is present in the spectrum of the comet, i.e. that at least one not blended peak appears at the positions of the band heads (there are three such heads per band, and these are all we can expect to detect at the resolution which was used);

(2) bl indicates that one or more of the band heads fall on top of other, well-known cometary emissions and that, consequently, the band in question is at least partially blended with or can be masked by these emissions.

We think it is significant that up to a value of the upper vibrational quantum number v' of about 10 all the bands that can be expected to have appreciable strength on the basis of the $q\nu^4$ factor are present in the cometary spectrum, even if blended in a number of cases.

The excitation mechanism of the CO Triplet bands was discussed by one of us a few years ago (Biermann, 1976).

TABLE 3

Franck-Condon Factors and Relative Intensities in the Triplet System $d^3\Delta - a^3\Pi$ of CO

v' \ v"	0	1	2	3	
0	0.019 1	0.091 3	0.194 3	0.249 1	a) b)
1	.063 bl 5	.165 7	.140 3	.022 -	
2	.112 bl 11	.140 bl 9	.016 -	.040 -	
3	.145 P 20	.064 P ,bl 6	.014 -	.095 3	
4	.152 P,bl 28	.009 bl 1	.067 5	.043 2	
5	.139 P,bl 32	.002 -	.080 8	- -	
6	.114 P?bl 33	.026 5	.048 6	.021 2	
7	.086 P?bl 31	.056 bl 14	.013 2	.054 6	
8	.061 P 27	.076 P 24	- -	.056 P? 8	
9	.042 P 22	.082 P,bl 32	.011 3	.032 6	
10	.027 bl 17	.077 P 36	.033 bl 11	.008 2	
11	.017 bl 13	.066 P,bl 37	.054 P ,bl 22	- -	
12	.010 9	.052 bl 34	.067 bl 32	.010 4	
13	.006 6	.037 bl 29	.070 P?bl 40	.031 13	
14	.003 4	.025 bl 22	.063 bl 42	.052 bl 26	

a) $q_{v'v"}$

b) $q_{v'v"}\nu^4_{v'v"}/q_{oo}\nu^4_{oo}$ (rounded-off)

Some transitions which are not reported by Krupenic were calculated and are included here.

It is clear that the usual fluorescence mechanism of production of the cometary emissions cannot work here because the rates of excitation of the upper Triplet states are much too low (see Fig.3). Direct collisional excitations are excluded also, because the particle densities are much too low, and the rather high energies required (~ 8 eV) are simply not available in sufficient numbers. The only plausible mechanism is the dissociative recombination (d.r.) of an ion containing CO (rate coefficient of the order of $10^{-7} cm^3 s^{-1}$) and releasing this molecule in the upper Triplet state, $d\ ^3\Delta$. This release would indead be followed immediately by the emission of the bands of the Triplet system. It is, at any rate, possible on energetic grounds up to $v' \simeq 10$ if the parent ion is HCO^+, up to $v'=5$ if it is CO_2^+, whereas the production of the Triplet bands from the recombination of H_2CO^+ would not be possible, since the difference between the ionization and the dissociation energy is only 6.35 eV in that case (see Fig. 3A).
Unfortunately, we have no experimental data nor any theoretical estimates for the relative probabilities of population of the various vibration levels through the d.r., so that we are unable to check the relative intensities of the bands other than to note, as we have done above that whenever $I^{\infty}_{v'v''}$ is high, i.e. whenever the radiative transition probability is high, the corresponding band occurs in the comet's spectrum.
Information on the absolute rates and on the branching ratios of the different possible channels followed in the d.r. process would be most welcome.
The limitation in the upper vibrational quantum number that we have just mentioned, provides a means of identifying the parent ion, and from the results presented above we suggest on this basis HCO^+ as a plausible precursor responsible for the emission of the CO Triplet bands after recombination.
This ion is predicted to be quite abundant in some theoretical models of cometary ionospheres (Ip and Mendis, 1977), and it is now known to be present in the interstellar medium (Snyder et al., 1976).

Using the estimated intensities of the CO Triplet bands and assuming they are produced by the d.r. process, we can now try to derive some information about the total amount of cometary gas associated with these emissions. We do this in two different ways:

a) First, on the basis of the brightnesses measured in the Triplet bands we can estimate approximately the number of parent ions.

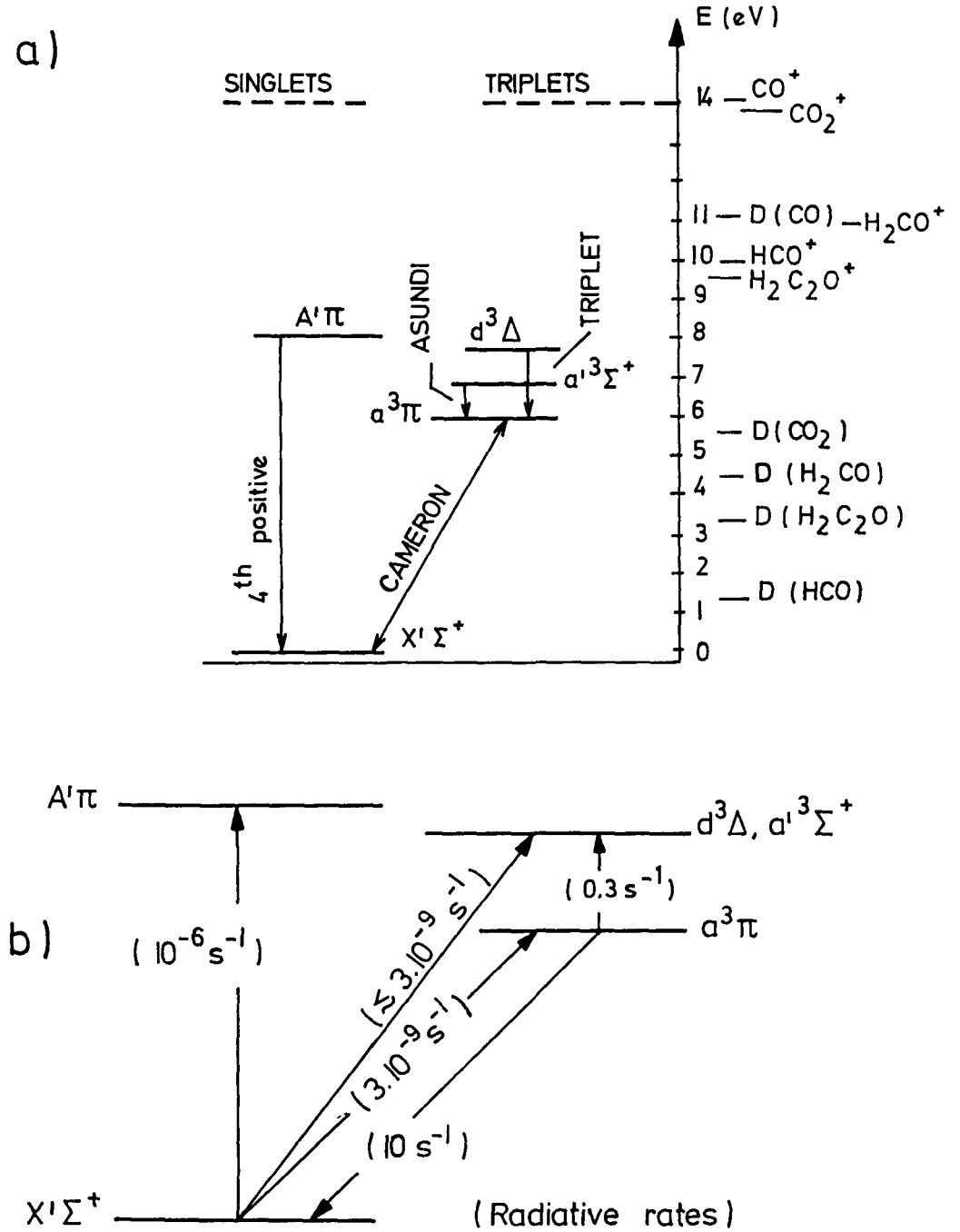

FIG. 3

a) Grotrian Diagram of the CO molecule (D = Dissociation energy) (only the up to now observed transitions).

b) Radiative rates for the relevant systems.

(HCO^+?) present in the coma.
The slit of the spectrograph used covered a length of about $2.6 \cdot 10^4$ km projected on the comet. Thus it is found that within a sphere of radius $\rho \simeq 10^4$ km there are

$$\mathcal{N}_i \simeq 3 \cdot 10^{30} - 3 \cdot 10^{32} \text{ ions},$$

using the informations of the brightness given in Table 1, depending on the values adopted for the recombination coefficient ($\sim 10^{-7}$ $cm^3 s^{-1}$) and for the mean electron densities (10^3-$10^5 cm^{-3}$).

These numbers are of the same order (although somewhat on the high side) as the total numbers of ions predicted by Ip and Mendis (1977) for their photochemical model of the ionosphere of a CO-rich comet with a nucleus a few km in radius.
On the other hand, the above values are also comparable to the total number of CO^+ ions that were found to be contained in a similar volume in the very active, CO-rich Comet Humason, 1962 VIII ($\sim 3 \cdot 10^{31}$) (Arpigny 1965).
On the contrary, they are somewhat larger when compared with the corresponding values given by Wyckoff and Wehinger (1976) for Comet Kohoutek, 1973 XII ($\sim 3 \cdot 10^{30}$ at r= 0.5 A.U. after perihelion).

b) Although the observations pertain to the innermost part (≤10000 km) of the emitting region, we can extrapolate outside this region and try to obtain an order of magnitude estimate for the production rate of the CO-containing parent molecules.
As discussed by one of us (Biermann, 1976), the ion and the electron densities are likely to decrease outward from the nucleus fairly slowly, disregarding the influence of the solar wind which disturbs the circular symmetry outside of perhaps 10000 km; under certain simplifying assumptions, n_e and n_i should vary like 1/r. Adopting a value of $3 \cdot 10^{-6}$ s^{-1} for the rate of primary photoionization at the solar distance in question (0.56 A.U.), we get a total luminosity and hence a production rate of

$$Q \gtrsim 3 \cdot 10^{30} \text{ } s^{-1} .$$

This, of course, is a very high production rate, but it should be recalled that it refers only to the days on which the spectra were taken and which, as it turned out later, were close to the occurrence of an unusual event (Cosmovici et al., 1982).

Furthermore, this estimate involves some uncertainties in the extrapolation and in the data used.

It is clear also that the high relative abundance of a molecule like HCO is not consistent with published results on the chemistry of dense interstellar clouds, but in this connection it should be considered that the most likely place of origin of the comets surrounding the solar system is not, as was believed until recently, the outer fringes of the presolar nebula, but another nearly fragment of the same interstellar cloud in which the presolar nebula came into existence 4 1/2 billion years ago (Biermann, 1981); obviously the chemical conditions in such a fragment require further study.

Conclusions

We have presented observational data and arguments which lead to the identification of a number of emission features seen in the visual region of the spectrum of Comet Bradfield 1980 t as belonging to the Triplet band system of Carbon monoxide.
These emissions are most probably produced as a consequence of the dissociative recombination of an ion such as HCO^+.
Rough estimates of the number of ions or of the production rates implied indicate rather high values, but the uncertainties are large.

The fact that CO emission lines were not detected before even in brighter comets leads to the conclusion that the Asiago observations are related to an exceptional event as shown in Fig. 2. It is possible that during the outburst large amounts of CO or its parent molecule were released from inside the nucleus.
A support to this hypothesis by UV-observations (IUE satellite) is unfortunately not available.
Thus only future high resolution observations of bright comets and cometary outbursts will be able to confirm the presence of visual emission of CO in cometary spectra.

REFERENCES

Arpigny, C.: 1965, A Study of Molecular and Physical Processes in Comets, Mem. Acad. Roy. Sc. Belg. 35, Fasc. 5.

Biermann, L.: 1976, Los Alamos Scientific Report LA-6289-MS.

Biermann, L.: 1981, Phil. Trans.R.Soc. Lond. A303,351.

Bortle, J.E.: 1981, Sky and Telescope, 3,271 and 4,295.

Cosmovici, C.B., Barbieri, C., Bonoli, C., Bortoletto, F., and Hamzaoglu, E.: 1982, Astronomy and Astrophysics, submitted

Feldman, P.D., and Brune, W.H.: 1976, Ap.J., 209, L45.

Fulle, M., and Milani, A.: 1982, Giornale di Astronomia, submitted.

Greenstein, J.L., and Arpigny, C.: 1962, Ap.J., 135, 892.

Huber, K.P., and Herzberg, G.: 1979, Constants of Diatomic Molecules (Van Nostrand Ed.).

Ip, W.H., and Mendis, D.A.: 1977, Icarus 30, 377.

Krupenie, P.H.: 1966, The Band Spectrum of CO, NSRDS-NBS 5, National Bureau of Standards, Washington.

McCallum, J.C., Nicholls, R.W., and Jarmain, W.R.: 1972, Franck-Condon Factors and Related Quantities - IV. Additional Diatomic Molecular Band Systems of CO and CO^+, CRESS, York University.

Smith, A.M., Stecher, T.P., and Casswell, L.: 1980, Ap.J., 242, 402.

Snyder, L.E., Hollis, J.M., Lovas, F.J., and Ulrich, B.L.: 1976, Ap.J. 209, 67.

Ulrich, B.L., and Conklin, E.K.: 1974, Nature, 248, 121.

Wyckoff, S., and Wehinger, P.A.: 1976, Ap.J., 204, 604.

Wollman, E.R., Geballe, T.R., Greenberg, L.T., Lacy, J.H., Townes, C.H., and Rank, D.M.: 1974, Icarus, 23, 599.

Woszczyk, A.: 1962, Mem. Soc. Roy. Sc., Liège, II. Fasc. 6.

FLUORESCENCE OF WATER MOLECULES IN COMETS

J. Crovisier
Observatoire de Meudon

Although most cometary models assume that water is the prevalent parent molecule in cometary atmospheres, the presence of this molecule has not yet been directly confirmed. This situation might change in the near future when it will be possible to observe the rotational and vibrational transitions of H_2O with suitable techniques at infrared and submillimeter wavelengths. The purpose of the present paper is to report an estimation of the excitation conditions of H_2O within cometary atmospheres, in order to prepare such observations and their interpretation. This work is part of a more comprehensive project to compute the synthetic spectrum of a typical comet in the infrared (Encrenaz et al., 1981, 1982), which was undertaken in order to prepare the infrared sounding of comet Halley by the Venera-Halley space probes (Crifo, 1981). We will more specifically study here H_2O fluorescence in the lower rotational transitions which might be observed by submillimeter telescopes at high altitude.

The excitation conditions of H_2O in the coma, as for the other molecules, are governed by :
a) collisions which tend to populate the energy levels according to the Boltzmann partition function (LTE) ;
b) excitation by the radiation field : UV excitation (electronic transitions) and infrared excitation (vibrational transitions) ;
c) spontaneous emission which leads the molecules to decay to the lowest energy levels.

Table 1 shows, for the water molecule, a summary of the level life-times, radiative pumping and collisional rates. For these evaluations we have assumed a heliocentric distance of 0.8 AU, a gazeous production rate $Q = 2\times10^{29}$ mol. s^{-1} (a possible value for P/Halley), a collisional geometric cross-section $\sigma = 2.5\times10^{-15}$ cm^2 (de Jong, 1973 ; Whipple and Huebner, 1976) ; for infrared pumping, only the solar radiation field (5500 K blackbody) was considered, but the nucleus and dust radiation may be important in the inner coma.

Proceedings of the ESO Workshop on "The Need for Coordinated Ground-based Observations of Halley's Comet", Paris, 29 – 30 April 1982.

Table 1 : Typical life-times and pumping rates of water molecules in comets at r = 0.8 AU.

transition	wave number (cm^{-1})	life-time of excited level (s)	solar pumping rate (s^{-1})
rotational	0.8 to 300	$\sim$100	-
vibrational			
ν_2	1630	0.06	2.8×10^{-4}
$2\nu_2$	3195	0.03	3.0×10^{-6}
ν_1	3690	0.2	1.3×10^{-5}
ν_3	3770	0.02	3.5×10^{-4}
$\nu_2+\nu_3$	4754	0.09	3.8×10^{-5}
$\nu_1+\nu_3$	6812	0.06	3.1×10^{-5}
$2\nu_1$	7312	$<$1.	2.2×10^{-6}
electronic	80600		1.6×10^{-8}
collisional rate	10^{-2} s^{-1} at 600 km from nucleus		
photodis. rate	1.9×10^{-5} s^{-1}		

We remark from Table 1 that :

a) UV pumping is negligible (the detectability of UV fluorescence is discussed by Smith et al., 1981) ;

b) in the infrared, a first-order evaluation needs only to consider the ν_2 and ν_3 vibrational bands which achieve 85% of the pumping ;

c) the life-times of the excited levels - including the rotational levels - are so small that UV and infrared pumping rates are not high enough to significantly populate these levels ;

d) radiative decay rates of the rotational levels are competitive with collisional rates at a distance $\rho\sim600$ km from the nucleus.

In order to specify this last point, we have computed the H_2O population distribution as a function of nucleus distance (ρ). We have only considered collisions and radiative decay within the rotational levels. In our model, molecules expand radially with v_{exp} = 1 km s^{-1} and an initial Boltzmann distribution (T_{kin} = 200 K) is assumed near the nucleus. The inelastic collision rate is

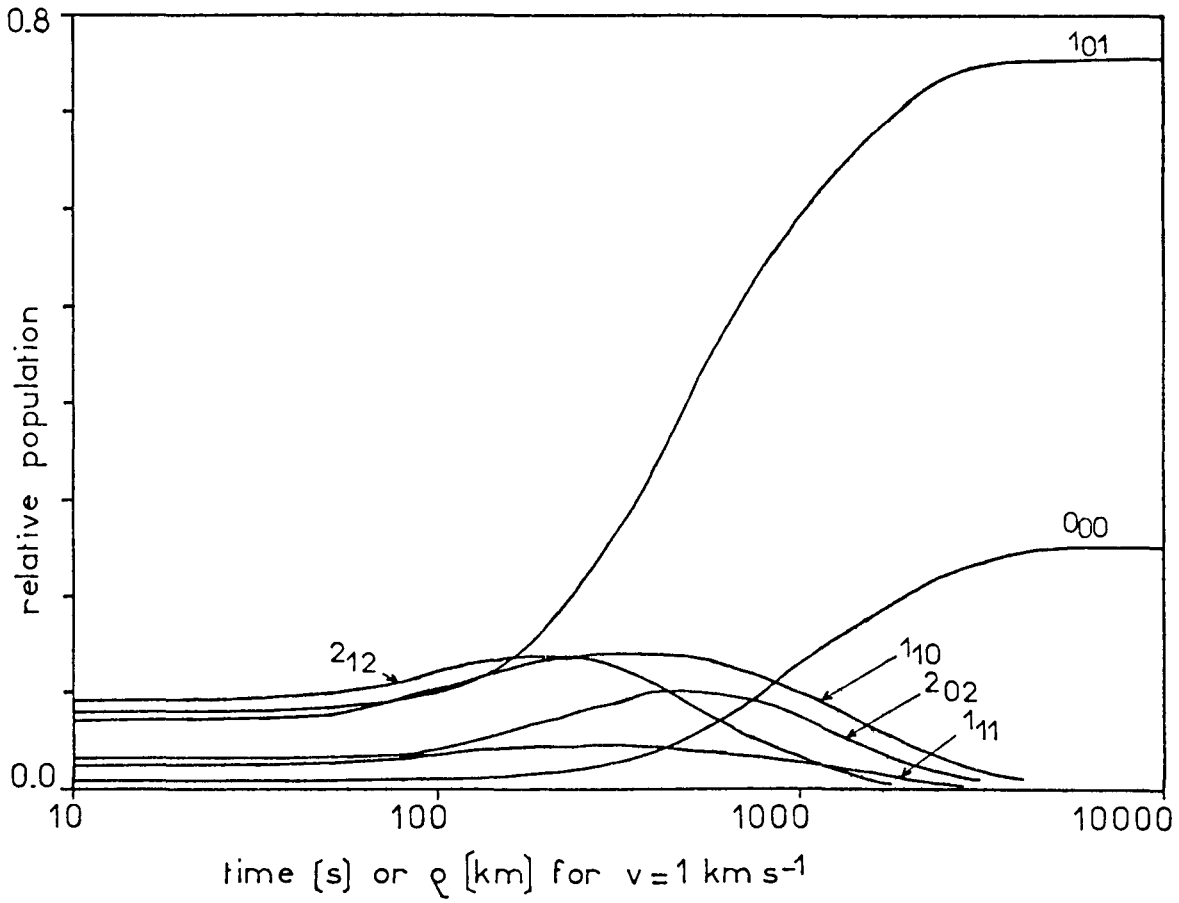

Figure 1 : Relative population of the lower levels of H_2O in the coma as a function of distance from the nucleus. Only collisions and radiative decay are taken into account.

$$\tau_{coll} = \frac{Q\sigma}{4\pi\varrho^2}$$

with $Q = 2\times10^{29}$ mol. s^{-1} and $\sigma = 2.5\times10^{-15}$ cm^2. Since rotational transition rates for $H_2O - H_2O$ collisions are unknown, we have assumed that each collision redistributes the shocked molecule on the rotational energy levels according to the Boltzmann partition function (T_{kin} = 200 K).

The results are shown in Figure 1 : within a few 100 km from the nucleus, collisions are sufficient to preserve thermalization. Beyond a few 1000 km, radiative decay prevails, and only the two lower levels 0_{00} and 1_{01} of the ortho and para states of H_2O are populated. An integration of the partition function over the whole coma shows that 98% of the water molecules are in these two lower states.

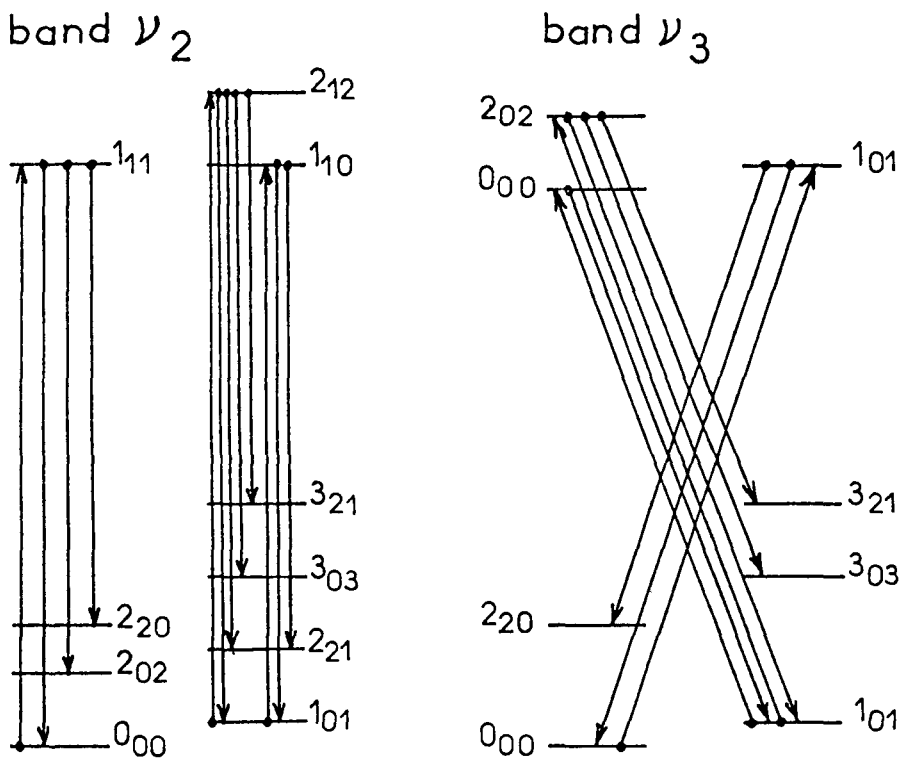

Figure 2 : Infrared excitation of H_2O from the 0_{00} and 1_{01} levels and subsequent fluorescence.

This model is not self-consistent, since H_2O radiative decay will efficiently cool the cometary atmosphere (Shimizu, 1976) whereas constant T_{kin} was assumed. Shimizu has shown that for $\rho \sim 200$ km the kinetic temperature may be as cold as 10 K and that the coma is heated by solar UV to temperatures ~ 400 K only for $\rho \gtrsim 5000$ km, where collisions are negligible. With such a temperature distribution the decay of H_2O to the lowest levels will be more rapid than in our model. Note also that a lower gazeous production rate or a greater heliocentric distance would decrease the inference of collisions. On the other hand, we have not taken into account collisions with ions which are not abundant in the inner coma, but which have a greater cross-section than neutrals.

In the following, we will assume that only the 0_{00} and 1_{01} levels are populated, which will enable us to compute line-by-line fluorescence in a very simple way. There are (Figure 2) only 3 lines starting from these levels in the ν_2 band, and 3 lines in the ν_3 band. The subsequent infrared fluorescent line intensities (9 lines for ν_2, 6 lines for ν_3) were given by Encrenaz et al. (1982). Since all these lines do not lead to the 0_{00} and 1_{01} ground state levels, there are cascading rotational transitions in the v = 0 state, shown in Figure 3.

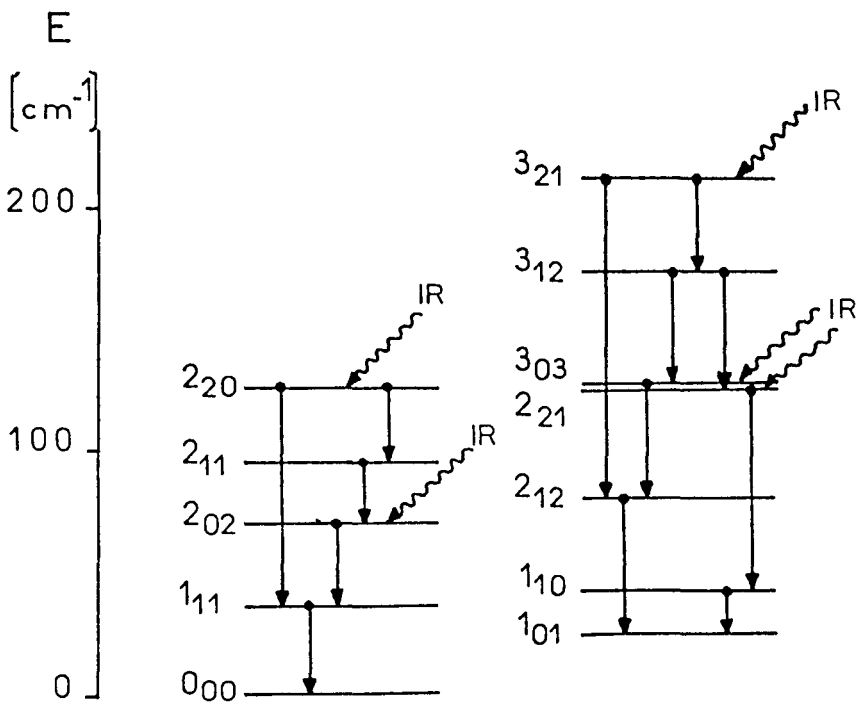

Figure 3 : H_2O fluorescence in the rotational levels of the vibrational ground state.

The fluorescence rates g of these transitions and the corresponding antenna temperatures (T_A/η for a lossless antenna) are given in Table 2. The antenna temperatures were computed for a comet of $Q = 2\times10^{29}$ mol. s^{-1} observed at $\Delta = 1$ AU with an 1' beam, assuming a 2 km s^{-1} line width and a 2.7 K background brightness temperature. The $1_{10} - 1_{01}$, $1_{11} - 0_{00}$ and $2_{12} - 1_{01}$ transitions, which lead to the lowest H_2O levels, are thick and strongly affected by radiation trapping, which explains their relatively low antenna temperature despite their high g-factor.

Irvine et al. (1981) have computed the rotational line emission of H_2O in comets assuming pure thermal excitation (T_{kin} = 150 K). Most of the corresponding emission rates are at least an order of magnitude greater than those of Table 2 ; we have shown above that thermal excitation is realistic only in the inner coma and thus concerns only a small fraction ($\sim$1%) of the water molecules.

The present fluorescence model does not predict any excitation of the H_2O rotational lines previously observed in the interstellar medium ($6_{16} - 5_{23}$ at 22 GHz ; $3_{13} - 2_{20}$ at 183 GHz ; $4_{14} - 3_{21}$ at 380 GHz). This is in agreement with the recent failures to detect the 22 GHz line in comets (Crovisier et al., 1981).

Table 2 : Expected submillimeter fluorescence of H_2O. (Pumping through the ν_2 and ν_3 bands only is assumed ; g-factors are computed for r = 0.8 AU.)

λ (μ)	ν (GHz)	transition	g-factor (10^{-5} mol.$^{-1}$ s^{-1})	antenna temperature T_A/η (K)
538	557	$1_{10} - 1_{01}$	5.71	0.6
399	752	$2_{11} - 2_{02}$	0.24	0.3
303	988	$2_{02} - 1_{11}$	1.77	1.6
273	1097	$3_{12} - 3_{03}$	0.14	0.1
269	1113	$1_{11} - 0_{00}$	5.19	0.2
260	1153	$3_{12} - 2_{21}$	0.02	0.01
258	1163	$3_{21} - 3_{12}$	0.16	0.1
244	1228	$2_{20} - 2_{11}$	0.24	0.1
179	1670	$2_{12} - 1_{01}$	15.7	0.2
175	1717	$3_{03} - 2_{12}$	13.3	3.9
108	2275	$2_{21} - 1_{10}$	5.71	0.4
101	2968	$2_{20} - 1_{11}$	3.42	0.3
75	3977	$3_{21} - 2_{12}$	2.40	0.1

Among the transitions listed in Table 2, those at 988 and 1717 GHz might be detectable with suitable submillimeter receivers, if the observations can be made above the absorbing atmospheric water.

References

Crifo, J.F., 1981, in "The Solar System and its Exploration", ESA SP-164 p. 229

Crovisier, J., Despois, D., Gerard, E., Irvine, W.M., Kazès, I., Robinson, S.E., Schloerb, F.P., 1981, Astron. Astrophys. 97, 195

Encrenaz, T., Combes, M., Crifo, J.F., Gerard, E., Bibring, J.P., Crovisier, J., 1981, BAAS 13, 707

Encrenaz, T., Crovisier, J., Combes, M., Crifo, J.F., 1982, Icarus (in press)

Irvine, W.M., Schloerb, F.P., Yngvesson, K.S., 1981, IAU Coll. 61, poster paper

de Jong, T., 1973, Astron. Astrophys. 26, 297

Shimizu, M., 1976, Astrophys. Space Science 40, 149

Smith, P.L., Black, J.H., Oppenheimer, M., 1981, Icarus 47, 441

Whipple, F.L., Huebner, W.F., 1976, Ann. Rev. Astron. Astrophys. 14, 143

Isotopic Abundances in Comets

by
A.C. Danks
E.S.O. Casilla 16317, Santiago 9
Chile

Introduction

Measurements of isotopic ratios in comets may indicate the origin of comets. That is we may be looking at a sample of the interstellar medium out of which the solar system was formed. This material has been preserved in "cold storage" for 4.6 billion years at the outer reaches of the solar system and may be especially interesting in studies of the chemical composition of the outermost planets. The alternative intriguing possibility is that some comets have been captured from outside the solar system and have a chemical composition closer to that of the interstellar medium today and so allow a closer study of the interstellar medium.

Evidence exists for variations of isotopic abundance ratios in the Galaxy. These variations are presumably due to nuclear processing of material in stellar interiors, which is subsequently returned to the interstellar medium by a variety of mechanisms, mass loss, supernova, etc. In Table 1 values are given for the most important isotopic abundances for the sun and the interstellar medium. Elements such as ^{13}C are principally produced in Hydrogen burning in the CNO cycle and ^{12}C in Helium burning. Similarly for other elements like ^{14}N and ^{16}O.

As pointed out by Festou earlier in this conference, absolute abundances are very difficult to determine. However, this is not the case for isotopic ratio's which should be easier to measure.

One ratio which lends itself to analysis in Comets is $^{12}C / ^{13}C$. The solar abundance is ~ 89 and as Carbon is abundant in Comets it should therefore be easily measurable.

Proceedings of the ESO Workshop on "The Need for Coordinated Ground-based Observations of Halley's Comet", Paris, 29 – 30 April 1982.

Table 1

Solar and interstellar medium isotopic ratios

Ratio	Solar	Interstellar
$D/_{H}$	1.4×10^{-4}	1.8×10^{-5}
$Li^{7}/_{Li^{6}}$	12.3	-
$^{12}C/_{^{13}C}$	89	40-60
$^{14}N/_{^{15}N}$	273	333-550
$^{16}O/_{^{18}O}$	500	500-300
$^{16}O/_{^{17}O}$	2.75×10^{3}	$1.6 \times 10^{3} - 9.9 \times 10^{2}$
$^{32}S/_{^{34}S}$	23	17.6 - 20.3

Further Wannier (1980) points out that this ratio in the interstellar medium in the Solar neighbourhood shows enrichment by a factor of 1.5 in ^{13}C yielding a $^{12}C/^{13}C$ ratio of $\simeq 60 \pm 8$.

The $^{12}C/^{13}C$ Ratio

The $^{12}C/^{13}C$ ratio is the only isotopic abundance which has been extensively looked for in comets to date. This ratio is the obvious candidate as the C_2 emission bands are strongly developed in comets and further the expected ^{13}C is only a factor $\sim$ 100 below the ^{12}C abundance. In addition, there is a further gain of a factor of 2 in the observed intensity ratio as $I(^{12}C^{12}C) / I(^{12}C\ ^{13}C) = a/_{2}$ (where a is the abundance of $^{12}C/_{^{13}C}$).

Substitution of a ^{13}C atom for a ^{12}C in the C_2 molecule produces a slightly different moment of inertia and a resulting wavelength shift. It also relaxes the homonuclear nature of the

molecule introducing a very small dipole moment which will be discussed later.

Stawikoswki and Greenstein (1964) were the first to attempt to measure the $^{12}C/^{13}C$ ratio in comet Ikeya 1963I (see Table 2). They logically selected the C_2(1-0) Swan band head at λ4737. The $^{12}C^{13}C$(1-0) head is shifted to the red into a relatively "clean" spectral region at λ4745. Extraction of $^{12}C/^{13}C$ was further thought to be simplified as the C_2 molecule is homonuclear resulting in the population of many rotational states which should produce a "smearing out" of the effects of resonance-fluorescence as there is no simple rotational ladder for depopulation. Unfortunately, the $^{12}C^{13}C$ band head lies on a weak but important NH_2 feature and in order to obtain an accurate $^{12}C/^{13}C$ ratio correction has to be made for these NH_2 lines.

Owen (1973) repeats the observations of Stawikoswki and Greenstein on comet Tago-Sato-Kosaka (1969IX) and by reference to a high resolution laboratory spectrum of NH_2 tried to make an accurate extraction of the NH_2 contribution to the observed $^{12}C^{13}C$ feature.

Table 2

* $^{12}C/^{13}C$ ratio's measured in comets to date

Comet	Ratio
Ikeya 1963I	70±15 Stawikoswki & Greenstein (1964)
Tago-Sato-Kosaka 1969IX	100±20 Owen (1973)
Kohoutek 1973XII	115(+30, -20) Danks et al (1974) 135(+65, -45)
Kobayashi-Berger-Milon 1975IX	132±30 Danks et al (this paper)
West 1976VI	60±15* Lambert & Danks (1982) 50±15

* See text

The first spectra to partially resolve the NH_2 lines from the $^{12}C^{13}C$ band head were made by Danks et al (1974) on comet Kohoutek (1973)XII. A low resolution spectrum, $\sim$ 0.4 Å, of Kohoutek is shown in fig.(1). This spectrum was taken with the McDonald 272-cm reflector and the Tull (1972) coudé scanner. Later scans at a resolution of 0.14 Å were made of the $^{12}C^{13}C$ + NH_2 λ4745 blend and these are shown in figs. (2) and (3). The violet-degraded ^{12}C ^{13}C band head begins at 4744.69 Å and the NH_2 blending lines occur at 4744.28, 4744.46, 4744.89 and 4745.19. The last 3 lines are from the (0, 14, 0) band and are classified by Dressler and Ramsay (1959). The line at 4744.28 probably belongs to the (1, 10, 0) band and will occur in the comet spectrum (Ramsay 1974)

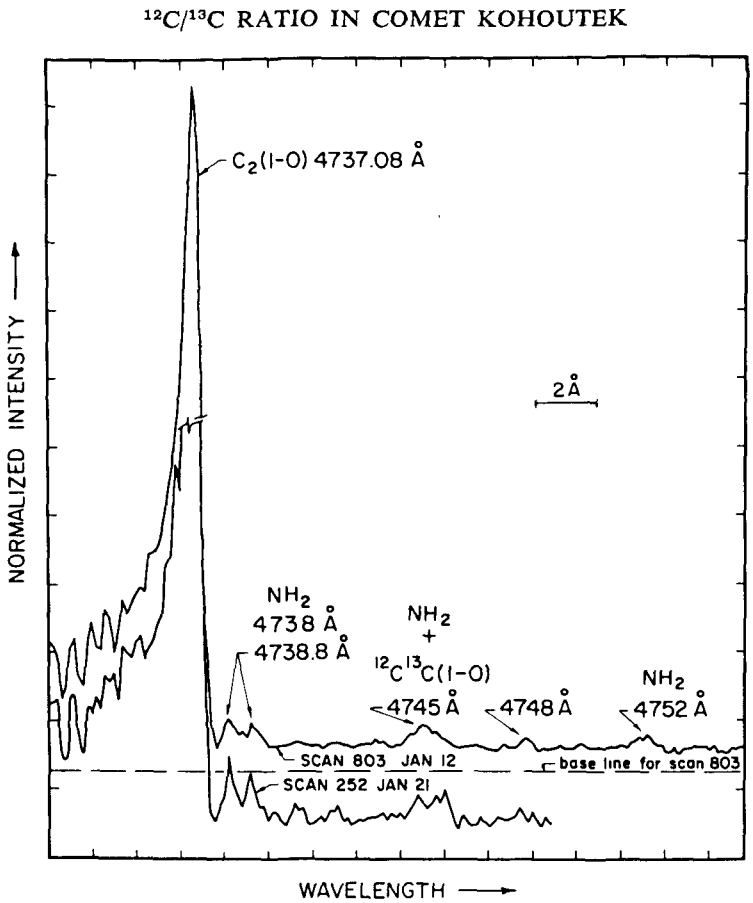

Fig.1 Medium resolution scans of Comet Kohoutek 73XII

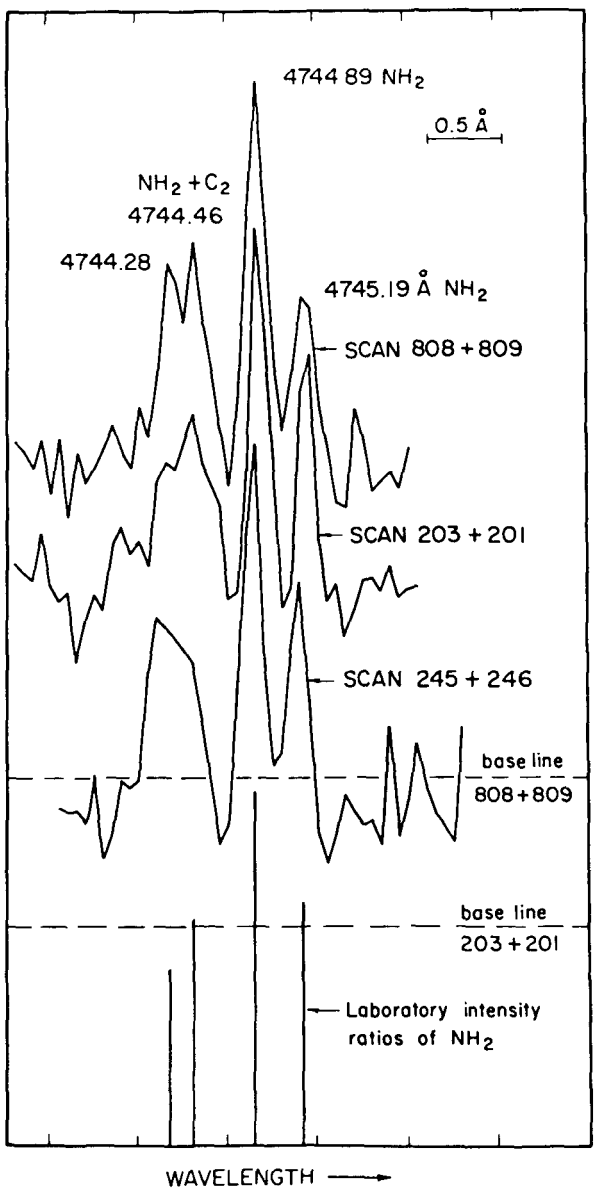

Fig.2 High resolution scans of the $^{12}C^{13}C$+NH_2 λ4745 blend in Comet Kohoutek

Naturally, the NH_2 line intensities must be corrected for the effects of Resonance-fluorescence before subtraction can be made. In fact, an approximation has to be made as complete information on the NH_2 spectrum and transition probabilities is not yet available. However the importance of subtraction is evident from fig. (3) where the λ4745 feature is seen to be composed of 82% NH_2.

In order to obtain an isotopic ratio a synthetic spectrum was generated and first fit to $^{12}C^{12}C$(1-0) band head by adjusting the excitation temperature.

The recipe for the spectrum is given in Danks et al (1974). In the case of Kohoutek the best fit was achieved for a $T_{exc} \simeq 3000°K$. In fact, the fit to the (1-0) band head is not very sensitive to temperature and where possible $\Delta v = +1$ sequence should be used, see Lambert and Danks (1982). The temperature derived from the $^{12}C^{12}C$(1-0) band head is now applied to the $^{12}C^{13}C$ head

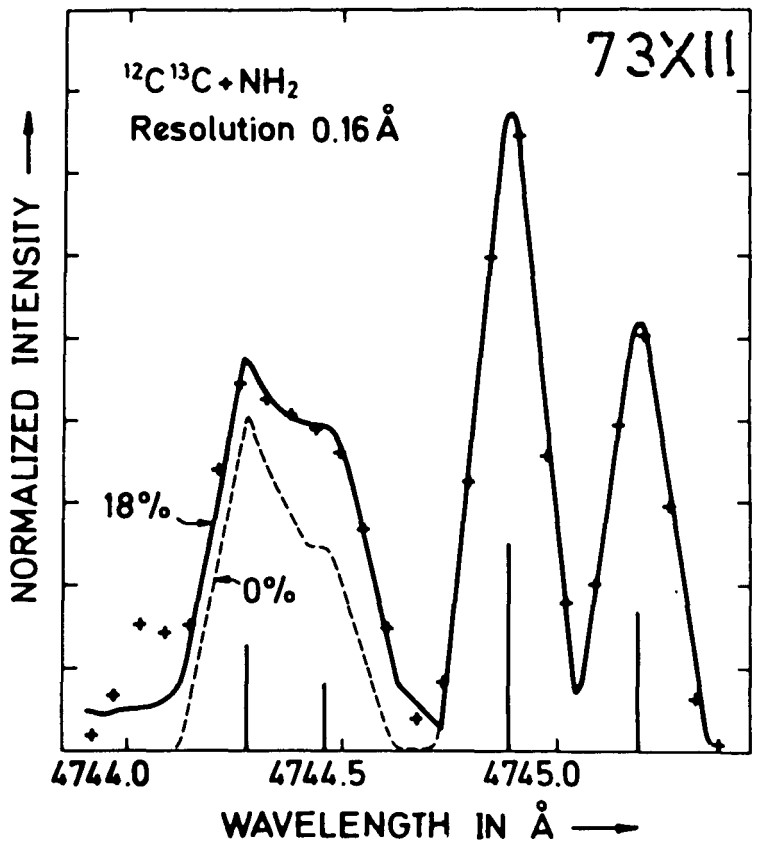

Fig.3 Observed (crosses) and synthesized (solid line) λ4745 blend of $^{12}C^{13}C+NH_2$

and once the % contribution of NH_2 has been estimated and extracted it is a simple matter to derive the $^{12}C/^{13}C$ ratio. The ratio's obtain for Kohoutek were 115 (+30, -20) and 135 (+65, -45) from low and high resolution spectra respectively.

Application of the same temperature to both the $^{12}C^{12}C$ and $^{12}C^{13}C$ heads needs justification as the $^{12}C^{13}C$ molecule is no longer strictly homonuclear and will have a small finite dipole moment. An idea of the strength of the dipole moment can be infered from the analogus molecular pair H_2 and HD. The dipole moment of HD in the vibrational ground state is approximately 5×10^{-4} debye which is to be compared with a typical value of the order of 1 debye for hetronuclear molecules. Bunker (1973) shows that for the

$^{12}C^{13}C$ molecule the dipole moment will be smaller by a factor of about 10^{-2}. The transition probabilities are proportional to the square of the dipole moment and therefore the assumption of identical excitation temperatures for $^{12}C^{12}C$ and $^{12}C^{13}C$ appears justified.

Similar observations of comet Kobayshi-Berger-Milon 1975IX were obtained at McDonald by L. Trafton and are shown in fig. (4) and (5) and have resolutions of 0.65 and 0.14 Å respectively. The spectra can be seen to be comparable although somewhat noiser than the Kohoutek spectra as Kobayashi-Berger-Milon was slightly fainter. From these observations I derived a $^{12}C/^{13}C$ ratio of 132±30 using a similar recipe as described for Kohoutek. The $^{12}C/^{13}C$ ratio's for all comets observed to date are shown in Table (2).

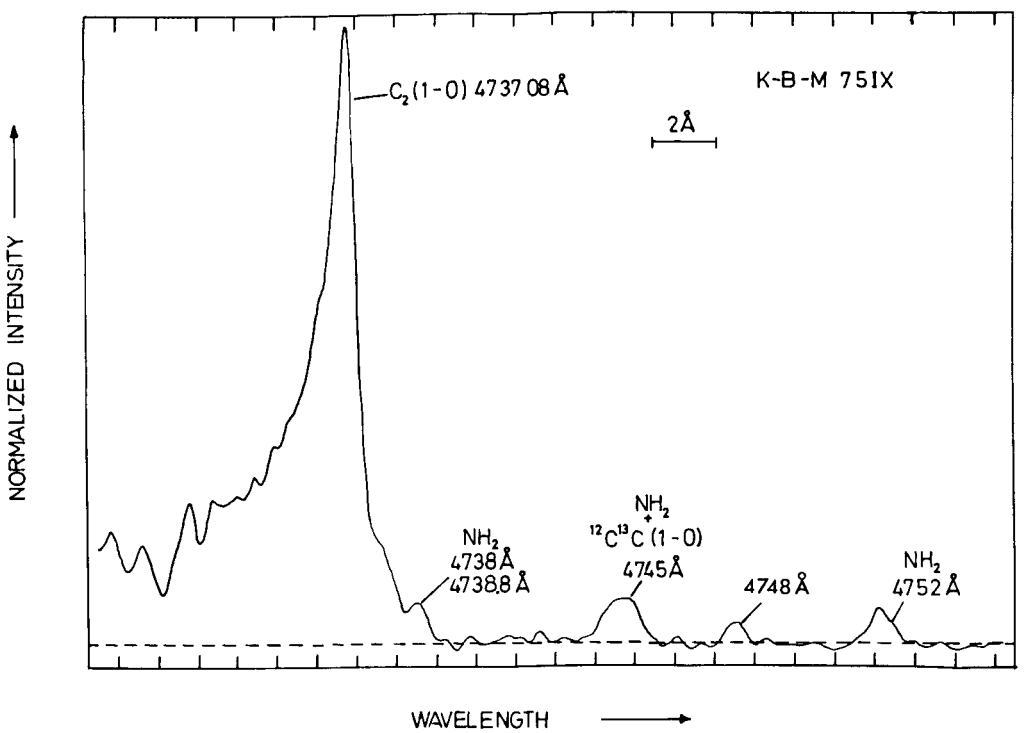

Fig.4 Medium resolution scans of Comet Kobayashi-Berger-Milon showing the $^{12}C_2$ (1-0) band head at λ4737, and the $^{12}C^{13}C$ blend with NH_2 at λ4745.

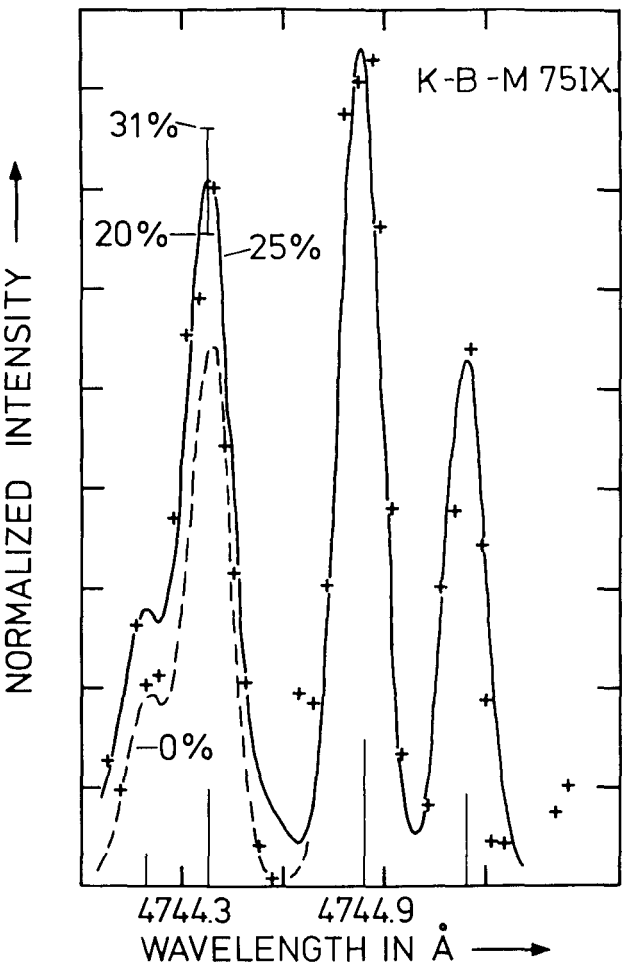

Fig.5 Observed spectrum (crosses) and synthesized (solid line) λ4745 blend of $^{12}C^{13}C+NH_2$ in Comet K-B-M.

The latest comet in which $^{12}C/^{13}C$ has been observed was West 1976VI by Lambert and Danks (1982). Our low resolution spectra 0.3 Å were taken again at McDonald with the Tull spectrograph and a Digicon detector and are shown in fig (6). This spectrum shows not only the C_2(1-0) band head but also the (2-1), (3-2), (4-3) and (5-4) band heads of the $\Delta v = +1$ sequence. The solid line drawn through the data is a synthetic spectrum fit for a $T_{exc} = 3500°K$.

The $^{12}C^{13}C+NH_2$ λ4745 feature is again evident. However, none of the observations carried out so far have achieved the precision necessary to distinguish solar system and interstellar $^{12}C/^{13}C$ ratios. The $^{12}C^{13}C$ head has been detected and the $^{12}C/^{13}C$ ratio measured to a precision of ±30 to 50%. The keys to a more precise result are 1) Improved resolution and higher signal-to-noise spectra, 2) a thorough treatment of the resonance fluorescence in $^{12}C_2$ and $^{12}C^{13}C$ and 3) an adequate discussion of the blended NH_2 lines.

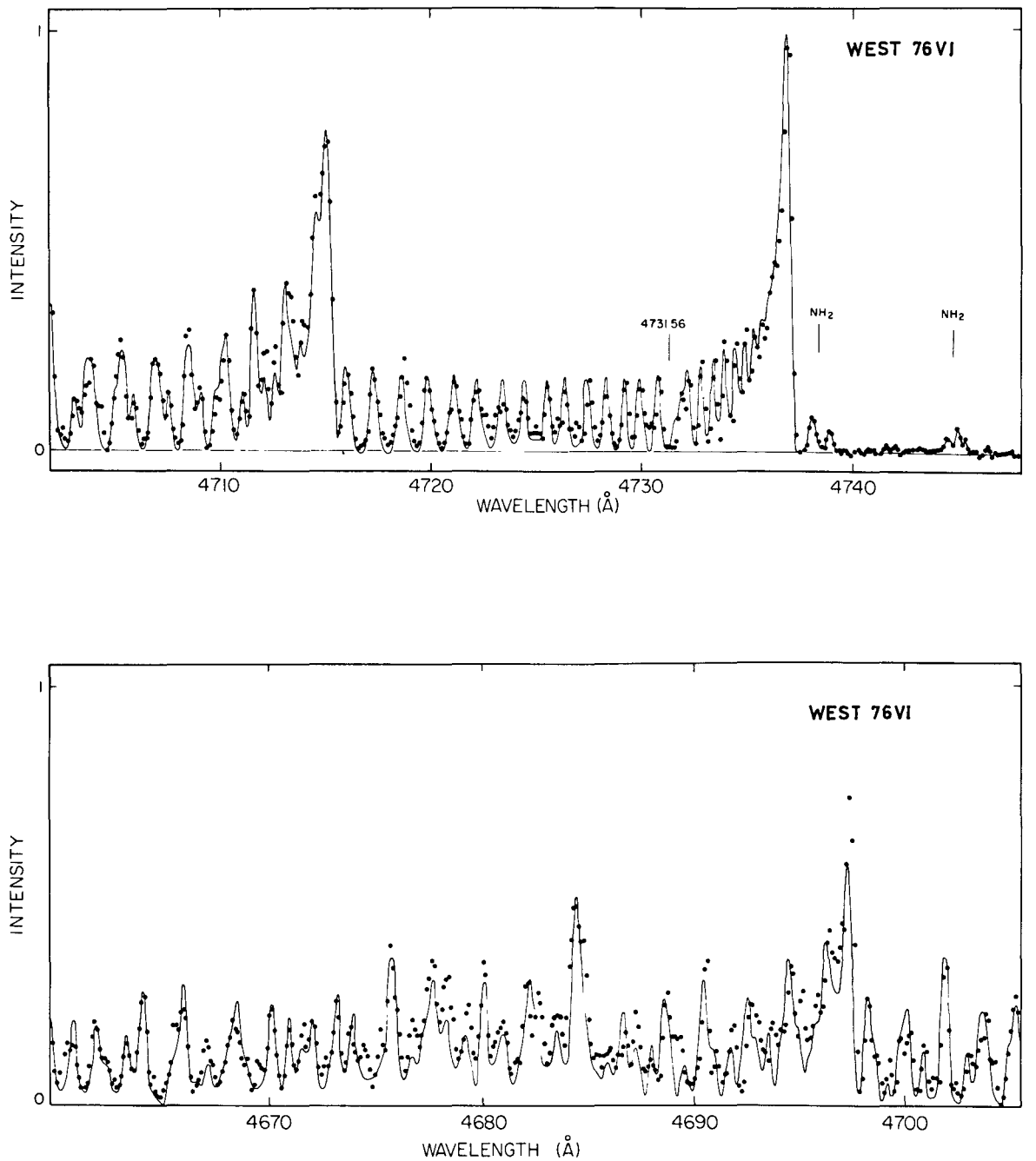

Fig.6 The C_2 Swan $\Delta v = +1$ sequence in Comet West on 1976 March 21. The contribution of sunlight scattered by dust grains in the comet has been removed (see text). The solid line is a synthetic spectrum corresponding to an excitation temperature of 3500 K.

Clearly with observations at only slightly higher resolution isolation of the $^{12}C^{13}C$ band head from the NH_2 lines is possible and both the McDonald scanner and the recently commissioned ESO Coudé Echelle Spectrograph are capable of routinely observing at this resolution. However, at this resolution, say approximately $\sim$ 0.1 Å other spectral regions may prove more fruitful. One region which is immediately interesting is the C_2(0-0) Swan band which is 4 times more intense than the (1-0) band. Here individual $^{12}C^{13}C$ lines rather than a complete band are displaced clear of $^{12}C_2$ lines and line lists reveal several $^{12}C^{13}C$ triplets which should be observable at high resolution. Our search in comet West was limited to portions of the interval between the (1-1) and (0-0) P branch band heads at λ5129 and λ5164. Six regions were selected for observation centered at wavelengths λ5132.2, λ5134.6, λ5136.3, λ5158.0, λ5159.1 and λ5160.6. The observations were made at resolutions of $\sim$ 0.1 to 0.15 Å over intervals of approximately 2 Å. Two further regions were selected but unobserved, centered at λ5131.2 (N" = 47) and λ5142.3 (N" = 41).

In fig (7) we show our highest quality spectra spanning the $^{12}C_2$ triplets $P_1(47)$, $P_2(46)$ and $P_3(45)$ and $R_1(18)$, $R_2(17)$ and $R_3(16)$ and include the $^{12}C^{13}C$ P branch triplet. Also shown is an acetylene flame spectrum of the same spectral region.

At higher resolution the flame spectrum shows the $^{12}C^{13}C$ triplet resolved in three components blended with $^{12}C_2$ Q branch triplet. At this resolution we can clearly resolve the Λ-type doubling of the $^{12}C^{13}C$ lines as shown in fig (8).

The six components blend into 3 features, labelled a, b and c; (for a full discussion refer to Lambert and Danks (1982)). Component b consists of three lines P_{1f}, P_{2f} and P_{3e} is unblended and the intensity of this feature relative to the $^{12}C_2$ P triplet in

the flame spectrum yields an isotopic abundance of $^{12}C/^{13}C \simeq 90$ or the expected terrestrial value.

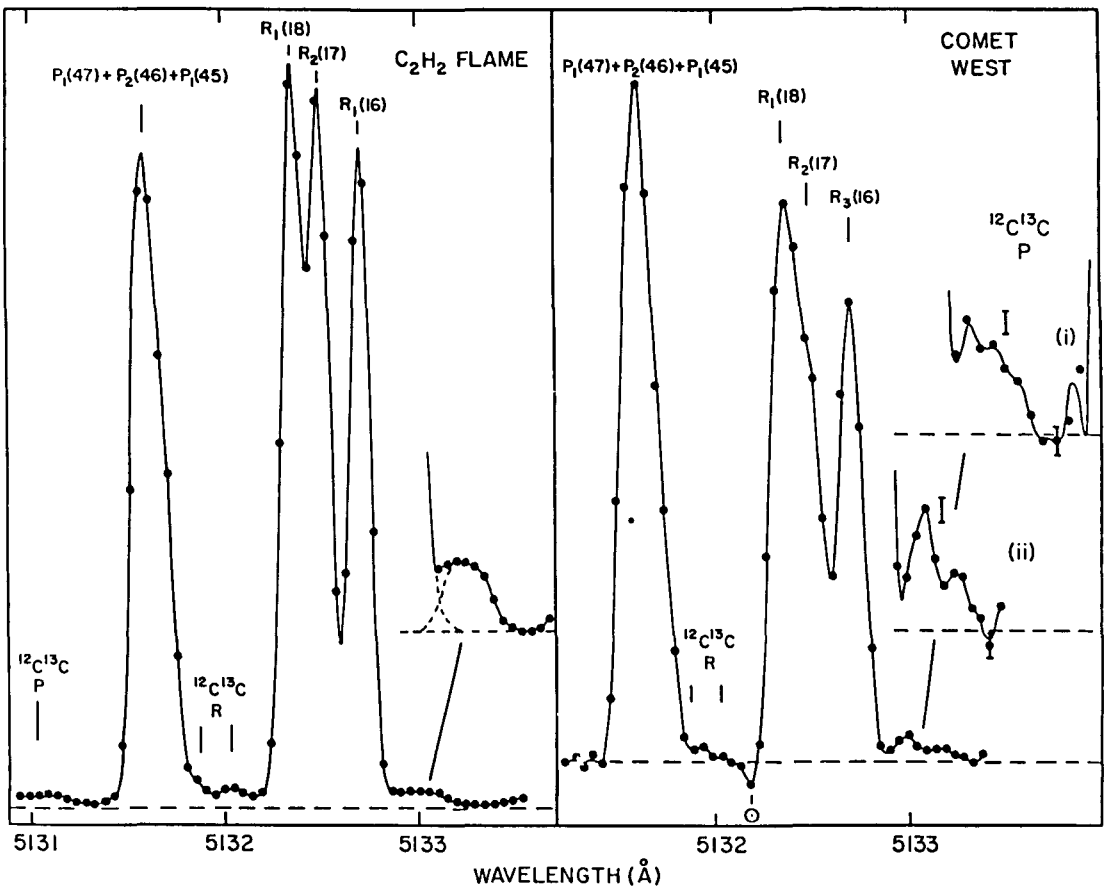

Fig.7 High resolution spectra of Comet West and an acetylene flame between 5131 and 5133.4 Å showing weak $^{12}C^{13}C$ features. The insets show on an expanded scale (x 5) the $^{12}C^{13}C$ P_1 (47) + P_2 (46) + P_1 (45) triplet corresponding to the $^{12}C_2$ triplet near 5131.6 Å. Inset (ii) corresponds to the full scale spectrum. Inset (i) is from a slightly lower resolution spectrum. The error bars shown with the insets are estimated from the total comet rate in the continuum and at the peak of the $^{12}C^{13}C$ feature.

At the resolutions employed in the Comet West observations the $^{12}C_2$ Q and $^{12}C^{13}C$ P triplets are blended. Spectrum synthesis would allow the $^{12}C^{13}C$ contribution to be extracted. We employed a similar method on the flame spectrum at this resolution, we measured the equivalent width of the blend and estimated the Q branch contribution by requiring that the corrected P triplet give the ratio

$^{12}C/^{13}C$ = 89. Then assuming the same mix of Q and P lines except for a reduction of Q relative to P in the comet arising from the higher vibrational temperature we obtain $^{12}C/^{13}C$ = 60±15. The lower resolution spectrum gives a similar result $^{12}C/^{13}C$ = 50±15.

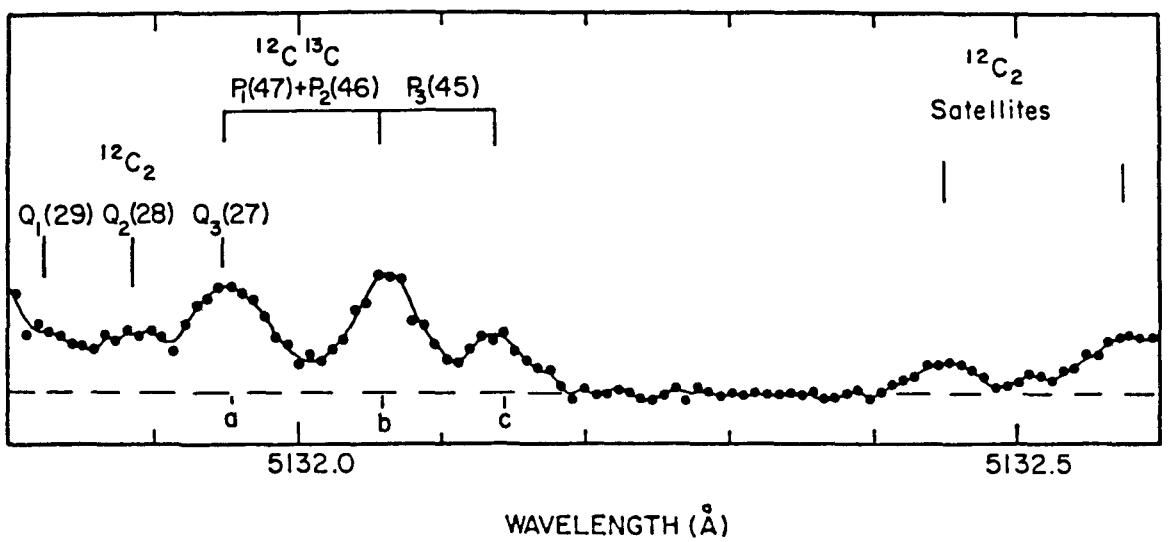

Fig.8 High resolution spectra of an acetylene flame showing three $^{12}C^{13}C$ P branch triplets, which are resolved into three principal components (a, b and c), and weak $^{12}C_2$ lines of either the Q or satellite branches.

We cannot rule out a weak unidentified line underlying the measured line and moreover our spectra of other potentially useful regions were of insufficient quality to provide a check on the ^{13}C excess in Comet West. Therefore we urge that our result not be taken as evidence of the $^{12}C/^{13}C$ ratio in comets is closer to the interstellar than the solar system value. The key point is the demonstration of the (0-0) band as a potential source of an accurate $^{12}C/^{13}C$ ratio in bright comets.

Other Isotopic ratios

After the extensive discussion of $^{12}C/^{13}C$ ratio it only requires a glance at Table 1 to realize the problems involved in detecting other isotopic abundances. The next most likely candidate would be $^{14}N/^{15}N$ and here the obvious molecule for detection is CN which has both well developed violet and red bands. The prefered choice would be the CN(0,0) violet band at λ3880. Unfortunately the (0,0) band is overlapped by the fainter CN (1,1). But the band is one of the strongest seen in Comets and falls in a region of high detector sensitivity. The band is strongly affected by resonance-fluorescence, however, this is well understood and extensively studied by both Arpigny (1964) and Malaise (1970). The rotational line separations are shown in fig (9) and it is immediately obvious that high spectral resolution is required in order to separate the individual rotational lines due to the small isotopic shifts. One promising region immediately evident is the region blueward of R (16) at λ3862.5.

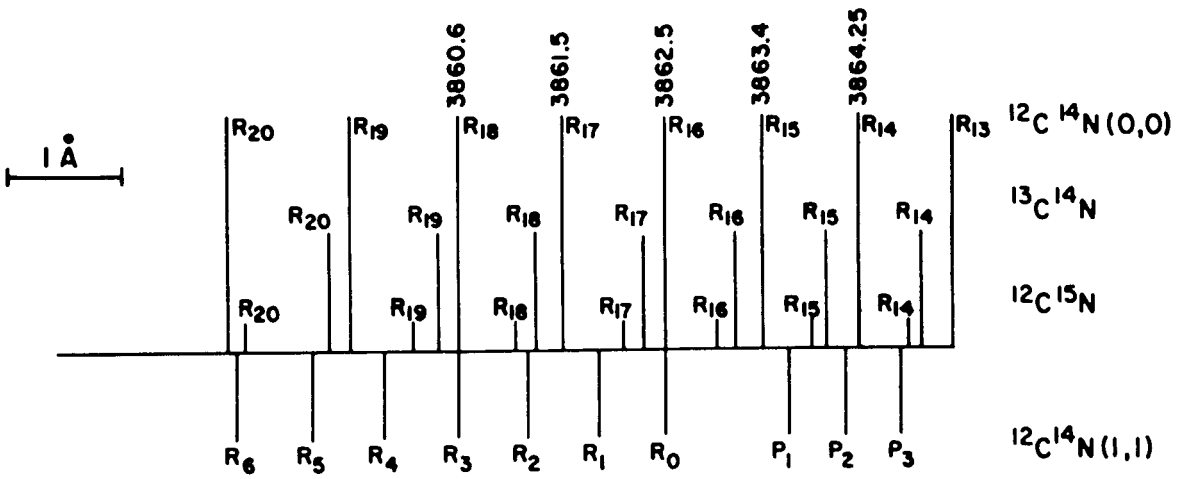

Fig.9 Approximate line separations of the CN(0,0) Violet band. The superimposed $^{12}C^{14}N(1,1)$ band is also shown.

Both the $D/_H$ and $^{16}O/^{17}O/^{18}O$ ratios are interesting astrophysically but appear inordinately difficult. In the visible it is possible that the OH (0,0) and OH (1,1) bands at λ3118 and λ3072 could be used either for OD or ^{16}OH, ^{17}OH and ^{18}OH. Although the OH bands are known to be intense from space observations they lie so close to the atmospheric cut off that they can only be studied well from exceptional high ground based observatories. This problem is probably best tackled from space. Although the Lyα is normally to broad it may be conceivable to measure the $D/_H$ ratio in certain comets fairly far out. But this ratio should be easily measurable directly by mass spectrometers on board Giotto. Similarly, an important ratio is Li^6/Li^7 which occurs at λ6708 and has not yet been measured in the interstellar medium. This could be searched for near perihelion spectroscopically yet again it may be more easily measured by on-board mass spectrometers. The ratio is modified by spalation and is likely to be both dependent on the density of interstellar matter and cosmic ray flux. Its measurement could reveal interesting history of the Solar system.

Again from space the $^{32}S/^{34}S$ ratio could be studied via the CS(0,0) λ2576 and (0,1) λ2663 bands. The isotopic shifts are of the order of 0.15 Å and 1 Å respectively for these bands and measurement should be well within the capability of IUE at high resolution or ST.

Conclusion

Ideally, the isotopic ratios discussed above should be measured directly by the space craft. However, many of them pose problems of mass separation and much of this information will only be obtainable from either ground based observations or from UV

spectrographs in Satellites (IUE), ST or on board the Shuttle.

Ground support of Giotto is absolutely imperative and only by combining ground based and space craft results will we increase our understanding of comets and perfect ground based techniques in order to observe future new "Unknown" comets. It should not be forgotten that many of the molecules of interest have interrelated transitions in the UV, visible and infrared.

Most of the measurements present here do not represent the present detector capabilities. Use of digital detectors enables extremely "clean" subtraction of the Fraunhofer spectrum. It should also be emphasized that as many independent methods of measuring an isotopic abundance as possible should be employed in order to increase credibility and ensure there are no fractionation effects.

Spectral resolutions of $\sim$ 100,000 are needed in most cases yet this resolution is now routinely possible with both the ESO Coudé Echelle Spectrograph (CES) at La Silla and the Tull scanner at the McDonald observatory.

Collaboration between the two instruments will allow similar resolution spectra to be obtained for both the Northern and Southern hemispheres.

Acknowledgment

It is a pleasure to thank Dr. L. Trafton for taking the spectra of Kobayashi-Berger-Milon 75IX and Dr. J. Tomkin for observing the flame spectra of C_2 H_2. I am grateful to Prof. D.L. Lambert for useful discussions.

References

Arpigny, C. 1964. Ann d'Ap 27, 393

Bunker, P.R. 1973. J. Mol Spectrosc. 46, 119

Danks, A.C., Lambert, D.L. and Arpigny, C. 1974. Ap. J 194, 745

Dressler, K. and Ramsay, D.A. 1959. Phil. Trans. Roy. Soc. London A. 251, 583

Lambert, D.L. and Danks, A.C. 1982. ESO Preprint no.

Malaise, D.J. 1970. Astr. and Ap. 5, 209

Owen, T. 1973. Ap. J 184, 33

Stawikoswki, A. and Greenstein, J.L. 1964. Ap. J 140, 1280

Tull, R.G. 1972. Proceedings ESO/CERN Conference on Auxiliary Instrumentation for Large Telescopes. Geneva, May 2-5. p. 259

Wannier, P.G. 1980. Ann. Rev. Astron. Astrophys. 18, 399

COMET ION FORMATION AND DYNAMICS

Max K. Wallis

Dept. Applied Maths & Astronomy, University College, Cardiff, Wales, U.K.

Summary - Solar photon and proton ionization may well supply average ion fluxes, but closer observation correlated with solar wind conditions is needed to distinguish creation of ion structures by intrinsic mechanisms (such as auroral discharges or ionizing flow instability) from the variable solar wind 'snow-plough'. Under steady conditions, the expected plasma flow is relatively smooth, varying over scales much larger than ion gyro-radii (the effective m.f.p.) and even the plasma bow shock would have limited physical significance. The inter-planetary field may be pictured as draping around the comet head, but Alfvén's picture needs modifying to include slipping over into the tail. The concept of one-fluid plasma picking-up fresh cometary ions is challenged, because relative drifts in the draped fields are inevitably major. Structures and tail rays as enhancements of density drift towards the tail axis, across the draped B. Magnetic forces become appreciable at order ten times the ionosphere radius, so the transition region of induced currents and fields should be very broad, unlike the Venus magnetosheath. Time sequenced observations at around 10-minute intervals are needed for tracing the evolution of ion structures in a Halley-sized comet.

Key words: cometary ionization, plasma dynamics, magnetic field, comet fluid models.

1. The Ionization Enigma

Solar protons and photons have frequently been considered inadequate for causing the ionized component of cometary gases: ionization rates of 10^{-6}/s or less (Jockers, this meeting) seemed to give fewer ions than observed and to conflict with structures and brightness flares with time scales as short as $10^{3.5}$s (Wurm 1963, Wurm and Mammano 1967). Electron-collisional ionization has therefore been proposed in various guises, with electrons energized

(i) in a collisionless plasma bow-shock (Axford 1964),

(ii) via the Alfvén mechanism, due to either boundary layer E-fields or plasma microinstabilities (Raadu 1981), or

(iii) via auroral-like discharge currents driven by solar wind potentials induced across the tail (Ip and Mendis 1976).

The first may be discounted as the bow-shock is probably weak and the streaming energy of the solar wind goes primarily to cometary ions (Wallis 1973a), mechanism (ii) found in laboratory experiments on the "critical velocity" (defined by the energy of ion-neutral streaming being equal to the ionization energy) may occur, depending on ion-electron relation processes, but one cannot extrapolate from laboratory to space conditions (Marochnik 1964). The intriguing proposal of auroral discharges (iii) draws on insecure analogies with the Earth's magnetosphere: the possibility is open and I shall return to discuss it on the basis of models developed below.

Cometary science has developed, on the other hand, in ways that weaken Wurm's original argument. Higher gas production at some 100 or 1000 times the CN and C_2

Proceedings of the ESO Workshop on "The Need for Coordinated Ground-based Observations of Halley's Comet", Paris, 29 – 30 April 1982.

is now established, with correspondingly more abundant photo-ions. Rapid dissociation and reshuffling of the ion species via ion-molecule reactions are now recognized, so that brightness flares are conceivably the result of injecting a different neutral species and of ionization of just a fraction of the total. The solar wind is now known to be highly inhomogeneous, so that early descriptions of corpuscular streams sweeping up coma ions into visible structures (Alfvén 1957, Marochnik 1962) are more plausible. At the leading edge of a high speed solar stream, the proton flux increases by up to a factor 10 within minutes (see the review of Ip and Axford 1982 for typical numbers). Increases from the occasional solar flare are even stronger. Thus one expects comets to respond to solar wind changes. What's surprising is the rather uncertain response and limited correlation with solar parameters (e.g. Jockers and Lüst 1973), but more data on this is needed. The 'envelope' ion structures (Ptitsina 1964) of some active comets recur too rapidly for solar wind streams. The rise-time of 10^3s in comet Morehouse (cf. Wallis 1977) is acceptable but the repeated formation of 3 or more envelopes at intervals of 10^4s would imply highly unusual solar wind structure.

2. Gasdynamic models of the plasma flow

Fluid descriptions of the solar wind penetration through the cometary coma are now commonplace. The coma itself is a collision-free radial expansion of gases, at 1 or a few km/s (except H-atoms, which expand at 10-30 km/s). Coma densities are extremely low, so particle collisions are almost absent, but charged particles in the magnetized plasma behave as a fluid over scales greater than the gyroradii (of 100-1000 km for protons). Alfvén (1957) predicted that a solar wind stream would therefore be preceded by a shock, while Marochnik (1962) pointed out there should be a second shock propagating back into the solar wind, whereas the inner shock would weaken and become collisonal as it reached higher density regions. Harwit and Hoyle (1962) at the same time as Marochnik conceived of the snow-plough effect, that cometary ions would couple to the magnetized solar plasma and be swept along with it.

Axford (1964) formulated similar ideas in depicting the steady solar wind decelerating by picking-up fresh cometary ions, in which case he predicted a stationary bow shock.

The stationary fluid model and relative scales as determined from more recent work are shown in Fig. 1, with a bow shock standing far ahead of the collisional region. In order to show all regions, this Figure (adapted from Wallis 1973b) uses a 'square root' scale in the radial direction, unlike the logarithmic scale in ESA's publicity (1981) which is internally inconsistent (the nucleus should be at $-\infty$) and highly exaggerates the inner regions: one needs to note that the collisional region is relatively minute - 100 times smaller in linear scale than

the shocked plasma region. The fluid model was first formulated by Biermann et al. (1967) in terms of conservation equations modified by source terms representing the infrequent ion-creation and plasma-neutral collision processes. However, their theoretical justification of the bow shock was faulty, and their calculations gave it the wrong position, wrong strength and wrong dependence on coma gases. The analytic solution to the quasi-1-D approximation to the flow (Wallis 1973a), confirmed by subsequent computations (Brosowski and Wegmann 1973), showed the shock to be weak and deep in the coma, at $R_s \simeq 3 \times 10^5$ km for outgassing rate $4\pi Q = 2 \times 10^{29}$ OH_n molecules/s (with $R_s \propto Q$). The shock lies just outside the position (broken line in Fig. 1) where the flow Mach number would be unity. Its strength depends on atmosphere steepness (for $d \ln N/d \ln R \simeq 2$, its Mach no. is $M \simeq 2$) while the need for a shock follows from the structure of the modified fluid equations being of saddle nature around the sonic point (Wallis 1977). The shock shape and strength depend hardly at all on downstream boundary conditions at the relatively tiny collisional or stagnation regions. Two recent papers (Beard 1981, Houpis and Mendis 1981) argue that the atmosphere varies more steeply and so the shock is stronger; the former argues that CO is blown back by radiation pressure on a 10^4 km scale, but there is no evidence for such a short scale and components such as O suffer little pressure and have the R^{-2} variation to large distance as in the model of Fig. 1. The second paper argues that ionospheric plasma and gas are collisionally coupled, but confuses the gas-plasma collision path with the smaller plasma-gas scale and ignores the penetration of any coupling layer by a fraction of the CO and other gases. Apart from H and He it is the longest-lived neutral species that populates the outer coma and fixes the shock strength (Jockers, this meeting). So the detailed flow fields calculated by Schmidt and Wegmann (1980, 1982) should be a good guide to a situation where photoionization is the dominant source of ions.

Transition from contaminated solar plasma to the inner cometary ionosphere is less clearly modelled. Ip (1980) interpolates across the 2 orders of magnitude in density, but avoids the issue of whether there are structures or a 'contact discontinuity' separating ions of a purely cometary origin. Suppose we estimate the coupling scales for neutrals (n) and ions (i) as where the mean free path in gas of density Q/VR^2 equals the radial distance R:

$$R_n = \sigma_{nn} Q/V \simeq 1.6 \times 10^3 \text{ km}, \qquad R_{ex} = \sigma_{in} Q/V \simeq 4 \times 10^3 \text{ km}, \tag{1}$$

differing because the ion-neutral charge exchange cross-section is larger- collisional cross-section taken as $\sigma_{nn} = 10$ Å^2. The existence of a contact discontinuity where cometary ion and incoming plasma dynamic pressures are equal (Marochnik 1962) depends on this position lying outside R_{ex}. First estimates (Wallis and Ong 1976) found the ionospheric pressure was too low by an order of

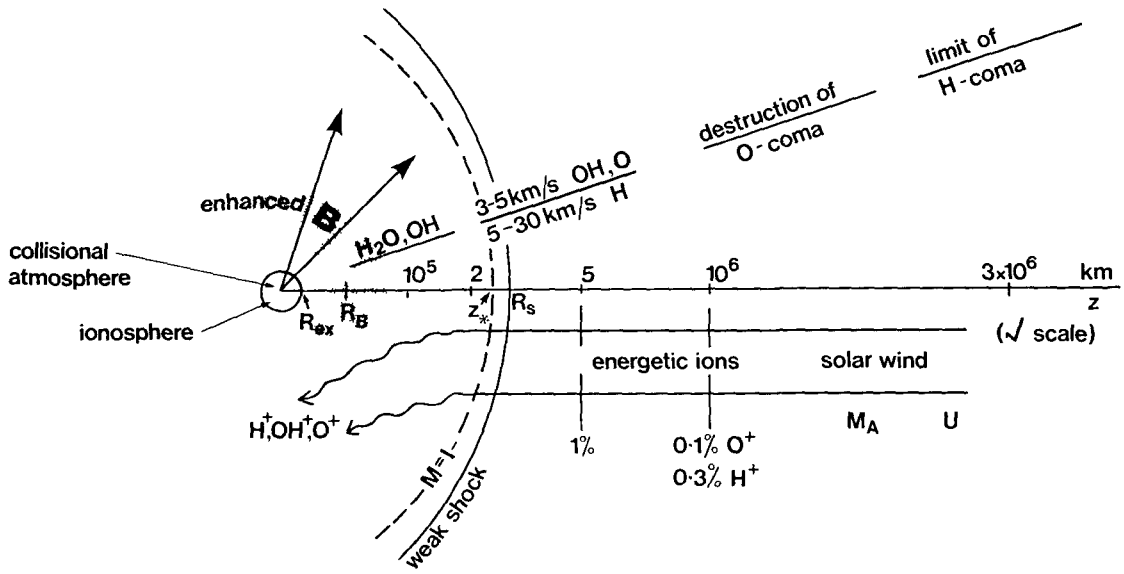

Figure 1 Scales in the coma and its interaction with the solar wind. Note that relative sizes are distorted by the 'square root' scale in radial distance. The physical scales R_S, R_B, and R_{ex} on based on symmetric outgassing at $4\pi Q = 2.5 \times 10^{29}$ molecules of H_2O /s at 1 km/s (Wallis 1973b) and all vary linearly with Q, but other constituents such as CO_2 or CO make little change.

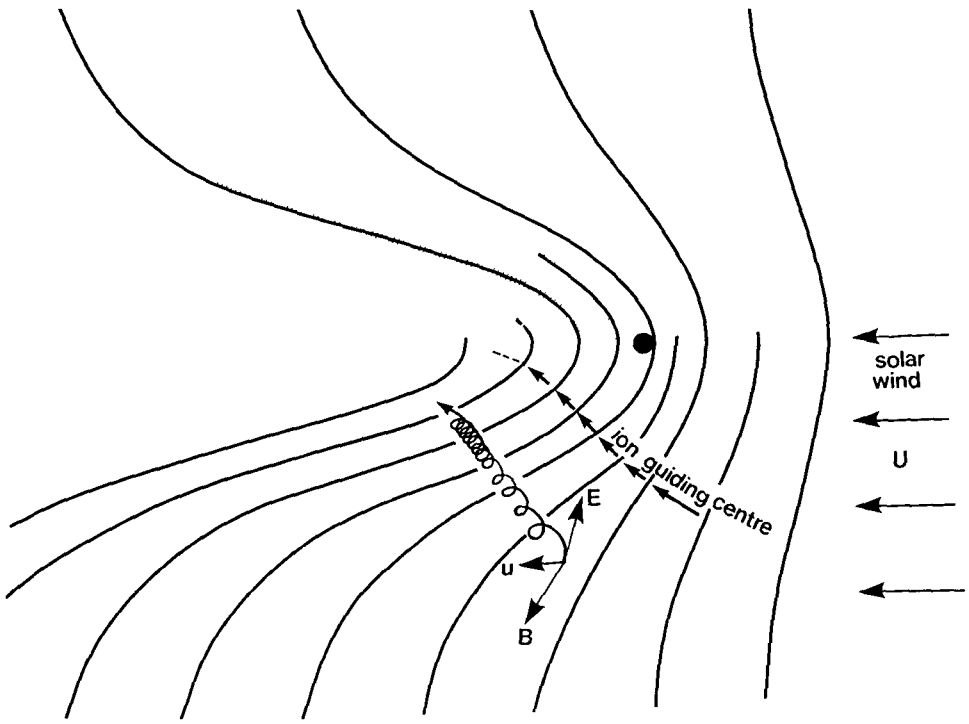

Figure 2 Magnetic field lines in the comet frame for the model velocity field (Eq. 2), showing the trajectory of a freshly created coma ion and schematic tail rays crossing B-lines. The length scale is linear and the central spot corresponds to the shaded region of Fig. 1 where magnetic pressure starts to distort the fluid motions.

magnitude. If the latest estimate from Munich (Schmidt and Wegmann 1982) is scaled down by 10^2 (one factor 10 for the increased heating arbitrarily assumed, a second factor 10 for over-high ion densities due to neglect of recombination reactions), any pressure balance position falls (at 60 km for Q as above) far inside R_n as well as R_{ex}; Ip and Axford (1982) find similar numbers. Thus the incoming plasma is balanced mainly by gas pressure, exerted through ion-neutral collisions over a thick region of order R_{ex}. Some mechanism for strongly enhanced ionization (Ip and Mendis 1976) might 'save' the contact discontinuity. Otherwise, plasma structures observed in the coma outside 10^4 km must arise from an intrinsic instability or from solar wind streams acting as 'snowploughs'.

3. Magneto-fluid properties

The notable sketch of field lines draping over the comet head (Alfvén 1957) has in recent years been questioned by that author, stressing that the "frozen-in" magnetic field concept is illegitimate in various situations (Alfvén 1981). However, on grounds that the regions of breakdown are limited, one can hope to treat them as boundary effects, considering carefully complete current-carrying circuits. Nevertheless, the question of whether MHD can describe the bulk flow still remains.

To model the draped-$\underline{B}$ structure, results of MHD computations of the Munich model are available (Schmidt and Wegmann 1980, 1982) but there are doubts on convergence and choice of boundary conditions. In the outer coma where $\underline{B}$ is weak and passive, solutions can be derived from Maxwell's equations taking infinite conductivity. As an example, Fig. 2 depicts results assuming the velocity field

$$\underline{u} = \underline{U}\{1 - g(x, y)\exp - (|z|/z_1)\} \tag{2}$$

with g a suitable even function of transverse coordinates x, y and $g(\infty) = 0$. The exponential variation with z has been chosen to allow exact integration, giving the field lines

$$\frac{z}{z_1} = \begin{cases} -\ln(g + 1/c), & z < 0 \quad \text{upstream} \\ \ln\{g + c(1 - g)^2\}, & z > 0 \quad \text{downstream} \end{cases} \tag{3}$$

corresponding to an unperturbed field transverse in the y-direction and in the comet's reference frame. The velocity field (2) does not incorporate the upstream bow shock, but such a modification would be small, though messy. The draped field lines as shown in Fig. 2 are constructed in the plane of symmetry $x = 0$ by taking $g(0, 0) = 0$. As in the MHD model, the field gets stronger into the head on the $-z$ axis: when the magnetic pressure approaches the dynamic pressure, our convected-$\underline{B}$ model breaks down - the magnetic pressure would move the plasma laterally in the x-direction, so the field can be approximated by that at $x = x_o$ where $g(x_o) = 1 - 1/c_o$. Hence we identify $c_o \simeq M_A - 1$ where the Alfvén mach number is

$M_A = \{\mu_o \rho U^2 / B_\infty^2\}^{\frac{1}{2}}$. Evidently the topography of the B-field of Fig. 2 differs from Alfvén's classical picture and illustrates B-lines 'slipping over' the head (though in the comet reference frame the lines are static). This topography closely resembles that found in laboratory simulation of a comet (Podgorny et al. 1979).

The trajectories of individual ions in the B and E fields can be readily derived: a typical ion starting from rest as an ionized coma atom is depicted. Gradient and inertia drifts (due to ∇B and changing u of (2)) move the ion's 'guiding centre' perpendicular to B as shown, substantially different from the ion pick-up or snow-plough conceptions derived for simple transverse B. The motion of ions from the inner coma injected into tail rays at speeds less than u can also be mapped and as depicted cross the B-lines. Generally, slower plasma drifts towards the axis, perhaps in the form of turning tail rays if the initial speeds decrease with time (Wallis 1968), while faster plasma drifts outwards. Marochnik (1964) assumed that appreciable disorder in B would give ion drifts equal to u, but in reality irregularities would just scatter the ion motions about the mean drifts. This could change if the relative drifts generate plasma microinstabilities (reviewed in Ip and Axford 1982) but these are hypothetical and would tend to occur only in denser inner regions.

Quantitatively, the present model B-field implies that magnetic forces become dynamically significant at radial distances of order $R_B = z_1 |\ell n(1 - M_A^{-1})|$, with z_1 related to the M = 1 scale (Fig. 1) by $z_1 \simeq z_* \ell n\gamma$ for γ the fluid adiabatic index. Thus $R_B = 0.1\, z_* \simeq 2.5 \times 10^4$ km for $M_A = 7$, $\gamma = 2$, so far outside the ionosphere and collisional atmosphere scales of (1), unlike the central source model of Ioffe (1967). This suggests there should be a broad magnetic transition and casts doubt on analogies with the boundary layer of induced currents and fields discovered by Pioneer Venus (Russell et al. 1982).

4. Conclusions

The tendency to identify rays with magnetic field lines can be misleading, especially close to the head. Alfvén's draped field picture needs modifying as in Fig. 2 and plasma rays do traverse field lines drawn consistently in the frame of the comet. Clouds and rays structures are not just luminous tracers of a general flow, but comprise regions of enhanced ion density with lower speeds for higher densities revealed by detailed study of the tail (Jockers 1981). In the large scale B-field of Fig. 2, slower moving structures would drift more rapidly towards the tail axis. It is not clear that homogeneous 1-fluid models in which field lines are drawn at arbitrary intervals (Schmidt and Wegmann 1982) relate in any way to observed ion structures.

The magnetic structure shown in Fig. 2 has not been justified here in terms of electric current circuits joining through the inner coma. Justification comes most readily through the topological similarity with Venus for which models are available with induced currents in the conducting ionosphere compatible with Venera and Pioneer observations (Breus 1979, Russell et al. 1982). But the finding that the magnetic field scale R_B far exceeds the ionosphere scale and ion-gyroradii means that interface instability and plasma cloud structure observed at Venus may not have a counterpart in comets. This magnetic topology implies currents across and along the tail (Ip and Axford 1982), analogous to the magnetospheric tail. The current along the tail can be estimated from Ampère's law, $\underline{j} = \mu_o^{-1} \nabla \times \underline{B}$, implying an electron flux $nv \simeq \ell B/\mu_o e R_B^2$ for tail $\ell \simeq 10^6$ km and R_B the lateral scale of variation. With $B = 10^{-4}$ gauss, this gives $nv \simeq 8 \times 10^7/cm^2 s$ at maximum energies from the cross tail potential of order $UBR_B/c \simeq 300$ eV. These values are small, e.g. compared with the solar wind's 3×10^8 protons/$cm^2 s$ at 1000 eV, but may still be significant because the electrons may concentrate into sheets or discharges, can penetrate more deeply from the tail into the coma, and would create several ions apiece. Thus tail currents might be important in limited regions and structures but on present estimates cannot rival the total photoions through the 10^4 km inner region (Ip and Mendis 1976).

A particular problem in observing plasma structures, especially in the comet head, is their rapid motion. Delsemme and Combi (1979) found significant changes between two 10 min exposures in H_2O^+ taken 20 min. apart, during which time structures seemed to move 2-5 x 10^4 km. Twenty minutes was also the interval for appearance of envelope structures in the exceptional comet Morehouse. Despite the observational and interpretation difficulties, short-exposure sequential imaging needs to be developed to identify the origin and evolution of structures. And, looking forward to comet Halley, we shall need such observations to help disentangle the mixture of temporal and spatial fluctuations measured by the Giotto plasma probes (Johnstone et al. 1981).

Acknowledgement - Part of this study was carried out in conjunction with Alan Johnstone when I held a S.R.C. Visiting Fellowship at the Mullard Space Science Laboratory of University College London. I am also grateful for an advance copy of the review by Tamara Breus, to appear in Space Sci. Rev.

References

Alfvén H 1957 *Tellus* 9 92

Alfvén H 1981 'Cosmic Plasma' Ch.II, D.Reidel.

Axford W A 1964 *Planet.Space Sci.* 12 719

Beard D B 1981 *Astrophys.J.* 245 743

Biermann L, Brosowski B, Schmidt H U 1967 *Solar Phys.* 1 257

Breus T K 1979 *Space Sci.Rev.* 23 253

Brosowski B, Wegmann R 1973 *Meth.Verfahren math.Phys.* 8 125

Delsemme A H, Combi M R 1979 *Astrophys.J.* 228 330

ESA (European Space Agency) 1981 'Giotto Mission'; also in ESA SP-155 p. 3

Harwit M, Hoyle F 1962 *Astrophys.J.* 135 875

Houpis H L F, Mendis D A 1981 *Moon & Planets* 25 95

Ioffe Z M 1967 *Astron.Zh.* 44 655 (=*Sov.Astron.A.J.* 11 1044)

Ip W-H, Axford W I 1982 in 'Comets' p. 588, ed. L L Wilkening, U.Ariz.P.

Ip W-H, Mendis D A 1976 *Icarus* 26 457

Jockers K 1981 *Icarus* 41 397

Jockers K, Lüst Rh 1973 *Astron.Astrophys.* 26 11[illegible]

Johnstone A *et al.* 1981 'Proc.Int.Meeting Giotto Mission' ESA SP-169 p. 17

Marochnik L S 1962 *Astron.Zh.* 39 678 & 1067 (=*Sov.Astron.A.J.* 6 532 & 828)

Marochnik L S 1964 *Usp.Fiz.Nauk.* 82 221 (=*Sov.Phys.Usp.* 7 80)

Podgorny I M, Dubinin E M, Potanin Yu N, Shkolnikova S I 1979 *Ap.Space Sci.* 61 379

Ptitsina N G 1964 *Bull.Komm.Komet.Meteor.* 9 12

Raadu M A 1981 'Relation between Laboratory and Space Plasmas' p. 13
ed. H Kikuchi, D.Reidel

Russell C T, Luhmann J G, Elphic R C, Neugebauer M 1982 in 'Comets' p. 561
ed. L L Wilkening, U.Ariz.P.

Schmidt H U, Wegmann R 1980 *Computer Phys.Comm.* 19 309

Schmidt H U, Wegmann R 1982 in 'Comets' p. 538, ed. L L Wilkening, U.Ariz.P.

Wallis M K 1968 *Planet.Space.Sci.* 16 1221

Wallis M K 1973a *Planet.Space.Sci.* 21 1647

Wallis M K 1973b *Astron.Astrophys.* 29 29

Wallis M K 1977 in 'Study of Travelling Interplanetary Phenomena' p. 279
ed. M A Shea *et al.*, D.Reidel

Wallis M K, Ong R S B 1976 in 'The Study of Comets' NASA SP-393, p. 856

Wurm K 1963 in 'The Moon, Meteorites and Comets' p. 573, ed. B M Middlehurst & G P Kuiper, U.Chicago P.

Wurm K, Mammano A 1967 *Icarus* 6 281

DISCUSSION

K. Jockers : You mentioned the model by Houpis and Mendis. To expect the ions to sweep the neutrals into the tail seems similar to a tail wagging the dog, because the neutrals are so much more abundant. Do you agree?

M.K. Wallis : Yes. In any case, the coupling-scale argument is fallacious as a proportion of the neutrals would penetrate the plasma "barrier".

E. Gérard: Do you think that the magnetic field intensity could reach 100γ on a large scale? If that is true, the Zeeman splitting of OH radio lines should be detectable (4 Hz per microgauss, hence perhaps 4 kHz).

M.K. Wallis: The tail instability analysis and other MHD arguments of Ershkovich seem to me convincing. Pressure balance in the head limits $|B|$ to $< 50\ \gamma$ at I AU under average solar conditions in a region of order 1-3x10 km radius sunward of the nucleus. For temporary enhancements produced by solar wind, high speed and dense streams, the PVO data from Venus would be a good guide, with $|B|$ up to about 150 γ. However medium fields in a large region of the coma are required for OH Zeeman splitting to occur. I would think fields of 100 γ could only be reached near the sun, at less than 0.3AU for short periods of high speed stream encounters.

AN ARTIFICIAL COMET EXPERIMENT

G. Haerendel, B. Häusler, H. Föppl, G. Paschmann, E. Rieger, and A. Valenzuela

Max-Planck-Institut für Physik und Astrophysik
Institut für extraterrestrische Physik
8046 Garching b. München

A plasma injection experiment will be conducted in the solar wind as part of a satellite mission called AMPTE (for Active Magnetospheric Particle Tracer Explorers). The experimental situation resembles that of a comet in that an expanding neutral gas (here barium) while being ionized will interact with the solar wind. Much of the plasma interaction processes occurring in cometary comae, like trapping of magnetic field, stretching of field lines, erosion and acceleration of cometary plasma are expected to take place although on a much smaller scale and for a limited period. These effects will be easily observable both by remote imaging and by in situ plasma diagnostics.

The AMPTE mission is a three-satellite project of the USA, W-GERMANY, and the United Kingdom. The German satellite with 16 release units (barium and lithium) and several plasma and field detectors, called Ion Release Module (IRM), will be accompanied by a UK subsatellite (UKS) at distances of several 100 km. Their orbit will be highly eccentric with apogee at 20 earth's radii and perigee height of a few 100 km. The NASA satellite CCE (for Charge Composition Explorer) with a set of mass and charge composition experiments will be inside the magnetosphere in an equatorial orbit of 9 R_E apogee. The whole stack of satellites is planned to be launched in August 1984 with a Thor Delta rocket from Cape Caneveral. The local time of apogee will initially be near 1400 LT.

The *scientific objectives* of the overall mission can be summarized as follows:

- Diagnostics of global plasma transport from the solar wind into the magnetosphere and inside the tail-magnetosphere system by (a) releasing and tracing of Ba- and Li-ions, and (b) by monitoring changes of the natural ionic composition.
- Plasma modification experiments with remote and in situ measurements of the interaction processes with the ambient plasma.
- Study of natural boundaries such as the magnetopause and its boundary layer, the bow shock and the tail neutral sheet.

Proceedings of the ESO Workshop on "The Need for Coordinated Ground-based Observations of Halley's Comet", Paris, 29 – 30 April 1982.

The CCE is equipped for the detection of rare ionic species over a wide range of energies (several eV to 100 MeV). The main task of the IRM is to inject (7 times during the mission) barium and lithium plasmas, both for the study of the local perturbations caused in a rarified plasma with weak magnetic field and for the subsequent tracing of the ions at large distance by the CCE. The UKS is assisting IRM in the in situ diagnostics of the plasma releases as well as in the study of the natural plasma boundaries at close distance thereby allowing the separation of spatial and temporal changes.

The mission will start with 2 or 3 Li^+ releases just outside the bow shock near the sun-earth line (see Figure 1). Lithium ions may penetrate the magnetopause predominantly in the magnetospheric cusps (high latitude magnetopause) or somewhere in the tail. Some of them may eventually reach the CCE orbit with sufficiently high density to be detected. Of interest are the observed delay times, density, and energization of the ions. They will provide insight into the global transfer and internal transport processes. Half a year later (March/April 1985), IRM (with UKS) will be in the magnetospheric tail where several releases will be actuated under varying geomagnetic condition for studies of the transport from the tail into the inner magnetosphere.

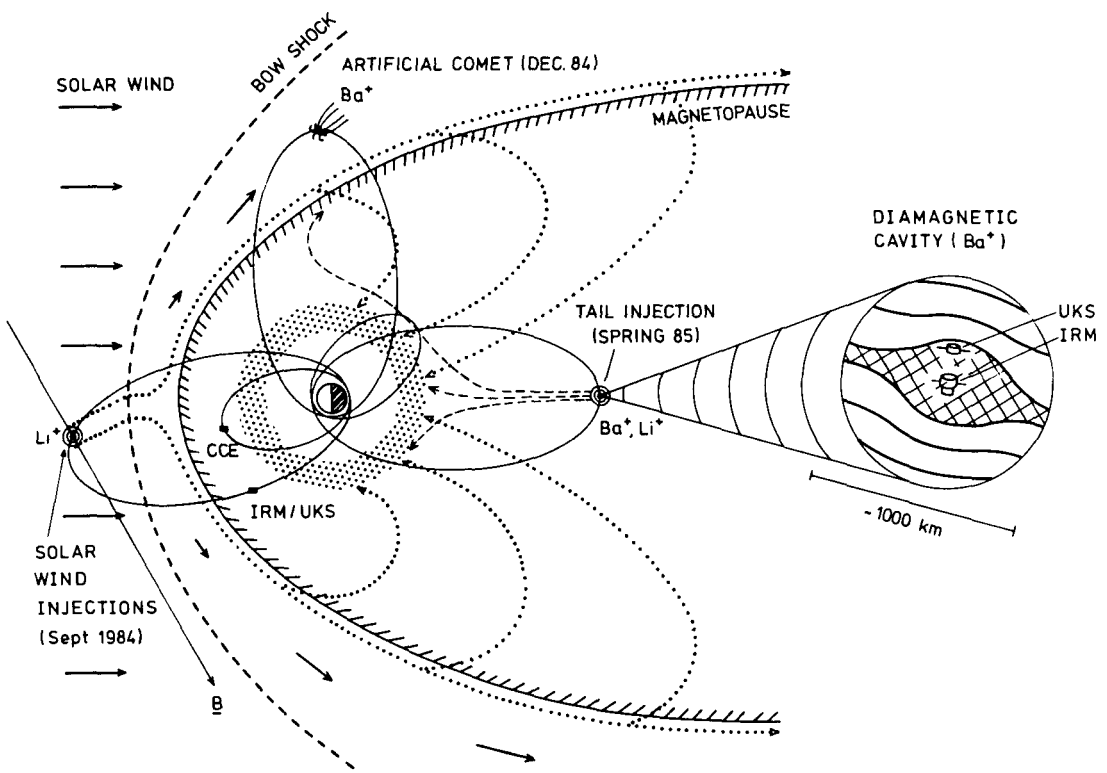

Figure 1

In this context we want to draw attention to a unique opportunity arising in December 1984 when the lines of apsides are directed towards dawn. IRM will have its apogee still outside the magnetopause in a region where the shocked solar wind is approaching Mach 1 again. In contrast to the preceding months the region near apogee is now observable from the dark hemisphere of the earth. This means that optical coverage of an artificial plasma cloud is possible. This will allow us to finally conduct the experiment which has motivated the development of the barium cloud technique in the early sixties, namely to simulate the cometary interaction.

The parameters are as follows:

- Total mass of barium atoms (ions)	2 kg $\hat{=}$ 10^{25} part.
- Size of diamagnetic core of plasma cloud (nucleus)	500 km ($\hat{=}$ 15 are minutes)
- Time-scale of initial expansion (diamagnetic phase)	$\lesssim$ 10 min
- Length of tail before loss of observations	$\approx$ 20 000 km
- Time-scale of plasma erosion	5 min
- Max. visual magnitude	BaI (5335 A): $m_v = + 3.0$ BaII (4934, 4554 A): $m_v = + 3.2$
- Max. surface brightness of plasma cloud	$\lesssim$ 25 kRayleigh
- Duration of optical phenomena - for naked eye - for low-light level TV	 10 - 15 min $\approx$ 40 min

Scientists who would like to participate in the observation of the artificial comet should contact Dr. G. Haerendel.

OBSERVATIONS OF HALLEY'S COMET WITH INTENSIFIED PHOTODIODE ARRAYS

G. Moreels, J. Clairemidi and J.P. Parisot
Observatoire de Besançon - 41 bis Avenue de l'Observatoire - 25000 BESANCON

I - THE SPECTRUM OF COMETS

The spectrum of comets presents the following components: fluorescence emissions from the coma and the tail, radiation scattered by dust and reflected flux by the surface of the nucleus. In the inner part of the coma, the optical thickness in the visible and the U.V. is too important to allow direct observation of the nucleus or to obtain spectra of the reflected radiation.

ATOME Å	H 1216	O 1304, 1356, 1972, 5577, 6300	C 1561, 1657, 1920	S 1820	Na 5893
MOLECULE Å	CO 1510, 1600, 2070	NO 1970, 2149	CS 2570, 2680	OH 2820, 3090 3142, 8450	NH 3360
MOLECULE OU ION Å	CN 3880	CH 4310	C_2 4700, 5160	C_3 4040	CO^+ 2190, 2300, 4012
MOLECULE OU ION Å	CO_2^+ 2890, 3370	N_2^+ 3914	OH^+ 2565	CH^+ 3960	H_2O^+ 7024
SUBSTANCE µm	H_2O 1.38	CH_4 1.66	NH_3 1.5	HCN 1.53	CO_2 1.57
SUBSTANCE µm	SO_2 BANDES DANS LA REGION VISIBLE	H_2CO			

Table 1 - List of the main cometary emissions observed in the coma and the tail. The wavelengths of the lines and bands are given in Å and micrometers (1), (2), (3), (4).

In the case of Halley's Comet, Figure 1 presents microphotometric records of spectra which were obtained in April, May and June 1910 (5). The intensity of scattered radiation decreases after perihelion with increasing distance from the Sun.

Proceedings of the ESO Workshop on "The Need for Coordinated Ground-based Observations of Halley's Comet", Paris, 29 – 30 April 1982.

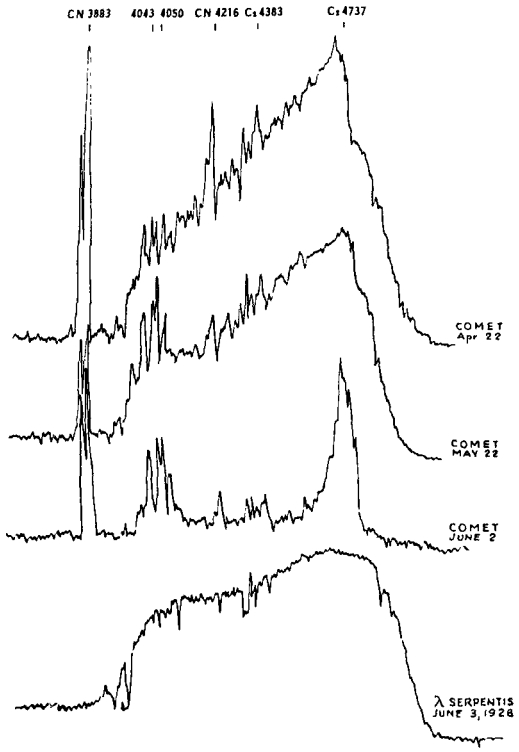

Figure 1 - Microdensitometric records of spectra of Halley's Comet obtained on April 22, May 22 and June 2, 1910. The C_3 band at 405 nanometers is not identified. The lower spectrum refers to λ Serpentis.

II - INTENSIFIED PHOTODIODE ARRAYS

Pictures of a comet in a spectral range as selective as possible around an emission feature have shown to be most useful for investigating the processes leading to the formation of the atoms and radicals in the coma (6), (7).

In order to reach both objectives: to proceed to a spectroscopic study of the radiation and to draw monochromatic maps of the comet, it is proposed to use a detector that is not at present time widely used in Astronomy. This detector is made of a microchannel plate image tube intensifier which is bonded to a photodiode linear or matrix array by using a fiber optics rectangular prism (Figure 2).

The spectral response of CCD type photodiode multielement detectors is limited towards lower wavelengths at 400 nm. By using an image tube in front of such a device it is possible to extend the useful spectral range to 120 nm (8) (Figures 3 and 4).

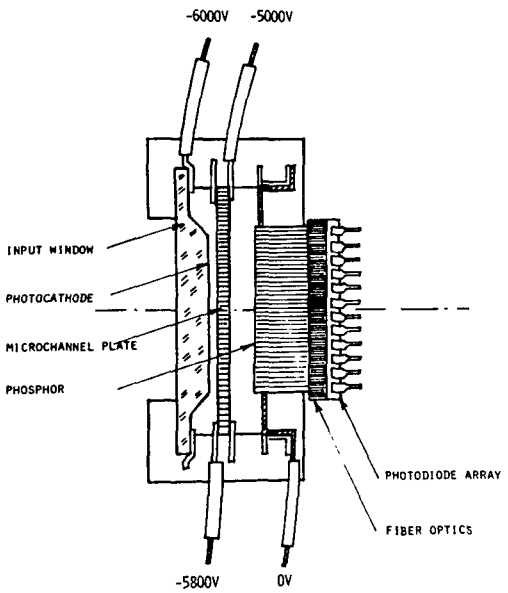

Figure 2 - Section of the intensified detector showing the image tube, the fiber optics coupling rectangular prism and the photodiode array.

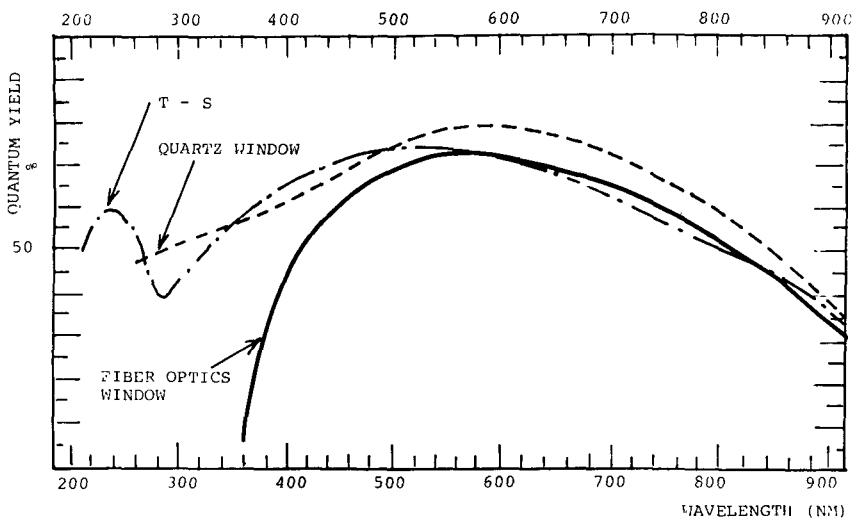

Figure 3 - Quantum yields of the different U.V. photocathodes available with image tube intensifiers. The spectral range of an S20 classic photocathode may be extended to 200 nm by using a quartz window.

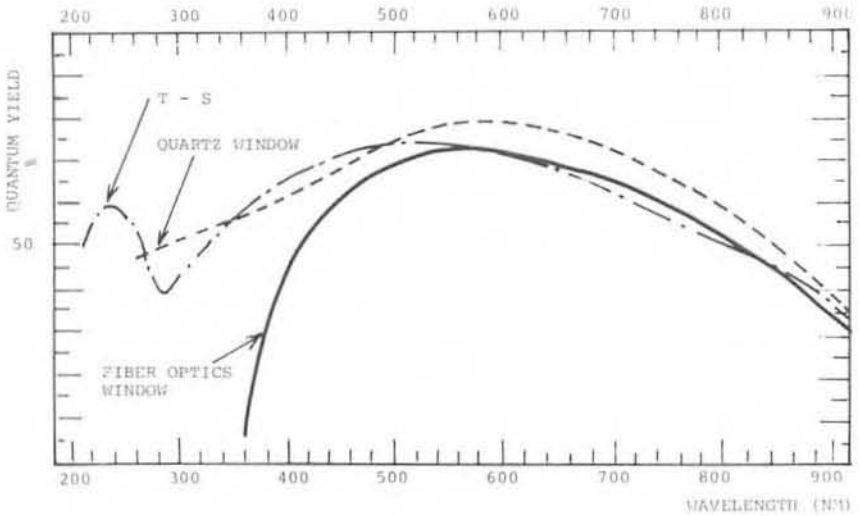

Figure 4 - Quantum yield of a Reticon linear photodiode array. The curve labelled T-S is taken from Ref. (9). The dashed line is for an array of the S series with a quartz window. The full line is for an array of the SF series with a fiber optics window.

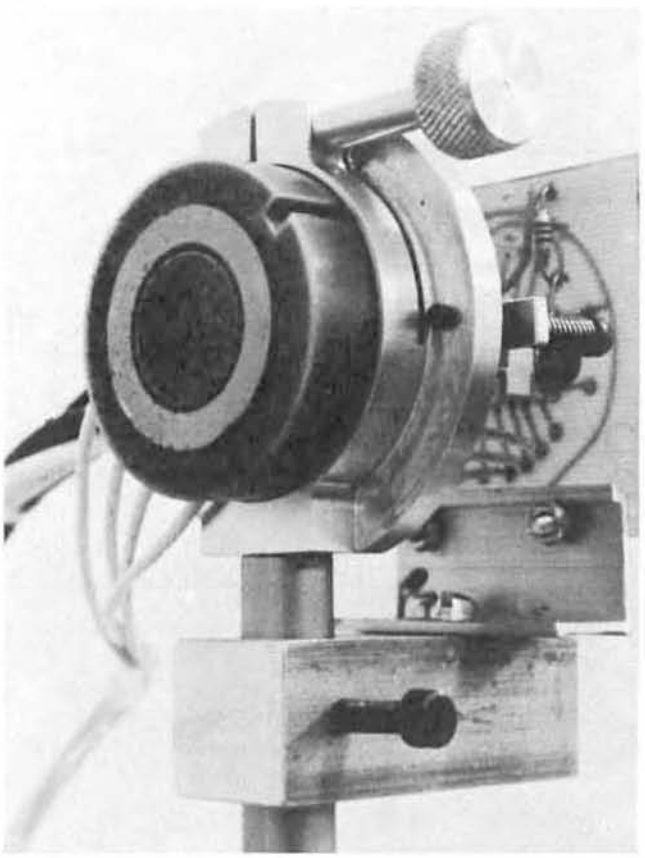

Figure 5 - Intensified detector. The front plane of the image tube in this set-up is made of fiber optics. The photocathode is of S20 type.

Such a detector has been built in the Observatory of Besançon (Figure 5). The detector includes an 18 mm RTC image tube with an optically flat output window and a Reticon 1024 linear multielement array. Two types of coupling may be done, the first with a Reticon linear array and the second with a bi-dimensional RCA matrix of 512 x 320 photosites. The pixel dimensions are: 25 μm x 2.5 mm in the first case and 30 μm x 30 μm in the second.

III - DIFFERENT SPECTROSCOPIC DESIGNS

Different types of design may be used depending upon the choice of the CCD array. In both cases, the radiation is dispersed by a concave holographic grating calculated for presenting a flat field. The spectrum is focused on the input screen of the image tube. If a matrix is used, individual spectra of the different points of an image of the comet along the entrance slit may be obtained.

In Figure 6 are presented the two optical schemes which have been studied in the design of the tri-canal spectrometer. This instrument covers the following wavelength ranges: 120 - 350 nm, 350 - 900 nm and 900 - 1000 nm. The secondary mirror of the telescope may be tilted in order to move the comet's image in the focal plane and obtain a monochromatic mapping of the object.

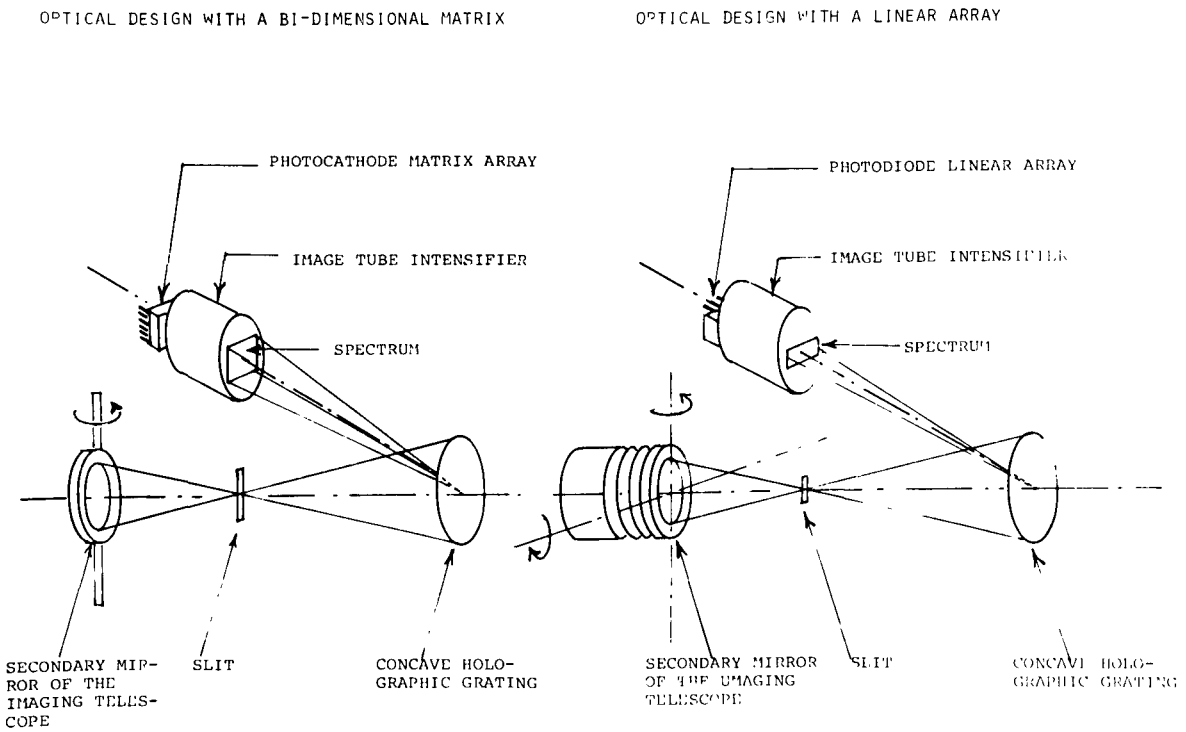

Figure 6 - Optical schemes of the tri-canal spectrometer. Two versions have been studied: with a matrix array and with a linear array.

IV - CONCLUSION

It is proposed to proceed to spectroscopic observations of Halley's comet in using an intensified detector which includes a photodiode array fixed on the output screen of an image tube intensifier. The coupling is made with a rectangular prism of fiber optics.

This detector extends the useful spectral range of CCD's to 120 nm.

From high altitude observatoires it is possible to measure the OH, NH, CN and CO_2^+ emissions. From stratospheric balloons, it should be possible to measure the NO, CO, CO^+ bands around 200 nm and detect the forbidden (^1S - ^3P) line of oxygen at 192.7 nm.

REFERENCES

(1) V.A. Chaubey (1979) Astrophys. Space Sci. 64, pp. 53-56.

(2) J.S. Neff, D. Ketelsen, G.D. Schmidt, J.B. Tatum (1976) Icarus 27, pp. 545-551.

(3) K.R. Sivaraman, G.S.D. Babu, M.K.V. Parthasaratym (1979) M.N.R.A.S. 189, pp. 897-906.

(4) P.D. Feldman, H.A. Weaver, M.C. Festou, M.F. A'Hearn, W.M. Jackson, B. Donn, J. Rahe, A.M. Smith and P. Benvenuti (1980) Nature 286, pp. 132-135.

(5) N.T. Bobrovnikoff (1931) Publ. Lick Obs. XVII, pp. 305-482.

(6) J.L. Bertaux, J.E. Blamont and M. Festou (1973) Astron. Astrophys. 25, p. 415.

(7) M. Festou (1978) Thèse de Doctorat d'Etat, Paris.

(8) P.D. Feldman and W.M. Brune (1976) Astrophys. J. Letters 209, pp. L45-L48.

(9) Y. Talmi, R.W. Simpson (1980) Applied Optics 19, pp. 1401-1414.

OPTICAL OBSERVATIONS: THE TAIL

THE COMETARY ION TAIL AND ITS RELATION TO SOLAR WIND PHENOMENA.

Klaus Jockers

Max-Planck-Institute for Aeronomy, Katlenburg-Lindau, FRG

Summary

Most cometary ions observed in the visible range are the ions of presumed mother molecules like H_2O, CO, CO_2, N_2. After reviewing the emissions of these ions an overview of our present understanding of the comet-solar wind interaction is given. Modulation effects on the different ions introduced by a change in solar wind flux are studied. Further topics include the general structure of the ion tail, tail rays and large-scale tail disturbances (tail disconnections). Recommendations for future ground-based observations are given.

1. Introduction

While the neutral molecules radiating in visible light are produced from the presumed mother substances by complicated and partly unknown chemical reactions, their ions (H_2O^+, CO_2^+, CO^+) are accessible for ground-based observations. In addition, the ion N_2^+ also has transitions in the visible part of the spectrum and may derive from N_2 as another possible mother substance. In view of this fact it is very surprising that physical studies of the cometary ions based on ground-based observations are almost totally missing. So far, most observers have not done more than to point out the existence of an ion emission in the spectrum and at best provided a rough qualitative estimate of the line strength. The reason for this may be two-fold. On one hand many plasma emissions are rather weak and therefore difficult to observe. This is particularly true in the near UV part of the spectrum, where extinction in the earth's atmosphere is important, especially if the comet is observed at low altitudes above the horizon. On the other hand, the cometary ions are influenced by the solar wind. Therefore, while simple models are available to describe the outflow of neutral species (Haser 1957, 1966, Combi and Delsemme 1980, Festou 1981) such models are so far not available for the ions.

It is the opinion of the present writer that the most interesting contribution, ground-based astronomy can provide to the study of comets using state of the art detectors and equipment, will come from observations of the ions. To explain this in more detail is the purpose of this article.

Proceedings of the ESO Workshop on "The Need for Coordinated Ground-based Observations of Halley's Comet", Paris, 29 – 30 April 1982.

2. The main spectral emissions of cometary ions.

Except for the newly identified ion H_2O^+ (Wehinger et al. 1974, Benvenuti and Wurm 1974) most emissions of cometary ions accessible to ground-based observations extend from the blue into the near-UV part of the spectrum. This is illustrated in Figures 1 and 2 which show an objective prism spectrogram of Comet P/Halley (Slipher and Lampland 1911) and a slit spectrogram of Comet Bester 1948I (Swings and Page 1950). In both figures, direct photographs of the comets are also shown.

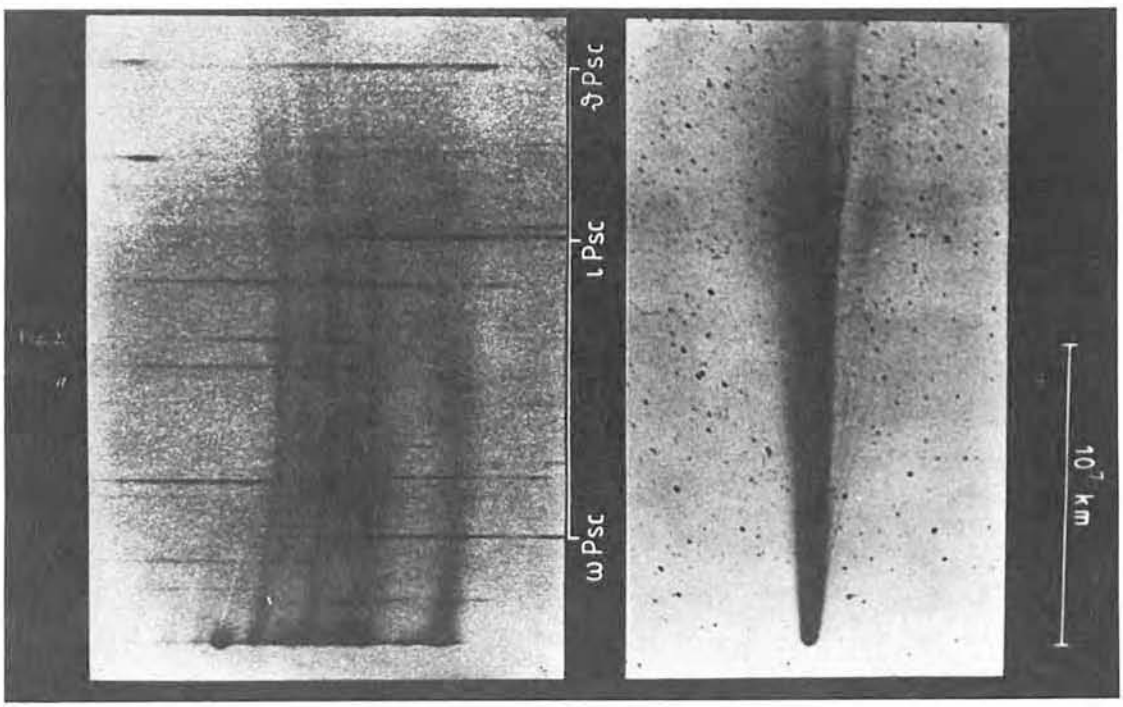

Fig. 1 Objective prism spectrum and direct photograph of Comet P/Halley taken May 4, 1910. (Slipher and Lampland 1911).

The strongest ion emission is due to CO^+, present in several vibrational bands of the $A^2\Pi_i - X^2\Sigma^+$ electronic transition, of which the 2-0 and 3-0 bands at 4251/4274 Å and 4002/4024 Å are especially strong. The doublet structure of these bands is apparent. Two emissions of the $B^2\Sigma_u^+ - X^2\Sigma_g^+$ emission of N_2^+ appear at 3914 and 4274Å. Both emissions are blended by the corresponding night glow emission and the stronger one at 3914 Å is quite close to the CN band head at 3882 Å. The CO_2^+ $\tilde{A}^2\Pi_u - \tilde{X}^2\Pi_g$ emission, which is much weaker than CO^+, is present in the UV at 3509 and 3674 Å. It is blended with some weak CO^+ emissions of the (non-resonance) Baldet-Johnson $B^2\Sigma^+ - A^2\Pi_i$ band system. Weak ionic emissions of the OH^+ and CH^+ ion are also present in this spectral range. The importance of OH^+ and CH^+ lies in the fact that the emission of the neutrals OH and CH are also available from the ground.

Figures 1 and 2 address still another problem of tail ion observations. The slit spectrum of Figure 2 provides high spectral resolution but covers a small

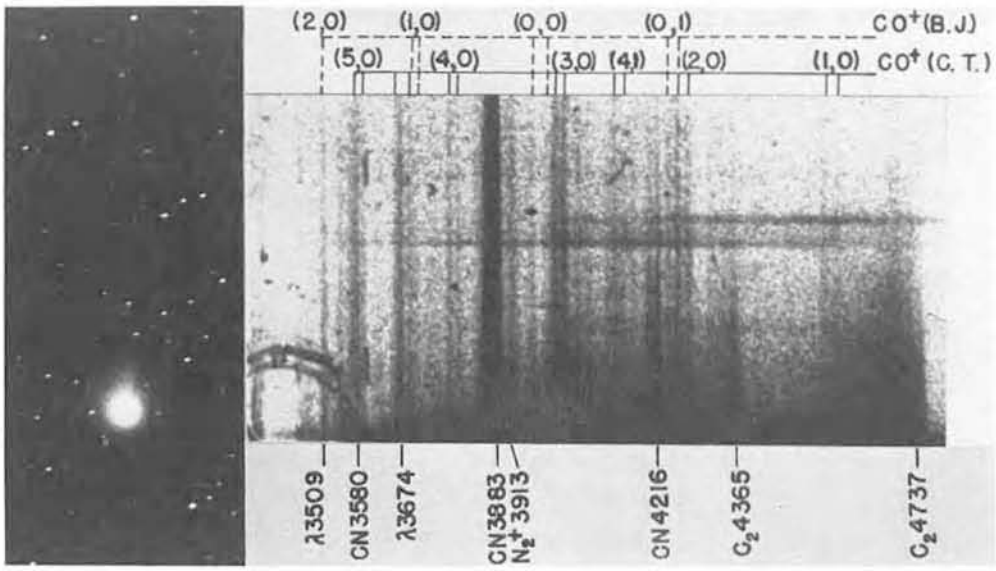

Fig. 2 Direct photograph and slit spectrum of Comet Bester 1948 I, showing the CO^+, N_2^+ and CO_2^+ bands (at λ 3509 and λ 3674). The spectrum covers only the coma of this dust-poor comet. Spectrum taken March 18 and direct photograph March 19, 1948 (Swings and Page 1950).

angle on the sky. The slit was put parallel to the antisolar direction, to catch the direction of the tail. It would have been still better to choose the aberration angle of the comet tail which respect to an average solar wind which usually differs from the radial direction by a few degrees (see Figure 6 below). It can be estimated that the ion tail probably is wider than the slit (in the direction of dispersion) so that not all light of the tail is admitted into the spectrograph. Besides of the light loss this makes it difficult to determine the number of radiating ions since a model of the tail, as compared to models of the neutral coma, is not available.

The slitless spectrogram of Comet P/Halley was obtained with a special camera of small size and an objective prism of rather high dispersion. Here the field covers a large portion of both, plasma and dust tails. The dust tail radiates mainly in the green part of the spectrum (in Fig. 1 a dust tail "absorption" feature in the green part of the spectrum is probably caused by a sensitivity gap of the emulsion on which the spectrum was photographed). The blue and violett emissions of the plasma tail are not strongly disturbed by the dust continuum. Nevertheless the sensitivity (signal/sky background) and spectral resolution are reduced as compared to the slit spectrum.

A spectrum of cometary H_2O^+ has been reproduced by Wyckhoff (1982). Between 5800 and 6300 Å H_2O^+ and weak CO^+ emissions exist in the same wavelength interval.

Plasma tails have been recorded in the light of the H_2O^+ ion even before it was identified (Miller 1980).

3. Theory of stationary solar wind - comet interaction.

Due to mathematical difficulties the existing theoretical models of the solar wind-comet interaction are still highly idealized. Ip and Axford (1982) have given a recent overview. Schmidt and Wegmann (1982) have done the most detailed numerical modelling (see also Wallis 1973). As will be explained in more detail below, CO^+ is the most important ion for the comet-solar wind interaction, because of its large abundance and because neutral CO has a rather long life time ($\sim 10^6$s) against photoionization or ionization by charge exchange with solar wind protons. If the CO atoms have a speed of 1 km s^{-1}, corresponding to the thermal ejection speed from the nucleus, they can reach a distance of 10^6 km from the nucleus before they are ionized. The existence of such a large cloud of neutral molecules serving as an extended source of cometary ions is a main feature of the presently accepted model of solar wind - comet interaction. Wurm (see e.g. Wurm 1968, Wurm and Mammano 1967) has very much opposed this notion of an extended ionization source and therefore stimulated proposals of other "anomalous" ionization mechanisms like impact ionization by energetic electrons from shock waves (Beard 1966), ionization by tail currents (Ip and Mendis 1976, Ip 1979) and by neutral molecular beams (Alfvén 1960, Formisano et al. 1981). These mechanisms may be important but in view of our limited knowledge it seems premature to include them in present-day interaction models.

In the extended, neutral cloud the neutral molecules are unaffected by the plasma flow. As soon as a particle becomes ionized it must gyrate around the lines of force of the magnetic field, which are imbedded in and moving with the solar wind. This way the newly formed ion aquires a quasi-random and a directed velocity, i.e. it is heated and at the same time accelerated to the solar wind speed. This mechanism of ion pick up is not restricted to comets only. Plasma instabilities associated with it are discussed by Ip and Axford (1982). The mass addition of cometary ions into the solar wind slows down the supersonic flow. As was pointed out by Axford (1964) and by Biermann et al. (1967), when the admixture of cometary ions has reached about a few percent, a shock transition must occur. The shock strength is much weaker than the strength of the earth's bow shock because of the continuous deceleration upstream of the shock. In a productive comet with a dense neutral source cloud a 1% ion admixture will already be reached at the edge of this cloud, i.e. the shock wave will form at a distance of about 10^6 km upstream of the nucleus. For comets with a smaller gas production the solar wind will penetrate more deeply into the cloud until it aquires an admixture of 1% cometary ions and the shock front will appear closer to the nucleus. Because of the

small admixture of cometary ions at the location of the shock the density increase of cometary ions is not strong enough to allow its detection with a telescope.

The existence of a shock wave in front of a comet is now fairly well established on theoretical grounds. In addition to the shock wave another surface has been postulated, the contact surface separating the solar wind flow field from a purely cometary flow field. Hydrodynamic theory predicts the distance of the contact surface from the nucleus by equating the dynamic pressure of the solar wind with the dynamic pressure of ion outflow from the cometary nucleus. For productive comets this gives a stand-off distance of 10^3 km. However, ion-neutral coupling or an ion temperature increased by exothermal chemical reactions could rise this distance. In their model calculation, Schmidt and Wegmann (1982) have assumed a standoff distance of the contact surface of 10^4 km to avoid excessive numerical problems. A result of their calculations is shown in Figure 3. In this model the magnetic

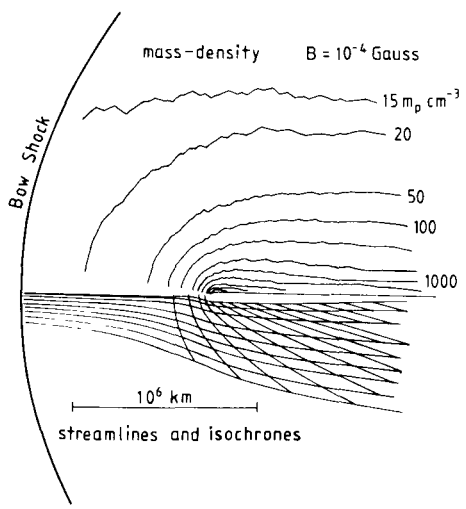

Fig. 3 Stationary interaction of the solar wind with a comet (Schmidt and Wegmann 1982).

force was averaged to produce an axi-symmetric flow. Ionization of CO with a rate constant of $10^{-6}s^{-1}$ and a cometary production rate of 2.10^{30} molecules s^{-1} was assumed. The shock wave is located at the edge of the neutral cloud. The lower part of the figure shows the stream lines and isochrones, i.e. surfaces which mark different epochs on the stream lines. In the subsonic region the flow is further decelerated by additional admixture of cometary ions. The upper part of the figure shows an observable quantity, the plasma density. The density increase is very much concentrated in a small inner part of the comet. A reduction

Table 1 : Typical life-times and pumping rates of water molecules in comets at r = 0.8 AU.

transition	wave number (cm^{-1})	life-time of excited level (s)	solar pumping rate (s^{-1})
rotational	0.8 to 300	$\sim$100	–
vibrational			
ν_2	1630	0.06	2.8×10^{-4}
$2\nu_2$	3195	0.03	3.0×10^{-6}
ν_1	3690	0.2	1.3×10^{-5}
ν_3	3770	0.02	3.5×10^{-4}
$\nu_2+\nu_3$	4754	0.09	3.8×10^{-5}
$\nu_1+\nu_3$	6812	0.06	3.1×10^{-5}
$2\nu_1$	7312	$<1.$	2.2×10^{-6}
electronic	80600		1.6×10^{-8}
collisional rate	10^{-2} s^{-1} at 600 km from nucleus		
photodis. rate	1.9×10^{-5} s^{-1}		

We remark from Table 1 that :

a) UV pumping is negligible (the detectability of UV fluorescence is discussed by Smith et al., 1981) ;

b) in the infrared, a first-order evaluation needs only to consider the ν_2 and ν_3 vibrational bands which achieve 85% of the pumping ;

c) the life-times of the excited levels - including the rotational levels - are so small that UV and infrared pumping rates are not high enough to significantly populate these levels ;

d) radiative decay rates of the rotational levels are competitive with collisional rates at a distance $\rho\sim600$ km from the nucleus.

In order to specify this last point, we have computed the H_2O population distribution as a function of nucleus distance (ρ). We have only considered collisions and radiative decay within the rotational levels. In our model, molecules expand radially with v_{exp} = 1 km s^{-1} and an initial Boltzmann distribution (T_{kin} = 200 K) is assumed near the nucleus. The inelastic collision rate is

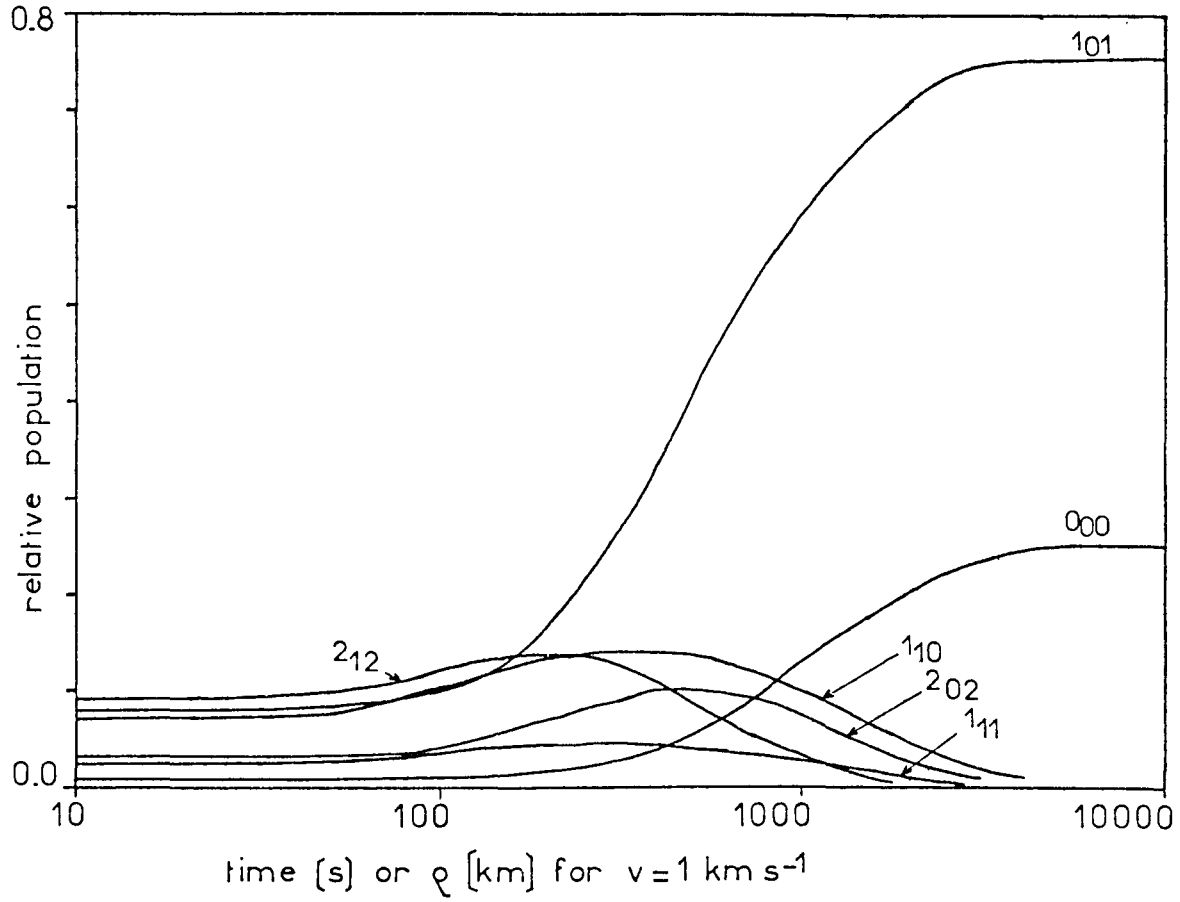

Figure 1 : Relative population of the lower levels of H_2O in the coma as a function of distance from the nucleus. Only collisions and radiative decay are taken into account.

$$\tau_{coll} = \frac{Q\sigma}{4\pi\varrho^2}$$

with $Q = 2\times10^{29}$ mol. s^{-1} and $\sigma = 2.5\times10^{-15}$ cm^2. Since rotational transition rates for $H_2O - H_2O$ collisions are unknown, we have assumed that each collision redistributes the shocked molecule on the rotational energy levels according to the Boltzmann partition function (T_{kin} = 200 K).

The results are shown in Figure 1 : within a few 100 km from the nucleus, collisions are sufficient to preserve thermalization. Beyond a few 1000 km, radiative decay prevails, and only the two lower levels 0_{00} and 1_{01} of the ortho and para states of H_2O are populated. An integration of the partition function over the whole coma shows that 98% of the water molecules are in these two lower states.

Such changes in flux by a factor of ten for periods of at least several hours are not rare. Much larger variations have been observed. Because of the enhanced charge exchange the size of the neutral source cloud is expected to shrink in linear proportion to the flux rise. The time scale of the shrinking is determined by the penetration time of the solar wind, i.e. is of the order of several hours (a solar wind of a speed of 100 km s^{-1}, i.e. somewhat decelerated by the mass loading process, moves a distance of $4 \cdot 10^5$ km in one hour). During this event a large part of the neutral cloud will be ionized very quickly. For a short period this will lead to an enhanced ion production. As the neutral particles move only with a speed of about 1 km s^{-1} as compared to the 100 km s^{-1} of the solar wind protons the recovery of the neutral cloud will take much longer than its partial destruction.

The different cometary species will vary in their response to the solar wind modulation. If the molecule has a small charge exchange rate as compared to the photoionization rate it will be less influenced. More important, molecules which have a small total ionization rate will be enriched in the outer parts of the neutral source cloud and therefore more affected by an enhanced solar wind flow.

Table 1
Ionization in Comets

Mother molecule	H_2O	CO	CO_2	N_2
Main photodestruction mechanism	Dissociation	Ionization	Ionization	Dissociation
Destruction rate (s^{-1})	1×10^{-5}	3×10^{-7}	7×10^{-7}	7×10^{-7}
Photoionization rate (s^{-1})	3×10^{-7}	"	"	3×10^{-7}
Charge exchange rate (s^{-1})				
average	8×10^{-7}	1.2×10^{-6}	6×10^{-7}	2×10^{-7}
compression region	4×10^{-6}	6×10^{-6}	3×10^{-6}	10^{-6}

In Table 1, in a simplified manner, the neutrals belonging to the main cometary ions are shown with their main destruction mechanism and destruction rates (the photochemical rates are taken from Huebner and Giguere 1980). If the enhanced charge exchange rates in the compression region of the high speed stream (bottom line of Table 1) compete with the main photodestruction rate a modulation effect is expected. Water is quickly dissociated into H and OH so that the size of the neutral H_2O cloud, producing the H_2O^+ ions is only 10^5 km. Therefore, despite of the high charge exchange rate, H_2O^+ production will not be strongly modulated because the solar wind flux will rarely be high enough to let the source cloud shrink below a size of 10^5 km. CO^+, on the other hand, will be strongly modulated because it is produced at large distances from the nucleus and has a high charge

exchange rate. CO_2^+ and N_2^+ will show an intermediate behaviour. In this discussion I have purposely assumed direct ionization from a neutral and not considered the ion-molecular reactions. At least in the outer part of the source cloud, ions are effectively removed by solar wind action. Models including the ion-molecular reactions and neglecting solar wind effects lead, however, to qualitatively similar results (Huebner and Giguere 1980, Feldman 1978).

5. The plasma tail

So far we have mostly considered the sunward side of the comet because it is the region of ion formation from the cometary neutrals. This region is very difficult to study observationally because of the presence of many emissions from neutral coma species. On the antisolar side the cometary plasma is collected in the plasma tail. In principle, the plasma tail should correspond in its structure to the sunward region of the coma. There should be an inner part of the tail which consists of cometary ions without solar wind admixture and represents the downstream extension of the contact surface. This inner tail should be of cylindrical shape (Ioffe 1966) and its width should be of the order of the lateral width of the contact surface. Since the solar wind magnetic field is frozen into the solar wind the inner tail should also be free of magnetic field and the flow

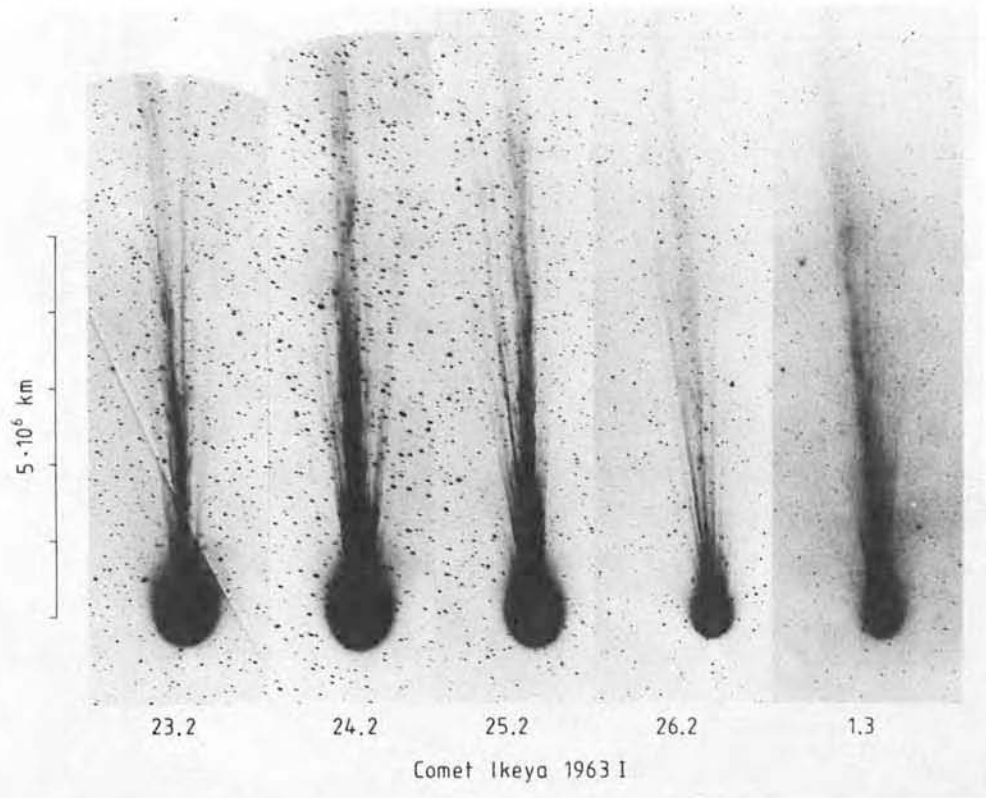

Fig. 6 Comet Ikeya 1963 I from Feb. 23 until March 1, 1963. (Boyden Observatory photographs, courtesy E. Geyer). The antisolar direction is vertical.

Table 2 : Expected submillimeter fluorescence of H_2O. (Pumping through the ν_2 and ν_3 bands only is assumed ; g-factors are computed for r = 0.8 AU.)

λ (μ)	ν (GHz)	transition	g-factor (10^{-5} mol.$^{-1}$ s^{-1})	antenna temperature T_A/η (K)
538	557	$1_{10} - 1_{01}$	5.71	0.6
399	752	$2_{11} - 2_{02}$	0.24	0.3
303	988	$2_{02} - 1_{11}$	1.77	1.6
273	1097	$3_{12} - 3_{03}$	0.14	0.1
269	1113	$1_{11} - 0_{00}$	5.19	0.2
260	1153	$3_{12} - 2_{21}$	0.02	0.01
258	1163	$3_{21} - 3_{12}$	0.16	0.1
244	1228	$2_{20} - 2_{11}$	0.24	0.1
179	1670	$2_{12} - 1_{01}$	15.7	0.2
175	1717	$3_{03} - 2_{12}$	13.3	3.9
108	2275	$2_{21} - 1_{10}$	5.71	0.4
101	2968	$2_{20} - 1_{11}$	3.42	0.3
75	3977	$3_{21} - 2_{12}$	2.40	0.1

Among the transitions listed in Table 2, those at 988 and 1717 GHz might be detectable with suitable submillimeter receivers, if the observations can be made above the absorbing atmospheric water.

References

Crifo, J.F., 1981, in "The Solar System and its Exploration", ESA SP-164 p. 229

Crovisier, J., Despois, D., Gerard, E., Irvine, W.M., Kazès, I., Robinson, S.E., Schloerb, F.P., 1981, Astron. Astrophys. 97, 195

Encrenaz, T., Combes, M., Crifo, J.F., Gerard, E., Bibring, J.P., Crovisier, J., 1981, BAAS 13, 707

Encrenaz, T., Crovisier, J., Combes, M., Crifo, J.F., 1982, Icarus (in press)

Irvine, W.M., Schloerb, F.P., Yngvesson, K.S., 1981, IAU Coll. 61, poster paper

de Jong, T., 1973, Astron. Astrophys. 26, 297

Shimizu, M., 1976, Astrophys. Space Science 40, 149

Smith, P.L., Black, J.H., Oppenheimer, M., 1981, Icarus 47, 441

Whipple, F.L., Huebner, W.F., 1976, Ann. Rev. Astron. Astrophys. 14, 143

Isotopic Abundances in Comets

by
A.C. Danks
E.S.O. Casilla 16317, Santiago 9
Chile

Introduction

Measurements of isotopic ratios in comets may indicate the origin of comets. That is we may be looking at a sample of the interstellar medium out of which the solar system was formed. This material has been preserved in "cold storage" for 4.6 billion years at the outer reaches of the solar system and may be especially interesting in studies of the chemical composition of the outermost planets. The alternative intriguing possibility is that some comets have been captured from outside the solar system and have a chemical composition closer to that of the interstellar medium today and so allow a closer study of the interstellar medium.

Evidence exists for variations of isotopic abundance ratios in the Galaxy. These variations are presumably due to nuclear processing of material in stellar interiors, which is subsequently returned to the interstellar medium by a variety of mechanisms, mass loss, supernova, etc. In Table 1 values are given for the most important isotopic abundances for the sun and the interstellar medium. Elements such as ^{13}C are principally produced in Hydrogen burning in the CNO cycle and ^{12}C in Helium burning. Similarly for other elements like ^{14}N and ^{16}O.

As pointed out by Festou earlier in this conference, absolute abundances are very difficult to determine. However, this is not the case for isotopic ratio's which should be easier to measure.

One ratio which lends itself to analysis in Comets is $^{12}C / ^{13}C$. The solar abundance is ~ 89 and as Carbon is abundant in Comets it should therefore be easily measurable.

Proceedings of the ESO Workshop on "The Need for Coordinated Ground-based Observations of Halley's Comet", Paris, 29 – 30 April 1982.

20-40 minutes. Similar tailward moving features on the solar side of a comet have been found in spectra of Comet Bennett 1970 II and Comet West 1976 VI in H_2O^+ and CO^+ profiles by Delsemme and Combi (1979) and Combi and Delsemme (1980). Usually envelopes and tail rays are formed so frequently that several of them can be seen at the same time. Sometimes a single pair of strong tail rays appears (Figure 9). Tail rays very often form in pairs but there are exceptions. Figure 10 shows a comparison of symmetric and one-sided ray formation. The latter phenomenon has

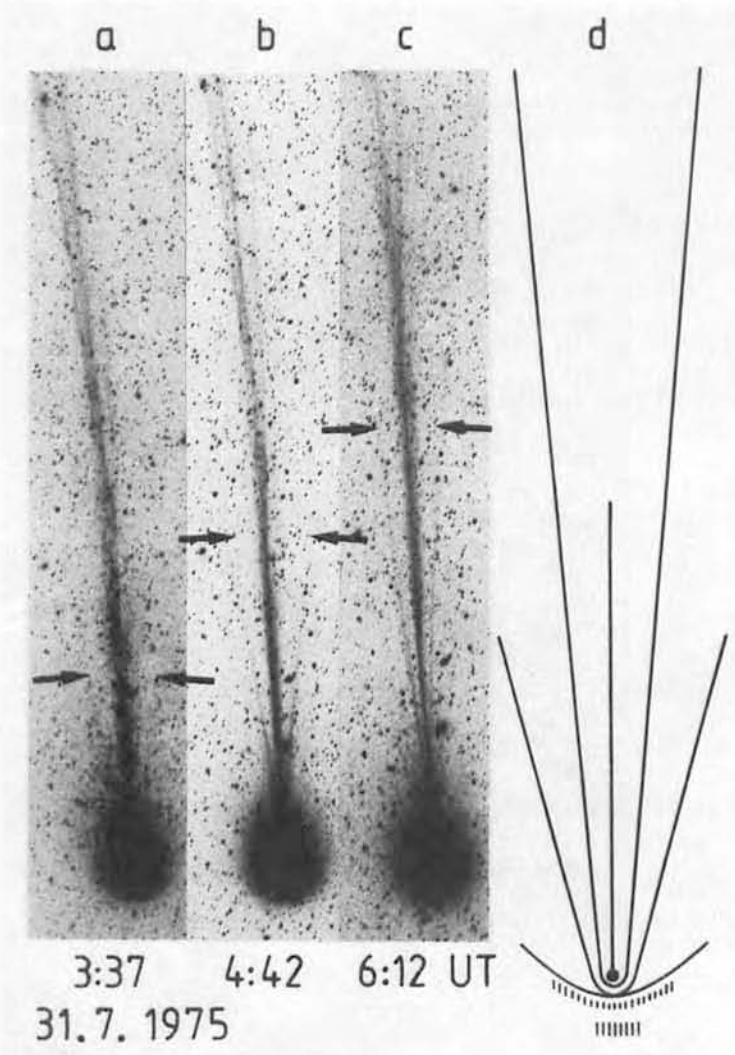

Fig. 9 Tail ray development in Comet Kobayashi-Berger-Milon 1975 IX. (Joint Observatory for Cometary Research photograph).

been called "plumes" by Miller (1979). It is very tempting to interpret plumes as side rays seen edge-on, indeed Figure 10 almost looks as if the same comet were shown in a front and side view. However such a conclusion cannot be justified on the base of the available observations. In fact, the spatial structure of the tail rays is not known. They may even represent conical surfaces of which only the part of the surface tangential to the line of sight is detectable. The formation of tail rays is related to solar wind disturbances. In fact, the iden-

tification of the repeated occurrence of enhanced tail ray activity in Comet P/Halley, when the comet met an interplanetary feature which was corotating with the sun led Biermann (1952) to predict the presence of continuous plasma outflow from the sun. Alfvén (1957) has interpreted the ray folding phenomenon as magnetic field lines, traced by cometary plasma, which are wrapped around the comet by the solar wind flow. In this simplistic form the model assumes a two-dimensional geometry and neglects the possibility that instead of getting collected in the cometary head three-dimensional topology allows the magnetic field lines to pass sideways along the comet. Nevertheless, as has been demonstrated rigorously by Lees (1964, see also Schmidt and Wegmann 1982), the flow field of a plasma containing an arbitrarily weak magnetic field around an obstacle cannot be axially symmetric. Instead, at the stagnation point the magnetic field lines will concentrate until its magnetic pressure can dynamically influence the flow to allow an increased convection in the direction perpendicular to the instantaneous magnetic

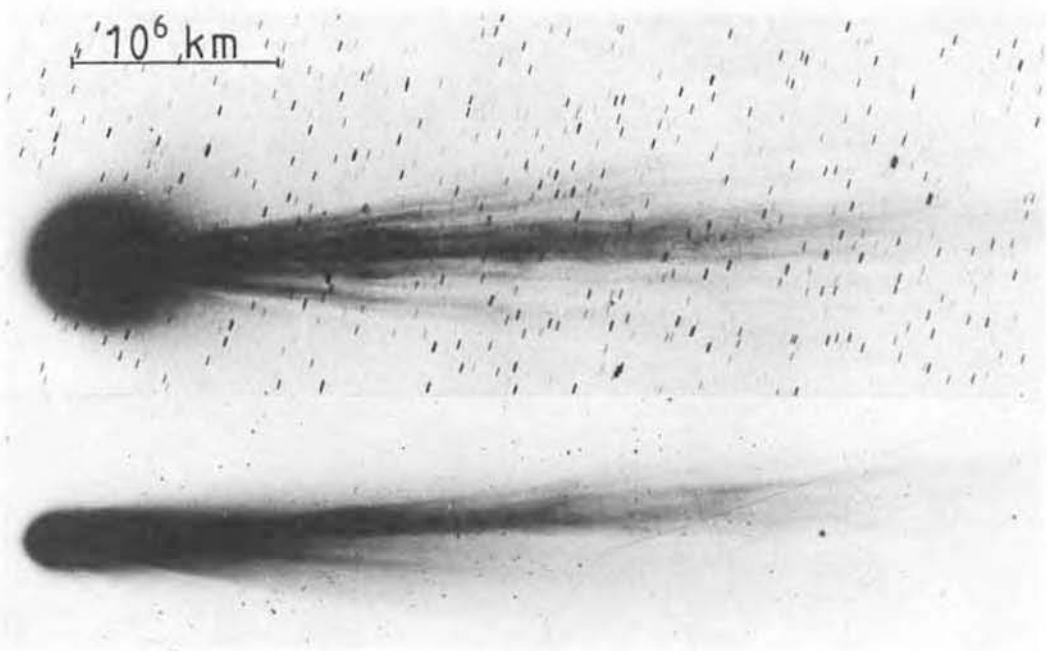

Fig. 10 Symmetric and asymmetric tail ray formation: Top: Comet 1963 I (Boyden Observatory photograph. courtesy E. Geyer). Bottom: Comet 1969 IX (Cerro Tololo Interamerican Observatory photograph, courtesy F.D. Miller).

field direction. This is sketched in Figure 11. The formation of such a magnetic barrier in front of a nonmagnetic obstacle has been observed in the case of Venus (see Russell et al. 1982). According to Schmidt and Wegmann (1982), balance of total pressure (plasma plus magnetic pressure) near the stagnation point requires a reduced plasma pressure (and density) in the region of increased magnetic field so that, in contrast to Alfvén's picture the tail rays would form in the region of reduced magnetic field. In addition, the magnetic field lines forming the magnetic

The first spectra to partially resolve the NH_2 lines from the $^{12}C^{13}C$ band head were made by Danks et al (1974) on comet Kohoutek (1973)XII. A low resolution spectrum, ∿ 0.4 Å, of Kohoutek is shown in fig.(1). This spectrum was taken with the McDonald 272-cm reflector and the Tull (1972) coudé scanner. Later scans at a resolution of 0.14 Å were made of the $^{12}C^{13}C$ + NH_2 λ4745 blend and these are shown in figs. (2) and (3). The violet-degraded ^{12}C ^{13}C band head begins at 4744.69 Å and the NH_2 blending lines occur at 4744.28, 4744.46, 4744.89 and 4745.19. The last 3 lines are from the (0, 14, 0) band and are classified by Dressler and Ramsay (1959). The line at 4744.28 probably belongs to the (1, 10, 0) band and will occur in the comet spectrum (Ramsay 1974)

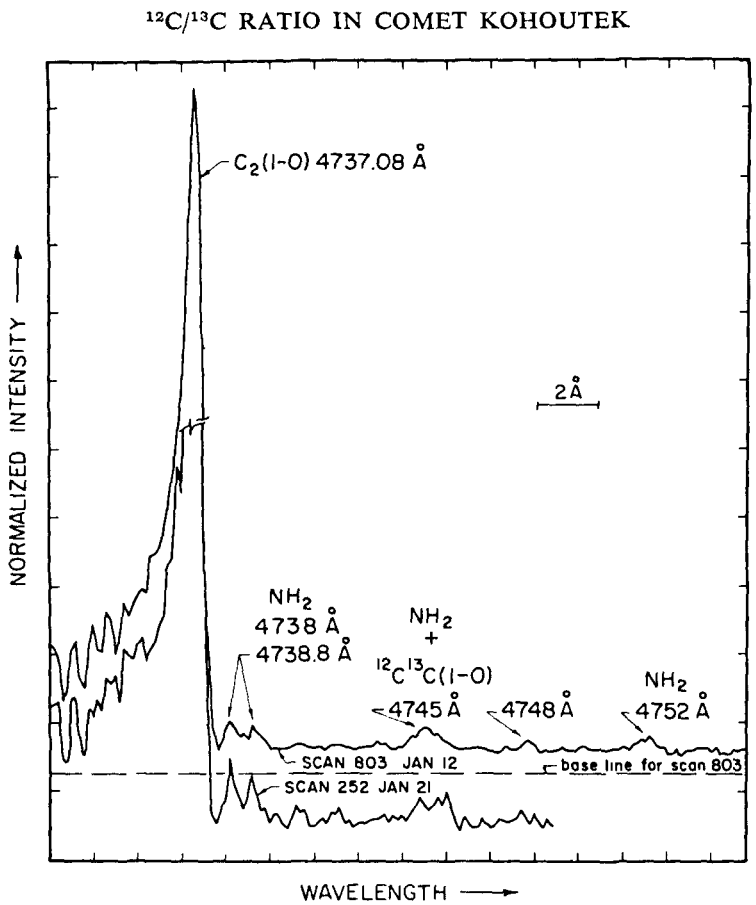

Fig.1 Medium resolution scans of Comet Kohoutek 73XII

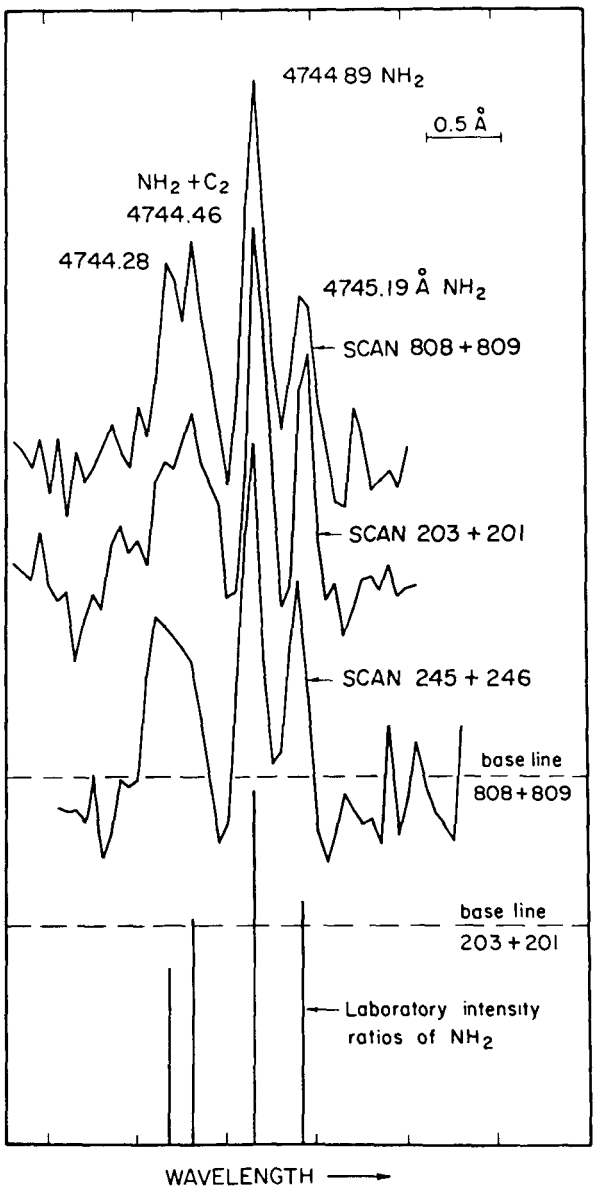

Fig.2 High resolution scans of the $^{12}C^{13}C$+NH_2 λ4745 blend in Comet Kohoutek

Naturally, the NH_2 line intensities must be corrected for the effects of Resonance-fluorescence before subtraction can be made. In fact, an approximation has to be made as complete information on the NH_2 spectrum and transition probabilities is not yet available. However the importance of subtraction is evident from fig. (3) where the λ4745 feature is seen to be composed of 82% NH_2.

In order to obtain an isotopic ratio a synthetic spectrum was generated and first fit to $^{12}C^{12}C$(1-0) band head by adjusting the excitation temperature.

The recipe for the spectrum is given in Danks et al (1974). In the case of Kohoutek the best fit was achieved for a $T_{exc} \simeq 3000°K$. In fact, the fit to the (1-0) band head is not very sensitive to temperature and where possible $\Delta v = +1$ sequence should be used, see Lambert and Danks (1982). The temperature derived from the $^{12}C^{12}C$(1-0) band head is now applied to the $^{12}C^{13}C$ head

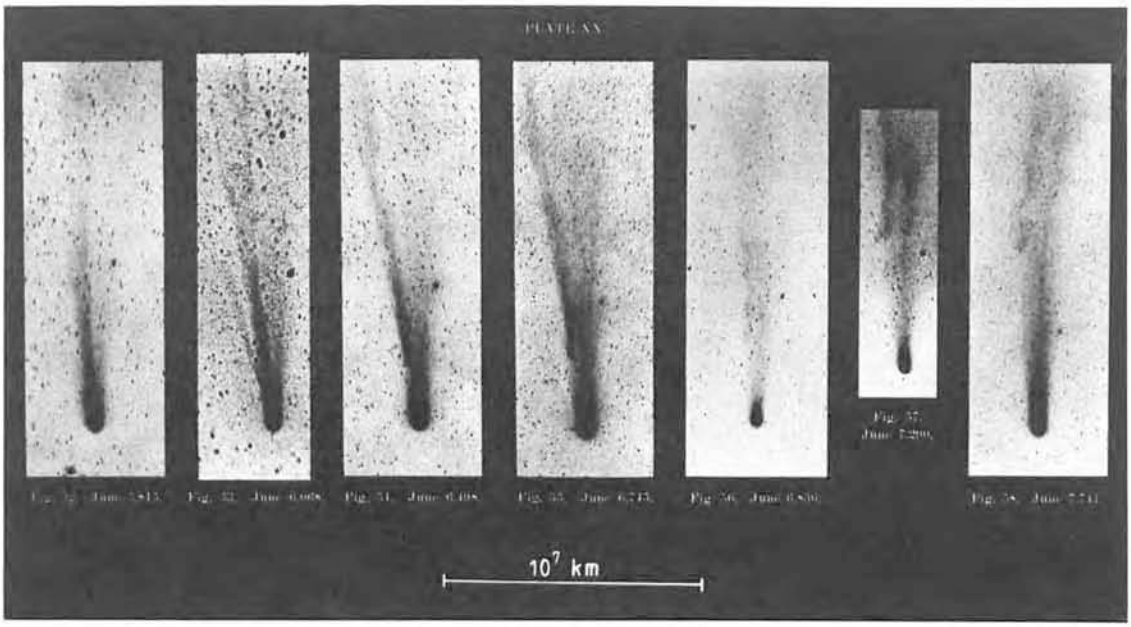

Fig. 13 A large-scale tail disturbance observed in Comet P/Halley June 5-7, 1910. (Bobrovnikoff, 1931).

there seems to be a continous transition to the regular tail ray phenomenon. So far, a clear phenomenological description does not exist. Necessary features are the presence of strong tail rays at the beginning of the event, bends in the tail and perhaps the formation of a plasma cloud as in Figure 12 or 13. Niedner et al. (1978) and Jockers (1981 a) have discussed an event which took place in Comet Kohoutek 1973 XII Jan 19/20, 1974, for which solar wind data from space craft are available. This event is summarized in Figure 14.
Two photographs of Comet Kohoutek, taken Jan 19, 18:27 UT and Jan 20, 01:56 UT are shown. They are brought to the same scale and oriented so that the antisolar direction is vertical. Drawings of the two photographs are included. Fig. 14c indicates the positions of the tail axis and two tail kinks marked with an = sign. Niedner et al. (1978) and Jockers (1981 a) agree that the tail bends can be explained by a mechanism first proposed by Jockers and Lüst (1973): a sudden solar wind direction change propagates across the comet tail. As illustrated in Figure 14 c in such a case the tail will consist of three segments. In segment 1 the comet tail points in the new solar wind direction and in segment 3 in the previous direction. The discontinuity in solar wind direction is at the border line between segments 2 and 3. Segment 2 consists of the part of the tail which has not yet reached equilibrium with the new solar wind direction. Along segment 2 the solar wind velocity vector is not parallel to the tail. As "predicted" by the working model discussed in Section 6 and illustrated in Figure 12, the tail should have one sharp and wavy and one diffuse side with streamers, which is indeed the case (Figure 14b). Both papers agree on the location of the directional discontinuity in the two photo-

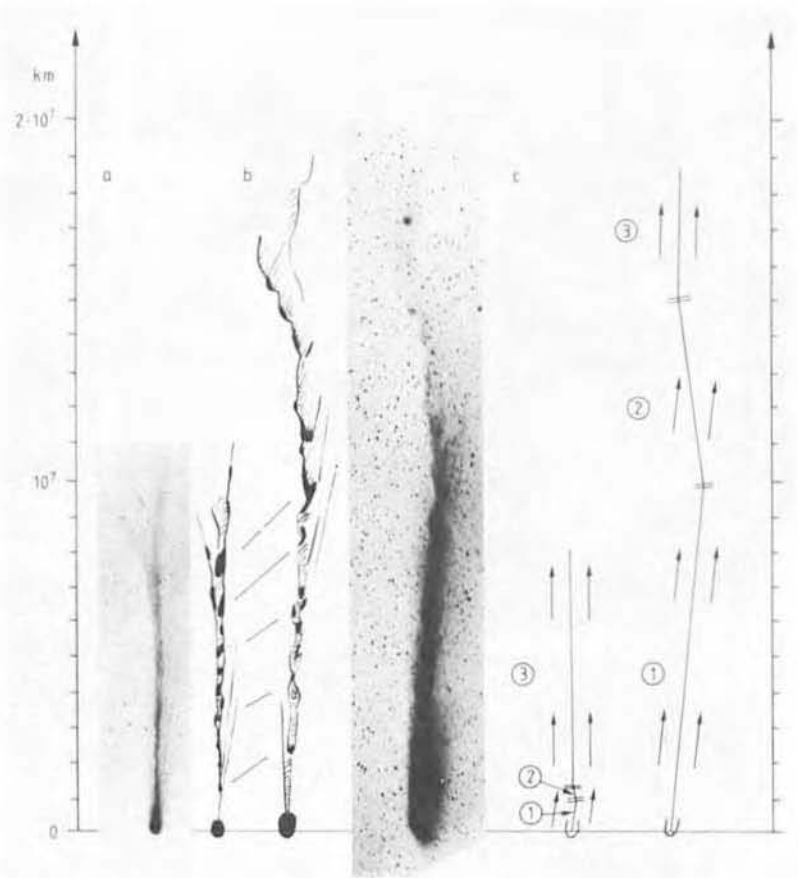

Fig. 14 A large-scale tail disturbance observed in Comet Kohoutek 1973 XII.
a) Photograph (Observatoire de Haute Provence, courtesy Ch. Fehrenbach) and sketch of comet on Jan. 19, 1974, 18:27 UT.
b) Sketch and photograph (Joint Observatory of Cometary Research, courtesy J.C. Brandt) on Jan. 20, 1974, 01:56 UT.
c) Schematic drawing of tail kinks as visible in the two photographs. The arrows indicate the presumed solar wind direction (see text).

graphs, Fig 14a and b. The vector velocity projected on the sky is consistent with solar wind measurements. The direction change is related to the passage of a solar wind high speed stream, where such direction changes are always observed (see Figure 5). The discontinuous change in solar wind direction moves down the tail with almost solar wind speed ($\sim$200 km s^{-1}). At the same time, condensations can be identified in Figure 14 a and b of which the speed has the usual value of about 90 km s^{-1}. The lines between Figure 14a and b connect features which are believed to be identical.

During the development of strong tail rays, i.e. mostly at the onset of large-scale tail disturbances, a thinning or absence of the main tail is often, but not always, observed. Two spectacular examples, which were observed in Comet Humason 1962 VIII, are shown in Figure 15 (see also Figure 6, March 1). Brandt and coworkers have introduced the term "disconnection event" to denote phenomena taking

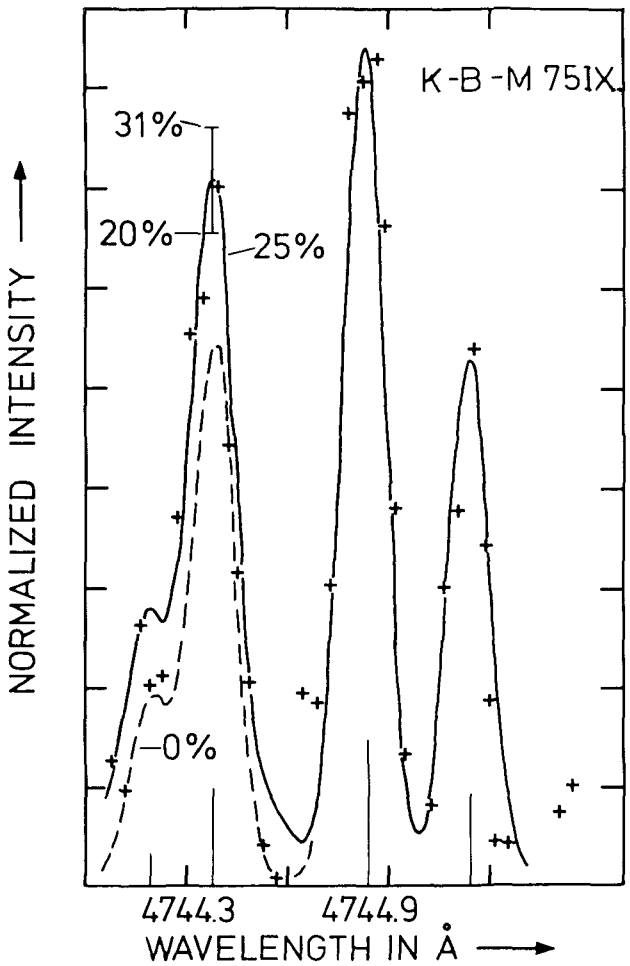

Fig.5 Observed spectrum (crosses) and synthesized (solid line) λ4745 blend of $^{12}C^{13}C+NH_2$ in Comet K-B-M.

The latest comet in which $^{12}C/^{13}C$ has been observed was West 1976VI by Lambert and Danks (1982). Our low resolution spectra 0.3 Å were taken again at McDonald with the Tull spectrograph and a Digicon detector and are shown in fig (6). This spectrum shows not only the C_2(1-0) band head but also the (2-1), (3-2), (4-3) and (5-4) band heads of the $\Delta v = +1$ sequence. The solid line drawn through the data is a synthetic spectrum fit for a $T_{exc} = 3500°K$.

The $^{12}C^{13}C+NH_2$ λ4745 feature is again evident. However, none of the observations carried out so far have achieved the precision necessary to distinguish solar system and interstellar $^{12}C/^{13}C$ ratios. The $^{12}C^{13}C$ head has been detected and the $^{12}C/^{13}C$ ratio measured to a precision of ±30 to 50%. The keys to a more precise result are 1) Improved resolution and higher signal-to-noise spectra, 2) a thorough treatment of the resonance fluorescence in $^{12}C_2$ and $^{12}C^{13}C$ and 3) an adequate discussion of the blended NH_2 lines.

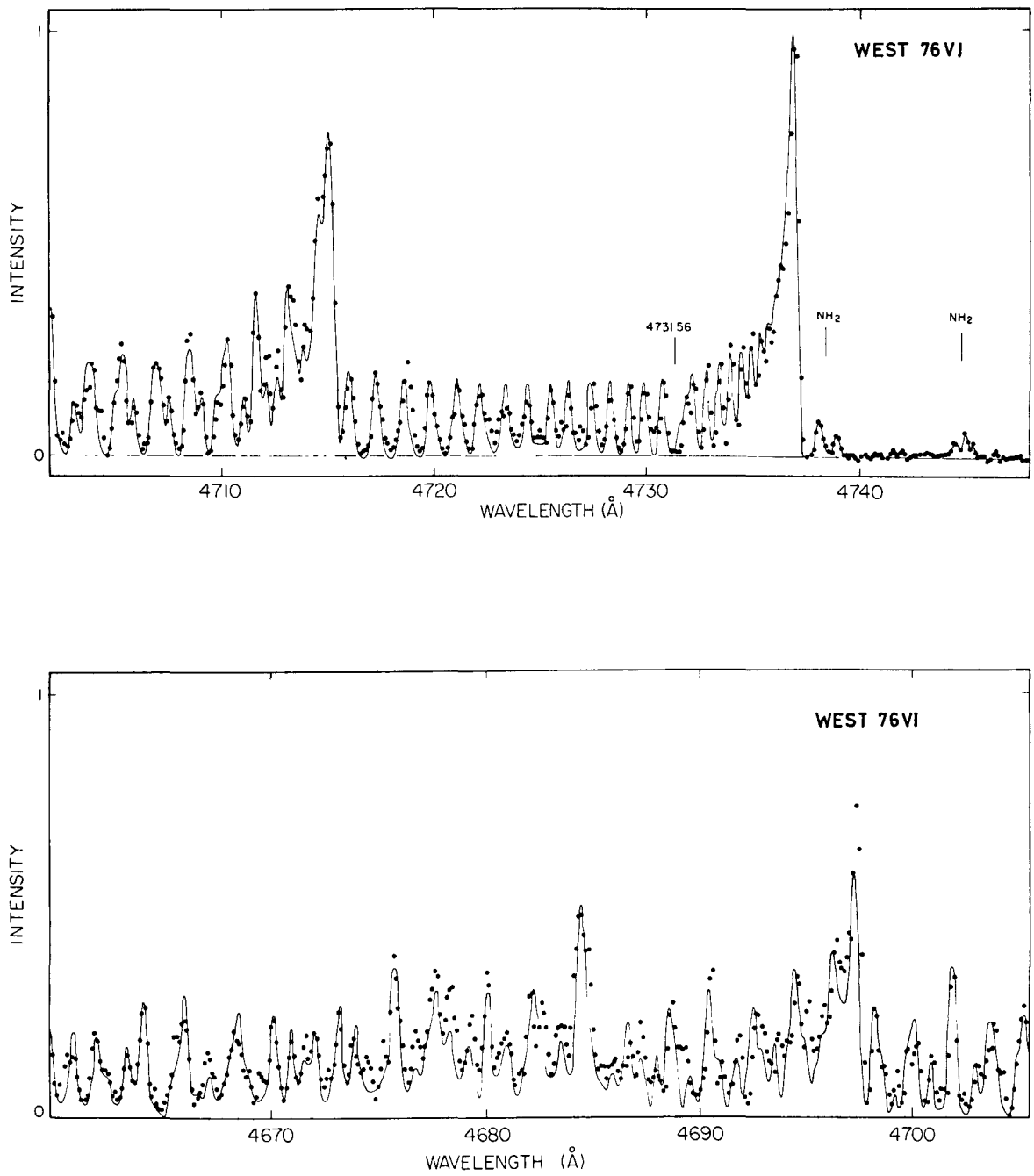

Fig.6 The C_2 Swan $\Delta v = +1$ sequence in Comet West on 1976 March 21. The contribution of sunlight scattered by dust grains in the comet has been removed (see text). The solid line is a synthetic spectrum corresponding to an excitation temperature of 3500 K.

full information on the spatial distribution of the individual ions is necessary. Moreover, the absolute light flux must be determined to allow the calculation of column densities of the observed species. Most comets, in particular Comet Halley on its next return, are very unfavourably placed in the sky and the time when the comet can be observed against a dark sky will be very limited. Therefore, to make most efficient use of the observing time, multichannel observations will be of great advantage.

Let us first discuss studies of plasma in the ionization region around comets From the discussion in Sections 3 and 4 it is clear that an area of several million kilometer around the nucleus should be observed. If the geocentric distance to the comet is of the order of 1 AU, this corresponds to a field ob about 1° on the sky. Therefore the usual astronomical spectrograph is of limited value because the slit length does not cover a sufficiently large angle on the sky. The prime focus or, even more, a focal reductor system with a re-collimated beam after the Ritchey-Chrêtien focus are most interesting for this work. To obtain spectral resolution, narrow-band interference filters may be sufficient in the outer parts of the coma. An imaging Fabry-Pérot system may be useful (Jockers 1981 b).

Studies of the tail proper require still a larger field of view. Here the plasma emission appears against the sky background and only low spectral resolution is necessary. However, high spectral resolution in limited wavelength bands may be useful to measure Doppler shifts or make isotopic studies of the tail ions. The classical instrument would be a small camera with a high-dispersion objective prism similar to the instruments employed by Slipher and Lampland (1911). Modern versions taking advantage of improved technology can be easily invented. Of particular importance would be a broad band filter to suppress the green part of the spectrum where there are no interesting plasma lines but where most of the sky back-ground radiation is emitted. In addition, close to the focal plane a neutral density filter should be employed to equalize photon flux of the major plasma emissions, a technique employed very successfully in observations of the solar corona. It should be noted that the spectra of stars, which appear trailed if the camera is guided to follow the comet, provide an ideal possibility to obtain absolute flux calibration. If a camera of small aperture is used together with an efficient detector system, narrow band filters or even a Fabry-Pérot étalon could be placed in front of the aperture.

This list of ideas is by no means exhaustive. Specially designed ground based cometary cameras would provide the opportunity not only to observe Comet Halley but also many more comets at relatively low cost.

References

Alfvén, H. (1957). On the theory of comet tails. Tellus 9, 12-96.

Alfvén, H. (1960). Collision between a non-ionized gas and a magnetized plasma. Rev. Mod. Phys. 32, 710-713.

Axford, W.I. (1964). The interaction of solar wind with comets. Planet. Sp. Sci. 12, 719-720.

Beard, D.B. (1966). The theory of type I comet tails. Planet. Sp. Sci. 14, 303-311.

Benvenuti, P. and Wurm, K. (1974). Spectroscopic observations of Comet Kohoutek (1973f). Astron. Astrophys. 31, 121-122.

Biermann, L. (1952). Über den Schweif des Kometen Halley im Jahre 1910. Z. f. Naturforschung 7a, 127-136.

Biermann, L., Brosowski, B. and Schmidt, H.U. (1967). The interaction of the solar wind with a comet. Solar Phys. 1, 254-284.

Brandt, J.C. (1982). Observations and dynamics of plasma tails, in L.L. Wilkening ed., Comets, Tucson, Univ. Arizona Press, 519-537.

Bobrovnikoff, N.T. (1931). Halley's comet in its apparition of 1909-1911. Publ. Lick Observatory 37, Part II, 309-482.

Combi, M.R. and Delsemme, A.H. (1980). Neutral cometary atmospheres I. An average random walk model for photodissociation in comets. Astrophys. J. 237, 633-640.

Combi, M.R. and Delsemme, A.H. (1980). Brightness profiles of CO^+ in the ionosphere of Comet West (1976 VI). Astrophys. J. 238, 381-387.

Delsemme, A.H., Combi, M.R. (1979). O(^{1}D) and H_2O^+ in Comet Bennett 1970 II. Astrophys. J. 228, 330-337.

Denskat, K.U., and Neubauer, F.M. (1982). Statistical properties of low-frequency magnetic field fluctuations in the solar wind from 0.29 to 1.0 AU during solar minimum conditions. Helios 1 and Helios 2. J. Geophys. Res. 87, A4, 2215-2223.

Eddington, A.S. (1910). The envelopes of Comet Morehouse (1908c). Mon. Not. Roy. Astron. Soc. 70, 442-458.

Ershkovich, A.I., and Chernikov, A.A. (1973). Nonlinear waves in type I comet tails. Planet. Sp. Sci. 21, 663-670.

Ershkovich, A.I. (1980) Kelvin-Helmholtz instability in type I comet tails and associated phenomena. Sp. Sci. Rev. 25, 3-34.

Feldman, P.D. (1978). A model of carbon production in a cometary coma. Astron. Astrophys. 70, 547-553.

Festou, M.C. (1981). The density distribution of neutral compounds in cometary atmospheres. Astron. Astrophys. 95, 69-79.

Formisano, V., Galeev, A.A. and Sagdeev, R.Z. (1981). The role of the critical ionization velocity phenomena in the production of inner coma cometary plasma. Space Research Inst. of Acad. Sci. USSR, Preprint 626.

Gosling, J.T., Hundhausen, A.J., Bame, S.J. and Feldman, W.C. (1978). Solar wind stream interfaces. J. Geophys. Res. 83, 1401-1412.

Haser, L. (1957). Distribution d'intensité dans la tête d'une comète. Bull. Acad. Roy. Belgique, Classe des Sciences 43, 740-750.

Haser, L. (1966). Calcul de distribution d'intensité relative dans une tête cométaire. Mem. Soc. Roy. Sci. Belgique Coll. in 8°, 12, 233-245 "Nature et Origine des Comètes".

Hasted, J.B. (1964). Physics of atomic collisions, London, Butterworth.

Houpis, H.L.F. and Mendis, D.A. (1980). Physicochemical and dynamical processes in cometary ionospheres. I. The basic flow profile. Astrophys. J. 239, 1107-1118.

Huebner, W.F., and Giguere, P.T. (1980). A model of comet comae II. Effects of solar photodissociative ionization. Astrophys. J. 238, 753-762.

Huppler, D., Reynolds, R.J., Roesler, F.L., Scherb, F. and Tranger, J. (1975). Observations of Comet Kohoutek (1973f) with a gound-based Fabry-Perot-spectrometer. Astrophys. J. 202, 276-282.

Ioffe, Z.M. (1966). Comets in the solar wind. Astron. Zt. 43, 175-180.

Ip, W.-H. and Mendis, D.A. (1976). The generation of magnetic fields and electric currents in cometary plasma tails. Icarus 29, 147-151.

Ip, W.-H. (1979). Currents in the cometary atmosphere. Planet. Sp. Sci. 27, 121-125.

Ip, W.-H., and Axford, W.I. (1982) Theories of physical processes in the cometary comae and ion tails, in L.L. Wilkening ed., Comets, Tucson, Univ. Arizona Press, 588-634.

Jockers, K., Lüst, Rhea, and Novak, Th. (1972). The kinematical behaviour of the plasma tail of Comet Tago-Sato-Kosaka 1969 IX. Astron. Astrophys. 21, 199-207.

Jockers, K., and Lüst, Rhea (1973). Tail pecularities in Comet Bennett caused by solar wind disturbances. Astron. Astrophys, 26, 113-121.

Jockers, K. (1979). An atlas of the tail of Comet Kohoutek 1973 XII. MPAE-W-100-79-37 preprint.

Jockers, K. (1981a). Plasma dynamics in the tail of Comet Kohoutek 1973 XII. Icarus 47, 397- 411.

Jockers, K. (1981b). Eine Fabry-Pérot-Kamera zum Studium von Ionen in der Koma von Kometen. Mitt. Astron. Ges. 54, 196-197.

Lees, L. (1964) Interaction between the solar plasma wind and the geomagnetic cavity. AIAA Journal 2, 1576-1582.

Lüst, Rhea (1962). Bewegung von Strukturen in der Koma und im Schweif des Kometen Morehouse. Z. Astrophys. 65, 236-250.

Miller, F.D. (1979). Comet Tago-Sato-Kosaka 1969 IX: Tail structure 25 Dezember 1969 til 12 January 1970. Icarus 37, 443-456.

Miller, F.D. (1980) H_2O^+ in the tails of 13 comets. Astron. J. 85, 468-473.

Niedner, M.B.jr., Rothe, E.D., and Brandt, J.C. (1978). Interplanetary gas XXII. Interaction of Comet Kohoutek's ion tail with the compression region of a solar-wind corotating stream. Astrophys. J. 221, 1014-1025.

Niedner, M.B.jr., and Brandt. J.C. (1979). Interplanetary gas XXIII. Plasma tail disconnection events in comets: evidence for magnetic field line reconnection of interplanetary sector boundaries? Astrophys. J. 223, 655-670.

Russell, C.T., Luhmann, J.G., Elphic, R.C., and Neugebauer, M. (1982). Solar wind interaction with comets: Lessons from Venus, in L. L. Wilkening ed., Comets, Tucson, Univ. Arizona Press, 561-587.

Schmidt, H.U., and Wegmann, R. (1982) Plasma flow and magnetic fields in comets, in L.L. Wilkening ed., Comets, Tucson, Univ. Arizona Press, 538-560.

Slipher, V.M., and Lampland, O.C. (1911). Preliminary notes on photographic and spectral observations of Halley's comet. Lowell Bulletin 2, No. 47, 252-254.

Swings. P. and Page, Th. (1950). The spectrum of Comet Bester (1974k). Astrophys. J. 111, 530-544.

Wallis, M.K. (1973). Weakly shocked flow of the solar wind plasma through atmospheres of comets and planets. Planet. Sp. Sci. 21, 1647-1660.

Wallis, M.K., and Dryer, M. (1976). Sun and comets as sources in an external flow. Astrophys. J. 205, 895-899.

Wehinger, P.A., Wyckhoff, S., Herbig, G.H., Herzberg, G.M, and Lew, H. (1974). Identification of H_2O^+ in the tail of Comet Kohoutek (1973f). Astrophys. J. 190, L43-L46.

Wolf, M. (1909). Über den Schweif des Kometen 1908 c (Morehouse). Astron. Nachr. 180, 1-12.

Wurm, K. (1968). Structure and kinematics of cometary type I tails. Icarus 8, 287-300.

Wurm, K., and Mammano, A. (1967). Dissoziation und Ionisation in Kometen. Icarus 6, 281-291.

Wyckhoff, S. (1982). Overview of comet observations, in L.L. Wilkening ed., Comets, Tucson, Univ. Arizona Press, 3-55.

Zirker, J.B. (1977), ed. Coronal holes and high speed wind streams, a monograph from Skylab Solar Workshop I. Boulder, Colorado Univ. Press.

DISCUSSION

C. d'Uston: You showed us nicely what is the chemistry in the environment of the comet. I would be interested to know more about the ion population dynamics. For example is the value of the speed of the neutrals expanding from the comet important in the charge exchange process?

K. Jockers: The speed of the solar wind protons varies between the speed of the undisturbed solar wind (∿ 400 km/s) down to about 10 km/s at close distances from the comet and the speed of the neutrals is about 1km/s (thermal speed at sublimation temperature).

S. Koutchmy: Would you comment on the observed fine structures over the dust tail of comets? Do you expect them to be related with solar wind disturbances?

K. Jockers: I am not an expert on this question but I could well think that the break-up of dust grains could be caused by enhanced charging of the grains during a solar wind disturbance.

D.K. Yeomans: Concerning the measured velocities of condensations in ion tails, is it your opinion that these movements are bulk motions or a wave phenomena?

K. Jockers: I would think it is bulk motion because the observed correlation between speed and cloud density would be hard to explain by wave motion.

COMET BRADFIELD 1979 X EVENT ON 1980 FEBRUARY 6 : CORRELATION WITH AN INTERPLANETARY SOLAR WIND DISTURBANCE

J.-F. Le Borgne (+)

European Space Research and Technology Centre
Noordwijk, The Netherlands

Abstract : The tail event observed by Brandt et al. (1980) on comet Bradfield 1979 X on 1980 February 6 is shown to be due to an interplanetary solar wind disturbance detected by instruments aboard Helios 2 and at Earth. The spacecraft was at 0.15 AU from the comet. The tail follows the bulk orientation of solar wind. Acceleration of cometary ions seems to result from small scale hydrodynamic instabilities. Cometary ion density and temperature are deduced.

1 - Observations

Observation of a very rapid turning of the tail of comet Bradfield 1979 X has been reported by Brandt et al. (1980). Three photographs taken on 1980 February 6 between 2 h 32.5 UT and 3 h 00 UT (mid-exposure) show a growing ondulation of the ion tail.
Spacecraft solar wind data have been gathered to look for an interplanetary disturbance which could have been responsible for this comet event. Spacecraft data come from ISEE 3, Helios 2, Helios 1 and Pioneer 12-Venus. Helios 2 was especially well situated relative to the comet (figure 1 and table I) :

	Distance from Sun	Heliocentric longitude	Heliocentric latitude
Comet	1. 13 AU	25°.3	- 4°.1
Helios 2	0. 98 AU	24°.5	- 5°2

Table I

(+) Now at Pic du Midi Observatory, Bagnères de Bigorre, France.

Proceedings of the ESO Workshop on "The Need for Coordinated Ground-based Observations of Halley's Comet", Paris, 29 – 30 April 1982.

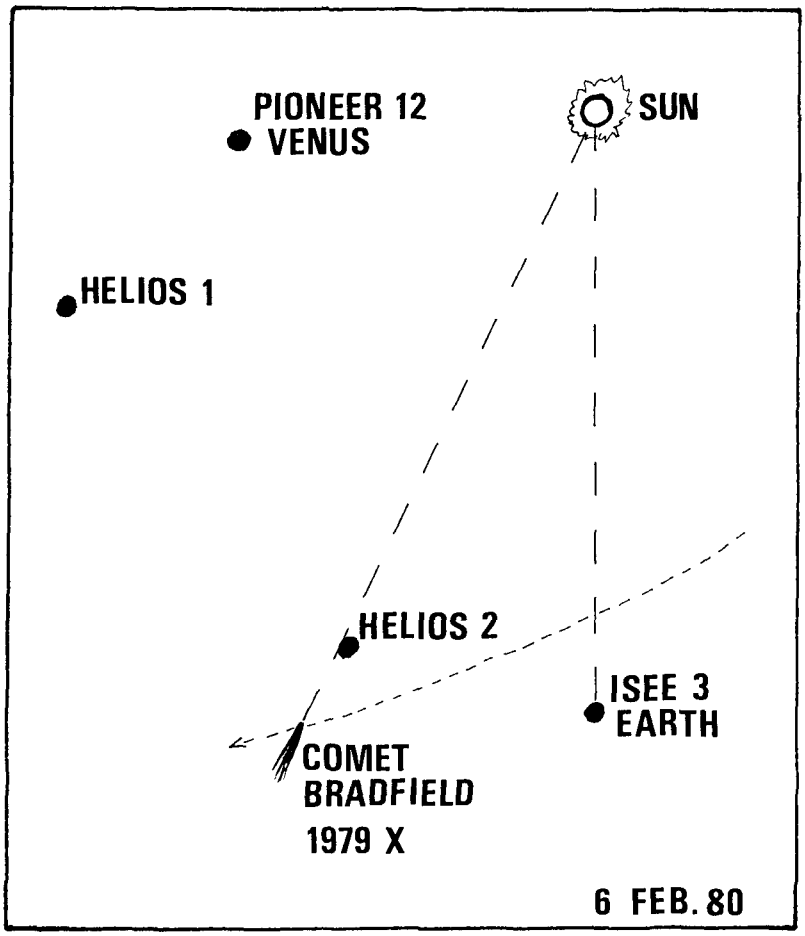

Figure 1 : Relative positions of Comet Bradfield, Earth and Spacecraft in the solar system.

Comet Bradfield and Helios 2, both clo. to ecliptic plane, were 0. 15 AU from each other and approximatively on the same solar radius. Helios 2 data (figure 2) show a solar wind disturbance on February 5 at 16 h 30 UT : solar wind velocity increases rapidly from 350 km s^{-1} to 880 km s^{-1} and decreases to 650 km s^{-1}. Then it decreases slowly from this velocity during the following days. This disturbance is preceded by an exceptional low solar wind density (<1 cm^{-3}). Density increase to 8 cm^{-3} when velocity goes up to 650 km s^{-1}. During disturbance, velocity orientation shows big changes with amplitudes of 20°. The disturbance is also seen on ISEE 3 data on 1980 February 6 at $\sim$ 3 h 00 UT (exact time is not available because of a data gap). At Earth, a sudden commencement (SSC) followed by a magnetic storm is reported by 21 geophysical observatories on February 6 at 3 h 20 UT (Solar Geophysical Data, n° 431, July 1980). ISEE3data does not show density variation during the disturbance. No disturbance has been observed by Pioneer 12 and Helios 1. But low density is recorded by Pioneer 12 (SGD, n° 426 and 427, February and March 1980) between January 30 and 31, and by Helios 1 between February 2 and 3.

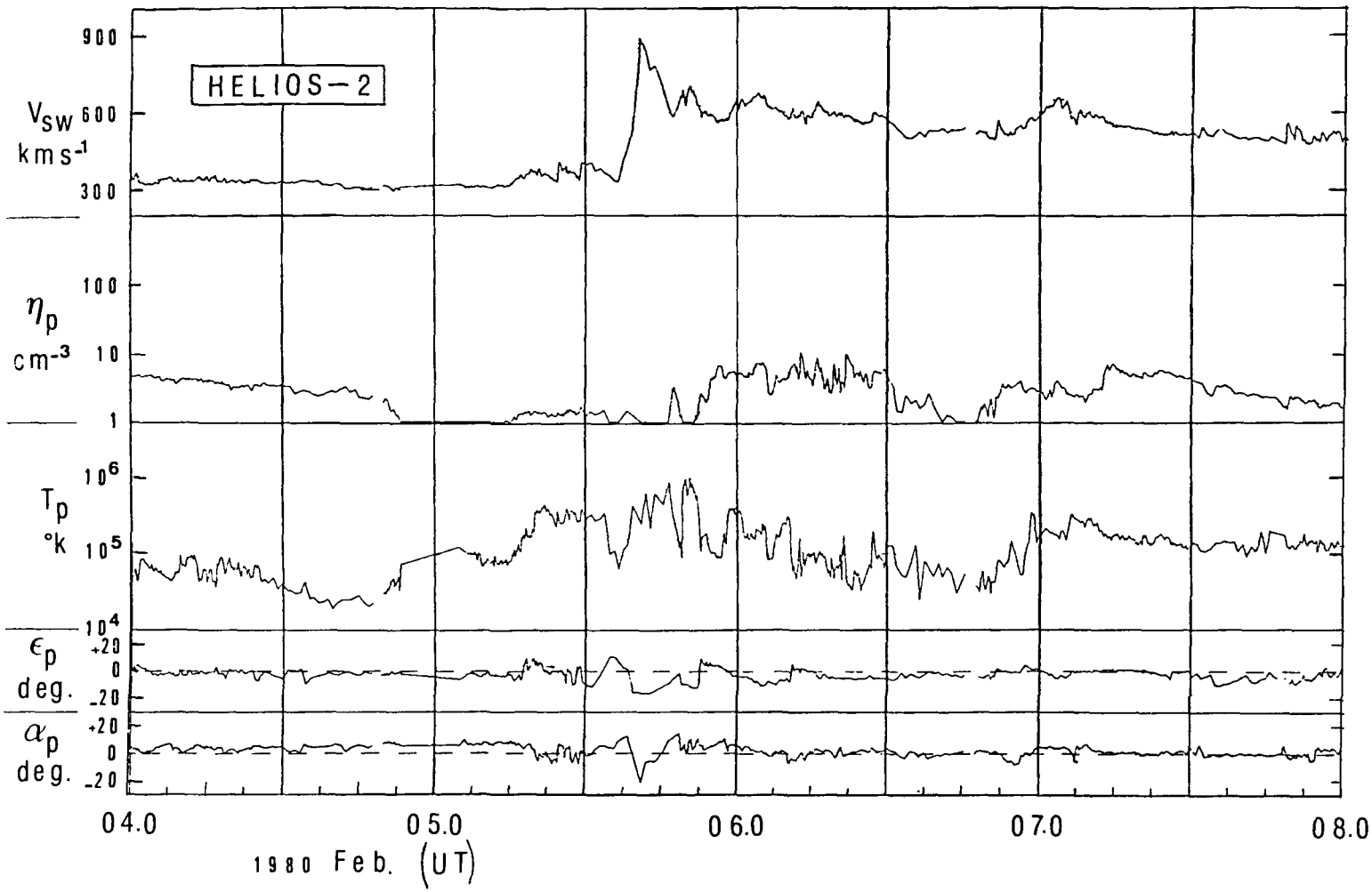

Figure 2 : Helios 2 solar wind data, between 1980 february 4 and 8.

2 - Discussion

The situation can be summarized as follow :

A low density zone seems to have rotated around the Sun at a speed of 17° per day at least between January 30 and February 6, between Venus and Earth, inside Earth orbit (a corotating feature is expected to rotate at 14°.2 per day). The low density feature no longer exists when it reaches Earth. A solar wind disturbance, originating on the Sun have propagated about this low density corotating zone, has been observed by Helios 2 instruments and at Earth.
Among the Hα solar flares observed from Earth, the most likely one to be responsible for the disturbance may be the flare which occured on the Sun on February 3 at 13 h 30 UT located at N 18°, E 13° (SGD, n° 247, March 1980), a little west relative to the radius comet-Helios 2-Sun, and associated with a type IV radioburst.

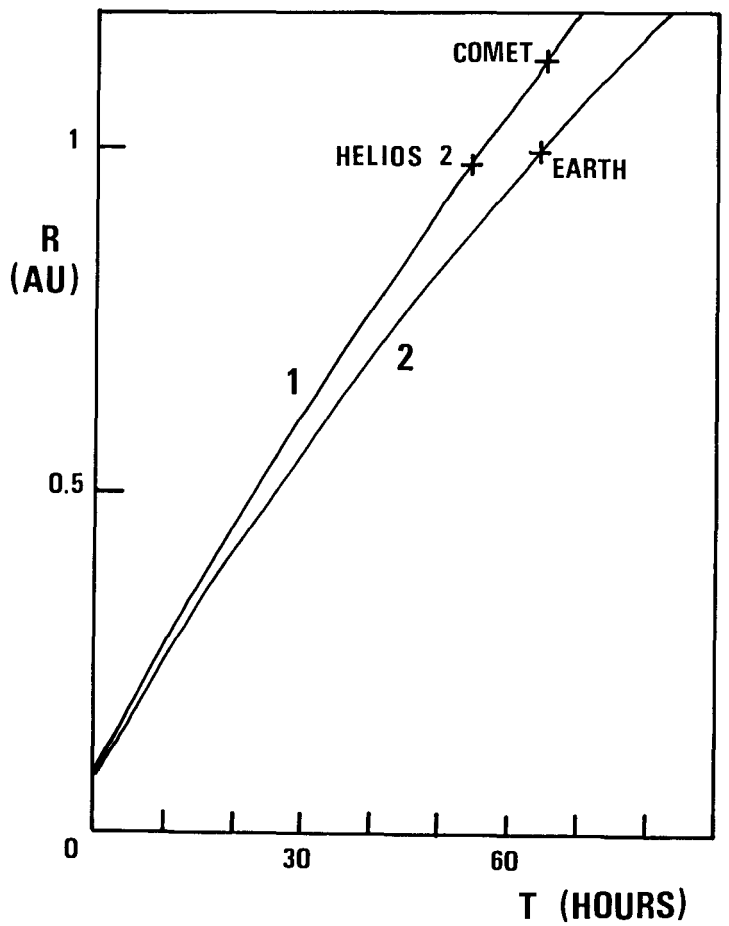

Figure 3 : Distance R (in AU) of disturbance front as a function of delay time t (in hours) for :

1) Sun - Helios 2 comet direction, and

2) Sun Earth direction.

Then the disturbance observed by Helios 2 should be the same which produced the comet Bradfield event. If we suppose this true, the mean velocity of the disturbance between Helios 2 and the comet is 623 km s^{-1}. The projection of maximum velocity of Solar-wind on the comet-Sun radius is 750 km s^{-1} : it is more than the apparent disturbance velocity. But considering that there is uncertainty on determination of distances, 750 km s^{-1} corresponds to 0.18 AU distance Helios 2-Comet. Then the error on the distance should be 0.03 AU.

According to commonly accepted models of propagation of solar flare associated disturbances (De Young and Hundhausen, 1971, D' Uston et al, 1981), observations of the disturbance at Helios 2, Comet Bradfield and Earth fit with the possibility of its origin on the Sun on February 3·56 as suggested earlier. Figure 3 shows adopted time evolution of disturbance front toward Earth and toward Comet-Helios 2. The curves have been obtained by fitting a power law $R = at^b + 0.084$ (R = Sun-disturbance front distance in AU, t = delay time in hours) (D'Uston et al, 1981).

A tentative of time sequence of the event is summarized on figure 4.

3 - Interaction model

Considering now that the picture of solar wind observed at Helios 2 has reached comet Bradfield without any change ten hours later, let us try to understand what influence the solar wind had on the comet tail shape. As Brandt et al. have foreseen from tail shape the Helios 2 data indicate that the solar wind has been oriented northward then southward. As a consequence the cometary ions seem to follow the bulk orientation of solar wind particles at the scale of 10^6 Km as the "wind sock" theory foresees it (Brandt and Rothe, 1976). If magnetohydrodynamic instabilities are responsible for cometary ions acceleration, they seem to act at smaller scale.

A qualitative tentative of finding comet tail shape from Helios 2 solar wind data has been done. Figure 5 shows the result : projection on the sky of the calculated comet tail seen from Earth. The model which fit exactly on Brandt's et al. photographs uses two kinds of cometary ion acceleration : in steady state (no disturbance) cometary ion velocity V_i grows exponentialy up to solar wind velocity V_{sw} :

$$V_i = V_{sw} \left[1 - \exp(-k_1 t)\right]$$

where t is the time (in mn) from ejection from the nucleus and k_1 a constant : $k_1 = 0.01\ mn^{-1}$. When disturbance arises ($V_{sw} > 500$ km s^{-1}) this model does not fit any more. A more powerful acceleration is needed. The model chosen for cometary ion acceleration a_i is then :

$$a_i = k_2 / (V_{sw} - V_i)$$

When V_i is close to V_{sw}, cometary ions are considered as part of solar wind. k_2 is a constant :

$$k_2 = 4.6 \ 10^{11} cm^2 s^{-3} .$$

According to Chernikov (1975) such an acceleration is likely to occure due to ion-sound instabilities, with

$$k_2 = 10^{-2} \omega_i (m_e/m_i)^{1/2} (n_p/n_i)^2 \ k \ T_e/m_p$$

where m_e, m_p, m_i are electron, proton, cometary ion masses respectively ; n_p, n_i are proton, ion densities ; T_e is the electron temperature ; ω_i is the cometary ion plasma frequency ; k is the Boltzmann constant. These instabilities occure when solar wind velocity exeeds a critical value V_{CR} :

$$V_{CR} = (n_i/n_p)\, v_s \left[1 + (m_i/m_e)^{1/2} (T_e/T_i)^{3/2} \exp(-3/2 - T_e/2T_i)\right]$$

where v_s is the sound velocity in cometary plasma, and T_i the ion temperature.

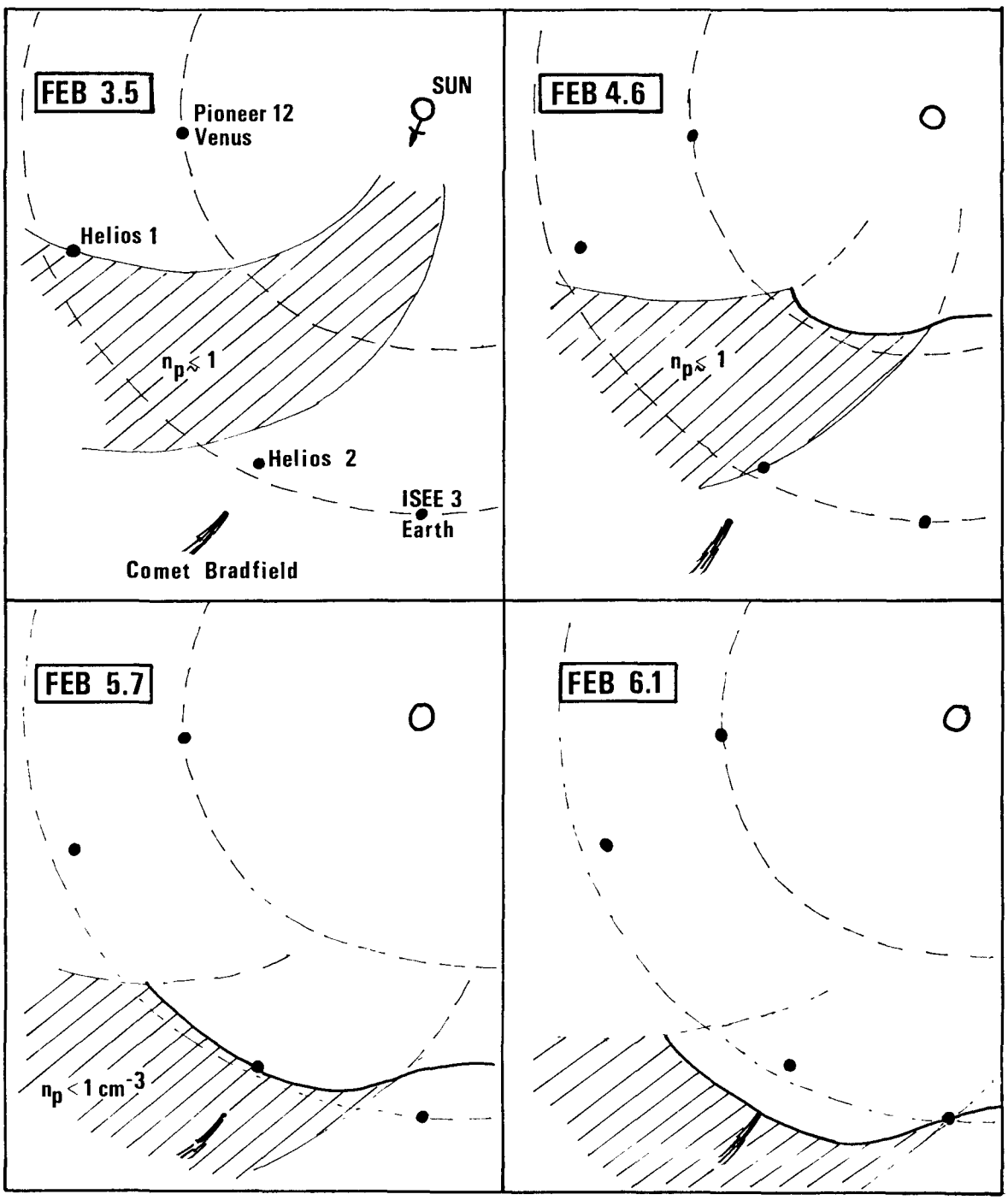

Figure 4 : Time sequence for comet Bradfield event.

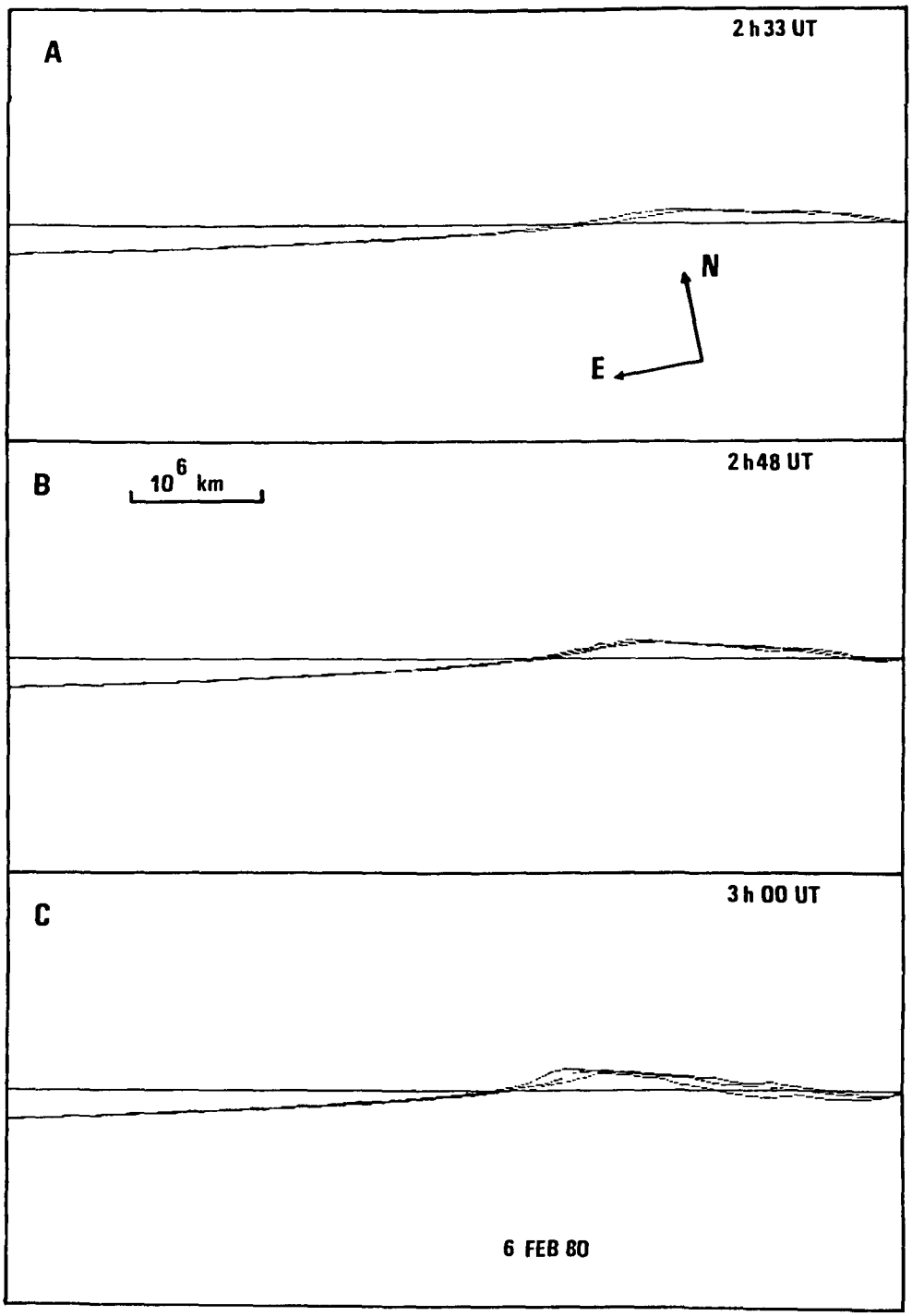

Figure 5 : Comet Bradfield tail shape evolution obtained with solar wind interaction model using Helios 2 data. Figure 5a, 5b, 5c correspond toplate 1 a,b,c, respectively of Brandt et al. paper.

If we take as an hypothesis that ion-sound instabilities have developped in comet Bradfield tail when $V_{sw} > 500$ Kms^{-1}, and that $k_2 = 4.6\ 10^{11}$ cm^2 s^{-3}, some cometary plasma parameters can be determined. For $n_p = 1$ cm^{-3} and $m_i = 25\ m_p$, the former values of k_2 and V_{CR}, when T_e has a value between 10^5 and 10^6 K, give n_i between 1 and 3.5 cm^{-3} and T_i between $5\ 10^4$ K and $9\ 10^4$ K. These values agree with commonly used values, though one generally uses higher values for n_i (10 to 1000 cm^{-3}).

Acknowledgements

The author would like to thank Dr Schwenn for Helios 1 and 2 data and Dr Domingo and Dr Rheinhard for their help. During the course of this work the author was supported by an ESA Research fellowship.

References

J.-C. Brandt, J.-D. Hawley, M.-B. Niedler,
1980, Ap. j. 241, L 51.

J.-C. Brandt, E.-D. Rothe,
1976, in Bonn et al.(eds.)
"The study of comets" (part 2), NASA -SP- 393, p 878.

A.-A. Chernikov,
1975, Soviet Astronomy, 18, 505.

D.-S. De Young, A.-S. Hundhausen,
1971, J.G.R., 76, 2245.

C. D'Uston, M. Dryer, S.-M. Han, S.-T. Wu,
1981, J.G.R., 86, 525.

DISCUSSION

Rh. Lüst : What was the ecliptic latitude of the comet at the time of the event you have shown?

J. Le Borgne : Both comet and Helios 2 spacecraft were close to the ecliptic plane and at a latitude of about -5°.

K. Jockers: Would you interpret your calculations to indicate that instabilities corresponding to the Chernikov model will not be produced?

J. Le Borgne: No; calculated density is low but acceptable since cometary ion density is believed to be between 1 to 1000 cm^{-3}.

K. Jockers: Do you agree that the direction of the tail close to the nucleus (right of the arrow) corresponds to the solar wind direction after the event

and the direction of the tail outward of the letter A (farther out) corresponds to the solar wind direction before the event?

J. Le Borgne: Yes.

A WORLDWIDE PHOTOGRAPHIC NETWORK FOR WIDE-FIELD OBSERVATIONS OF HALLEY'S COMET IN 1985-1986

M. B. Niedner, Jr., Laboratory for Astronomy & Solar Physics, NASA/GSFC
J. Rahe, Remeis Sternwarte, Universität Erlangen-Nürnberg
J. C. Brandt, Laboratory for Astronomy & Solar Physics, NASA/GSFC,

ABSTRACT

A worldwide network of ground-based observatories with wide-field imaging capability would be of inestimable value in the study of Halley's Comet in 1985/1986, in that it would: 1.) provide a set of images of high time resolution necessary for a detailed study of highly variable plasma-tail phenomena, 2.) permit the "calibration" of plasma-tail events with solar-wind properties (measured in situ by the Halley missions and by near-Earth spacecraft) required for the general use of comets as solar-wind probes, and 3.) serve as a "barometer" of the large-scale state of the comet as the Giotto, Venera, and Planet A spacecraft fly by, thus assisting the interpretation of the in situ data.

We have recently been selected (John C. Brandt, Discipline Specialist) by the International Halley Watch (IHW) to administer the Large-Scale Phenomena portion of its full and diverse program. As a preparatory action in the event of our selection, we have in the last three years sent out several calls for support, and the responses have been very encouraging: >40 observers/institutions around the world have indicated a desire to collaborate with us in a wide-field network for Halley observations. A large fraction of the proposed instruments are fast (~f/2) Schmidt cameras (typical FOV = 5^{o}-10^{o}), which are probably the ideal (but not the only useful) telescope for wide-field imaging of the plasma tail, an extended (>10^{o}) object of moderate to low surface brightness.

Our modus operandi exactly parallels that of the IHW: participating institutions are asked to forward data (in this case, film copies of the best plates or, when possible, the original plates) to the IHW for analysis in the context of the worldwide data as a whole, and for inclusion in the Halley Archive, but--and this goes without saying--they retain full proprietary rights to the analysis of their own data. This arrangement has seemed very satisfactory and fair to most of the observers and institutions we have contacted.

Proceedings of the ESO Workshop on "The Need for Coordinated Ground-based Observations of Halley's Comet", Paris, 29 – 30 April 1982.

Far from regarding the present wide-field network as complete, we consider it only a "good start". We welcome your support in this very important scientific venture.

I. Introduction: The Need for Wide-Field Cometary Networks

Commenting on the spectacular and unusual tail structures seen in a photograph he had taken of comet Morehouse on 1908 October 15 (shown below in Figure 1), structures which were not visible in Yerkes Observatory photographs

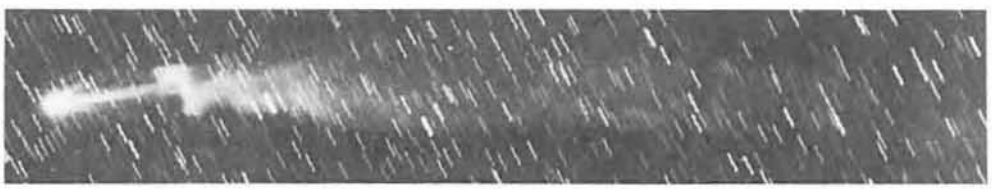

Figure 1. Comet Morehouse on 1908 October 15 (Yerkes Obs. photo)

taken the previous night, E. E. Barnard had the following to say (Barnard 1908):

> "Photographs of the comet...made in the early evening of the 15th in England or on the continent ought to show the masses quite close to the head of the comet....It will be a great pity if photographs were not made in Europe to give a complete history of the transformation of some of these masses throughout their visible existence."

Thus, as Barnard recognized, the great changes in the tail were much too rapid to follow from photographs taken on successive nights at one (namely, Yerkes) observatory, and greater coverage was needed. Fortunately, Pidoux at the Observatory of Geneva and Quenisset at Juvisy Observatory had both secured photographs early on October 15 which did show an earlier stage of development of the tail disturbance (Barnard 1909).

The event recorded by Barnard, Pidoux, and Quenisset is one of a general class of tail structures known as disconnection events (or DEs), in which the entire plasma tail uproots itself from the head of the comet, recedes in the anti-Sunward direction, and is replaced by a "new" plasma tail. The phenomenon--by no means confined to anomalous comet Morehouse--was well known

to Barnard (1899, 1920) and his contemporaries, and it is undoubtedly the most spectacular wide-field phenomenon exhibited by comets. It also takes place extremely rapidly, as the above example illustrates. DEs will be discussed further in the next section.

Concerning observations of plasma (type I) tails in general, Barnard clearly saw the need for obtaining many photographs closely-spaced in time:

> "The day-to-day history of a comet has too great an interval, and the changes are not necessarily at all connected. It is the hour-to-hour history that must be studied to understand the changes taking place in the comet. In the case of a very bright comet, exposures at intervals of half an hour should be made as long and as continuously as the conditions will permit. By this means it will be possible to determine the exact value of the motion of the particles in the tails of various comets...."
> (Barnard 1905)

By 1909, when plans were being formulated for observations of Halley's Comet at its 1910 apparition, the inadequacy of photographic observations of previous bright comets (due to gaps in coverage) was a matter of record. The Committee on Comets of The Astronomical and Astrophysical Society of America, therefore, recommended a coordinated, worldwide effort directed at Halley,

> "To give a permanent record, as continuous as possible, of the phenomena and changes, (1) in the tail of the comet, with special reference to outgoing masses; (2) in the head and nucleus of the comet, particularly as to the formation of envelopes and jets." (Committee on Comets Report, 1915)

Space does not permit a full summary of the accomplishments and shortcomings of the 1910 Halley network. Suffice it to say, however, that the Committee on Comets' call for observations did result in a wealth of data which might not otherwise have been obtained. The network's principal failings were in not collecting all the data which it had inspired, and in not fully analyzing all those data which were forwarded. The former is only now being corrected by J. Rahe, J. Brandt, and B. Donn, who have collected most of the available 1910 photographs and spectra of Halley and are assembling an "Atlas of Comet Halley 1910II: Photographs and Spectra" (Rahe et al. 1982). In the same spirit, an atlas of wide-field photographs of comet Kohoutek was compiled by K. Jockers from plates taken at 18 observatories in 9 countries (Jockers 1979).

Although the 1910 network fell short of its goals, several excellent time sequences of the comet were obtained; perhaps the best and most well known one is shown in Figure 2. From top to bottom, the three photographs were taken on $15^h.8$ GMT June 6 (Yerkes Observatory, by Barnard), $18^h.5$ June 6 (Honolulu, by Ellerman), and $7^h.0$ June 7 (Beirut, Syria; by Joy). The 15 hr sequence shows the evolution of a dramatic DE; note the recession of the detached tail from the head and the obvious growth of the new (attached) tail with time. This event is only one of five DEs known to have occurred in Halley's Comet during the 1910 apparition (Niedner 1981), and there is no reason to expect any less tail activity during the upcoming appearance of the comet. A proper study of DEs and of other highly time-dependent plasma phenomena will require a wide-field network.

II. Wide-Field Plasma Phenomena and Associated Observational Techniques

A. Instrumentation and Techniques

1. Tail Lengths and Required Telescope Field-of-View

Halley's is one of a class of comets which display prominent plasma ("type I") and dust ("type II") tails simultaneously. In most of the discussion which follows, however, we will be emphasizing plasma-tail phenomena since the associated timescales for major change (e.g., Figures 1 and 2) are much less than those of dust phenomena. Although a network is probably not necessary for the study of the dust tail, an added benefit of having an effective wide-field network would be the existence of images suitable for such studies.

Comets of Halley's brightness generally have plasma tail lengths $\geq 2 \times 10^7$ km for heliocentric distances $r \leq 1$ AU. Such a linear size corresponds to an appreciable number of degrees on the plane of the sky, as Figure 3, a 3-element mosaic of comet Kohoutek 1973f on 1974 January 15, shows. The mosaic elements were all taken with the Joint Observatory for Cometary Research (JOCR) Schmidt telescope, an f/2 instrument which records an $8^\circ \times 10^\circ$ field onto 4"x5" plates. The plasma tail of the comet on this particular date was visible out to $\sim 25^\circ$ from the cometary head. Given a geocentric distance of $\rho = 0.81$ AU and a foreshortening angle of $\beta = 94^\circ.8$, the corresponding linear length was 5.9×10^7 km (~ 0.4 AU). The heliocentric distance was $r = 0.63$ AU.

The observing geometry will not be so favorable for Halley in 1985/1986 as it was in 1910. As Figure 4 shows, perihelion (1986 February 9) will occur close to superior conjunction, and solar elongation angles $\geq 45^\circ$ will occur

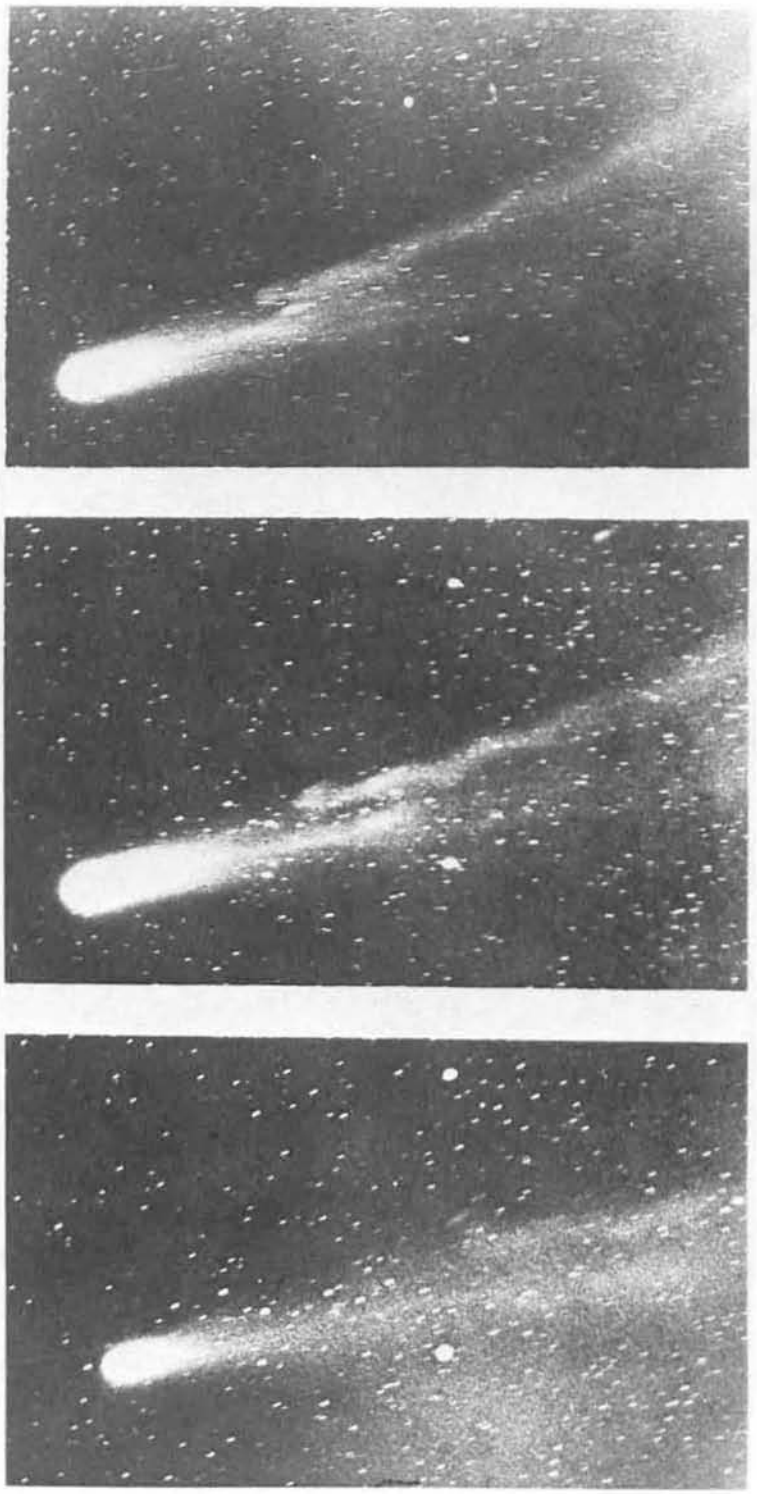

Figure 2. 15 hr time sequence showing a disconnected tail in Halley's Comet on 1910 June 6-7.

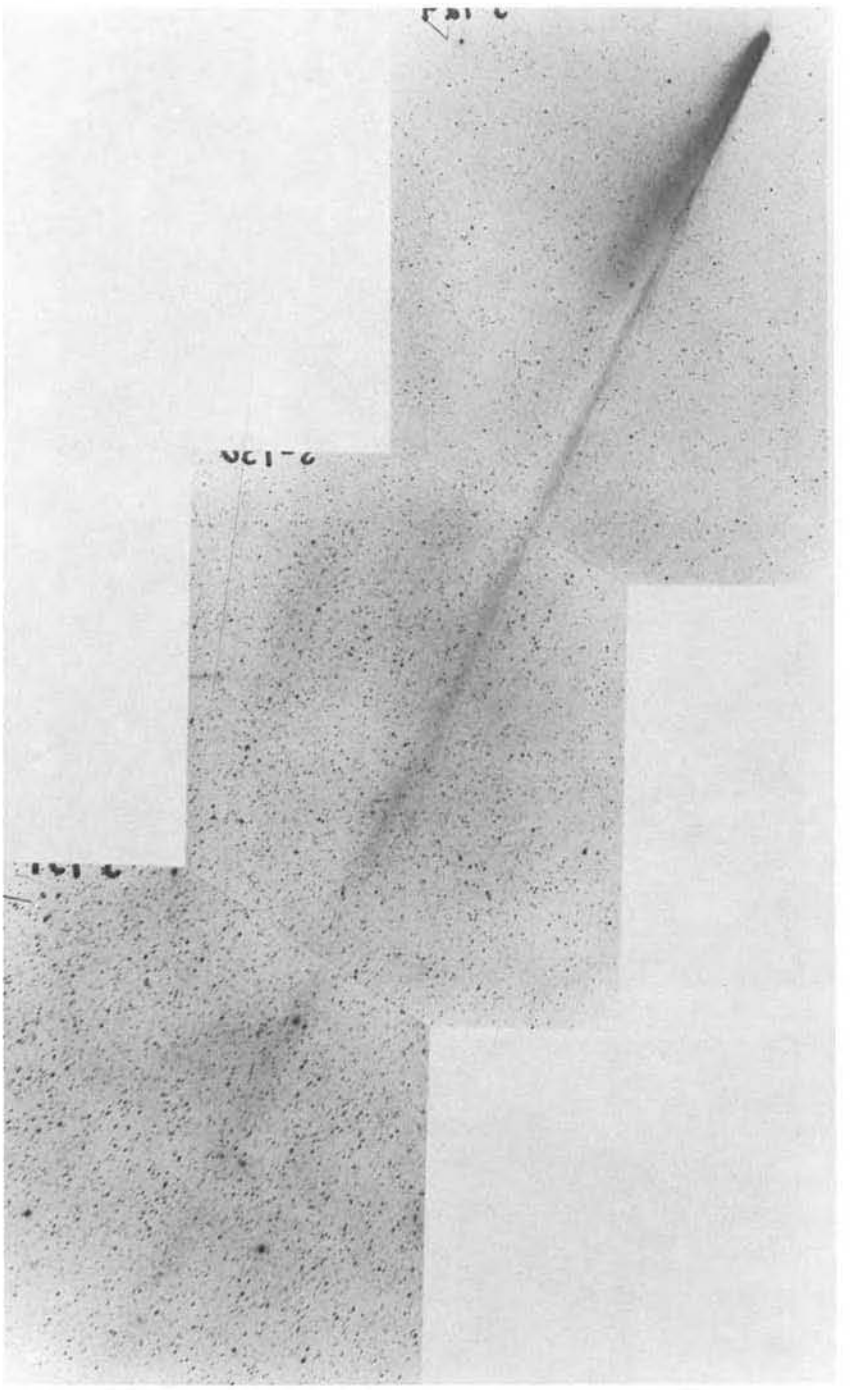

Figure 3. Photographic mosaic of comet Kohoutek on 1974 January 15 (JOCR photographs).

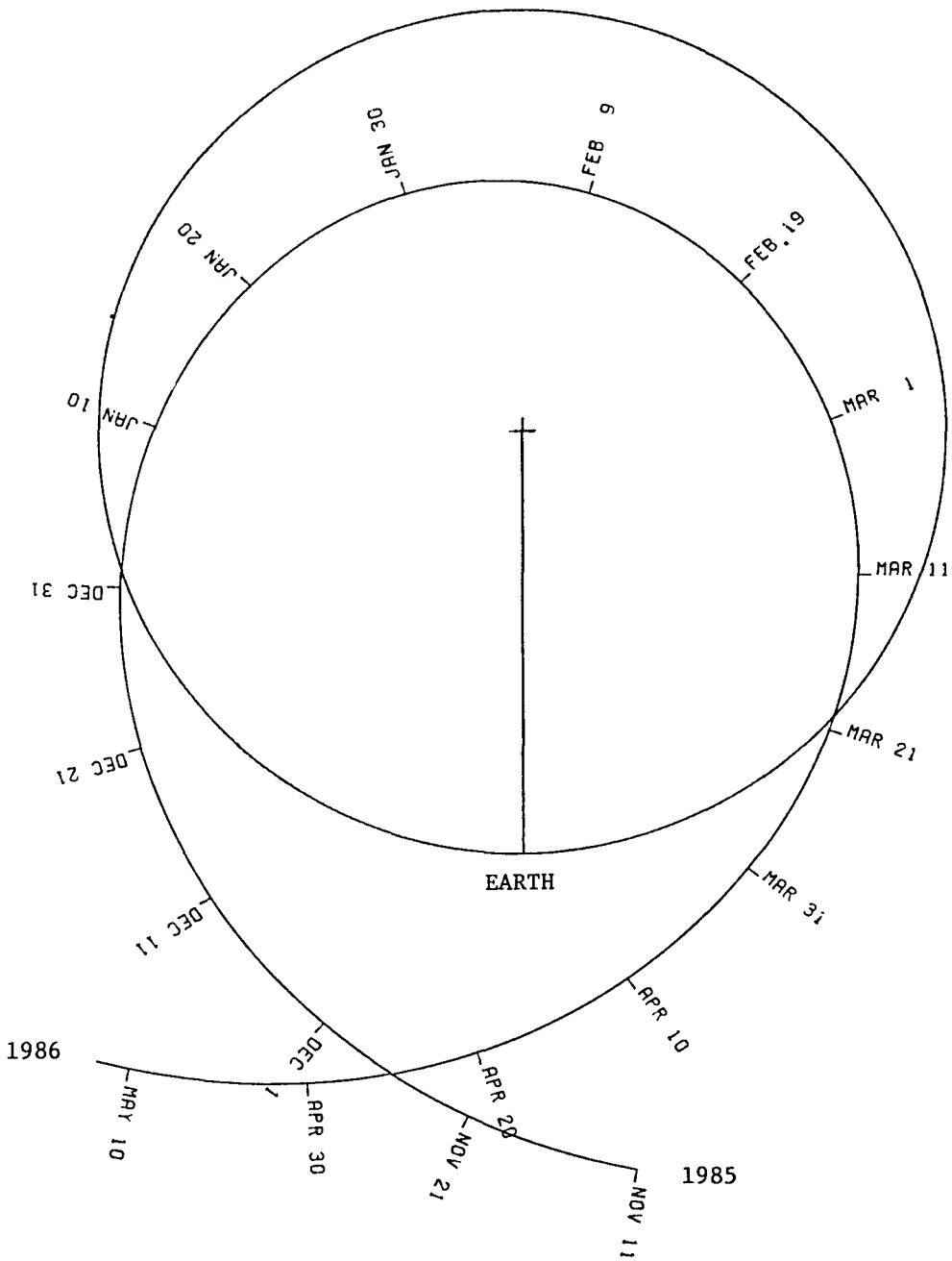

Figure 4. Earth-Sun-comet geometry for Halley's Comet in 1985/1986. Note that the Sun-Earth line is fixed.

only outside heliocentric distances of r = 0.90 AU (inbound) and r = 0.81 AU (outbound), times when the comet will be significantly below maximum intrinsic luminosity. Assuming the tail length will be a minimum of 2 x 10^7 km for r < 1 AU, Table 1 lists the expected minimum angular extent of the plasma tail for the 1985/1986 apparition. Note that despite the poor observing geometry

Table 1

Anticipated Minimum Tail Lengths for Halley's Comet

Date	r	ρ	β	S	
1/1/86	1.01	1.16	126°.6	5°.0	Northern
1/10	0.87	1.32	132°.0	4°.0	hemisphere
1/20	0.74	1.47	143°.1	2°.9	object
	Comet Unobservable				
3/1	0.72	1.27	128°.9	4°.4	Southern
3/10	0.84	1.06	118°.5	6°.0	hemisphere
3/20	0.99	0.81	113°.8	8°.0	object

(large ρ when r < 1 AU), angular lengths approaching S = 8°-10° are still expected, especially when the comet is a Southern hemisphere object in 1986 March-April. Thus, Schmidt cameras with fields-of-view ≥ 5° will be the most productive instruments for the wide-field imaging of the tail. The periods of closest approach to Earth--1985 late-November (Northern hemisphere) and 1986 early-April (Southern hemisphere)--occur at large r (1.55 and 1.33 AU, respectively), where both the tail's brightness and linear extent are difficult to predict.

2. Emulsions, Filters, and Exposure Times

The spectral energy distributions of plasma and dust tails are greatly different, a property of significant importance when choosing an emulsion/filter combination for Halley's Comet observations. Plasma tails radiate principally via resonance fluorescence of the CO^+ molecule, whose strong band system at λ4273 dominates the spectral response range of blue-sensitive photographic plates. In contrast, the light from dust tails is reflected solar light and hence peaks at ~λ5500. Yet, it has been our experience at JOCR--from observations of comets Kohoutek and West 1975n--that

unfiltered IIa-O plates yield very satisfactory results for both the plasma and dust tails simultaneously. A noticeable weakening of the plasma tail is seen when either IIa-F or IIa-E plates are used.

For the plasma-tail studies we have proposed to the IHW, there is no particular advantage in having monochromatic tail images for the purpose of separating spatial distributions of different tail ions (e.g., CO^+ and H_2O^+). Our view here is, first, that spectroscopic work will be definitive in establishing the CO^+/H_2O^+ ratio (for example), and second, that there is no good physical reason to expect different spatial distributions in the tail for various ionic species. What is important is to obtain observations of the overall plasma-tail structure and morphology, and it is our experience that unfiltered IIa-O yields very reliable results.

The correct exposure times for plasma-tail photographic imaging is less a matter of calculation than of experimentation. Generally speaking, however, a fast system like the JOCR Schmidt (f/2) records deep, usable tail images on unfiltered IIa-O in 3-10 minutes for the inner tail regions, whereas the most distant tail regions usually require exposure times >20 minutes. For example, moving outward from the head, the three image elements in the Figure 3 mosaic of comet Kohoutek had exposure times of 8, 14, and 22 minutes.

B. Expected Wide-Field Plasma Phenomena in Comet Halley

1. Disconnected Plasma Tails

The disconnection of plasma tails is perhaps the most spectacular form of cometary activity and a highly visible DE in Halley's Comet during the 1910 apparition was shown in Figure 2. Niedner and Brandt (1978, 1979) have pointed out that such occurrences are not rare and that they show a correlation with interplanetary magnetic field sector boundaries observed at Earth and corotated to comets. At least five DEs are known to have occurred in Halley during the 1910 return.

Niedner and Brandt have proposed that the pressing together in the cometary ionosphere of reversed magnetic fields at sector boundary crossings strips away--via magnetic reconnection--the magnetic flux which was captured in the first sector and which formed the "roots" of the existing tail as in the model of Alfvén (1957). The result is a disconnected tail followed by the capture of flux from the new sector, which results in the formation of a new tail, as observed. Alternative models have been proposed by Ip and Mendis (1978) and by Jockers (1981).

Securing good time sequences of DEs in Halley's Comet during 1985/1986 would be a high priority item in the proposed observing program (as it was in

1910). Of special interest is the possibility of using calibrated plates to explore the question of whether magnetic reconnection at sector boundary crossings produces ionospheric heating and associated brightness increases.

2. Helices and Waves

Observations of this phenomenon in cometary plasma tails during the last 85 years are not uncommon, and a good example is the helical system observed in comet Kohoutek on 1974 January 13 and shown in Figure 5. Hyder, Brandt, and Roosen (1974) interpreted the helices as resulting from the classical kink instability, which is excited when large field-aligned currents ($I = 10^8 - 10^9$ A) flow down the tail. The axial field produced by the current is what kinks the flux tube and the observed speed (Hyder *et al.* measured $V = 200$ km s^{-1}) is interpreted as the Alfvén speed of the tail medium.

Ershkovich (1979 and earlier papers) has adopted a different approach in which the helices are produced by the Kelvin-Helmholtz instability at the discontinuous interface between the tail plasma and the solar wind. Ershkovich has computed both linear and nonlinear models, and on his scheme, the observed recession speeds are equal to material speeds, in contrast to the mechanism of Hyder *et al.*, in which the helices travel at the local Alfvén speed in the frame of reference of the tail plasma.

High time resolution observations of such features by the comet Halley network should shed additional light on this very interesting class of plasma tail activity.

3. Large-Scale Orientation of the Plasma Tail

A long-known property of plasma tails is that they lag the radius vector in the direction opposite to the directon of orbital motion. Biermann (1951) interpreted this propety within the framework of the interaction of a comet with a continuous flow of "corpuscular radiation", which is now called the solar wind. Alfvén (1957) added the effects of a magnetic field frozen in the solar wind and the result was the "windsock model" of plasma tails, in which the large-scale orientation of the tail in space is governed by the simple vector equation:

$$\vec{t} = \vec{w} - \vec{V} \qquad (1)$$

Here, $\vec{t}$ denotes the tail direction, and $\vec{w}$ and $\vec{V}$ are, respectively, the solar-wind velocity and the orbital velocity vector of the comet.

Equation (1) has been used in conjunction with a set of over 600 plane-of-the-sky plasma tail orientations to determine the long-term (85 years),

Figure 5. 1974 January 13 photograph of comet Kohoutek, showing a system of helices in the plasma tail (JOCR photograph).

global solar-wind velocity field to solar latitudes well beyond the range traversed by interplanetary satellites (e.g., Brandt, Roosen, and Harrington 1972). In nearly every case in which the comet results could be compared to those obtained from satellites, excellent agreement has been found, which thus confirms the value of plasma tails as solar-wind velocity probes.

A major objective during the Halley apparition of 1985/86 would be the measurement of tail position angles and the comparison of the inferred solar-wind speeds with any observed in situ by spacecraft (not necessarily spacecraft sent to the comet).

III. Network Objectives

The first and foremost objective of our network will be the study of the plasma phenomena mentioned in the previous section using the high time resolution images obtained from the network. Additional goals not previously discussed will be:

A. Support for Missions to Halley's Comet. Examples of such support or collaboration are:

1.) To provide extensive coverage of the large-scale structure of the coma and tail of the comet during the flybys. While the spacecraft are carrying out their brief but crucial in situ observations, they will be constrained to studies of fine-scale structure of limited portions of the comet. The ground-based imaging network will ensure simultaneous coverage of the entire comet, thus providing a record of transient phenomena which may be necessary for the interpretation of the in situ data.

2.) To obtain stereoscopic views of the comet if suitable companion images are available from any of the spacecraft. Such an approach could be used to infer the comet's three-dimensional structure.

B. Calibration of the Comet/Solar Wind Interaction. We are beginning to understand the correlation between solar wind properties and cometary phenomena such as tail orientations, disconnection events, brightness fluctuations, and other transient events. These relationships can be tested directly and extended by a study of wide-angle images obtained simulaneously with spacecraft in situ measurements of the solar-wind speed, density, and magnetic field, as well as the same quantities in the mixed cometary/solar-wind plasma at the time of closest approach.

IV. Approach

To carry out the objectives described above it is necessary to be able to obtain wide-angle images at approximately one hour intervals for extended periods during the prime observing periods from earth, roughly November-December 1985 and March-April 1986, and during the period of spacecraft closest approach, roughly March 7-10 1986. To achieve this objective requires a network of observatories as uniformly distributed in longitude as the presence of land masses will permit, as near the equator as possible, and in both northern and southern hemispheres. Figure 6 shows the locations of observers who have access to wide-field (mostly Schmidt) telescopes and who have expressed a desire to participate in our network. While the minimum needs of our investigation are satisfied by this network, there are exceptions. Coverage is needed at longitude ~75°E (India) and negotiations are currently in progress to provide for it. Coverage is also needed at longitude ~30°W. A site in the Canary Islands would help fill this gap and we understand that a Schmidt telescope (Swedish) is being moved there. A telescope in eastern Brazil would also be useful. While we are pleased with this initial response to our network call, we are also mindful that a relative lack of Southern hemisphere observers/instruments presently exists in our coverage. We would welcome additional support there and elsewhere.

V. Results Expected and Data Plan

1. Results Expected

The resulting raw data from the network will be a large number of calibrated (see below) photographic plates. It is proposed that these plates be copied onto a transfer emulsion for subsequent study by the network team, and the original plates be returned to the observatories. Institutions not wishing to send original plate material would be requested to provide film copies (preferably on Kodak Fine Grain Positive Film 7302, or equivalent) of the best plates. The data will be used in several different ways by the team:

A. Working quality pictures will be provided to the IHW project as quickly as possible to be used by other investigator teams and mission support as needed.

B. The best time sequences in the data set will be digitized and computer processed to a uniform intensity level and scale. These images will then be

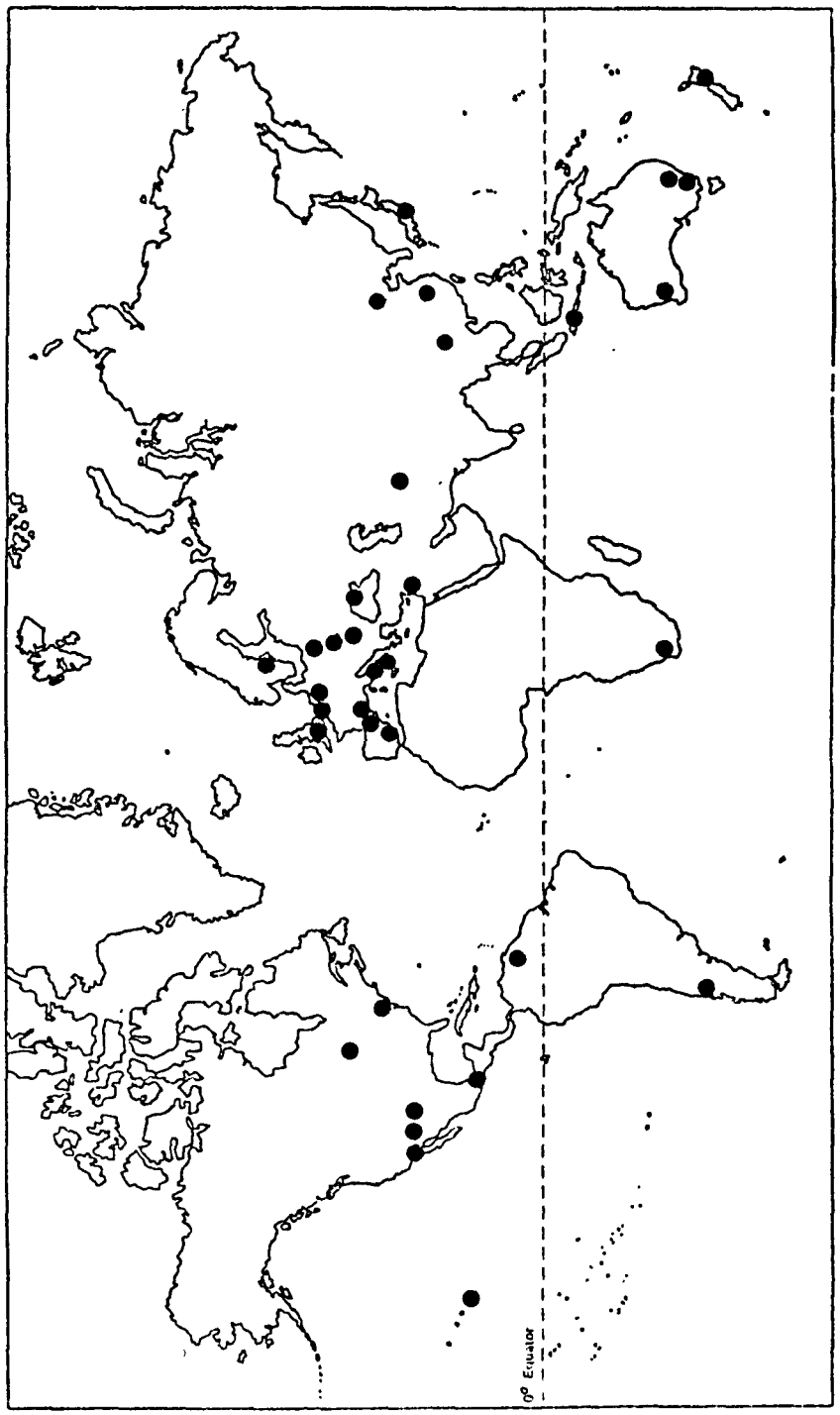

Figure 6. The Wide-Field Network (at present).

combined into motion picture format for the study of the time history of cometary activity by the network team and others.

C. The best 1000 frames will be published as an atlas of Halley's Comet as part of the IHW archiving activity.

We regret that the charter of the IHW will not accomodate renumeration of observatories for their support (e.g., plates, film, and mailing costs).

2. Data Analysis

Since the photographic data will be obtained from many different locations under a variety of observing conditions, it will be necessary to give the utmost attention to the calibration of the individual images. The calibration method to be used will be an outgrowth of the technique proposed by John Kormendy (A. J., 78, 255; 1973). Use of his method requires obtaining the brightness profile of standard stars obtained with the same telescope/emulsion combinations that will be used for the comet Halley observations. The shapes of the standard stars will determine the relative intensity transfer and their known magnitudes, along with photo-electric sky background measures, and will provide the absolute zero point of the intensity scale. Errors of the order of ~0.05 mag are expected. The procedure must be applied to each telescope in the network since the measured shape of the star profiles will depend on the optical condition within that telescope. We will request that each observatory provide us with a sequence of plates of a large, well-studied, extended object (for example M31 in the northern hemisphere and M83 in the southern hemisphere) near the time of the comet observations, so that we may calibrate their telescope in the condition that the comet images are obtained.

VI. Summary

The plasma tail of a comet is the site of many interesting and often spectacular phenomena, such as knots, helices, disconnected tails, rays, and condensations, all of which have been known and observed since the late-1800's. Central to the need for a ground-based Halley network are, first, the knowledge that these phenomena develop and evolve extremely rapidly (≤hours) and second, the belief that such structures are produced by, or are related to, the solar wind, and that the relevant physics involves some of the most interesting plasma physics processes studied today. As examples, the following can be sited: magnetic reconnection (Niedner and Brandt 1978, 1979), the rippling and tearing modes (Morrison and Mendis 1979), the

classical kink instability (Hyder, Brandt, and Roosen 1974), the Kelvin-Helmholtz instability (Ershkovich 1979), and the flute instability (Ip and Mendis 1978). The cometary environment, and the plasma tail specifically, should be considered a giant cosmic plasma laboratory. Clearly, a major observational and theoretical effort directed at understanding the plasma tail of Halley's Comet in 1985/1986 can be justified on the basis of providing important information about cometary structure and about solar-wind and plasma physics problems of interest. A network would also provide critical support to Halley Space Missions.

To be effective, our network requires the participation and cooperation of as many observers and institutions as possible. We need and invite your support.

References

Alfvén, H. 1957, Tellus, 9, 92.

Barnard, E. E. 1899, Mon. Not. Royal Ast. Soc., 59, 354.

Barnard, E. E. 1905, Astrophys. J., 22, 249.

Barnard, E. E. 1908, Astrophys. J., 28, 292.

Barnard, E. E. 1909, Astrophys. J., 29, 65.

Barnard, E. E. 1920, Astrophys. J., 51, 102.

Biermann, L. 1951, Zs. f. Ap., 29, 274.

Brandt, J. C., Roosen, R. G., and Harrington, R. S. 1972, Astrophys. J., 177, 277.

Ershkovich, A. I. 1979, Planet. Space Sci., 27, 1239.

Hyder, C. L., Brandt, J. C., and Roosen, R. G. 1974, Icarus, 23, 601.

Ip, W.-H., and Mendis, D. A. 1978, Astrophys. J., 223, 671.

Jockers, K. 1979, "An Atlas of the Tail of Comet Kohoutek XII", MPAE-W-100-79-37.

Jockers, K. 1981, Icarus, 47, 397.

Morrison, P. J., and Mendis, D. A. 1979, Astrophys. J., 226, 350.

Niedner, M. B. 1981, Astrophys. J. (Suppl.), 46, 141.

Niedner, M. B., and Brandt, J. C. 1978, Astrophys. J., 223, 655.

Niedner, M. B., and Brandt, J. C. 1979, Astrophys. J., 234, 723.

Rahe, J., Brandt, J. C., and Donn, B. 1982, in preparation.

LARGE-SCALE PHOTOGRAPHIC OBSERVATIONS, PHOTOMETRY COLORIMETRY AND POLARIMETRY OF COMETARY TAILS

Philippe L. LAMY
Laboratoire d'Astronomie Spatiale du CNRS, Marseille

Serge KOUTCHMY
Institut d'Astrophysique du CNRS, Paris

INTRODUCTION

In his historical introduction of his monumental study of Halley's Comet, Bobrovnikoff (1931) wrote: "Experience with preceding comets, notably Comet Morehouse (1908 III) showed that a continuous photographic record of the comet would be of utmost importance. Accordingly, several astronomical observatories and societies sent out expeditions to observe the comet under the most favorable conditions". Photography indeed largely contributed to the study of Halley's Comet in 1910 and although new powerful observational technics have appeared in the mean-time, it will remain the foremost tool for investigating the large-scale properties of this comet in 1986.

In 1910, the plan for collecting the best photographs and observational data failed (chiefly because of the abundance of material) and it is imperative that this question be carefully examinated before the next return. Furthermore, photographic has now evolved to a quantitative science allowing precise photometry, colorimetry and polarimetry of extended objects. The benefit of these progress should be fully exploited and photometric aspect as well as reduction procedures must be looked at very seriously.

Although large-scale observations deal with both types of tail I (plasma) and II (dust), this contribution will concentrate on the dust tails first, because of the interest of the authors and second, because plasma tails are fully discussed by K. Jockers (this volume). It is clear however that several problems such as those mentioned above pertaining to the observations themselves and their reduction are common to both phenomena.

SCIENTIFIC INTEREST OF LARGE-SCALE OBSERVATIONS

A simple analysis of the geometry of dust tails already produces

Proceedings of the ESO Workshop on "The Need for Coordinated Ground-based Observations of Halley's Comet", Paris, 29 – 30 April 1982.

a wealth of information on the nature of the dust grains, the forces acting upon them and their temporal dynamical evolution. This is thanks to the mechanical theory originally proposed by Bessel and Bredichin and reformulated by Finson and Probstein (1968a) which allows to compare the photographs with two types of trajectories of the dust grains with respect to the nucleus:
i) the synchrones are the loci of grains emitted at the same time τ but subjected to various radiation pressure forces;
ii) the syndynes are the loci of grains emitted continuously with zero initial velocity from the nucleus but subjected to a constant β (ratio of radiation pressure force to solar gravity).
This theory has been very successful to explain the geometry of tails and anti-tails (for instance, Arend-Roland and Kohoutek) and has enabled Vskhsrjatsky to establish the synchronic origin of most dust tails some 20 to 30 years ago. It allows further to follow their temporal evolution (bursts) and to conclude that the dynamics of the grains is entirely controlled by the gravitational and radiation pressure forces. Finally, from the values of β obtained from the syndyne analysis, one can fairly well infer the size and composition of the grains via the functions $\beta(s)$ calculated for various materials (see Burns et al., 1980). Most results are compatible with silicates as also deduced from infrared observations.
A few very structured tails -so-called striated tails- cannot be explained by the mechanical theory as their striae are definitively not coincident with the synchrones (Fig. 1). The recent case of Comet West 1976 VI has been studied thanks to the availability of sequences of photographs over a sufficiently long period. We showed that the motion of individual stria could be followed over a period of several days very much like the structures of plasma tails and that they propagate with velocities of 10 to 40 km sec^{-1} before diluting in the interplanetary medium (Koutchmy and Lamy 1978, 1979; Lamy and Koutchmy 1979). We favored a brief interaction on a synchronic dust emission of the electromagnetic type; indeed the system of striae became more and more complex (e.g., large angle bifurcations) with increasing distance from the nucleus very much like the more and more turbulent motion of plasma tails. Sekanina and Farrell (1979) studied 16 inner almost parallel striae using small-scale photographs and found that their motion could be explained by fragmentation of friable dust grains after their ejection from the nucleus and the only action of solar attraction and

radiation pressure. This particular question of striated tails shows very well the importance of monitoring the activity of dust tails and of obtaining series of continuous records.

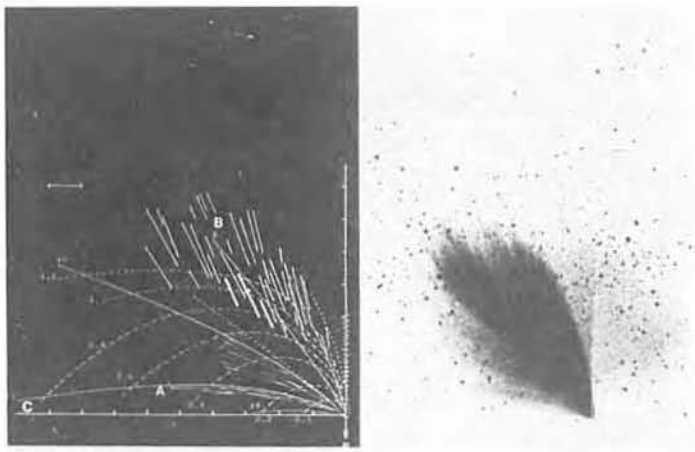

Fig. 1 : Comet West 1976 VI observed by D. Elmore on March 5.5, 1976. The drawing represents the plane of the sky projection of synchrones (solid thin line) and syndynes (dashed thin lines) labelled with the corresponding values of τ (time of ejection from perihelion) and β (see text). Note the simultaneous presence of synchronic structures such as "A" along the synchrone $\tau = 12$ and striae (region "B") which are clearly non synchronic.

After the analysis of the geometry, the next step is to take advantage of the photometry via the Finson and Probstein (1968a) analysis. By treating the motion of the dust grains as a hypersonic, collision-free flow in the (β, τ) coordinate system, these authors were able to derive simple expressions for the surface density of dust tails which depends upon the grain size distribution function and their production rate. Theres quantities may be determined by fitting the two-dimensional isophotes to the calculated surface density assuming proper values for the albedo and mass density of the grains. Full application of this method has been performed for comets Arend-Roland 1957 III (Finson and Probstein, 1968b) Bennett 1970 II (Sekanina and Miller 1973) and Seki-Lines 1962 III (Jambor, 1973).

The dust production rates at perihelion has been obtained for:
Arend-Roland 1957 III: 7.5×10^5 g sec^{-1}
Bennett 1970 II : 2×10^7 g sec^{-1}

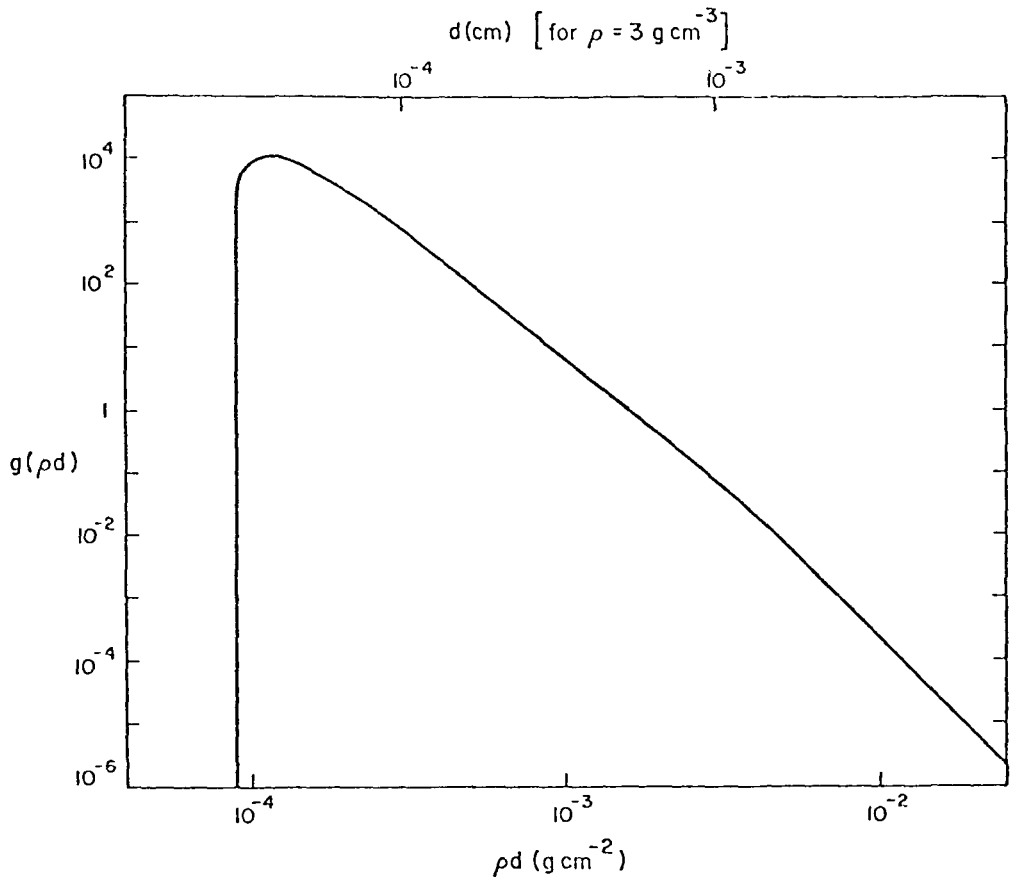

Fig. 2: The size distribution function of the dust grains of comet Bennett 1970 II as obtained by Sekanina and Miller (1973) where d is the diameter of the grains (cm) and ρ, their density (g cm^{-3}).

The result for comet Bennett, which supposedly ressembles best Halley's comet, have been used as a baseline for all present models of this comet.

The Finson and Probstein analysis has also been performed for two other comets D'Arrest and Encke by Sekanina and Schuster (1978a, b) but for observations far from perihelion and the results concern only the larger grains of the distribution function.

The next step involve more complex observations of cometary dust tails, polarization and color. Unfortunately, there exists no general framework such as the Finson and Probstein analysis to readily interpret those observations which contain potential information on the composition, the shape and the surface aspect of cometary grains. Few such observations have been carried out and their interpretation have remained limited. Let us mention:

i) photographic photometry and polarimetry of the tail and anti-tail of Comet Kohoutek 1973 XII performed by Bücher et al. (1975) showing that the polarization reaches quite large values, up to 50 %.

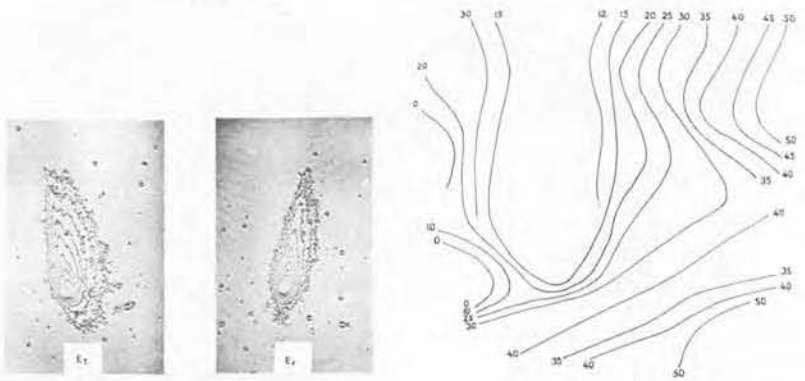

Fig. 3: Comet Kohoutek observed by Bücher et al. (1975).
Left: polarized photographs in two perpendicular directions.
Right: isoplepths of equal polarization in the external parts of the coma and anti-tail; data are in percent.

ii) multicolor photometry and polarization of Comet Ikeya-Seki (1965 VIII) obtained by Weinberg and Beeson (1976) with a scanning photoelectric polarimeter. Worth pointing out is the presence of positive and negative polarization with the phase angle of the neutral point varying with both color and with time.

The scientific goals of large-scale observations are therefore of utmost importance and the morphological and photometric studies of the tails and related outer coma features as well as their temporal evolution may be summarized as follows:

i) development and geometry of the tails:
ii) detection of detached structures, bursts, striae and large-scale extensions of the coma and tails;
iii) determination of the integrated magnitudes from the blue (B) to the near infrared (I);
iv) absolute photometry of the tails plus colorimetry and polarization of the dust tails.

Subsequent analysis of the data should allow to investigate fundamental questions of cometary science such as:

i) dynamical evolution of the tails; nature of the forces at work;

ii) gas and dust production rates as function of time;
iii) physical nature and properties (size distribution) of cometary dust grains.

PHILOSOPHY OF OBSERVATIONS

We now discuss several specific points pertaining to the technics of large-scale photographic observations

1. Optics

Current predictions of the maximum extent of the tails of Halley's comet give 25° approximately. Therefore, a larger field-of-view is required, with 30° as a minimum, to record the tails and also, the adjacent background together with a resolution of $\lesssim$ 1 arc min. Schmidt telescopes will be helpfull when the tails are of smaller extent ($\simeq$ 5°) or by taking adjacent overlapping fields. Wide-field optics are probably preferable and should be as fast as possible the drawback being a substantial vignetting of the field.

2. Spectral coverage

Photographic films and plates presently available on the market covers the spectral range of interest for ground-based observations. It should be kept in mind that OH clouds usually preclude wide-field observations in the near infrared.

3. Spectral selection (filters)

A good separation of the dust and plasma tails may be a happy result of a favorable viewing geometry (e.g., Comet West). But it does not work when the two tails converge to the coma and it may not work at all under unfavorable viewing geometry. A proper spectral selection will solve this problem and will further allow the colorimetric study of the dust tail. The spectrum of plasma tails is usually dominated by the lines of CO^+ (hence the blue appearance on color emulsions) and in order of decreasing importance, H_2O^+ with upper vibronic levels at 5489, 5799, 6158, 6542, 6987 and 7468 Å (Wehinger et al., 1974), CO_2^+ and N_2^+. The spectrum of dust tails may be considered of solar type, probably slightly redder than the sun. Taking into account all these conditions, filters should be selected to isolate clean regions of the continuum and to offer a good spectral coverage while other filters may proove of interest of isolate some spectra lines of the plasma tails. This process may

even lead to the recommendation of a standard set of filters such as the one defined by IAU Commission 15 for the photoelectric photometry of the coma.

4. Polarizors

Polaroid foils mounted in front of the optics appear a satisfactory solution. They are readily available on the market and should be selected according to the desired spectral range.

5. Calibrations

Relative calibration of the film may be performed by various methods. We are familiar with the step wedge properly illuminated. We have been recently testing a square matrix of 6 × 6 densities ranging from 0 to 4 and directly illuminated by attenuated (10^{-6}) solar light.

Absolute calibration using selected stars in the field is also a routine procedure. Care must be taken of the spectral type of the stars as only solar type ones should be retained for proper photometry. Corrections for the effective passbands of cometary observations which may notably differ from the UBVR system must obviously be introduced.

6. Color emulsions

The advantage of color emulsions is to record the color information in the spectral range 4300-6500 Å approximately on a single exposure. If a polarizor is further introduced, the polarization may even be studied as a function of wavelength. The spectral selection is operated at the microdensitometer by measuring the films through appropriate filters. The standard trichrome selection uses three filters whose central wavelengths are 4550 Å for the blue, 5420 Å for the green and 6350 Å for the red. The method was described by Koutchmy (1978) and successfully applied to the solar corona. It requires that the step wedge be divided in three parts each covered by a different filters and correctly illuminated (color of the source) to determine the H-D curves for the three colors and the inter-image effects or coefficients. It has been shown by Koutchmy (1978) that these interimage effects are negligible between the blue and the red but must be taken into account between the green and the blue and the green and the red.

This method is presently applied to color photographs of Comet

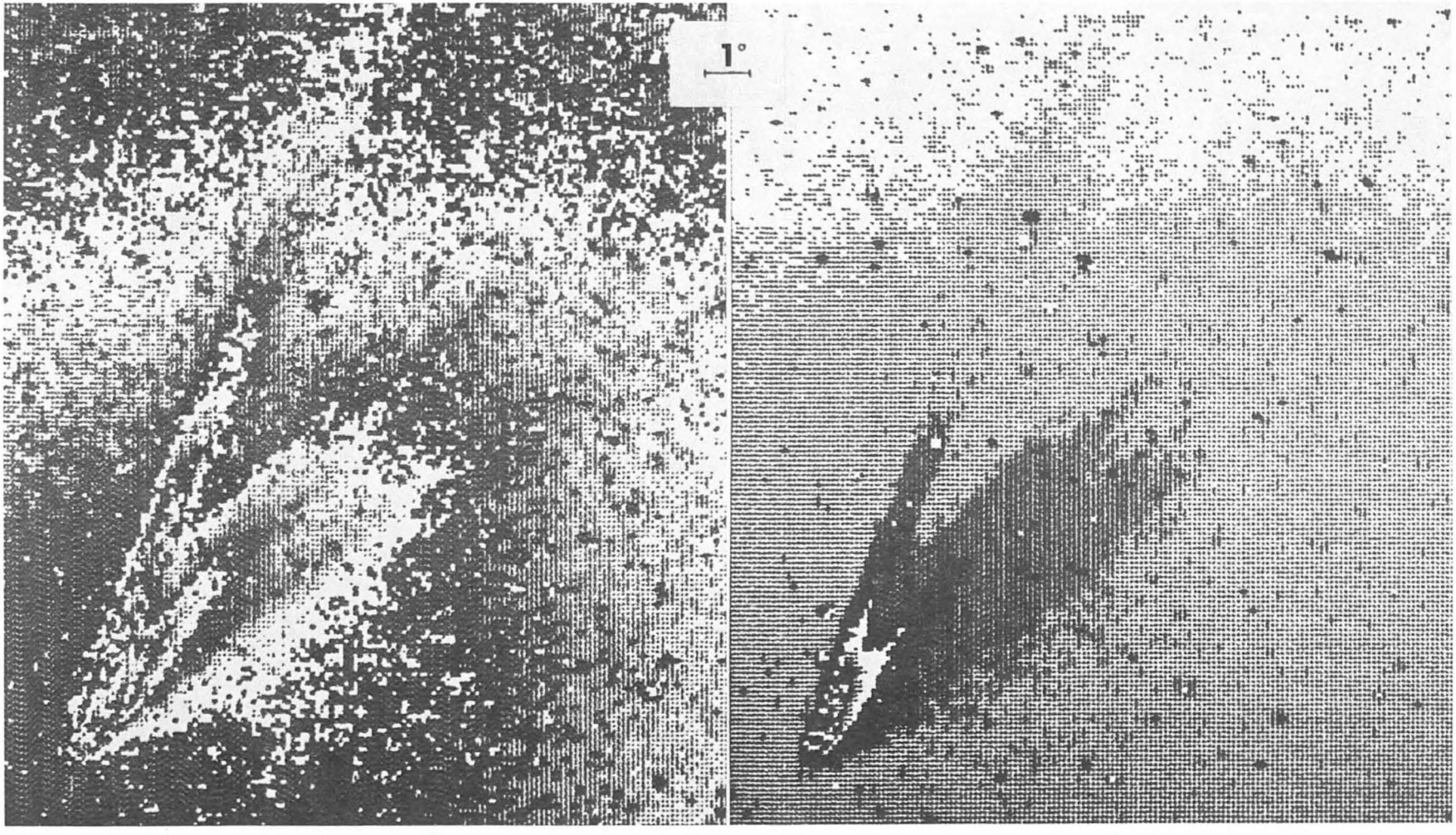

Fig. 4: Isophotes of Comet West at 4550 Å for two directions of polarization, perpendicular (left) and parallel (right).

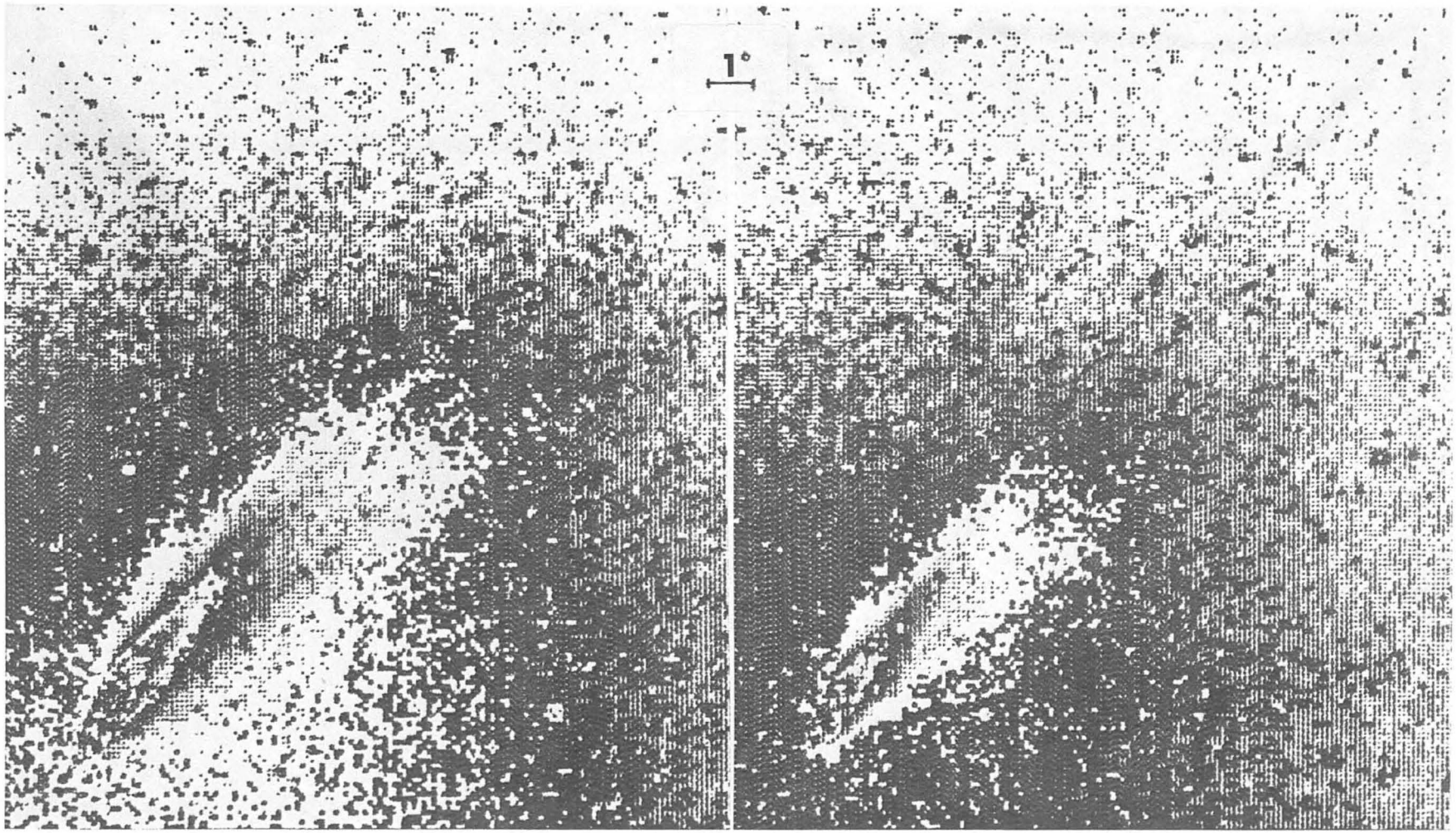

Fig. 5: Isophotes of Comet West at 6350 Å for two directions of polarization, perpendicular (left) and parallel (right).

West obtained at Sacramento Peak Observatory on March 12, 1976 with and without polarizers. Fig. 4 and 5 show preliminary results for two orthogonal directions of polarization (// and $\perp$) in the blue and in the red. A simple comparison already suggests a large polarization. Note also the near total absence of the plasma tail for the red filter.

DATA REDUCTION

Even with modern interactive image processing facilities such as the one operated by Laboratoire d'Astronomie Spatiale, the reduction of photographs always remains a large amount of work which should not be overlooked for the campaign of observation of Halley's Comet which may produce thousands of images. Establishing a procedure as automatic as possible is probably an essential task in the preparation of the observations. Let us just mention a few important steps of a possible standard procedure:

- non linear-filtering (to improve the S/N ratio)
- reduction of step wedge images → H-D curve
- conversion densities → intensities
- identification of stars
- correction for vignetting
- correction for atmospheric absorption
- photometry of selected stars
- removal of stars
- determination of background and cancellation

The scientific analysis may then proceed and may require further processing such as enhancement of details, special spatial filtering, etc...

TOWARD AND ORGANIZED NET OF IDENTICAL CAMERAS

The analysis of the above constraints and conditions as well as our own experience with photographic observations of cometary dust tails has led us to conclude that an organized net of identical cameras is the realistic key to adequatly performing the large-scale observations, photometry, colorimetry and polarimetry of Halley's Comet. The selection of the camera type will be investigated; it may be either a standard commercially available camera or may have to be specifically designed and built. The observations should be carried out with identical equipment that is identical films or plates, identical filters if any, identical polarizors and identical

Plate I: Color photograph of Comet West 1975n obtained on March 12, 1976 at Sacramento Peak Observatory by S. Koutchmy. Emulsion: Ektakrome 64, exposure time: 15 m; field: 30° x 40°. Such color pictures allow an easy separation of dust and gaz in the tail.

sensitometers. It is only under these conditions that a relatively fast reduction of the photographs may be considered through an automatic procedure as outlined above. Naturally, the cameras will have to be set up at judiciously chosen sites taking into account the best visibility of the comet, an appropriate coverage in longitude (i.e., good coverage of the temporal evolution of the tails) and local weather conditions.

A SPATIAL WIDE-FIELD CAMERA

It may well be that the ultimate solution to a large fraction of the above problems consists in a spatial instrument. The Very Wide Field Camera of the Laboratoire d'Astronomie Spatiale to be flown aboard Spacelab I (P.I. G. Courtès) appears to be well suited to the observations of the large-scale phenomenae of Halley's Comet.

It is an all-reflection (i.e., achromatic) camera of the hyper-Schmidt type having an unvignetted field of 56°. An hyperbolic mirror diaphragmed at one of its long foci gives a large field while a Schmidt camera operating as a focal reducer gives a high f-number. It has two modes of operation:

i) an imaging or photometric mode (f = 30 mm, f/1.8, resolution 6 mn of arc) with 3 filters;

ii) a spectrographic mode (f = 45 mm, f/1.8) operating as a nebular spectrograph with a dispersion of 30 Å/mm. In its present configuration, the VWFC is equipped with a 40 mm proximity-focused intensifier including microchannel plate with a CsTe photocathode and a MgF_2 window to operate in the 1150-3400 Å spectral range. As the cometary tails are best observed in the visible/near-infrared, a detector with a S20R photocathode would be preferred with a sensitivity extending from 3000 to 9000 Å. Likewise, the grating of the spectrograph would be changed to be adapted to the new spectral domain.

REFERENCES

Bobrovnikoff,N.T. 1934, Pub. Lick. Obs. Vol XVII, Part II

Bücher,A., Robley,R. and Koutchmy,S., 1975, Astron. Astrophys. 39, 289

Burns,J.A., Lamy,Ph.L. and Soter,S. 1979, Icarus 40,1

Finson,M.L. and Probstein,R.F. 1968a, Astrophys. J. 154,327

Finson,M.L. and Probstein,R.F. 1968b, Astrophys. J. 154,353

Jambor,B.J. 1973, Astrophys. J. 185,727

Koutchmy,S. 1978, Proc. ESO Modern Techniques in Astronomical Photography (Eds, R.M. West and J.L. Heudier) 225

Koutchmy,S. and Lamy,Ph.L. 1978, Nature 273,522

Koutchmy,S., Coupiac,P., Elmore,D., Lamy,Ph.L. and Sèvre,F. 1979, Astron. Astrophys. 72,45

Lamy,Ph.L. and Koutchmy,S. 1979, Astron. Astrophys. 72,50

Sekanina,Z. and Farrell,J.A. 1980, Proc. Symp. IAU N°90, p. 267

Sekanina,Z. and Miller,F.D. 1973, Science 179,565

Sekanina,Z. and Schuster,H.E. 1978a, Astron. Astrophys. 65,29

Sekanina,Z. and Schuster,H.E. 1978b, Astron. Astrophys. 68,429

Wehinger,P.A., Wyckoff,S., Herbig,G.M., Herzberg,G. and Lew,H. 1974, Astrophys. J. 190,L43

Weinberg,J.L. and Beeson,D.E. 1976, Astron. Astrophys. 48,151

DISCUSSION

J. Klinger: Is is well known that comets are more or less dusty. Are there any attempts to find out whether these differences in dustiness are due to more or less dusty nuclei or due to more or less important take off of particles by gas? This last effect may give some indications about surface temperature.

P. Lamy: The answer is not clear cut; the situation may be more complex and, for instance, Brin and Mendis have shown that two behaviours may take place depending upon whether or not the nucleus keeps a dust "crust" around it (bald versus non - bald nuclei). There will also be a difference between new comets and old short-periodic comets. The two alternatives which you present will remain open until we know more about the physics of the near-nucleus environment.

THE SIGNIFICANCE OF PHOTOPOLARIMETRIC MEASUREMENTS FOR THE EXPLORATION OF COMETARY DUST

R.H. Zerull R.H. Giese
Bereich Extraterrestrische Physik
Ruhr-Universität Bochum, F.R.G.

Introduction.

The scattering features of dust particles are closely related to their physical properties, i.e. shape, structure, size, and material. Therefore, scattering measurements can be a useful tool for the exploration of cometary dust. Appropriate data are available for several comets, however they are contradictory in some aspects, especially concerning the color dependence of polarization. Ground based photopolarimetry of comet Halley along with observations from space provide therefore an important opportunity to resolve still existing ambiguities.

Comparison of Observations.

The quantities usually measured are the intensity and the degree of linear polarization at different scattering angles and wavelengths (for definitions see Kerker, 1969).

The most observations available are consistent concerning the following typical scattering features of dust in the cometary coma: Intensity is clearly enhanced toward backscattering and slightly reddened with respect to the solar spectrum. The degree of linear polarization reaches a positive maximum of 25 - 30% at a scattering angle $\theta \simeq 90^{\circ}$, has a neutral point at $\theta \simeq 160^{\circ}$ followed by a branch of slightly negative polarization down to about -5% (Michalsky, 1981; Kiselev et al., 1978 and 1981).

Qualitatively similar characteristics are found for the empirical scattering functions of interplanetary dust, derived from Zodiacal Light measurements (Dumont et al., 1975; Leinert et al., 1981), and for dusty surfaces, as well (Dollfus et al., 1971).

There are, however, discrepancies concerning the color dependence of polarization:
The degree of positive polarization at medium scattering angles

Proceedings of the ESO Workshop on "The Need for Coordinated Ground-based Observations of Halley's Comet", Paris, 29 – 30 April 1982.

clearly decreases with increasing wavelength for interplanetary dust (Leinert et al., 1981) and dusty surfaces (Dollfus et al., 1971), as well. The data reported for cometary dust, however, range from only insignificant color changes (Michalsky, 1981; Kneissel et al., 1982) to clear increase with wavelength (Doose et al., 1974; Kiselev et al., 1981).

Comet West is represented in both groups, thus the discrepancies can not only be due to consideration of different comets. The observational conditions of comet Halley's apparition in 1986 seem to be sufficient to overcome these uncertainties.

Observational Conditions during Halley's Passage.

The scattering angles relevant during comet Halley's 1985/86 passage range from $107^{\circ} \leq \theta \leq 178.7^{\circ}$, covering the domain of all typical features mentioned in the previous section.

Possible ground based measurements include in the preperihelion phase (Nov. - Dec. 1985) the range $126.4^{\circ} \leq \theta \leq 178.7^{\circ}$ and during post-perihelion (Mar. - Apr. 1986) $113.8^{\circ} \leq \theta \leq 159.1^{\circ}$ with the expected total brightness between 5.7^{m} and 7.1^{m}, or 4.0^{m} and 4.6^{m}, respectively (Yeomans, 1981). Observations of comet Halley's perihelion passage will not be possible from the ground because of the unfavorably small angle sun-earth-comet.

Direct in situ probing of Halley's coma will provide intensity and polarization measurements of dust within 4 wavelength bands and at a scattering angle of 107° by the OPE-experiment onboard the GIOTTO-spacecraft encountering Halley in March 1986 (Levasseur-Regourd et al., 1981).

Models of Cometary Grains.

Models for cometary grains must not only meet the scattering features addressed in this paper but also be consistent with the conception of cometary origin and results concerning chemistry, infrared properties, and dynamics.

Several models have been proposed which reproduce the typical run of polarization vs. scattering angle. Oishi et al. suggested models containing spheres of graphite, iron, and silicates. These models fit their own and observations of Ney et al. (1976), even including color, but their validity is restricted to spherical particles. These

models might not be transferable to irregular dust grains, especially if the dielectric component deviates from spherical symmetry, because negative polarization properties vanish for nonspherical dielectric particles in the size range considered (Zerull et al., 1980). A mixture of dielectric and absorbing irregular particles was proposed by Giese (1980). This model also describes the polarization observations quite well, expect the negative values at scattering angles $\theta \gtrsim 160^{o}$. There are also two models considering low density particles: Greenberg et al., 1981, achieved good agreement with observations proposing bird's nest-like structures consisting of (ice-mantled) dielectric cylinders. According to laboratory measurements (Schwill, 1979) "fluffy" particles containing dielectric and absorbing constituents are also a promising conception (Giese, 1980). Both "low density-models" reproduce in addition to positive polarization at medium scattering angles also a domain of negative polarization at large scattering angles. An important criterion for the validity of these models will be the color dependence.

Conclusions.

To make use of all information hidden in the light scattering properties of P/Halley's dust the following efforts are necessary:

1) Multicolor intensity- and polarization measurements from ground, completed by results obtained from the OPE-experiment onboard the GIOTTO probe. Spacelab measurements during the interval where measurements from earth are impossible would also be highly desirable.

2) Laboratory scattering measurements with special emphasis on color effects for clear interpretation of the observational data.

3) Close cooperation between the scientists engaged in the tasks mentioned above.

References.

Dollfus. A., Titulaer, C.: Astron. Astrophys. 12, 199 (1971).

Doose, L.R., Coffeen, D.L.: in Planets, Stars and Nebulae Studied with Photopolarimetry (ed. T. Gehrels), Univ. of Arizona Press, 818 (1974).

Dumont, R., Sanchez, F.: Astron. Astrophys. 38, 405 (1975).

Giese, R.H. in: Halliday I. and McIntosh (eds.) Solid Particles in the Solar System, 1-13 (1980).

Greenberg, J.M., Gustafson, B.Å.S.: Astron. Astrophys. 93, 35 (1981).

Kerker, M.,: The Scattering of Light and other Electromagnetic Radiation, Academic Press, New York (1969).

Kiselev, N.N., Chernova, G.P.: Sov. Astron. 22, 607 (1978).

Kiselev, N.N., Chernova, G.P.: Icarus 48, 473 (1981).

Kneissel, B., Schwehm, G.H., Leinert, C., Richter, I., Planck, B.: Comet West 1976 VI: Photopolarimetry by the Helios 2 Zodiacal Light Experiment, Paper presented at COSPAR Ottawa (1982).

Leinert, C., Link, H., Pitz, E., Giese, R.H.: Astron. Astrophys. 47, 221 (1976).

Leinert, C., Richter, I., Pitz, E. and Planck, B.: Astron. Astrophys. 103, 177 (1981).

Levasseur-Regourd, A.C. et al.: Proc. International Meeting on the GIOTTO Mission, ESA SP-169, 121 (1981).

Michalsky, J.J.: Icarus 47, 388 (1981).

Ney, E.P., Merrill, K.M.: Science 194, 1051 (1976).

Oishi, M., Okuda, H., Wichramasinghe, N.C.: Publ. Astron. Soc. Japan 30, 161 (1978).

Schwill, S.: Mikrowellen-Analogie-Messungen und qualitative Diskussion zum optischen Streuverhalten loser Partikelagglomerate (Fluffy Particles), Wiss. Prüfungsamt Bochum (Staatsexamensarbeit) 1979.

Yeomans, D.K.: The Comet Halley Handbook, JPL Publication 400-911 (1981).

Zerull, R.H., Giese, R.H., Schwill, S. and Weiss, K. in: Schuerman D.W. (ed.) Light Scattering by Irregularly Shaped Particles, Plenum Press New York and London (1980).

RECOVERY OF HALLEY'S COMET AND ORBIT DETERMINATIONS

Table 1

Observed magnitudes for comets 1974 XII, 1975 II and 1977 IX

Object	JD 2440000+	Obs. Code	m	r	m(r,1)
1974 XII	2363	675	17.0T	6.06	13.44
	2366	372	17.0T	6.06	13.44
	2371	372	17.0T	6.06	13.43
	2374	879	17.0T	6.07	13.42
	2384	372	18.0T	6.07	14.37
	2398	372	18.0T	6.09	14.31
	2426	372	18.0T	6.12	14.14
	3083	809	20.0T	8.18	15.65
1975 II	2840	809	16.5T	7.39	12.37
	2842	693	16.5N	7.39	12.37
	2844	485	17.0N	7.40	12.87
	2857	809	16.5T	7.43	12.37
	2864	809	16.5T	7.45	12.36
	2893	485	17.5N	7.52	13.29
	2900	485	17.4N	7.54	13.16
	3172	809	18.5N	8.39	13.99
	3312	474	18.9N	8.91	14.10
	3516	809	19.5T	9.74	14.62
	3841	809	>19.0	11.16	>13.80
	4160	809	>20.5	12.62	>15.01
	4166	809	>22.0	12.65	>16.51
	4262	809	>22.5	13.07	>16.97
1977 IX	2868	413	17.5T	6.57	13.31
	3520	809	17.0T	5.75	13.12
	3528	372	16.0T	5.76	12.16
	3546	372	16.0T	5.79	12.27
	3570	885	15.0T	5.84	11.41
	3578	885	15.5T	5.85	11.95
	3580	885	15.5T	5.86	11.96
	3593	372	16.0T	5.88	12.51
	3596	046	16.0T	5.89	12.52
	3606	046	16.6T	5.91	13.13
	3608	046	15.8T	5.92	12.33
	3629	046	17.0T	5.97	13.49
	3632	046	17.4T	5.98	13.89
	3900	381	17.0T	6.86	12.90
	3955	801	18.0T	7.08	14.01
	3961	381	18.8T	7.10	14.80

The usual brightness law for comets is:

$$m = m_o + 5 \log \Delta + 2.5 \cdot n \cdot \log r,$$

where m_o is the intrinsic brightness at unit distance from the sun and the earth, Δ is the geocentric and r the heliocentric distance. The value of n is poorly known at large r. For comet Halley at its last apparition (1910 II), a pre-perihelion value of n = 5.2 is given by Yeomans (1981) and Ferrin (1982) finds n = 6.0 from a re-reduction of the available, visual magnitude estimates. Both of these values are larger than the "standard" n = 4.0, i.e. the comet was fainter at large distances than predicted by the "standard" law. 1910 II was first observed (by Wolf in Heidelberg) when it was at r = 3.6 A.U., and the quoted values of n therefore only describe the brightness variation within this distance. Nevertheless, the current recovery attempts are taking place while Comet Halley, according to the improved, orbital calculation by Yeomans (1977) is still beyond 12 A.U. A brightness $23^m.8$ is predicted by Yeomans at the end of April 1982, i.e. at the very limit of detectability with current equipment. Should the comet, however, follow Ferrin's prediction (n = 6.0, m_o = 5.0), then it will only reach $24^m.0$ in September 1983.

In order to cast more light on the brightness variation of comets at very large heliocentric distances, we have investigated the behaviour of three comets, 1974 XII van den Bergh, 1975 II Schuster, and 1977 IX West, all of which have been well observed while beyond r = 5 A.U. Observations of comets at these distances are relatively rare; Kresak (1977) cites 1 comet (1927 IV) observed at r = 11.52 A.U., a total of 4 beyond r = 9 A.U., 7 beyond 8 A.U., and 12 beyond 7.4. A.U., respectively. The three comets were selected, a) because they were observed within the last decade with modern equipment, b) because they were followed during periods of at least 2 years and over significant r-intervals and c) because they have large perihel distances and not having been very close to the sun, may better compare with Comet Halley before perihelion (no periodic comets have ever been discovered or recovered before perihelion at these distances).

2. The Observations

The compilation of published magnitudes was greatly facilitated by the availability at ESO of the latest magnetic tape version of the MPC-catalogue, recently published by the IAU Minor Planet Bureau

(Marsden, 1982). The following total numbers of astrometric observations were listed: 44 for 1974 XII, 46 for 1975 II and 60 for 1977 IX. In all cases where a magnitude estimate was indicated, the literature source was consulted for details. An effort was made to include only reasonably reliable magnitudes by well-established observers. In addition, some plates in the ESO archive were inspected and the magnitudes determined. As far as known, all magnitudes are blue (obtained on 103a-O, IIa-O or IIIa-J emulsions).

The resulting list is given in Table 1. The columns are: 1. Name of object, 2. Julian Date, 3. Observatory code (cf. Minor Planet and Comet Circulars 4766-70, 1979 July 1), 4. Magnitude (T = "total", N = "nuclear"), 5. Heliocentric distance r A.U., 6. "Heliocentric" magnitude $m(r,1) = m - 5 \log \Delta$, i.e. as seen at geocentric distance $\Delta = 1$ A.U. It should be noted that all magnitudes are visual estimates on photographic plates and that they must therefore necessarily be somewhat uncertain. However, since the estimates were made by experienced observers working at their "own" equipment with which many estimates of other objects have been made and subsequently verified, it is believed that the commonly quoted uncertainties, $\pm\ 0^m.5$ in most cases, are indeed realistic. Taking into account the exposure time and in particular, the seeing, empirical corrections can be made, even in the absence of photometric sequences on the same plate. In what follows, we have not attempted to apply any corrections in order to transform "nuclear" magnitudes into "total", since the comet tails, if at all seen, are quite faint.

Some comments about the individual objects:

Comet 1974 XII van den Bergh

This object was discovered with the Palomar 48-inch Schmidt telescope, about three months after perihel passage at the then record distance of 6.02 A.U. It was observed regularly during two seasons (1974-75) and one additional plate was obtained with the ESO 1 m Schmidt telescope in October 1976 (IAU Circular No. 3045). The osculating orbit is slightly hyperbolic and from a backward extrapolation to the "original" orbit, it is seen that this comet is "new" (Marsden et al., 1978).

Comet 1975 II Schuster

This "new" comet still has the largest known perihel distance, 6.88 A.U.; it was discovered with the ESO Schmidt telescope one year

after perihel passage. It was observed for the last time at r = 10.1 A.U. in April 1978 at Flagstaff. The $19^{m}.5$ image at r = 9.74 A.U. on a January 1978 ESO Schmidt plate is shown in Figure 1. Until January 1980, four more attempts to photograph 1975 II were made at ESO by H.-E. Schuster and R.M. West, but all were negative. On two occasions, JD 2443841 and 4160, deep Schmidt plates with off-set motion were obtained and later, limiting IIIa-J plates were exposed at the prime focus of the ESO 3.6 m telescope. Although these plates were subsequently photographically amplified by the diffuse contact printing method, the comet still remained invisible. In case of the negative observations, very conservative upper brightness limits were established, taking into account the seeing and the slight residual comet image motion on the plates, due to the unavoidable, mechanically introduced deviation of actual tracking rate from the theoretical.

Comet 1977 IX West

Originally found at ESO in January 1978, prediscovery observations were later uncovered with the 48-inch UK Schmidt Telescope at Siding Spring in March-April 1976. The perihel distance is 5.61 A.U. and the latest, recorded observation was made at the Harvard Agassiz station in June 1979. The published magnitudes show a somewhat larger scatter than is the case for 1974 XII and 1975 II; it might therefore be that this comet is intrinsically variable over short time periods.

3. The Brightness Law

Figure 2 shows m(r,1) plotted against the heliocentric distance r on a logarithmic scale. For each object the best fitting straight line was found by the method of least squares. The coefficients n and m_o and their variance are given in Table 2, together with the r.m.s. scatter around the lines. Forcing the inclination (i.e. n) to be the same, a combined solution for all three objects was also made. The upper magnitude limits for 1975 II at large heliocentric distances were not included in the solutions.

As expected, the coefficients for the individual solutions are relatively uncertain. It is noteworthy, however, that the values of n are all greater than 4.0 and, within the errors, rather similar. Indeed, the combined solution does not appreciably increase the residual scatter and yields a mean value of $n = 7.1 \pm 1.0$. This

Table 2 Brightness law for comets 1974 XII, 1975 II and 1977 IX

$$m = m_o + 5 \log \Delta + 2.5 \cdot n \cdot \log r$$

	N	m_o	n	r.m.s.
1974 XII	8	+2.4 ± 2.9	5.80 ± 1.46	± 0.44
1975 II	10	-3.0 ± 2.4	7.19 ± 1.08	± 0.35
1977 IX	16	-2.2 ± 4.2	7.67 ± 2.11	± 0.67
Combined	34	-	7.10 ± 0.98	± 0.53

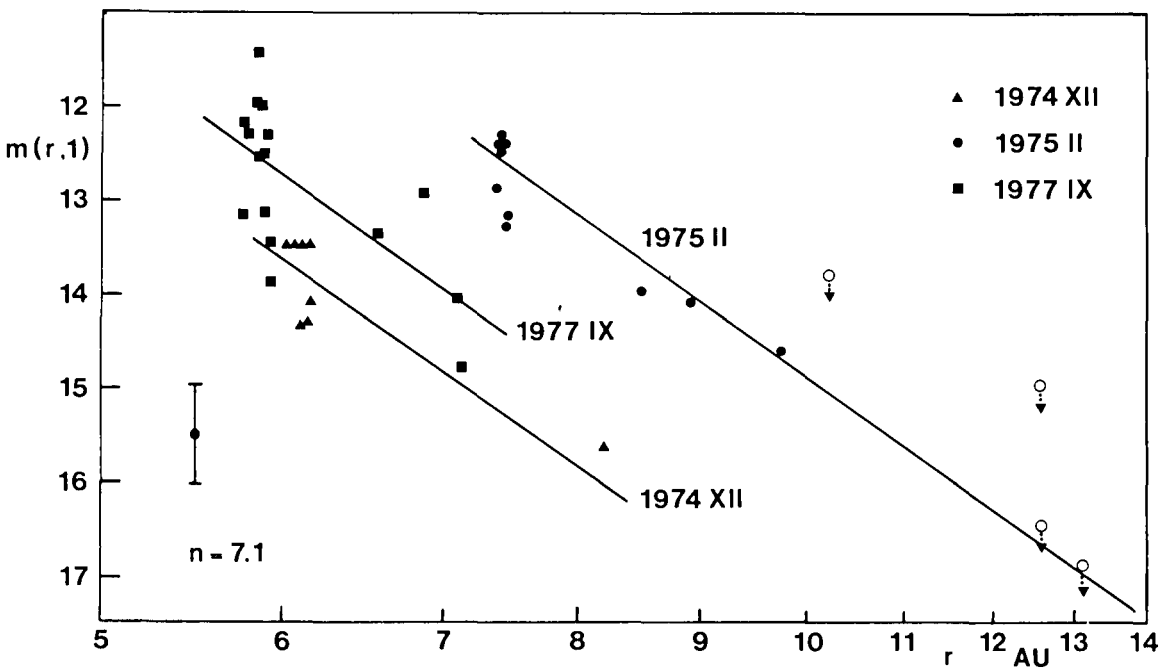

Fig. 2 Heliocentric magnitudes m(r,1) vs. heliocentric distance r. The fitted lines correspond to n = 7.1 (cf. text) and the r.m.s. (± $0^m.53$) is indicated with a vertical bar. The open circles indicate upper brightness limits for 1975 II. They were not used for the line-fitting.

value is also supported by the unsuccessful 3.6 m observations which, if the upper limits are included in the solution for 1975 II alone, give n = 6.82 ± 0.26 and r.m.s. = ± $0^{m}.32$.

The deduced values of m_o are all very bright, but they are of course not necessarily of physical reality, since none of the comets can be observed at small heliocentric distances.

4. Conclusions

The values of n derived for 1974 XII, 1975 II and 1977 IX (5.6 A.U. < r < 9.7 A.U.) indicate that the brightness decrease at large heliocentric distances is steeper than what is normally observed nearer to the sun. Our best value, n = 7.1 ± 1.0 is even larger than those quoted by Yeomans (1981) and Ferrin (1982) for Comet Halley (1910 II) and supports the statement by Ferrin and Narango (1980) that "the light curve of a comet tends to get steeper, the farther the comet is from the sun".

Before applying this result to Comet Halley at its current return, it must of course be emphasized that none of the three comets investigated here are periodic, that their perihel distances are large, that they are "new", and that they therefore have not been subject to periodic solar heating as Comet Halley. Nevertheless, this finding does support the widespread opinion that n increases with heliocentric distance and it offers a plausible explanation as to why Comet Halley has not yet been recovered. If this comet were to follow an n = 7.1 law when beyond r = 5 A.U., then m = 24 will not be reached before 1984. Only time can tell whether this is indeed so, but it will in any case be of great common interest to study the brightness variation of Comet Halley from recovery to perihel and onwards as long as it is observable with the Space Telescope.

Acknowledgements

It is a pleasure to thank Mr. C. Madsen for photographic work with the 3.6 m 1975 II plates and Mrs. E. Völk for typing the manuscript.

References

Ferrin, I., 1982, Astron. & Astrophys., 107, L7

Ferrin, I., Narango, O., 1980, Month. Not. Roy. Astr. Soc. 193, 667

Kresak, L., 1977, Bull. Astron. Inst. Czech., 28, 346

Marsden, B., Sekanina, Z., Everhart, E., 1978, Astron. J., 83, 64

Marsden, B., 1982, Computer magnetic tape with 266722 observations of minor planets and comets, Minor Planet Center, Cambridge, Mass., USA

Yeomans, D.K., 1977, Astron. J., 82, 435

Yeomans, D.K., 1981, The Comet Halley Handbook, An Observer's Guide, International Halley Watch

DISCUSSION

J. Rahe : Comet Halley 1910 II was last photographed around May 30, 1911, when it was about Jupiter's distance from the sun, with a photographic magnitude of almost $18.^{m}.0$. According to H.L. Giclas from Lowell observatory, the comet's brightness had dropped by more than one magnitude during the previous five days.

D. Malaise: It is indeed very important to measure or give estimates of n for distant comets especially the one you showed which have long perihelia (q >5). In this case there is no question that water did not contribute to the activity. Whether the index n found for these comets can apply to a comet reaching the inside of earth's orbit is not clear. We have to learn much more about comet's activity before answering this question. Your measurement surely contributes to this question.

R. West: Thank you. Perhaps it would not be a bad idea if astrometrists could more often give magnitude estimates, in addition to positions.

J. Klinger: I am convinced that there is no general brightness law to be found. As brightness may depend on chemical composition and physical state of the matter in the nucleus, I suggest to examine if there exist groups of comets that in the preperihelion branch follow a similar law and to look what the orbital parameters are. The same work can be done for the post-perihelion branch.

R. West: I fully agree that we might expect differences in behaviour between individual comets and I certainly do not wish to say that Comet Halley necessarily must be similar to the three comets investigated here. Still, I be-

lieve that the result is indicative of what may happen at large distances. Unfortunately, there are very fey observations available, due to obvious observational difficulties and we cannot compare large numbers of comets (yet).

AN ATTEMPT AT DETECTING COMET P/HALLEY AT THE 3.60M C.F.H. TELESCOPE IN DECEMBER 1981

J.P. Picat, J. Guérin, M. Combes, E. Gérard, J. Lecacheux, G. Lelièvre

1. Introduction

An early recovery of comet P/Halley is of importance not only for preparing the space missions Giotto and Vega but also for studying the nuclear activity at large distance from the sun.

According to Yeomans (1981), the nuclear magnitude M_2 of P. Halley could be fit with the following formula :

$$M_2 = M_2^\circ + \log 5 \log \Delta + 10 \log r \qquad (1)$$

(where Δ and r are the geometric and heliocentric distances respectively) when the 1909 and 1911 pre and post-perihelian observations are considered up to 3.6 and 5.4 AU respectively. Should the r^{-4} law hold up to r = 12.8 AU, then M_2 is expected to reach M_2 = 24.0 during the 1981/82 opposition, well within the detection capability of the Lallemand electronographic camera at the prime focus of the 3.6 m C.F.H. Telescope (Hawaii).

2. Observations

The Lallemand electronographic camera built by the "Meudon Camera Group" is currently in operation at the C.F.H.T. prime focus. The capability of measuring limiting magnitude of 25.2 (at 5σ) in the V band has been demonstrated during previous experiments (Baudrand et al. 1982).

A search for Comet P/Halley was carried out during the night of 2/3 December 1981 : two 90 min. exposures in the V band were made starting at 12:05 and 13:38 UT, respectively. The field of view is 7 arc min. and the scale 65.6 μ/arc sec. The telescope was tracking the assumed position of the comet with an accuracy of about 1 arc sec. following the ephemeris kindly provided by B. Morando from Bureau des Longitudes in Paris.

The absolute position of the comet is believed to be good within 10 arc sec. according to Yeomans (1982).

These exposures have been calculated using stars in the neighbouring field of PKS 0736 + 01 which have been previously measured by Vanderriest and Herpe (1980). No extinction corrections have been made.

The nuclear plates have been digitized on a PDS microphotometer at the CDSI of Orsay and the data processed on the VAX computer of the Meudon Observatory.

Proceedings of the ESO Workshop on "The Need for Coordinated Ground-based Observations of Halley's Comet", Paris, 29 – 30 April 1982.

The seeing determined as the FWHM of a star profile is 1.7 arc.sec. and the signal has been integrated on 5.27 square arc.sec. which has been shown to achieve the best signal-to-noise ratio.

The limiting magnitude was estimated by two ways :

- first, by measuring the signal-to-noise ratio on the empty sky background,

- second, by measuring the magnitude of several stellar objects in the same field and extrapolating the result to a signal-to-noise ratio of 5.

Both methods lead to the same limiting magnitude of 25.2 $\pm$ 0.2 at a 5σ detection level. This result is to be compared to V $\geq$ 24.3 "at the level of one standard deviation above the mean level of the sky in 2.6 times the FWHM of the seeing function", as reported by Belton and Butcher (1982). The probability that the comet is hidden by any one star trail is less than 10%.

3. Discussion

Our results clearly rule out the possibility that the visual brightness follows the r^{-4} law defined in equation 1 up to r = 12.8 AU : a steeper dependence is suggested according to :

$$M_2 = M_2^{\circ} + 5 \log \Delta + 2.5\, n \log r \qquad (2)$$

with n > 4 beyond 5 AU.

It is easy to show (Sekanina, 1976) that the actual solid nucleus of a comet has never been observed even on photograph where the cometary image looks stellar" ; a true nucleus brightness must follow the same law as an asteroïd i.e. equation (2) with n = 2 where the phase effect is negligible at a large heliocentric distance. Many comets show evidence for activity at distances of 6 AU (e.g. P/ Schwanmann-Wackmann 1) and even 9 AU (West, 1982). Clearly P/Halley is active at 5 AU and may be up to 12 AU and its brightness could be due to the scattering of sunlight by dust and ices rather than by the true nucleus itself. In fact one cannot exclude that P/Halley is active all along its trajectory. On the other hand our upper result may be interpreted assuming that the nucleus is inactive at 12 AU and that sunlight is directly reflected from its surface. In such a case, we obtain an upper limit to the product Pv . D^2 (where Pv and D are respectively the geometric albedo and the diameter of the nucleus). Table 1 shows the upper limit on D for typical values of Pv (Morrisson, 1977).

Table 1

	Pv	D(upper limit) km
C-type asteroïd	0.035	12.5
S-type asteroïd	0.15	6.1
Fresh ice	0.70	2.8

4. Conclusion

The present work sets constraints on both the goemetric albedo and the diameter of the nucleus of comet Halley. Our limiting magnitude 25.2, is 0.9 magnitude below that obtained by Belton and Butcher (1982) resulting in somewhat bitter limit to the diameter.

Onservations during the next opposition 1982/1983 at Δ = 9.6, 10.6 should be critical. If the comet remains undetected, the upper limit to its diameter will be lowered by a factor 1.5. Should the comet be detected, one must establish the light curve before attributing the brightness to the true nucleus or to the onset of activity of the comet.

5. Acknowlegements

We are grateful to J. Baudrand for running the electronic camera for us.

6. References

1. Baudrand J., Chevillot A., Dupin J.P., Guérin J., Bellenger R., Felenbok P., Picat J.P., Vanderriest C., 1982, *Nouvelle Revue d'Optique* 13.

2. Belton M.J.S. & Butcher H., 1982, preprint.

3. Morrisson B., 1977, in "Comets, Asteroïds and Meteorites", *ed. A.H. Delsemme*, University of Toledo, p. 177.

4. Sekanina Z., 1973, *Astrophys. Letters*, 14, 175.

5. Sekanina Z., 1976, in "The Study of Comets", *ed. B. Donn, M. Mumma, W. Jackson, M.A.' Hearn & R. Harrington*, NASA SP-393, p.537.

6. Vanderriest C., Herpe G., 1980, *Astron. Astrophys. Suppl. Ser.* 39, 395.

7. West R., 1982, *ESO Workshop* 29-30 April 1982, I.A.P. Paris.

ASTROMETRIC OBSERVATIONS AND THE MOTION OF COMET HALLEY

Donald K. Yeomans
Jet Propulsion Laboratory
Pasadena, California U.S.A.

The recovery attempts for the coming apparition of comet Halley began in November 1977 when unsuccessful observations were made using the four meter telescope at Kitt Peak and the 5.1 meter telescope at Mt. Palomar. At the time the comet's predicted nuclear magnitude was 26 and the heliocentric distance was 19.3 AU. More recent unsuccessful attempts to recover the comet in December 1981 by astronomers at Kitt Peak and Mt. Palomar established a limiting magnitude of approximately 24.5. Following the technique of Houziaux (1959), this places upper limits upon the comet's effective radius of 1.7 and 4.2 km for assumed Bond Albedos of 0.6 and 0.1 respectively. Observations of an inactive comet Halley at great heliocentric distances will place important constraints upon the size and albedo of the comet's nucleus. However, it is the astrometric observations of an active comet Halley at closer heliocentric distances that are the most important for orbit determination purposes. Cometary activity in the sun's neighborhood not only increases the difficulty of making accurate position observations but this activity also increases the difficulty in determining the comet's motion itself.

Cometary Orbit Determination and Nongravitational Accelerations

Beginning with the work of Bessel on the 1835 apparition of comet Halley, it became apparent that comets may undergo substantial nongravitational perturbations due to the rocket-like effect of an outgasing cometary nucleus. Whipple (1950, 1951) put these so-called nongravitational effects on a firm theoretical framework when he introduced his icy conglomerate model for a cometary nucleus. Marsden (1968, 1969) modeled these nongravitational effects with a semiempirical term in the cometary equations of motion. Marsden, Sekanina, and Yeomans (1973) scaled the nongravitational acceleration model so as to approximate the theoretical expression for water snow vaporization flux as a function of heliocentric distance. The cometary equations of motion are written:

Proceedings of the ESO Workshop on "The Need for Coordinated Ground-based Observations of Halley's Comet", Paris, 29 – 30 April 1982.

$$\frac{d^2\vec{r}}{dt^2} = -K^2\frac{\vec{r}}{r^3} + K^2\sum_{i=1}^{9} m_i\left[\frac{\vec{r}_i' - \vec{r}}{\rho_i^3} - \frac{\vec{r}_i'}{r_i'^3}\right] + A_1 g(r)\hat{r} + A_2 g(r)\hat{T}$$

$$g(r) = \alpha\left(\frac{r}{r_o}\right)^{-m}\left[1 + \left(\frac{r}{r_o}\right)^{n}\right]^{-k}$$

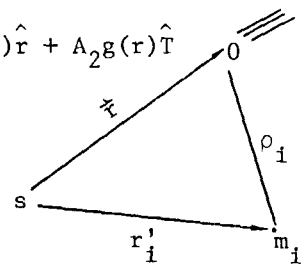

The acceleration is given in astronomical units per (ephemeris day)^2, K is the Gaussian constant. The scale distance r_o is the heliocentric distance where reradiation of solar energy begins to dominate the use of this energy for vaporizing the comet's nuclear ices. For water ice r_o = 2.808 AU and α is a normalizing constant defined such that g(1) = 1. The exponents m, n, and k are respectively 2.15, 5.093, and 4.6142. The terms $A_1 g(r)$ and $A_2 g(r)$ represent nongravitational accelerations acting upon the rotating comet in radial and transverse directions. The radial unit vector $\hat{r}$ is directed along the sun-comet vector $\vec{r}$ and the transverse unit vector $\hat{T}$ is directed along a vector defined by $(\vec{r} \times \vec{v}) \times \vec{r}$ where $\vec{v}$ is the comet's orbital velocity vector. An acceleration component in the direction normal to the orbit plane has been found to have an undetectable effect upon the motion of short period comets. Marsden, et. al., (1973) have demonstrated that if the Bond albedo in the visible range is assumed equal to the infrared albedo of the cometary ices, the scale distance (r_o) is related to the vaporization heat (L) of the volatile ice by the expression:

$$r_o = \frac{4.0 \times 10^8}{L^2}$$

where r_o and L have respective units of AU and calories per mole.

Yeomans (1977) investigated the nongravitational effects acting upon comet Halley. Using observations over the 1607-1911 interval, various orbit determination solutions were computed for several input values of the scale distance (r_o). The most successful orbital solution was consistent with an outgasing water ice nucleus in direct rotation. The well determined, nongravitational acceleration parameter in the transverse direction (A_2) was found to be time independent over the obverved 1607-1911 interval. Using the ancient Chinese observations (837 A.D. - 87 B.C,) as constraints, Yeomans and Kiang (1981) integrated comet Halley's motion back to 1404 B.C. The nongravitational acceleration parameters (A_1 and A_2) were held constant over the entire integration interval. The successful fitting of the observational data back to at least 87 B.C. suggests that the nongravitational accelerations have changed very little over nearly two millennia. In turn, this suggests that the comet's spin axis orien-

tation and ability to outgas have not changed substantially over the same interval.

The Astrometry Network of the International Halley Watch

In an attempt to encourage and coordinate accurate astrometric observations of comet Halley, an Astrometry Network is being established within the International Halley Watch program. The Discipline Specialist for astrometry will be Donald K. Yeomans of the Jet Propulsion Laboratory (JPL) in Pasadena, California. Serving in an advisory capacity will be two experienced scientific collaborators, Brian G. Marsden of the Center for Astrophysics in Cambridge, Massachusetts and Robert S. Harrington of the U.S. Naval Observatory in Washingron, D.C. Dr. Marsden is director of the I.A.U. Central Bureau of Astronomical Telegrams and Dr. Harrington is head of the astrometry division of his observatory. Participation of experienced astrometric observers within the Astrometry Network will be encouraged. It is hoped that, in spite of the paucity of observers now doing astrometry for comets, enough observatories will participate to provide good coverage in longitude for both the northern and southern hemisphere of the Earth. Once the members of the Astrometry Network have been identified, standardized observation and data reduction procedures will be agreed upon and lines of communication established between the observing members and the orbit determination center at the office of the Astrometry Discipline Specialist (at JPL). Observing members will retain the right to publish and use their data as they see fit; they will only be asked to grant permission to use their data in orbital computations prior to publication. Astrometric data on comet Halley sent to the Office of the Discipline Specialist (JPL) will be processed, validated, and stored chronologically in a central computer file. This master data file will be used to periodically update the comet's orbit and ephemeris.

Support of the Halley Flight Projects by the Astrometry Network

The European spacecraft Giotto is scheduled to flyby comet Halley on March 13, 1986. In addition, two spacecraft each from Japan and the Soviet Union are scheduled for March 1986 flybys of the comet. The ability of each spacecraft to fly closely past the comet will depend, to a large degree, upon the uncertainties in the comet's ephemeris. Final mid-course maneuvers for each spacecraft will depend upon accurate ephemerides in early March 1986. Unfortunately, the comet will be unobservable behind the sun from mid January to late February 1986 (see Table 1). Accurate astrometric observations in late February and early March 1986 are, therefore, critical if an accurate, up-to-date ephemeris is to be delivered to the flight projects of ESA, Japan, and the Soviet Union. Hence, the successful support of the Halley Flight Projects will depend upon a group of dedicated, experienced observers who are capable of

making and reducing their observations very quickly. Many of these critical observations will have to be made from southern hemisphere observatories. During this critical late February, early March period the master data file at JPL will be used to nearly continuously update the comet's orbit and ephemeris. The information on the master data file and the derivative orbital and ephemeris data will be made available to requesting flight projects. The computer software for data processing, orbit determination, and ephemeris generation is being constructed at JPL; it will also be made available to the European Space Operations Center (ESOC) at Darmstadt, FRG. In addition, some observers will be asked to send their astrometric observations to ESOC as well as JPL.

Support of Ground Based Observers by the Astrometry Network

Many ground based observers using wide field telescopes will require only the traditional geocentric ephemerides that are usually published for comets. However, parallax effects in April 1986 could amount to $\sim$ 20" and observers using a narrow field of view will require topocentric ephemerides generated for a paticular observatory location. Optical observers making high resolution spectroscopic observations will also require information on the heliocentric and topocentric comet velocities. Radio emission line or continuum observations and radar observations present addition problems. Apart from radio observations of OH emission, radio and radar observations are usually made near the limit of equipment detection capabilities. Imprecise cometary ephemerides can easily ruin an observing program that might otherwise have been successful. Recent radio observations of OH emission have shown that the Swings effect is important for interpreting some radio spectral line observations. As with optical spectroscopy, radio spectroscopy may require accurate heliocentric and topocentric velocity information as well as accurate position predictions.

While the office of the Astrometry Discipline Specialist will have the capability for providing special ephemerides for particular observatories, many observatories already have their own ephemeris generation computer software. In this latter case, only periodic updates of the comet's osculating orbital elements will be required from the Astrometry Discipline Specialist. However, care must be taken because the published cometary elements are usually given with an osculating epoch and perihelion passage time in ephemeris, not universal, time. If an observatory's ephemeris generation program is based upon a two body formulation and does not include the effects of planetary perturbations, then additional care must be taken. For the most precise cometary ephemeris computations, using a two body formulation, the ephemeris time interval should not be more than a few weeks different from the osculating epoch of the input orbital elements. To check their ephemeris generation software, radio telescope

Date(1985)	Dark Hours North Lat. 45°	30°	South Lat. 30°	45°	Appar. Magn. m_1	m_2	Date(1986)	Dark Hours North Lat. 45°	30°	South Lat. 30°	45°	Appar. Magn. m_1	m_2
Jan. 1	11.6	10.9	6.8	3.5		17.9	Jan. 6	2.6	2.3	0.5	0	5.1	7.7
11	10.7	10.0	6.9	3.9		17.8	16	1.3	1.1	0	0	4.4	7.2
21	9.7	9.1	7.2	4.6		17.7	26	0	0	0	0	3.6	6.7
31	8.7	8.1	5.6	5.3		17.7	Feb. 5	0	0	0	0	3.0	6.2
Feb. 10	7.7	7.2	5.0	3.7		17.6	15	0	0	0	0	3.1	6.2
20	6.8	6.4	4.4	3.3		17.6	25	0	0.3	0.7	0.5	4.3	6.4
Mar. 2	5.8	5.5	3.9	2.9		17.5	Mar. 7	0.2	0.9	2.0	2.0	5.0	6.8
12	4.9	4.7	3.4	2.5		17.5	17	0.5	1.5	3.3	3.7	4.8	7.0
22	4.0	4.0	2.9	2.1		17.4	27	0.7	2.3	5.3	6.2	4.3	6.9
Apr. 1	3.2	3.2	2.4	1.8		17.4	Apr. 6	0	3.8	9.1	9.4	4.0	6.7
11	2.3	2.5	1.9	1.4		17.3	16	6.0	8.3	10.0	9.9	4.4	7.2
21	1.4	1.7	1.5	1.0		17.2	26	6.2	8.0	9.2	10.0	5.5	8.5
May 1	0.5	1.0	1.0	0.6		17.1	May 6	5.5	5.1	7.7	8.3	6.5	9.7
11	0	0.3	0.5	0.2		17.0	16	2.7	4.3	6.7	7.3	7.3	10.7
21	0	0	0	0		16.8	26	1.9	3.5	6.0	6.5	7.8	11.4
31	0	0	0	0		16.7	June 5	1.0	2.8	5.3	5.8	8.3	12.2
June 10	0	0	0	0		16.5	15	0.2	2.1	4.6	5.1	8.8	12.8
20	0	0	0	0		16.3	25	0	1.5	4.0	4.5	9.3	13.3
30	0	0	0	0		16.1	July 5	0	0.9	3.4	3.9	9.8	13.8
July 10	0	0	0.3	0.1		15.9	15	0	0.4	2.7	3.2	10.3	14.2
20	0	0.5	0.8	0.5	14.8	15.7	25	0	0	2.1	2.5	10.8	14.6
30	0.5	1.2	1.3	0.9	14.4	15.4	Aug. 4	0	0	1.5	1.9	11.3	14.9
Aug. 9	1.4	1.9	1.7	1.3	14.1	15.1	14	0	0	0.9	1.2	11.8	15.2
19	2.3	2.6	2.1	1.6	13.7	14.7	24	0	0	0.3	0.5	12.3	15.5
29	3.2	3.3	2.5	1.9	13.2	14.4	Sept. 3	0	0	0	0	12.7	15.7
Sept. 8	4.1	4.0	2.9	2.2	12.7	13.9	13	0	0	0	0	13.1	16.0
18	5.0	4.8	3.3	2.5	12.2	13.5	23	0	0	0	0	13.4	16.2
28	5.9	5.6	3.8	2.8	11.6	12.9	Oct. 3	0	0	0	0	13.6	16.3
Oct. 8	6.9	6.4	4.3	3.1	10.9	12.3	13	0	0.1	0.4	0	13.8	16.5
18	8.0	7.3	4.9	3.5	10.1	11.6	23	0.4	0.8	0.8	0.4	13.9	16.6
28	9.2	8.5	5.7	4.1	9.3	10.8	Nov. 2	1.2	1.5	1.2	0.7	14.0	16.8
Nov. 7	10.7	10.0	6.8	5.0	8.3	10.0	12	2.0	2.2	1.7	1.0	14.1	16.9
17	11.1	10.6	7.3	4.9	7.2	9.0	22	2.7	2.8	2.3	1.4	14.1	16.9
27	10.6	9.8	7.0	4.2	6.4	8.4							
Dec. 7	7.7	7.1	4.4	3.6	6.1	8.1							
17	5.5	5.1	2.8	1.0	5.9	8.1							
27	3.9	3.6	1.5	0	5.6	8.0							

TABLE 1. Ground-Based Observing Data, Comet Halley 1985-1986. For a particular observer's latitude, the number of dark hours is defined as the time interval during which the sun is below the local horizon by at least 18 degrees and the comet is simultaneously above the local horizon. Magnitude estimates are based upon comet Halley's observed behavior in 1909-1911.

observers may wish to align a small optical telescope with their radio telescope by simultaneous observations of a bright planet. Subsequent radio observations of comets would be facilitated by noting ephemeris errors with the optical telescope.

To enable observers to make spectroscopic observations in absorption and continuum optical depth studies of the inner coma, the office of the Astrometry Discipline Specialist will issue periodic updates for possible cometary occultations of stars and radio sources in 1985-1986. Observers who desire to begin planning their observation schedules should consult The Comet Halley Handbook (Yeomans, 1981) for preliminary ephemeris data. Finally, it should be pointed out that the return of comet Halley in 1985-1986 will be accompanied by the very favorable return of short periodic comet Giacobini-Zinner. Comet Giacobini-Zinner will reach eighth magnitude near its perihelion passage on September 5, 1985 and will be well placed for ground based observations for several months on either side of perihelion (see Figure 1). The opportunity to nearly simultaneously observe two completely different types of comets with the same instrumentation should considerably enhance our understanding of cometary phenomena. The Fall of 1985 and the Spring of 1986 should be a period of unprecedented cometary research.

References

1. Houziaux, L., (1959), Bull. Acad. Belg., 45:218.

2. Marsden, B. G., (1968), Astron. J., 73:367.

3. Marsden, B. G., (1969), Astron. J., 74:720.

4. Marsden, B. G., Sekanina, Z., and Yeomans, D. K., (1973), Astron. J., 78:211.

5. Whipple, F. L., (1950), Astrophys. J., 111:375.

6. Whipple, F. L., (1951), Astrophys. J., 113:464.

7. Yeomans, D. K., (1977), Astron. J., 82:435.

8. Yeomans, D. K., (1981), The Comet Halley Handbook: An Observer's Guide. NASA Document, JPL 400-91, Jet Propulsion Laboratory, Pasadena, CA.

9. Yeomans, D. K. and Kiang, T., (1981), MNRAS, 197:633.

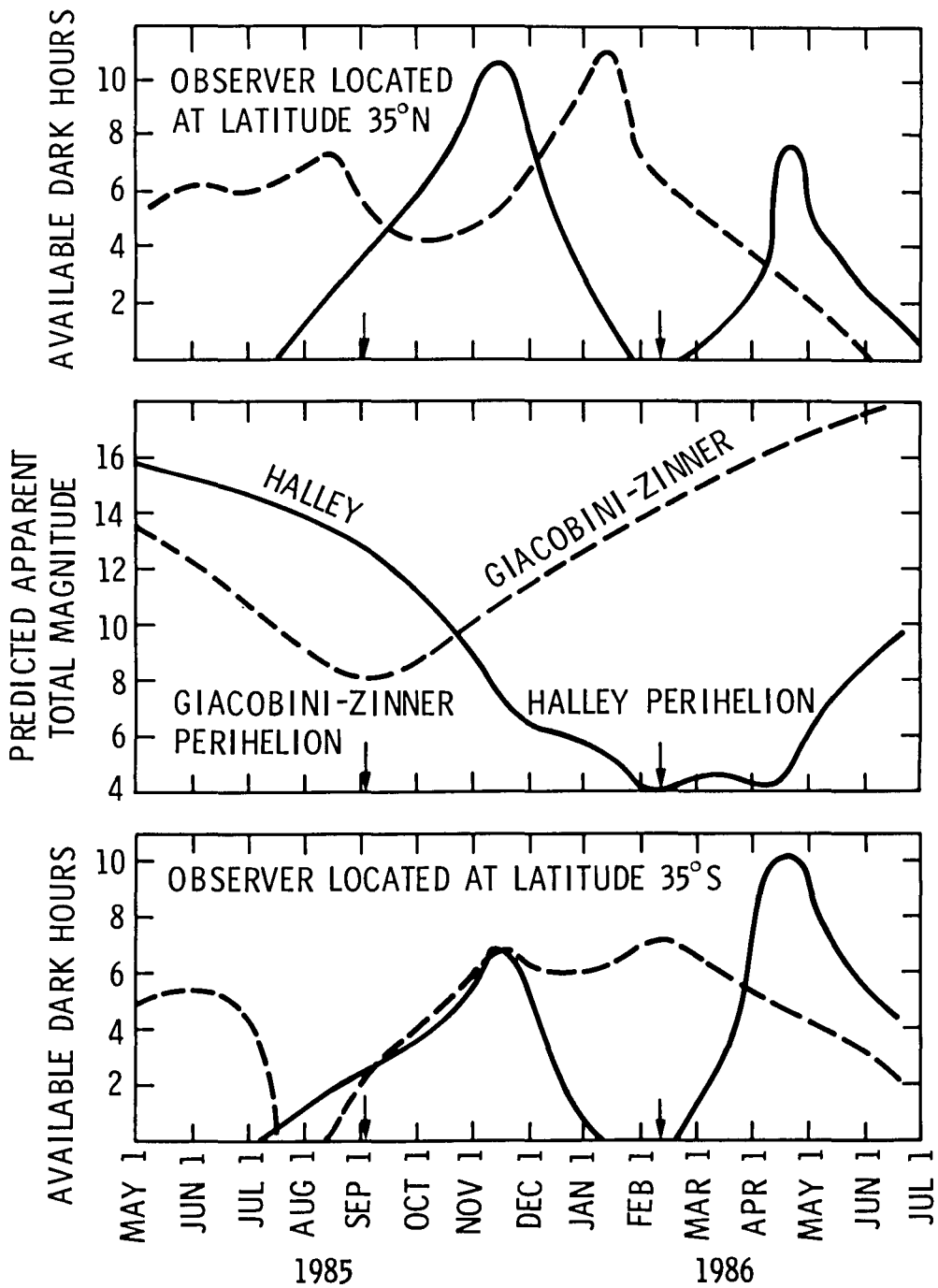

FIGURE 1. Observing Conditions for Comets Halley and Giacobini-Zinner in 1985-1986.

DISCUSSION

M.K. Wallis: The 1973 nongravitational dependence on heliocentric r does not fit iceevaporation models at small r as the latter $\sim r^{-2}$. I suggest instead r^{-2} exp $-(r/r_1)^{4.5}$ for an anistropically-heated comet, rotating with a few hours period. Both these models apply only to single-component nucleus, which does not agree with ideas of an icy conglomerate of H_2O, CO_2, CH_4, etc...

D.K. Yeomans: The nongravitational force model now in use is an empirical fit of Delsemme's theoretical expression for the vaporization flux of water ice as a function of heliocentric distance. This model has allowed Marsden, Sekanina and myself to successfully represent almost all comets whose motions are affected by nongravitatonal forces and whose periods are on the order of 6 years. However, some of the intermediate period comets (P$\sim$ 70 years) have nongravitational effects that do not behave in strict accordance with the nongravitational model now in use. At JPL, Sekanina and I are now in the process of trying alternative models for comet Halley. Perhaps we could try your expression to see whether or not the orbital solution is improved.

J. Klinger: I am very glad to hear that your considerations on non-gravitational forces lead to the conclusion that the activity of Halley's comet must have been very constant during past apparitions. The model for the nucleus based on phase transition of ice I presented yesterday led qualitatively to the same conclusion.

P. Lamy: What is the typical accuracy on the Chinese data (i.e. on the determination of perihelion time)?

D. Yeomans: The accuracy in determining perihelion passage times from the ancient Chinese observations depends upon how close the comet passed by the Earth. For a close passage, the cometary apparition was obvious and well documented. In addition, the comet's apparent motion on the sky during a close approach is rapid and hence the perihelion passage for that apparition is very sensitive to the time of a perticular position measurement. In 837 A.D. comet Halley made its closest approach to the Earth (0,04 AU) ever and the Chinese observations allowed the time of perhelion passage to be determined to within $\pm$ 0.05 day. This is not a typical error of course but usually a well observed aparition will allow the perihelion passage time to be determined to within a few days.

A. Danks: How reliable are your magnitude predictions and how did you arrive at them?

D.K. Yeomans: The magnitude estimates as a function of time for the evening coming apparition of comet Halley were determined by fitting the 1909-11 observations with a formula of the following form $m = M + 5 \log \Delta + n \log r$. Here Δ and r are the geometric and heliocentric distances in AU. From several estimates of the comet's apparent magnitude (m) in 1909-11, the absolute magnitude (M) and the index (n) were found to be 5.0 and 13.1 respectively.

Post perihelion observations in 1910-11 did not seem to follow this standard equation and these observations were fit with a Chebychev series. The 1985-86 magnitude predictions will be corrected if the comet's brightness in the coming apparition behaves as it did in 1909-1910. However it should be noted that some of the 1910 observations, particularly post perihelion, showed a 0.5-1 magnitude scatter.

DETERMINATION OF PRECISE PHOTOGRAPHIC POSITIONS WITH THE AUTOMATIC MEASURING MACHINE IRIS

G. Hahn and C.-I. Lagerkvist
Astronomiska observatoriet, Uppsala, Sweden

I. INTRODUCTION

To determine precise photographic positions of solar system bodies is an important task in astrometry. Rapidly calculated and published positions of newly discovered objects allow orbit determinations and calculations of ephemerides for follow-up observations. Accurate positions of known asteroids and comets are used for improvement of their orbits and to provide better ephemerides.

At the Uppsala observatory a programme for determination of accurate positions of asteroids has been in progress for several years, using the Schmidt telescopes at Kvistaberg and Mount Stromlo observatory as well as the telescopes at ESO at La Silla, Chile.

At the Institute of Physics IV at the Royal Institute of Technology in Stockholm we have had the opportunity to use the automatic measuring machine IRIS. One of us (GH), when working at the Institute of Physics IV, developed the interactive computer routine ASTEROID, which allows automatized measurements and reductions of photographic positions.

II. THE MEASURING MACHINE IRIS

IRIS, which stands for Image Reading Instrument System, was developed by N. Åslund and his collaborators in the 1970's and has since then been continously improved during the last few years. For a techical description see Åslund et al. (1975) and Åslund et al. (1981). IRIS is a two-channel micro-densitometer with vibrating prisms as scanning devices. The rapid scanning (60 Hz) produces an intensity profile of the measured object in both coordinates. The controlling computer programme determines the median of this profile and the measuring table is moved to the corresponding position. A servo system, including stepmotors, Heidenhain rulers and digital encoders, performs all motions for the table. The machine works in several measuring modes, allowing both manual and automatic setting. All functions are computer- as well as operator-controlled, which allows interactive handling.

The machine must be in a temperature-controlled environment (takes about 1-2 hours to establish thermal stability). For short measuring runs (up to 15 minutes or so) the temperature drift is negligible.

Proceedings of the ESO Workshop on "The Need for Coordinated Ground-based Observations of Halley's Comet", Paris, 29 – 30 April 1982.

III. THE INTERACTIVE COMPUTER ROUTINE ASTEROID

The overall philosophy for the development of this programme was to facilitate and automatize as much as possible the procedures used in the determination of photographic positions; selection and identification of reference stars, coordinate measurements and reductions.

In the following a step-by-step description of a typical measuring run is given in order to illustrate the procedure (compare fig. 1).

Preparations before start:

Identification and marking of the unknown objects on the plate.
Compilation of necessary data such as telescope and plate parameters (the information on the plate cover is normally sufficient).

The programme starts with a request for certain initial parameters which must be entered first (e.g. focal length, plate size, coordinates of the plate center, observatory coordinates).

The procedure starts by selecting an appropriate number of catalogue stars from magnetic tape and writing them on a disc file. At the moment we have the AGK3 and the SAO catalogues on magnetic tape, with the AGK3R and Perth 70 in preparation.

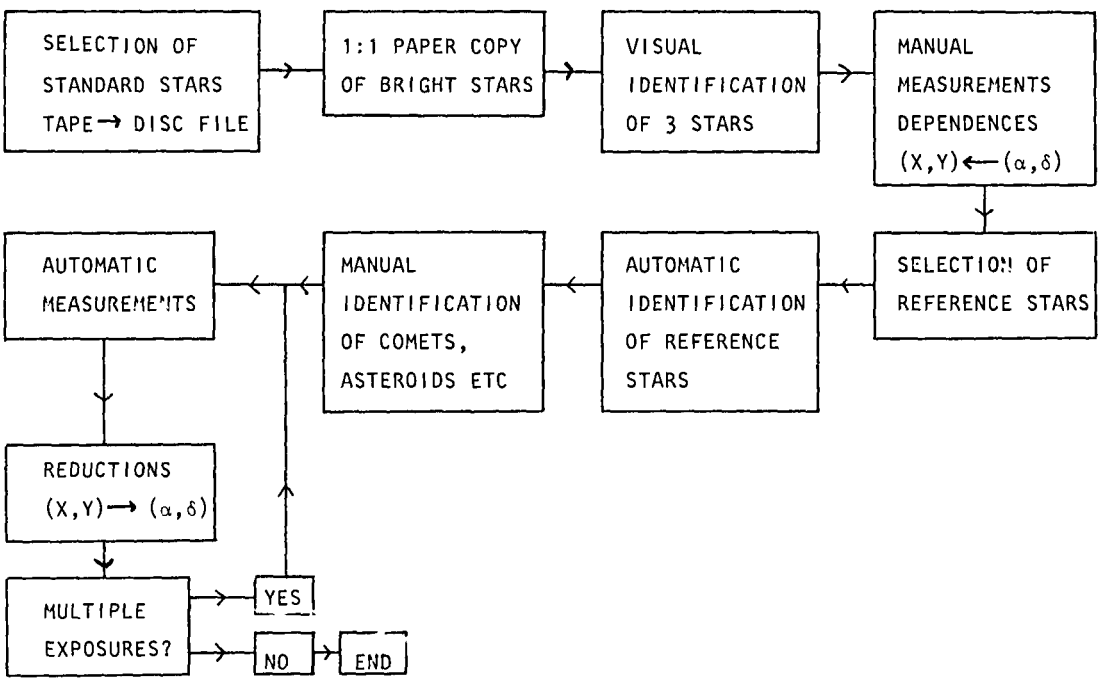

Selection of bright stars

Next the compiled disc file is searched for bright stars and those found to be on the plate are plotted on a TV screen. When enough stars are found (at least three around the plate center) a 1:1 scale paper copy is produced on a plotter. Superposing this plot on the plate on a light board gives an easy identification of the stars. The plate center and the unknown objects are marked on the copy. No marks are needed on the plate - only the orientation need be determined.

Visual identification

After the identification of the three stars the plate is mounted into IRIS (plates up to 30 x 30 cm can be measured). The plateholder and the measuring table can be moved manually in order to inspect the plate on a projection screen with approximately 8x magnification. The marked objects thus can easily be found. In the center of this screen is seen the measuring window into which the image must be positioned. This window defines the area to be scanned and is of variable size, allowing the measurements of large and small images. There is also a separate glass plate behind which a light point indicates the approximate position of the table. On this plate the copy can be attached and orientated so that all stars can be indentified.

Coordinate transformation

The zero point of the IRIS coordinate system is chosen at the plate center. The coordinate transformation between the X and Y coordinates and the spherical coordinates is performed by measuring three stars, thus forming a Dependence triangle around the plate center. The operator positions on each star and presses a button, the computer reads the coordinates and uses the stored α and δ of the stars to calculate the transformation, as well as the α and δ of the plate center (which is to be considered to be the tangential point).

Selection of the reference stars

Now the reference stars are selected from the disc file. This is done by moving the plate to a point which will be considered the center around which the reference stars are searched for in the disc file. The size of the field is defined by the operator as well as the magnitude interval. All stars found will be displayed on the TV screen. The procedure can be repeated if necessary, in order to select the appropriate number of reference stars optimally distributed around the unknown objects. A running numbering of the stars allows their subsequent identification.

Automatic identification

With the aid of the transformation the reference stars found are identified automatically by IRIS, which positions on each star, allowing the operator to decide whether the star is to be measured or not. In this way only well-defined and unblended images are selected. The operator also sets the appropriate parameters for the automatic measuring mode. When a star has been accepted, the programme calculates the necessary corrections for proper motion between the catalogue epoch and the plate epoch and determines the standard coordinates ξ and η, using the earlier determined tangential point.

Identification of the unknown objects

After the reference stars the images of the unknown objects have to be identified The operator inspects the image, decides whether the measurement can be performed automatically or has to be done manually. (Very poor or faint images cannot be fully automatically measured; instead the operator must position on the image and an automatic reading will be performed after the automatic measuring run).

When all images to be measured are identified their X and Y coordinates are stored on a disc file (for some possible later use; e.g. remeasurement).

Automatic measurements

Before the actual automatic measuring run starts the sidereal time of the exposure for the image in question is requested. The programme calculates the UT of the exposure, which is stored together with the later determined α and δ.

In the automatic measuring mode IRIS positions on each image automatically. Up to eight settings per image are made by successive displacements of 10 microns off the image in different directions and following resettings. The measured coordinate values are displayed on the terminal. Points which deviate more than 5 microns are rejected and remeasured. The repeatability on an image of average quality is better than one micron. The mean value of all settings is determined, together with the standard deviation. The latter is displayed on the screen after the measuring run, allowing the operator to check the quality of the measurements and to decide about a possible remeasurement. The measured coordinates are stored on a disc file. This allows a separate reduction of the data later on as well as a possible rereduction if necessary.

Data reduction

The distribution of all measured objects on the plate is displayed on the TV. From the reference stars the operator selects some control stars. Their number depends on the overall number and the distribution of the reference stars.

These control stars (normally 1-3) are considered as unknown objects and their coordinates are determined and then compared with their known α and δ from the catalogue. This gives a quality control for the measurements. All the other stars are taken as reference stars.

The programme provides six different reduction modes:

1) linear terms only
2) + a magnitude term
3) + magnitude and coma terms
4) linear and quadratic terms
5) + a magnitude term
6) + magnitude and coma terms

The errors in α and δ and the standard deviation of the reduction are displayed, as well as the errors of the control stars. The operator may, after inspection of these data, decide whether some reference stars are to be excluded from the reduction and may perform a new reduction. The calculated coordinates of the asteroids, control stars and the errors are stored on a disc file.

IV. RESULTS

The measuring time for one plate with three exposures is approximately 45 minutes, including the reduction of the coordinates. The repeatability of one measurement is about ±0.5 micron. The errors of the determined positions are comparable with the errors of the used reference star catalogue.

REFERENCES

Carlsson, M., Hahn, G. and Lagerkvist, C.-I. :1980, Astron. Astrophys. Suppl. 41, 117.

Hahn, G., Lagerkvist, C.-I. and Svensson, B. :1981, Astron. Astrophys. Suppl. 44, 317.

Pettersson, B., Hahn, G. and Lagerkvist, C.-I. :1982, Astron. Astrophys. Suppl. 47, 533.

Åslund, N., von Gersdorff, N., Norberg, R. and Nordin, J.A. :1975, ed. de Jager and Niuwenjuijzen. Proc. of the Conf. on Image Processing Techniques in Astronomy (Utrecht), p. 229.

Åslund, N., von Gersdorff, N., Hahn, G. and Petersson L. :1981, Proc. of the Second Conf. on Image Analysis (Helsinki), ed. E. Oja and O. Simula, p. 421.

PHOTOGRAPHIC FACILITIES OFFERED BY THE SCHMIDT TELESCOPE AT CALERN OBSERVATORY

Jean Louis HEUDIER
C.E.R.G.A.
Caussols
06460 SAINT VALLIER DE THIEY
FRANCE

The Schmidt telescope located at Calern Observatory is operated by Centre d'Etudes et de Recherches Géodynamiques et Astronomiques (C.E.R.G.A.) for the Institut National d'Astronomie et de Géophysique (I.N.A.G.).
Calern Observatory is in the south east of France, close to the cities of Nice, Cannes and Grasse.
The overall characteristics of the instrument are the following:

Longitude	- 27 min 42.3 sec
Latitude	43° 44' 53"
Elevation	1270 m.
Aperture	90 cm.
Mirror diameter	152 cm.
Focal length	315 cm.
Plate size	30 x 30 cm.
Field Size	5° 16' x 5° 16'

Filters available : UG 11, UG 1, GG 385, GG 455, GG 495, RG 610, RG 630, RG 715.

Emulsions available : IIaO, IIaD, 103aF, 103aE, IIIaJ, IIIaF, IV N, I Z.
Hypersensitization can be achieved either by baking in Nitrogen or Forming Gas, or by bathihg in a solution of Silver Nitrate.

The instrument is not presently involved in a survey programm; therefore, plates can be taken for many different astronomers.

Proceedings of the ESO Workshop on "The Need for Coordinated Ground-based Observations of Halley's Comet", Paris, 29 – 30 April 1982.

The request for new plates must be sent to the telescope where a scientific committee check them.
The plates are taken by the telescope staff, but astronomers are welcome when th eir programs are run.
After the exposure and processing, the plate is carefully examined and the main observing parameters are encoded and stored in a computer. An interactive program can be used from any telephone set that can be connected to the Centre Interrégional de Calcul Electronique (CIRCE); then anyone has the possibility to find the plates that correspond to a variety of criteria such as given coordinates, given emulsion, filter, date of acquisition, quality and so on.
Once he has found the plate he wanted, the astronomer can receive a copy and start working on the field.
We also have the possibility to use the PDS microdensitometer located at Nice Observatory (i.e. one hour by car from the telescope) and digitization and numerical processing of the images can be achieved very quickly after the exposure if needed. As an example figures 1 - 2 show the images of the numerical treatment obtained on comet SCWASSMANN WACHMANN 1 on plates taken on April 16 and 18 1982, digitized and computer processed on April 19.

This instrument, in conclusion, can be used very easily by people who need cometary observations: it is possible to find the available plates in the file by using the database and the interactive procedure and get copies of the needed plates; it is also possible to get new plates, especially taken for new programs. To receive the application forms contact the Telescope staff at the address mentioned in the title of this paper.

P/ SCHWASSMANN WACHMANN 1

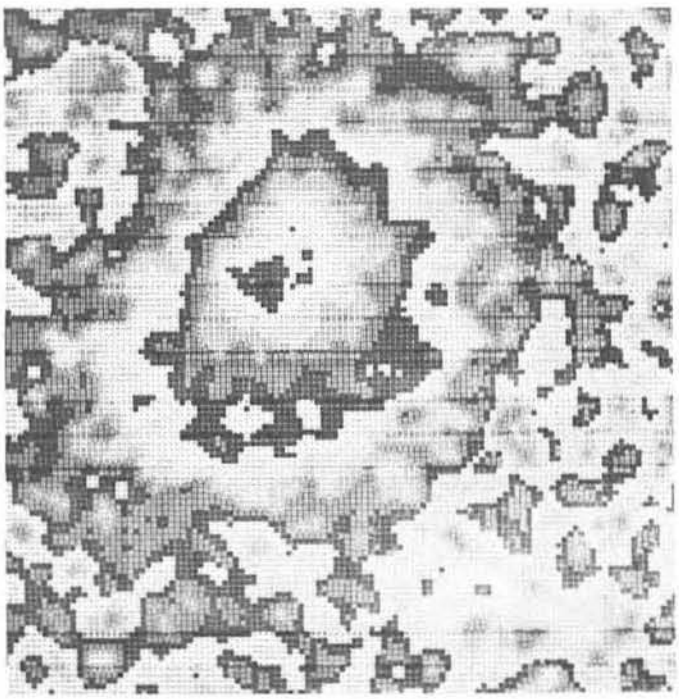

1. April 16 20h 29 U.T.

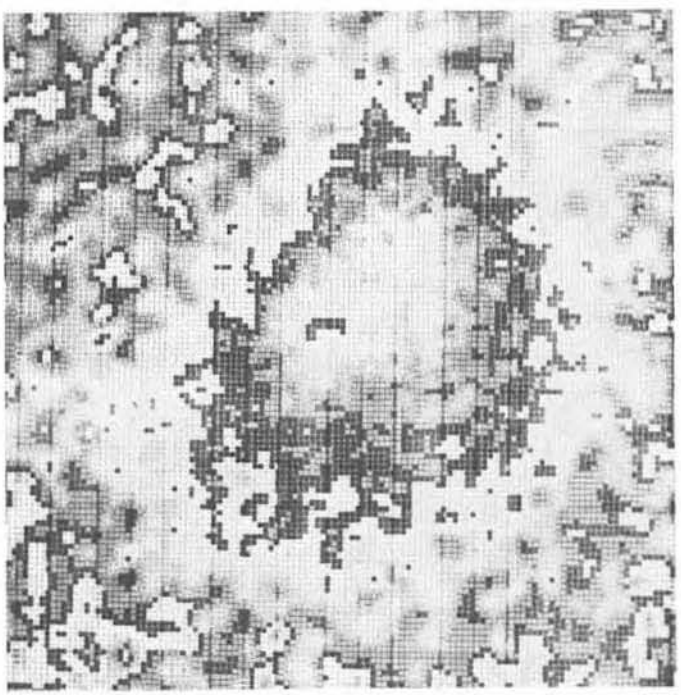

2. April 18 20h 53 U.T.

The field size is about 1 arcmin square

THE CONTRIBUTION OF FRENCH ASTRONOMERS TO THE ORBIT DETERMINATION OF HALLEY'S COMET.

B. MORANDO (Bureau des Longitudes - Paris)

The next reappearance of Halley's comet in 1986 will give French astronomers an opportunity to develop studies of the orbits of comets and to organize the observations of these bodies for astrometric purposes.

Bureau des Longitudes in Paris is specialized in the celestial mechanics of the solar system and the building of ephemerides for planets and satellites. We have applied to Halley's comet a numerical integration program with variable step using the Cragg-Bulirsch-Stoer method (Bulirsch-Stoer 1966), the initial conditions were taken in Yeomans (Yeomans 1981) as well as the model for the non gravitational forces (Yeomans 1977). The integration was carried through from 1982 to 1987 and the results agree with Yeoman's to the precision he gave (Yeomans 1981).

This allowed us to obtain a file on magnetic tape of the coordinates of the comet from now through the period of its passage through perihelion. This file will be used to predict risings, settings etc... for would be users.

Moreover the numerical integration program is being altered so that the derivatives of the elements with respect to the initial conditions may be obtained. This will lead to the improvement of the orbit when observations after rediscovery are obtained.

Another field of research could be the study of the motion of the comet since it was first observed as soon as a tape of all observations is available.

As far as observations are concerned an effort will be made to stimulate good amateur observers and to give them advice. Other plans by professional astronomers are described in this volume by J.-L. Heudier.

Proceedings of the ESO Workshop on "The Need for Coordinated Ground-based Observations of Halley's Comet", Paris, 29 – 30 April 1982.

References

Burlisch R. , Stoer J. 1966.Num. Math. 8,1.
Yeomans D.K. 1977. Astron. Journal vol. 82, n°6 .
Yeomans D.K. 1981. The Comet Halley Handbook.

THE INTERNATIONAL HALLEY WATCH

THE INTERNATIONAL HALLEY WATCH

Jürgen Rahe

Remeis-Observatory Bamberg
Astronomical Institute
University Erlangen-Nürnberg
Bamberg, F.R.G.

Ray L. Newburn, Jr.

Jet Propulsion Laboratory
California Institute of Technology
Pasadena, California, U.S.A.

Abstract. The International Halley Watch (IHW) is a program designed to promote cooperation, standardization, and archival documentation in all phases of study of Comet Halley during its 1985-86 apparition. Discipline Specialists have been selected to create cooperative nets of ground-based observers encompassing seven different technical areas and to coordinate the observations and publication of results in each. The IHW will promote cooperation among ground-based and space studies of comet Halley wherever reasonable and feasible. More specifically, the IHW will make ephemerides from the astrometric net available to any country flying a deep space mission. It will coordinate special Halley Watch Days with the arrival dates of space probes or periods of observation from Earth orbit. And the IHW will provide a permanent archive in published form of all scientific observations of comet Halley.

Proceedings of the ESO Workshop on "The Need for Coordinated Ground-based Observations of Halley's Comet", Paris, 29 – 30 April 1982.

The IHW is an organization dedicated to advocating, assisting, coordinating, and ultimately archiving a worldwide effort to study comet Halley from the ground, the air, and space by every means possible and to present the plans for and results of these activities to an interested public. In particular, a large ground-based effort is necessary to place space probe results in their proper context within the overall apparition and because this is the first time modern, quantitative astronomy has had the opportunity to study one of history's most famous astronomical objects. It will also be the first time fully coordinated and correlated studies involving all astronomical technology will have been devoted to any comet. It is important that the ground-based effort be coordinated in order to achieve the greatest scientific benefit from the effort that is sure to take place, and it is equally important that the results be widely disseminated in a technical archive for present and future scientists and in non-technical format to the public.

The IHW activity will include four phases:

(1) creation of observing nets and setting standards for their operation;

(2) trial run on an available comet;

(3) comet Halley operations;

(4) data publication and archiving.

The general organization of the IHW is outlined below:

IHW ORGANIZATION

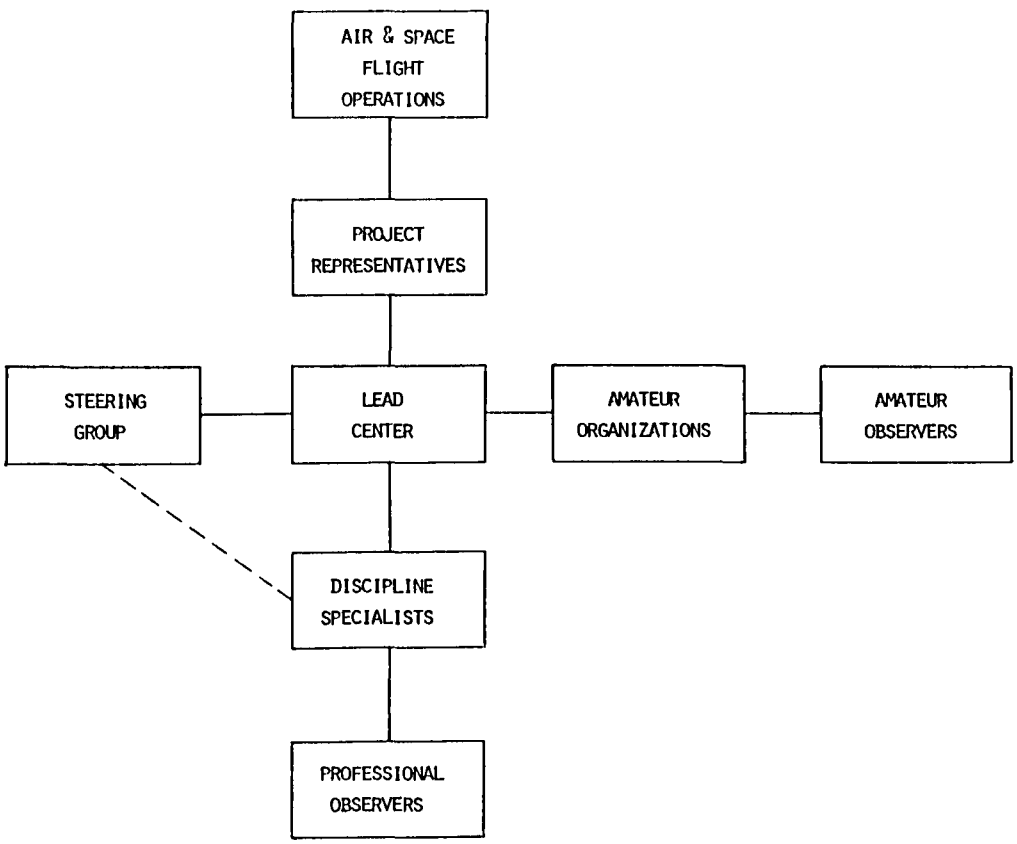

The basic structure of the IHW consists of a Halley Watch Leader, Ray L. Newburn, Jr. at the JPL, U.S.A., and a Co-Leader for Europe, Africa and Asia, Jürgen Rahe at Bamberg, F.R.G., and their offices, a Steering Group of international comet specialists, and the Discipline Specialists. To this basic structure will be added appendages for communicating with amateur astronomers, with educational facilities such as planetariums, and with the mass media. Project representatives for space missions to Comet Halley, for Earth-orbiting instruments for Halley studies, and for any non-orbiting flight instruments (aircraft, balloon, sounding rocket), will help provide careful planning of useful cooperation between the ground-based and fligth studies, as well as a rapid communication link when necessary.

The Halley Watch Leaders will coordinate the activities of the Discipline Specialists and serve as the communications link among all elements of the IHW. They will set general goals and will be responsible for publication of the Halley Archive, a compendium of results from all disciplines, independent of the prior individual journal publications of net members. This Halley Archive will be established at JPL in Pasadena, U.S.A. and at the Remeis-Observatory in Bamberg, F.R.G. In consultation with the Discipline Specialists (DS), they will set Halley Watch Days for coordinated observations by two or more disciplines. They will oversee preparation of information about comet Halley for distribution to amateurs, to planetariums, and to the news media, as well as to professional IHW participants.

The IHW Steering Group is an international group of comet experts appointed by NASA to advise the Halley Watch Leaders. Members of the Steering Group are listed below. They meet with the IHW Leaders semi-annually, and their first task has been to review all proposals for Discipline Specialist nominations. The activities of the Discipline Specialists will be reviewed annually by the Steering Group.

IHW STEERING GROUP MEMBERS

M.K.V. Bappu	-	India	A. Massevitch	-	USSR
M.J.S. Belton	-	USA	C.R. O'Dell	-	USA
J. Blamont	-	France	R. Reinhard	-	The Netherlands
G. Briggs	-	USA	H.E. Schuster	-	Chile
A. Delsemme	-	USA	V. Vanysek	-	Czechoslovakia
B. Donn	-	USA	J.F. Veverka	-	USA
H. Fechtig	-	West Germany	K.W. Weiler	-	USA
I. Halliday	-	Canada	G. Wetherill	-	USA
G. Herbig	-	USA	F.L. Whipple	-	USA
Y. Kozai	-	Japan	L.L. Wilkening	-	USA
R. Lüst	-	West Germany	Ya.S. Yatskiv	-	USSR

The IHW Discipline Specialists are the backbone of the IHW. In consultation with other experts in that discipline, they will recommend standards, data formats, and objectives and priorities for observations. They will provide facilities for reducing data of those willing to observe but unwilling or unable to go beyond that first step. In some cases, proper standardization may require that data be uniformly processed at one reduction center.

DISCIPLINE SPECIALISTS

- Will be a specialist in a class of observing techniques
- Will create an observing net dedicated to use of those particular techniques
- Will develop standardization and coordination within a net
- Will provide facilities to handle data as required
- Will provide a means of rapid communication with net members
- Will cooperate with the Lead Center in setting up interdisciplinary studies
- Will report regularly to the Lead Center and Steering Group on progress and problems in the net
- Will transmit net data to the Halley Archive

The Discipline Specialists will create nets of ground-based observers and coordinate their work in one of the following areas:

Large-Scale Phenomena. This net will study phenomena of large angular extent and relatively low surface brightness, especially the ion tail, dust tail, and related outer coma features.

Near-Nucleus Studies. This net will study physical features of small to medium scale and low contrast such as the photometric nucleus, jets, shells, and any other non-uniformities of the inner coma.

Spectroscopy and Spectrophotometry. This net will include observers making compositional studies in the wavelength range 3000-10000 Å using grating or prism dispersion.

Photometry and Polarimetry. This net will include observers making compositional studies or particulate studies in the wavelength range 3000-10000 Å and using interference filter wavelength discrimination for the former.

Infrared Spectroscopy and Radiometry. This net will include observers working in the wavelength range 1-500 μm whether studying composition, scattering properties, or thermal emission of dust, gas, or the nucleus.

Radio Science. This net will include observers, working at wavelengths greater than one-half millimeter whether studying composition, thermal emission, or non-thermal mechanisms.

Astrometry. This net will include observers furnishing positional data on comet Halley. At least some observers must be found who will reduce plates to astrometric positions within 24 hours. The Discipline Specialist is prepared to furnish new ephemerides in equally short time, based upon a fully perturbed theory including non-gravitational force terms.

In order to make the IHW more truly international, to help overcome communication problems caused by time differences, and to help assure continuity of effort, the individual Discipline Specialists

(DS) have Deputies, so that the DS and the Deputy DS are citizen of and resident in different countries which are separated by a minimum of five time zones.

The Discipline Specialists (DS) and their Deputies (DDS), are:

Large Scale Phenomena	- J.C. Brandt (DS), M.B. Niedner (DDS), J. Rahe (DDS)
Near Nucleus Studies	- J. Rahe (Co-DS), Z. Sekanina (Co-DS), S. Larson (DDS)
Spectroscopy & Spectro-photometry	- S. Wyckoff (Co-DS), P.A. Wehinger (Co-DS), M. Festou (DDS)
Photometry & Polarimetry	- M.F. A'Hearn (DS), V. Vanýsek (DDS)
IR Spectroscopy & Radiometry	- M.F. Knacke (DS), T. Encrenaz (DDS)
Radio Studies	- W.M. Irvine (DS), F.P. Schloerb (Co-DS), E. Gerard (DDS)
Astrometry	- D.K. Yeomans (DS), R.M. West (Co-DS)

Approved and planned flight projects, dedicated fully or in part to observations of Halley's comet (Giotto, Vega, Planet-A, Space Telescope, Spacelab OSS-3), will communicate with the IHW through the Project Representatives.

These Project Representatives will

- set up, together with the IHW Leaders and Discipline Specialists, special Halley observation periods to take full advantage of simultaneous remote-sensing and in situ experiments,
- serve as a communication link for the inevitable technical questions that flight projects and IHW observers will have about the nature of observations being attempted by the other (workshops with participation of ground-based observers and space experimenters may prove helpful here),
- receive from and provide to the IHW data describing the state of the interplanetary medium and warnings of sporadic cometary behaviour such as jets, secondary nuclei, disconnection events, etc.,
- support the IHW in its attempts to receive and archive the flight data in a manner satisfying the interests of individual flight project experiments as well as the needs of the IHW archive.

For the transmission of ephemeris data to the flight projects, planning Halley encounters, a separate direct link will be established between the Discipline Specialist for Astrometry and the Flight Operations Personnel of these flight projects.

An Inter-Agency Steering Group, with delegations from the USSR, Japan, NASA, and ESA, and three working groups were formed in September 1981, during the First Inter-Agency Meeting on Space Missions to Halley's Comet and Related Activities, promoting the IHW as the coordinator of all ground-based and near earth Halley observations. The next meeting is scheduled to take place in Budapest, Hungary in November 1982, in conjunction with an international meeting on Comet exploration.

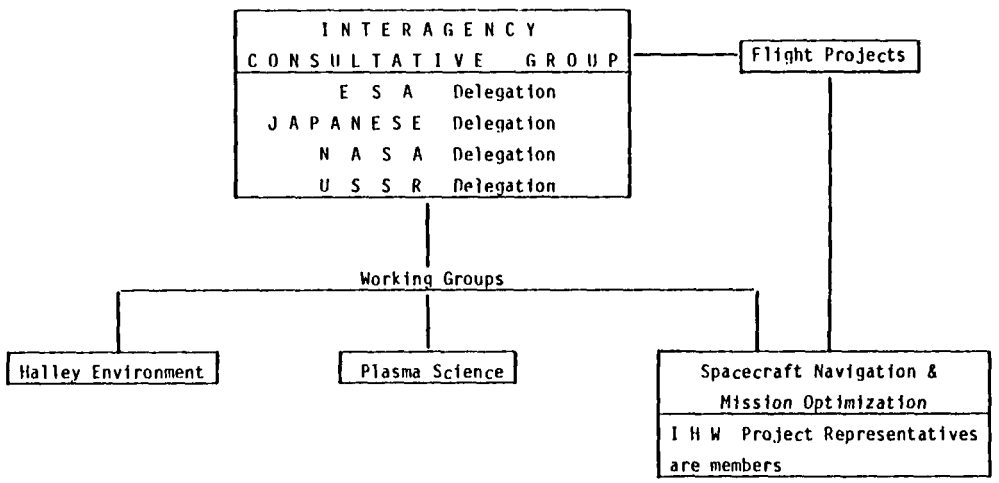

The Excetutive Committee of the International Astronomical Union (IAU) has endorsed the goals of the IHW, and has recognized it as the international co-ordinating agency for comet Halley observations. Formal announcement of the IHW will be made during the 1982 IAU-General Assembly in Patras, Greece.

DISCUSSION

Ph. Lamy: Those who have been faced with the problem of comparing several photographs such as K. Jockers and myself agree that the basic problem lies with the differences in the observations (focal length, emulsion, ...). I emphasize, as I said in my communication, that the probable key to the problem is the setting of a net of observers - not necessarily numerous - using identical cameras capable of producing readily comparable photographs whose reduction may be made almost automatic.

J. Klinger: Did IHW make any decision until now about periods when Halley will be observed at the same moment with different techniques. Since some techniques, space missions for example, need a long preparation time, those kind of decisions should be made rather early.

J. Rahe: "Halley Watch Days" and /or "Periods" have not been set up, but it will be done in due time.

K. Jockers: Referring to a question by Prof. Blamont, I consider it very important that innovating observations which cannot be proposed worldwide through an organization like Halley Watch are not a priori excluded from obtaining observation time.

L. Woltjer: Three types of observations should probably be considered.
1) Observations for specific needs, like the astrometric data needed for space projects. These will be performed by ESO staff under an agreement with the relevant space organizations.
2) Observations of a basic nature, like for example the photographs (with standardized filters and calibrations) to be obtained over a relatively long period. With input from the community a programme of such observations will be developed and ESO staff will execute it.
3) Other observations of particular aspects will certainly be proposed by many researchers. We would expect that proposals for such observations will be made to ESO by individual researchers or groups of researchers and evaluated in the normal way.

K. Jockers: Is there a possibility to obtain financial support from ESO for the development and adaptation of special comet instrumentation to ESO instruments or to obtain a commitment that special instrumentation which is to be developed will be granted observation time.

L. Woltjer: ESO is not a funding organization and as such cannot support individual projects. It is sometimes possible to obtain some support in instrumentation projects of interest to a broader community of users. Observing time can be committed only on the basis of a scientific programme, which may of course have related instrumental aspects.